# Counting Degrees of Freedom in Quantum Field Theory Using Entanglement Entropy



by

Márk Mezei

M.Sc., Eötvös Loránd University (2009)

Submitted to the Department of Physics
in partial fulfillment of the requirements for the degree of

Doctor of Philosophy in Physics

at the

MASSACHUSETTS INSTITUTE OF TECHNOLOGY

June 2014



Signature redacted

Author .....
Department of Physics
May 23, 2014

Signature redacted

Certified by...
Hong Liu
Associate Professor
Thesis Supervisor

Signature redacted

Accepted by .....
Krishna Rajagopal
Associate Department Head for Education

# Counting Degrees of Freedom in Quantum Field Theory Using Entanglement Entropy

by

Márk Mezei

Submitted to the Department of Physics
on May 23, 2014, in partial fulfillment of the
requirements for the degree of
Doctor of Philosophy in Physics

## Abstract

We devote this thesis to the exploration of how to define the number of degrees of freedom in quantum field theory. Intuitively, the number of degrees of freedom should decrease along the renormalization group (RG) flow, and should be independent of the RG scale at a conformal fixed point. We argue that a refinement of entanglement entropy is a promising candidate for such measure. Indeed, in two and three spacetime dimensions the number of degrees of freedom defined this way can be proven to monotonically decrease under RG flows.

Firstly, we define renormalized entanglement entropy (REE) and show that it is finite in the continuum limit in a renormalizable field theory. We argue that it is most sensitive to degrees of freedom at a scale determined by the size of the entangling region, and interpolates between the ultraviolet and infrared RG fixed point vales. We discuss how it can be used to count the degrees of freedom at a given scale.

Secondly, we test whether REE is monotonic along the RG flow. In two dimensions it was known to be monotonic before our study. In higher dimensions, we study REE in free theory examples and in the framework of holography. Holography is tailor-made for the study of RG flows, and allows an efficient determination of entanglement entropy. We make use of its power and flexibility to conjecture that in three spacetime dimensions REE is monotonic, while in four dimensions it is neither monotonic nor positive. Subsequent work has proven the conjecture.

Thirdly, we count the degrees of freedom in three-dimensional superconformal field theories that are the infrared limit of supersymmetric gauge theories with matter. Supersymmetric localization reduces the computation of entanglement entropy to a matrix integral. We solve this matrix model in the large $N$ number of colors limit using two different methods; in a saddle point approximation we obtain the next-to-leading order expression in $1/N$, while mapping the matrix model to a non-interacting Fermi gas enables us to determine the result to all orders in $1/N$. We match the leading piece with $N^{3/2}$ scaling – a strong coupling phenomenon in the field theory – with the holographic duals of these theories.

Establishing a measure for the number of degrees of freedom provides nonperturbative understanding of RG fixed points and flows. Our hope is that the constraints coming from RG monotonicity can be efficiently used to constrain the long-distance physics of certain systems of interest. The first applications are only starting to emerge.

Thesis Supervisor: Hong Liu
Title: Associate Professor

# Acknowledgments

I would first like to thank my advisor Hong Liu for mentoring me from the very start of my graduate studies to the writing of this thesis. He was a constant source of ideas and inspiration, and taught me how to capture the essence of complicated problems and not to let go until every detail was understood.

I thank my spectacular collaborators Ethan Dyer, Nabil Iqbal, and Silviu Pufu for the countless hours working together on exciting problems, and sharing the excitement of research with me. I also thank Andrea Allais, Paolo Glorioso, Qimiao Si, Josephine Suh, and David Végh for working together on smaller projects. I have learnt a great deal from discussions with faculty, postdocs, and fellow students at the Center for Theoretical Physics: Allan Adams, Tarek Anous, Koushik Balasubramanian, Michael Crossley, David Guarrera, Mark Hertzberg, Timothy Hsieh, Yonatan Kahn, Shelby Kimmel, Vijay Kumar, Jaehoon Lee, Mindaugas Lekaveckas, John McGreevy, Michael Mulligan, Duff Neill, Daniel Park, Daniel Roberts, Maksym Serbyn, Shu-Hang Shao, Julian Sonner, Brian Swingle, Iain Stewart, Washington Taylor, Yifan Wang, Frank Wilczek, Sho Yaida, and Barton Zwiebach. It has been a transformative experience to be part of this community.

I thank my high school Physics teacher, Mihály Rácz, the KöMaL (Mathematical and Physics Journal for Secondary Schools), and my undergraduate advisor Péter Forgács for making my early encounters with physics an exciting experience. I thank the Princeton Center for Theoretical Science for offering me the terrific opportunity to spend the next three years as a postdoctoral fellow there. I will try to be up for the challenge.

I would like to thank my friends in Cambridge and back in Hungary for making the past five years as much fun as they were. Finally, I would like to thank my wife Anna and my family at home for their love and support.

# Contents

# Chapter 1

# Introduction

## 1.1 How do strongly interacting systems behave at long distances?

The quest to understand the basic constituents of nature and the laws determining their dynamics has been highly successful. We have a solid understanding of phenomena occurring from the electroweak scale, $10^{-18}\,m$ to the Hubble distance, $10^{26}\,m$. Navigating through these 44 orders of magnitude requires us to be able to relate physics at different scales.

The renormalization group (RG) provides a framework for an effective description of the system at the scale we are probing it. Starting from microscopic laws, we average over short distance degrees of freedom in small steps, until we reach the scale of interest. The task is highly non-trivial, and in practice one needs to expand in some small parameter, or use an appropriate approximation scheme. Finding the best way to perform RG is a creative enterprise and this versatile tool has found its applications in practically all branches of physics, ranging from particle physics, through astrophysics, to biological systems.

In this thesis we will have particle and condensed matter physics examples in mind. A central challenge is to understand the dynamics of systems, governed by simple microscopic laws, at long distances. When interactions are weak, perturbation

theory provides a powerful tool in obtaining answers of extreme precision.[1] However, when strong interactions are involved, there can be a dramatic change in the nature of the degrees of freedom as we vary the scale at which we probe the system. In quantum chromodynamics (QCD) the short distance degrees of freedom are quarks and gluons. At long distances however, these partons get bound into the zoo of hadrons, and the properties of microscopic constituents are transformed beyond recognition. In condensed matter physics, at short distances we have electrons and ions interacting though the Coulomb interaction. These simple constituents give rise to a myriad of condensed matter systems, including the fascinating example of the fractional quantum Hall liquids, which have excitations carrying fractional electric charge.

The RG enables us to organize the theoretical description of these systems. Let us think about the averaging procedure as a step in the infinite dimensional space of all Hamiltonians. Then going from one scale to another corresponds to a flow in the space of Hamiltonians. Thinking in terms of the RG flow makes it possible to identify the following notions:

1. The RG flow goes between fixed points that are scale invariant. The fixed points have their basin of attraction, called the universality class.

2. If we perturb a trajectory in a direction, the perturbed trajectory can either converge back to the original one, or diverge from it. The former case is called an irrelevant, the latter a relevant deformation. In the vicinity of a fixed point the question of relevance is decided by the scaling dimension of the fields.

3. In Lorentz-invariant systems recent advances show that one can add a height function to the RG picture; the RG always flows in a direction that decreases this function. This does not mean that the RG is a gradient flow, as the flow does not necessarily go in the steepest direction.[2]

[1] A triumph of quantum electrodynamics is the prediction of the anomalous magnetic moment of the electron, known to $10^{-9}$ accuracy. In the RG language the anomalous magnetic moment is a term in the effective action of the electron at very low energies in a background magnetic field. The calculation involves averaging over all standard model fields.

[2] In $d = 2$ spacetime dimensions the RG is a gradient flow, but for $d > 2$ it is believed not to have this property.

These points are illustrated in Fig. 1-1.

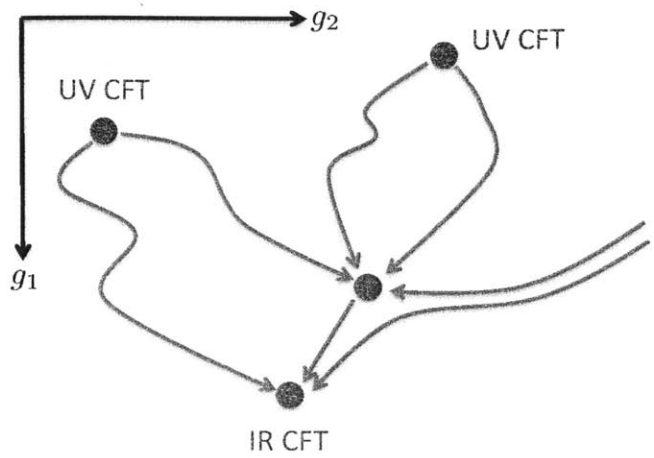


(a) Cartoon of the RG flow of a relativistic system in the space of coupling constants $g_i$. Short distance (UV) fixed points are denoted by purple, while long distance (IR) fixed points by red dots. Scale invariance in relativistic systems is believed to enhance to conformal invariance, hence the fixed points are conformal field theories (CFT).

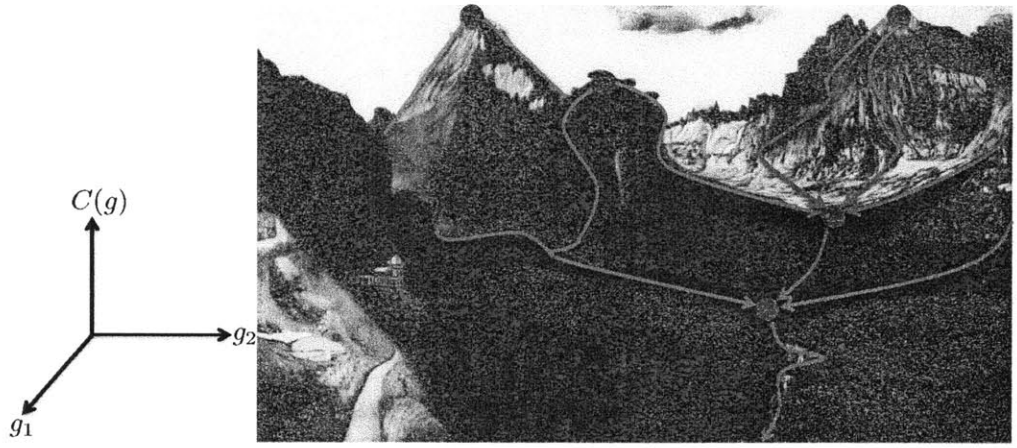


(b) A height function adds an extra dimension to the space of couplings, making it into a landscape. The RG flow can only descend on this landscape.

Figure 1-1: Cartoons illustrating how we think about RG flows of relativistic systems. Fixed points organize the space of Hamiltonians into universality classes, and a height function provides additional structure.

The discussion of the thesis revolves around the height function, which is to be interpreted as the number of degrees of freedom at a given scale. Its monotonicity along the RG flow is then very plausible: a massive field would contribute to the count at short distances, but drops out at distances large compared to its Compton

wavelength. The existence of a height function formalizes the intuition about the loss of degrees of freedom along the RG flow.[3] It turns out that to define the number of degrees of freedom in a general field theory in any spacetime dimension $d$, we have to use entanglement entropy. Hence, in the following we introduce entanglement entropy, expand on what we require from the number of degrees of freedom, and combine these two notions.

## 1.2 Entanglement entropy

There is a dramatic difference between classical and quantum entropy. While in classical physics if we divide a composite system $AB$ into two subsystems $A$ and $B$, it is always true that

$$S_{\rm cl}(AB) \geq \max\left(S_{\rm cl}(A),\, S_{\rm cl}(B)\right) \ , \tag{1.2.1}$$

this is not true in a quantum system. In particular, if $AB$ is in a pure state, dividing it into two parts generally produces mixed states for $A$ and $B$. Then it is obvious that (1.2.1) is violated.

Entanglement entropy is a specific subsystem entropy, when the subsystems correspond to geometric regions. Let us specialize to a system governed by local dynamics in its unique ground state, and take a geometric region $V$. The Hilbert space of states factorizes into the degrees of freedom corresponding to those in the region $V$ and its complement $\bar{V}$, $\mathcal{H} = \mathcal{H}_V \otimes \mathcal{H}_{\bar{V}}$. We can define the reduced density matrix corresponding to $V$ by

$$\rho_V = \operatorname*{Tr}_{\mathcal{H}_{\bar{V}}} |0\rangle\langle 0| \ , \tag{1.2.2}$$

where $|0\rangle$ is the vacuum state of the theory. Then the entanglement entropy of region $V$, or more conveniently across the boundary surface $\Sigma = \partial V$ is the entropy of this

[3]By the number of degrees of freedom we mean the number of fields needed to provide the continuum description of the system. Hence, it is not the number of lattice sites for a lattice system.

density matrix:

$$S^{(\Sigma)} = -\operatorname*{Tr}_{\mathcal{H}_V} \rho_V \log \rho_V \ , \tag{1.2.3}$$

where we assumed that the density matrix is normalized, $\mathrm{Tr}_{\mathcal{H}_V}\ \rho_V = 1$.

Quantum entanglement has been seen to play an increasingly important role in our understanding and characterization of many-body physics (see e.g. [2,3]). Entanglement entropy for spatial regions provides an important set of observables to probe quantum correlations that go beyond the information encoded in $n$-point correlation functions. It plays a major role in the characterization of topological phases of matter, where it serves as an order parameter for the detection of non-trivial phases.

In spacetime dimensions higher than two, however, the entanglement entropy for a spatial region is dominated by contributions from non-universal, cutoff-scale physics [4,5]. This implies that for a region characterized by a size $R$, the entanglement entropy is sensitive to the physics from scale $R$ all the way down to the cutoff scale $\delta$, no matter how large $R$ is. As a result the entanglement entropy is ill-defined in the continuum limit.

The common practice is to subtract the UV divergent part by hand, a procedure which is not unique and often ambiguous, in particular in systems with more than one scale. Even with the UV divergent part removed, the resulting expression could still depend sensitively on physics at scales much smaller than the size $R$ of the entangled region. As a result, in the limit of taking $R$ to infinity, one often does not recover the expected behavior of the IR fixed point (see for example the case of a free massive scalar in Sec. 3.2).

Such a situation is clearly awkward both operationally and conceptually. We should be able to probe and characterize quantum entanglement at a given macroscopic scale without worrying about physics at much shorter distance scales.

In this thesis, we show that there is a simple fix of the problem [6].[4] Consider a quantum field theory on $\mathbb{R}^{1,d-1}$ which is renormalizable non-perturbatively, i.e.,

[4]See also [7] for a discussion based on free theories.

equipped with a well-defined UV fixed point. Suppose $S^{(\Sigma)}(R)$ is the entanglement entropy in the vacuum across some smooth entangling surface $\Sigma$ characterized by a scalable size $R$.[5] We introduce the following function

$$\mathcal{S}_d^{(\Sigma)}(R) = \begin{cases} \frac{1}{(d-2)!!}\left(R\frac{d}{dR}-1\right)\left(R\frac{d}{dR}-3\right)\cdots\left(R\frac{d}{dR}-(d-2)\right)S^{(\Sigma)}(R) & \text{d odd} \\ \frac{1}{(d-2)!!}R\frac{d}{dR}\left(R\frac{d}{dR}-2\right)\cdots\left(R\frac{d}{dR}-(d-2)\right)S^{(\Sigma)}(R) & \text{d even} \end{cases} . \tag{1.2.4}$$

We will be mostly interested in the cases $d = 2, 3$, where (1.2.4) takes the form[6]

$$\begin{aligned} \mathcal{S}_2(R) &= R\frac{dS(R)}{dR} , \\ \mathcal{S}_3^{(\Sigma)}(R) &= \left(R\frac{d}{dR}-1\right)S^{(\Sigma)}(R) . \end{aligned} \tag{1.2.5}$$

In Sec. 2.2 we show that it has the following properties:

1. It is UV finite in the continuum limit (i.e. when the short-distance cutoff is taken to zero).

2. For a CFT it is given by an $R$-independent constant $s_d^{(\Sigma)}$.

3. For a renormalizable quantum field theory, it interpolates between the values $s_d^{(\Sigma,\mathrm{UV})}$ and $s_d^{(\Sigma,\mathrm{IR})}$ of the UV and IR fixed points as $R$ is increased from zero to infinity.

4. It is most sensitive to degrees of freedom at scale $R$.

The differential operator in (1.2.4) plays the role of stripping $S^{(\Sigma)}(R)$ of short-distance correlations. The stripping also includes finite subtractions and is $R$ dependent; it gets rid of not only the UV divergences, but also contributions from degrees of freedom at scales much smaller than $R$.[7]

[5] For this definition we consider $\Sigma$ to be a closed connected surface. For the strip case, we have to modify our discussion. Also note that not all closed surfaces have a scalable size. In Sec. 2.2 and Appendix 2.A we make this more precise.

[6] In $d = 2$, $\Sigma$ is just two points, hence we omit the superscript.

[7] $\mathcal{S}_d^{(\Sigma)}(R)$ can also be used at a finite temperature or finite density where it is again UV finite in the continuum limit. In the small $R$ limit, it reduces to the vacuum behavior while for large $R$, we expect it to go over to the thermal entropy.

$\mathcal{S}_d^{(\Sigma)}(R)$ may be considered as the "universal part" of the original entanglement entropy, a part which can be defined intrinsically in the continuum limit. Below we will sometimes refer to it as the "renormalized entanglement entropy" (REE), although this name is clearly not perfect. We believe such a construction gives a powerful tool for understanding entanglement of a many-body system.

## 1.3 The number of degrees of freedom

The first step towards understanding the physics of a system is to identify its relevant degrees of freedom, and the role they play in the dynamics. A fundamental question is how many degrees of freedom the system has. A continuum system has an infinite dimensional phase space, hence it is challenging to provide a finite measure for the degrees of freedom. Because the dynamics of a quantum field theory is organized by scale, we would like to characterize how the number of degrees of freedom changes with scale.

The first measure that comes to mind is the number of fields needed to describe the system. However, this cannot be correct: we know quantum field theories, that do not admit a Lagrangian formulation,[8] and the discovery of dualities has taught us that one system can have multiple equivalent descriptions with different number of fields. To avoid these problems, counting degrees of freedom is ought be based on an observable quantity. As discussed above, based on intuition from RG, this observable should be a monotonic function of the RG scale. We also require that it is computable with only the effective action at our disposal, i.e. it should not be UV sensitive. Finding a quantity that satisfies the above criteria is very difficult; rather than giving plausibility arguments for why entanglement entropy is the quantity to base the definition on, we sketch the road paved by landmark results that led to the current understanding.

In $d = 2$ Zamolodchikov solved the problem of counting degrees of freedom in a spectacular manner [8]. Because degrees of freedom have energy and momentum it is

[8]The $d = 6$ $(2, 0)$ theory is an example of a consistent theories without a Lagrangian.

reasonable to base the measure on the energy momentum tensor. Because $\langle T_{\mu\nu}\rangle = 0$ in the vacuum, we can use two point functions. In Euclidean signature, let us define the following functions:

$$\begin{aligned} F(r^2) &= 4\pi^2\, z^4 \langle T_{zz}(z,\bar{z})\, T_{zz}(0,0)\rangle \ , \\ G(r^2) &= 16\pi^2\, z^3 \bar{z} \langle T_{zz}(z,\bar{z})\, T_{z\bar{z}}(0,0)\rangle \ , \\ H(r^2) &= 64\pi^2\, z^2 \bar{z}^2 \langle T_{z\bar{z}}(z,\bar{z})\, T_{z\bar{z}}(0,0)\rangle \ , \end{aligned} \tag{1.3.1}$$

where we introduced the complex coordinates $z$, $\bar{z}$, and used rotational invariance to conclude that the functions only depend on $r^2 = z\bar{z}$. Using $r$ as a proxy for scale we can define the number of degrees of freedom by:

$$C(r^2) = 2F - G - \frac{3}{8}H \ . \tag{1.3.2}$$

Using the conservation of the energy momentum tensor, $\bar{\partial} T_{zz} + \partial T_{z\bar{z}} = 0$ we conclude that:

$$\frac{dC}{d\log r^2} = -\frac{3}{4}H \leq 0 \ , \tag{1.3.3}$$

where theinequality follows from unitarity.[9] $C$ is stationary if and only if $T_{z\bar{z}} = 0$, implying that the theory is a CFT. Then $C = c$, the central charge of the CFT.[10] For a flow between a UV and and IR CFT (1.3.3) implies that

$$c_{UV} \geq c_{IR} \ . \tag{1.3.4}$$

After the problem in $d = 2$ had been solved, the quest for appropriate higher dimensional generalizations began. Because – as discussed below – the central charge $c$ can be isolated from many different observables, it is not *a priori* clear which quantity provides a good definition of the number of degrees of freedom in higher

[9] In the Euclidean version of the theory that we invoked here, $H \geq 0$ follows from reflection positivity.

[10] We define $T_{ab} = -\frac{2\pi}{\sqrt{g}} \frac{\delta S}{\delta g^{ab}}$, and $c$ by $\langle T_{zz}(z,\bar{z})\, T_{zz}(0,0)\rangle = c/8\pi^2 z^4$ .

dimensions. To illustrate how the subject developed, we provide a list of attempts for a higher dimensional generalizations.

- Perhaps the asymptotic growth of the density of states $\rho(E)$ is the most intuitive quantity to base the definition for the number of degrees of freedom on, as it directly involves counting states. We are interested in the finite temperature partition function:

$$Z(T) = \int dE\, \rho(E)\, e^{-E/T} \,. \tag{1.3.5}$$

  In a $d = 2$ CFT the Cardy formula [9] determines the high temperature limit of the partition function and hence of the free energy:

$$\begin{aligned} Z(T) &\sim \exp\left[\frac{\pi c}{12} LT\right] \,, \\ F &= -\frac{\pi c}{12} LT^2 \,, \end{aligned} \tag{1.3.6}$$

  where $L$ is the system size. The asymptotic growth of the density of states is then read off:

$$\rho(E) \sim \exp\left[\sqrt{\frac{\pi c L E}{3}}\right] \,. \tag{1.3.7}$$

  The coefficient of the thermal free energy, or equivalently the asymptotic growth of the density of states was proposed to be a height function [10], but (1.3.4) fails even for the simple example of the $d = 3$ critical $O(N)$ model flowing to the Goldstone phase with $N - 1$ free bosons [11, 12].

- $c$ is the coefficient of the energy momentum tensor two-point function, but this coefficient is not monotonic either in $d = 3$ [13], or in $d = 4$ [14, 15].

- $c$ is also the coefficient of the trace anomaly

$$\langle T^a{}_a \rangle = -\frac{c}{24\pi} R \,. \tag{1.3.8}$$

Trace anomalies are present in even dimensions, but for $d > 2$ there are multiple independent anomaly coefficients:

$$\langle T^a{}_a \rangle = -2(-1)^{d/2} A E_d + \sum_i B_i I_i \ , \tag{1.3.9}$$

where $E_d$ is the Euler density, and $I_i$ are Weyl invariants. Note that for $d = 2$ the Euler density is $E_2 = R/4\pi$, there are no Weyl invariants, and $A = -c/12$.[11] More than twenty years ago, Cardy conjectured that $A$ obeys the analogue of the $c$-theorem [16]. Only very recently was it proven for $d = 4$ [17, 18].

- The universal logarithmic piece in the $S^d$ free energy of an even dimensional CFT is also related to $A$ by

$$\begin{aligned} F &= -\log Z_{S^d} \ , \\ \frac{dF}{d\log R} &= -\int_{S^d} \langle T^a{}_a \rangle = 4\,(-1)^{d/2}\, A \ , \end{aligned} \tag{1.3.11}$$

  where $R$ is the radius of the sphere. The universal logarithmic term in the $S^d$ free energy is equal to the negative of the universal terms in the entanglement entropy across $\Sigma = S^{d-2}$ [19]. Hence isolating the number of degrees of freedom for an even dimensional CFT from either of these quantities is equivalent.

- The last point suggests a generalization to odd dimensions: we should isolate universal terms in the $S^d$ free energy, or equivalently in the entanglement entropy across $\Sigma = S^{d-2}$.

Recent developments show that the most fruitful generalization to higher dimensions is through entanglement entropy. In addition to providing a measure for the number of degrees of freedom, a monotonic quantity imposes constraints on the space

[11] We normalize the Euler density so that $\int_{S^d} E_d = 2$. In $d = 4$ we use the convention

$$\langle T^a{}_a \rangle = -\frac{c_4}{16\pi^2} W_{abcd} W^{abcd} + 2a_4 E_4 \ , \tag{1.3.10}$$

with $W_{abcd}$ the Weyl tensor and $E_4 = \frac{1}{32\pi^2}\left(R_{abcd}R^{abcd} - 4R_{ab}R^{ab} + R^2\right)$ the Euler density.

of quantum field theories. We briefly discuss how such invaluable information can be used in applications in Sec. 1.4.5.

## 1.4 Entanglement entropy and the number of degrees of freedom

### 1.4.1 Relating entanglement entropy to the number of degrees of freedom

In Chapter 2 we focus on the behavior of $\mathcal{S}_d^{(\Sigma)}(R)$ in the vacuum, studying its possible connections to RG flows and the number of degrees of freedom along the flow. The material presented is based on [6]. In the discussion below (1.2.4), especially item (4) indicates that $\mathcal{S}_d^{(\Sigma)}(R)$ can be interpreted as characterizing entanglement correlations *at scale* $R$. Thus, in the continuum limit, as we vary $R$ from zero to infinity, $\mathcal{S}_d^{(\Sigma)}(R)$ can be interpreted as describing the RG flow of the REE from short to large distances. In contrast to the usual discussion of RG using some auxiliary mass or length scale, here we have the flow of a physical observable with real physical distances. Its derivative

$$R\frac{d\mathcal{S}_d^{(\Sigma)}(R)}{dR} \tag{1.4.1}$$

can then be interpreted as the "rate" of the flow. With the usual intuition that RG flow leads to a loss of short-distance degrees of freedom, it is natural to wonder whether it also leads to a loss of entanglement. In other words, *could* $\mathcal{S}_d^{(\Sigma)}(R)$ *also track the number of degrees of freedom of a system at scale* $R$*?* which would imply (1.4.1) should be negative, i.e. $\mathcal{S}_d^{(\Sigma)}(R)$ should be monotonically decreasing.

For $d = 2$,[12] a previous result of Casini and Huerta [20, 21] shows that $\mathcal{S}_2(R)$ is indeed monotonically decreasing for all Lorentz-invariant, unitary QFTs, which provides an alternative proof of Zamolodchikov's $c$-theorem [8]. We present the proof in Sec. 1.4.3.

[12]for which $\Sigma$ is given by two points and there is no need to have a superscript in $\mathcal{S}_2(R)$.

In higher dimensions, the shape of $\Sigma$ also matters. We argue in Sec. 2.5 that $\mathcal{S}_d^{(\text{sphere})}(R)$ has the best chance to be monotonic. At a fixed point, $\mathcal{S}_d^{(\text{sphere})}(R)$ reduces to the previously proposed central charge in all dimensions.[13] Its monotonicity would then establish the conjectured $c$-theorems [16,20,21,23–25] for each $d$. (For notational simplicity, from now on we will denote the corresponding quantities for a sphere simply as $S(R)$ and $\mathcal{S}_d(R)$ without the superscript.)

### 1.4.2 Calculating entanglement entropy and testing monotinicity

In Chapter 3 we test the monotonicity of $\mathcal{S}_3(R)$ and $\mathcal{S}_4(R)$ [6]. Entanglement entropy is extremely hard to calculate in a general field theory. One can provide a path integral definition of entanglement entropy through Rényi entropies, which themselves are important measures of entanglement properties of quantum states. They are defined as

$$S_n^{(\Sigma)} \equiv -\frac{1}{n-1} \log \operatorname{Tr} \rho^n \ . \tag{1.4.2}$$

The entanglement entropy can be obtained from them by analytic continuation in $n$:

$$\lim_{n\to 1} S_n^{(\Sigma)} = S^{(\Sigma)} \ . \tag{1.4.3}$$

The Rényi entropies can be obtained by the replica method; one has to calculate the path integral on an $n$-fold cover of $\mathbb{R}^d$ branched over $\Sigma$. The analytic continuation (1.4.3) is in general very hard and has only been performed in a few examples.

This situation leaves us with very few tractable examples:

- A massive free theory undergoes an RG flow from a massless free CFT to the empty theory. The tracing over the outside degrees of freedom can be performed explicitly, and the eigenvalues of the reduced density matrix can be obtained. For the $d = 3$ free scalar we perform this analysis is Chapter 3. The analogous

[13] That the entanglement entropy could provide a unified definition of central charge for all dimensions was recognized early on in [22] and was made more specific in [20,21] including proof of a holographic $c$-theorem.

test for a free massive fermion was performed in [26]. Another free theory that undergoes an RG flow in $d = 3$ is the compact $U(1)$ gauge theory; it flows from the non-compact Maxwell theory in the UV to a non-compact massless scalar in the IR.[14] The dimensionful gauge coupling constant is playing the role of the physical scale in this example. The entanglement entropy was obtained along this RG flow in [27].[15]

- As discussed above, for $\Sigma = S^{d-2}$ in a CFT one can map the problem to the calculation of the $S^d$ free energy. One can then use a variety of techniques to do the calculation. In Chapter 5 we use supersymmetric localization and matrix model techniques to calculate the entanglement entropy for $\mathcal{N} \geq 4$ gauge theories with classical gauge groups.

- In theories with holographic duals there is a very simple approach to calculating entanglement entropy. Holographic duality maps a large $N$ gauge theory in the 't Hooft limit to weakly interacting string theory on a weakly curved asymptotically $\mathrm{AdS}_{d+1} \times \mathcal{M}$ spacetime.[16] The field theory can be thought of as living on the boundary of $\mathrm{AdS}_{d+1}$, and the radial direction geometrizes the RG flow. The radial direction stands for the RG scale, and different radial slices encode the field theory degrees of freedom at different scales. In contradistinction to the other cases, entanglement entropy is easily calculated in these theories. In the gravitational description, we have to determine the area of the minimal surface anchored on the entangling surface $\Sigma$, giving

$$S = \frac{A_{\min}}{4G_N} , \tag{1.4.4}$$

where $G_N$ is the $d+1$-dimensional Newton's constant. We cannot resist to emphasize the elegance of this prescription and its profound connection to the

[14]The $d = 3$ $U(1)$ gauge theory is dual to the theory of a compact scalar, the two formulations are related by $*F = d\phi$.

[15]We note that for this example $\mathcal{S}_3 \to -\frac{1}{2}\log(g^2 R)$ for $R \to 0$, i.e. the REE diverges in the UV. The reason for this is that in the UV we do not have a CFT.

[16]The duality is believed to be exact for all $N$ and any coupling, but we will only use it in the limit, when the supergravity description of string theory is appropriate.

Bekenstein–Hawking black hole entropy.

Holography is a tailor-made approach to studying the monotonicity of REE along RG flows. The RG trajectory is encoded in the geometry, and one can study a family of examples. We devote most of Chapter 3 to this study. We find that $\mathcal{S}_3(R)$ is monotonic in all holographic examples, however some cases give non-monotonic $\mathcal{S}_4(R)$.

### 1.4.3 Monotonicity from strong subadditivity

Entanglement entropy obeys powerful inequalities. Let us take two geometric regions $A$ and $B$. The strong subadditivity property of entanglement entropy states that

$$S(A) + S(B) \geq S(A \cup B) + S(A \cap B) \ . \tag{1.4.5}$$

In $d = 2$, using only Lorentz invariance, unitarity, and that $\mathcal{S}_2(R)$ is finite for a renormalizable theory one can prove the entropic version of the $c$-theorem [20, 21]. We present the proof here to demonstrate how powerful (1.4.5) is, and to give a flavor of how the proof in the $d = 3$ case goes, which is based on the same minimal set of ingredients, but proceeds through a more elaborate geometric construction [28]. We note that these methods cannot establish the monotonicity of REE in higher dimensions, in accord with our findings about $\mathcal{S}_4(R)$.

Let us examine the spacetime diagram in Fig. 1-2. In a Lorentz-invariant theory the entanglement entropy is the property of the casual development[17] of a region. If we used time slices that were identical to the usual flat slices outside, but deviated from them inside the light cone (drawn by blue), the entanglement entropy associated to the inside part of the Cauchy surface would be the same, see Fig. 1-2a. Hence on Fig. 1-2b the regions $R$, $A \cup C$, $B \cup D$, and $A \cup r \cup D$ have the same entanglement entropy. [18]

[17] i.e. the union of the past and future light cone

[18] These regions have lightlike segments. A suitable limiting procedure is required to make the proof precise.

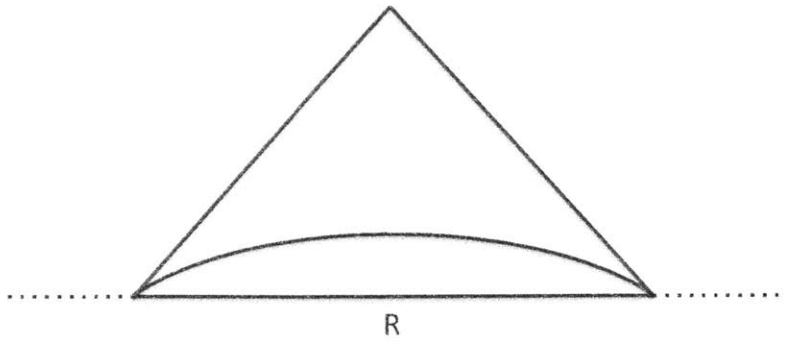


(a) In a Lorentz invariant theory entanglement entropy is the property of the casual development; using either of the time slices in the inside region, we get the same result for the entanglement entropy.

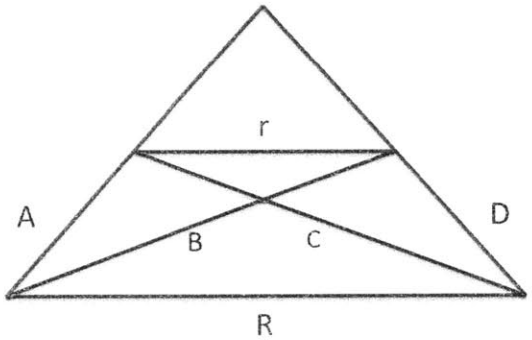


(b) The future light cone of $R$ and the intervals we need for the proof.

Figure 1-2: Spacetime diagram for the proof of the entropic $c$-theorem.

As the vacuum of the theory is Lorentz-invariant, the entanglement entropy of an interval can only depend on its invariant length. Then we can write:

$$\begin{aligned}
2S(B) &= S(B) + S(C) && B \text{ and } C \text{ have equal invariant length,} \\
&= S(A \cup r) + S(r \cup D) && B\,(C) \text{ has the same casual development} \\
& && \text{as } A \cup r\,(r \cup D), \qquad (1.4.6) \\
&\geq S(A \cup r \cup D) + S(r) && \text{strong subadditivity (1.4.5),} \\
&= S(R) + S(r) && A \cup r \cup D \text{ has the same casual development as } R.
\end{aligned}$$

Using the names of the intervals to denote their invariant length, we have $B = \sqrt{rR}$.

Taking $r = R - \epsilon$ and expanding to second order in $\epsilon$ we obtain:

$$0 \geq RS''(R) + S'(R) = \frac{d\mathcal{S}_2(R)}{dR} \ . \tag{1.4.7}$$

This completes the proof.

### 1.4.4 Behavior in the vicinity of fixed points

In Chapter 4, based on [6, 29], we investigate the behavior of REE across $\Sigma = S^{d-2}$ in the vicinity of conformal fixed points in the framework of holography. For a (UV) fixed point perturbed by a relevant operator of dimension $\Delta < d$, we find that

$$\mathcal{S}_d(R) = s_d^{(\mathrm{UV})} - A(\Delta)(\mu R)^{2(d-\Delta)} + \cdots \ , \quad R \to 0 \tag{1.4.8}$$

where $\mu$ is a mass scale with the relevant (dimensional) coupling given by $g = \mu^{d-\Delta}$, and $A(\Delta)$ is some *positive* constant.

Based on REE, one can introduce an "entropic function" on coupling space, by trading the $R$ dependence along a trajectory for the dependence on the coupling constants. Then (1.4.8) leads to an entropic function given by

$$\mathcal{C}_d(g) = s_d^{(\mathrm{UV})} - A(\Delta) g_{eff}^2(\Lambda), \qquad \Lambda \to \infty \tag{1.4.9}$$

where $g_{eff}(\Lambda) = g\Lambda^{\Delta-d}$ is the effective dimensionless coupling at scale $\Lambda$. Equation (1.4.9) has a simple interpretation that the leading UV behavior of the entropic function is controlled by the two-point correlation function of the corresponding relevant operator, and we would expect (1.4.9) to be valid universally. Curiousy, low dimensional free theories defy this expectation [30–33]. It is an outstanding challange to determine a formula valid for all field theories.

Near an IR fixed point, we find that the large $R$ behavior of $\mathcal{S}(R)$ has the form

$$\mathcal{S}_d(R) \ = \ s_d^{(\mathrm{IR})} + \frac{B(\tilde{\Delta})}{(\tilde{\mu}R)^{2(\tilde{\Delta}-d)}} + \cdots$$

$$+\begin{cases} \frac{s_1}{\tilde{\mu}R}+\frac{s_3}{(\tilde{\mu}R)^3}+\cdots & \text{odd } d \\ \frac{s_2}{(\tilde{\mu}R)^2}+\frac{s_4}{(\tilde{\mu}R)^4}+\cdots & \text{even } d \end{cases}, \quad R\to\infty\,, \tag{1.4.10}$$

where $\tilde{\Delta} > d$ is the dimension of the leading irrelevant operator, $\tilde{\mu}$ is a mass scale characterizing the irrelevant perturbation, and $B(\tilde{\Delta})$ is a constant. The first line, similar to (4.1.4), has a natural interpretation in terms of conformal perturbations of the IR fixed point. The coefficient $B(\tilde{\Delta})$ is expected to depend only on physics of the IR fixed point. In terms of irrelevant coupling $\tilde{g} = \tilde{\mu}^{d-\Delta}$ corresponding to the leading irrelevant operator, equation (4.1.8) leads to

$$\begin{aligned} \mathcal{C}(\Lambda) &= s_d^{(\mathrm{IR})} + B(\tilde{\Delta})\tilde{g}_{eff}^2(\Lambda)+\cdots \\ &\quad + \begin{cases} s_1\tilde{g}_{eff}^{\frac{1}{\tilde{\Delta}-d}}(\Lambda)+\cdots & \text{odd } d \\ s_2\tilde{g}_{eff}^{\frac{2}{\tilde{\Delta}-d}}(\Lambda)+\cdots & \text{even } d \end{cases}, \quad \Lambda\to 0\,, \end{aligned} \tag{1.4.11}$$

where $\tilde{g}_{eff}(\Lambda) = \tilde{g}\Lambda^{\tilde{\Delta}-d}$ is the effective dimensionless coupling at scale $\Lambda$. It is amusing that the "analytic" contributions in $1/R$ in (1.4.10) lead to non-analytic dependence on the coupling while non-analytic contributions in $1/R$ lead to analytic dependence on the coupling. Note the first line dominates for

$$\tilde{\Delta} < \begin{cases} d+\frac{1}{2} & \text{odd } d \\ d+1 & \text{even } d \end{cases} \tag{1.4.12}$$

i.e. if the leading irrelevant operator is not too irrelevant. Note in this range $B(\tilde{\Delta}) > 0$. The second line of (1.4.10)-(1.4.11) can be expected from a geometric expansion. As discussed in Chapter 2 the contributions of any degrees of freedom at some lengths scale $\ell \ll R$ should be packaged into terms that come with integer powers of $R$. Thus the coefficients $s_n$ are expected to depend on the RG trajectory from the cutoff scale $\delta$ to $R$.[19]

[19]Since here we consider the $R\to\infty$ limit $s_n$ should thus depend on the full RG trajectory from $\delta$ to $\infty$.

### 1.4.5 Applications

For a strongly interacting systems obtaining the effective long distance description in general involves guesswork. We base our considerations on symmetry, various expansions, and approximation schemes. Non-perturbative results are a valuable aid in the quest of obtaining the correct description. The established monotonicity property of REE in $d = 2, 3$ together with the $a$-theorem in $d = 4$ gives us such a tool. We do not discuss in detail how one can apply these abstract results to concrete physical systems, we only mention the most recent application of entanglement monotonicity to the question of confinement in $d = 3$ gauge theories. For example, we can conclude that QED with $N_f \geq 12$ fermion flavors has to deconfine [34,35], and detailed analysis of the dynamics reveals that $N_f = 12$ is indeed the smallest number of fermions that deconfines the theory [35].

In Chapter 5, based on [36], we discuss another application: calculating entanglement entropy in M2-brane theories enables us to count the number of degrees of freedom in these supersymmetric CFTs. Applying the holographic correspondence to the worldvolume theory of $N$ M2-branes, we obtain that in the large $N$ limit the number of degrees of freedom scales as $N^{3/2}$. It was a longstanding challenge to reproduce this result from field theory considerations. The number of degrees of freedom in vector like theories scales as $N$, while for matrix large $N$ theories as $N^2$. The peculiar $N^{3/2}$ behavior hence cannot be reproduced by either of these, and is a strong coupling phenomenon. Recent advances in supersymmetric field theories allow us to determine the $S^3$ free energy [37], which as discussed above is equal to the entanglement entropy across $S^1$.

## 1.5 Plan of the thesis

Above we introduced the main thread of the thesis. We aimed at presenting the main ideas, and glossed over many important details. In this section we list the topics discussed in the following chapters of the thesis.

In Chapter 2 we introduce the REE and elucidate its properties. The chapter is

based on [6]. Firstly, we argue for the divergence structure of entanglement entropy. Secondly, we show that REE, which is obtained from entanglement entropy by acting with the differential operator (1.2.4), is well-defined in the continuum limit. Thirdly, we show how it interpolates between UV and IR fixed points, and speculate about its relation to the number of degrees of freedom at a given scale. Our main focus is the vacuum state of quantum field theories, but having defined a cutoff insensitive quantity, we can use scaling arguments to learn about its behavior in systems at finite temperature and chemical potential. We also obtain REE, and hence entanglement entropy, for systems with a Fermi surface including non-Fermi liquids.

In Chapter 3 we explore the monotonicity properties of REE through examples. The chapter is based on [6]. We analyze free field theories, and theories with a gravitational dual. For the latter category we develop effective calculational techniques that determine REE in terms of asymptotic data of the minimal surface. For closely separated fixed points we prove that REE decreases along the RG flow. We study a variety of examples numerically and conclude with a conjecture: $\mathcal{S}_3$ decreases under RG flow.[20] However, we find that $\mathcal{S}_4$ is neither monotonic, nor positive in general. We also observe "phase transitions" in REE, which could encode information about the reorganization of the degrees of freedom at a scale.

In Chapter 4 we study the behavior of REE near fixed points in the framework of holography. The chapter is based on [6, 29]. We discuss how REE can be translated into an entropic function on coupling space. We concentrate on spherical entangling regions. The case of UV fixed points is treated in perturbation theory in a straightforward way. The study of IR behavior is considerably more difficult; we use separate expansions in the UV and IR regions of the geometry, and match them in an intermediate matching region. We provide an exhaustive list of possible IR behaviors, and determine the first few terms in the long distance expansion of REE. The techniques developed are powerful enough to discuss entanglement entropy of arbitrary shapes in a thermal state; we show that the leading piece in the long distance expansion is always equal to the thermal entropy.

[20] The conjecture was subsequently proven in [28], as discussed above.

In Chapter 5 we calculate the entanglement entropy of $d = 3$ $\mathcal{N} \geq 4$ supersymmetric CFTs, the IR limits of gauge theories with $U(N)$, $O(N)$, and $USp(2N)$ gauge groups and matter hypermultiplets in the fundamental and two-index tensor representations. The chapter is based on [36]. We present the brane construction, the Coulomb branch of moduli space, and the gravity dual of these theories. Supersymmetric localization reduces the computation of REE to a matrix model that we solve in the large $N$ limit using two different methods. The first method is a saddle point approximation first introduced in [38], which we extend to next-to-leading order in $1/N$. The second method generalizes the Fermi gas approach of [1] to theories with symplectic and orthogonal gauge groups, and yields an expression for the REE valid to all orders in $1/N$. In developing the second method, we use a non-trivial generalization of the Cauchy determinant formula.

# Chapter 2

# A refinement of entanglement entropy and the number of degrees of freedom

## 2.1 Introduction

In this chapter, we introduce a "renormalized entanglement entropy" which is intrinsically UV finite and is most sensitive to the degrees of freedom at the scale of the size $R$ of the entangled region. We illustrated the power of this construction by showing that the qualitative behavior of the entanglement entropy for a non-Fermi liquid can be obtained by simple dimensional analysis. We argue that the functional dependence of the "renormalized entanglement entropy" on $R$ can be interpreted as describing the renormalization group flow of the entanglement entropy with distance scale. The corresponding quantity for a spherical region in the vacuum, has some particularly interesting properties. For a conformal field theory, it reduces to the previously proposed central charge in all dimensions, and for a general quantum field theory, it interpolates between the central charges of the UV and IR fixed points as $R$ is varied from zero to infinity.

## 2.2 A refinement of entanglement entropy

In our discussion below we will assume that the system under consideration is equipped with a *bare* short-distance cutoff $\delta_0$, which is much smaller than all other physical scales of the system. The continuum limit is obtained by taking $\delta_0 \to 0$ while keeping other scales fixed. The entanglement entropy for a spatial region is *not* a well-defined observable in the continuum limit as it diverges in the $\delta_0 \to 0$ limit. The common practice is to subtract the UV divergent part by hand, a procedure which is often ambiguous. The goal of this section is to introduce a refinement of the entanglement entropy which is not only UV finite, but also is most sensitive to the entanglement correlations at the scale of the size of the entangled region.

### 2.2.1 Structure of divergences in entanglement entropy

In this subsection we consider the structure of divergent terms in the entanglement entropy. We assume that the theory lives in flat $\mathbb{R}^{1,d-1}$ and is rotationally invariant. The discussion below is motivated from that in [39] which considers the general structure of local contributions to entanglement entropy in a gapped phase.[1] We will mostly consider the vacuum state and will comment on the thermal (and finite chemical) state at the end.

Let us denote the divergent part of the entanglement entropy for a region enclosed by a surface $\Sigma$ as $S_{\rm div}^{(\Sigma)}$. Then $S_{\rm div}^{(\Sigma)}$ should only depend on *local* physics at the cutoff scale near the entangling surface. For a smooth $\Sigma$, one then expects that $S_{\rm div}^{(\Sigma)}$ should be expressible in terms of local geometric invariants of $\Sigma$, i.e.

$$S_{\rm div}^{(\Sigma)} = \int_\Sigma d^{d-2}\sigma \sqrt{h} F(K_{ab}, h_{ab}) \ , \tag{2.2.1}$$

where $\sigma$ denotes coordinates on $\Sigma$, $F$ is a sum of all possible local geometric invariants formed from the induced metric $h_{ab}$ and extrinsic curvature $K_{ab}$ of $\Sigma$. Note that here we are considering a surface embedded in flat space, all intrinsic curvatures and their

[1] We thank Tarun Grover for discussions.

derivatives can be expressed in terms of $K_{ab}$ and its tangential derivatives, thus all geometric invariants can be expressed in terms of the extrinsic curvature and its tangential derivatives. The proposal (2.2.1) is natural as $S_{\rm div}^{(\Sigma)}$ should not depend on the spacetime geometry away from the surface nor how we parametrize the surface. Thus when the geometry is smooth, the right hand side is the only thing one could get after integrating out the short-distance degrees of freedom. In particular, the normal derivatives of $K_{ab}$ cannot appear as they depend on how we extend $\Sigma$ into a family of surfaces, so is not intrinsically defined for the surface itself.

Here we are considering a pure spatial entangled region in a flat spacetime, for which the extrinsic curvature in the time direction is identically zero. Thus in (2.2.1) we only have $K_{ab}$ for the spatial normal direction. In more general situations, say if the region is not on a spatial hypersurface or in a more general spacetime, then $\Sigma$ should be considered as a co-dimensional two surface in the full spacetime and in (2.2.1) we will have $K_{ab}^{\alpha}$ with $\alpha$ running over two normal directions.

Given (2.2.1), now an important point is that in the vacuum (or any pure state),

$$S^{(\Sigma)} = S^{(\bar{\Sigma})} \tag{2.2.2}$$

where $S^{(\bar{\Sigma})}$ denotes the entanglement entropy for the region outside $\Sigma$, and in particular

$$S_{\rm div}^{(\Sigma)} = S_{\rm div}^{(\bar{\Sigma})} \ . \tag{2.2.3}$$

Recall that $K_{ab}$ is defined as the normal derivative of the induced metric and is odd under changing the orientation of $\Sigma$, i.e., in $S_{\rm div}^{(\bar{\Sigma})}$ it enters with an opposite sign. Thus (2.2.1) and (2.2.3) imply that $F$ should be an *even* function of $K_{ab}$. In a Lorentz invariant theory, there is also an alternative argument[2] which does not use (2.2.2) or (2.2.3). Consider a more general situation with both $K_{ab}^{\alpha}$ as mentioned above. The $\alpha$ index has to be contracted which implies that $F$ must be even in $K_{ab}^{\alpha}$. Then for a purely spatial surface we can just set the time component of $K_{ab}^{\alpha}$ to zero, and $F$ is still even for the remaining $K_{ab}$.

[2]We thank R. Myers for pointing this out to us.

As a result one can show that for a *smooth* and *scalable* surface $\Sigma$ of size $R$, the divergent terms can only contain the following dependence on $R$

$$S_{\rm div}^{(\Sigma)} = a_1 R^{d-2} + a_2 R^{d-4} + \cdots \ . \tag{2.2.4}$$

See Appendix 2.A for a precise definition of scalable surfaces. Heuristically speaking, these are surfaces whose shape does not change with their size $R$, i.e. they are specified by a *single* dimensional parameter $R$ plus possible other dimensionless parameters describing the shape. For such a surface, one can readily show that various quantities scale with $R$ as (see Appendix 2.A for more details)

$$h_{ab} \sim R^2, \qquad K_{ab} \sim R, \qquad D_a \sim R^0 \tag{2.2.5}$$

where $D_a$ denotes covariant derivative on the surface. As a result, any fully contracted quantity which is even in $K$, such as $F$ in (2.2.1), can only give rise to terms proportional to $R^{-2n}$ with $n$ a non-negative integer, which then leads to (2.2.4). Below we restrict our discussion to scalable surfaces.

Now let us consider a scale invariant theory in the vacuum. On dimensional ground, the only other scale can appear in (2.2.4) is the short-distance cutoff $\delta_0$. We should then have

$$a_1 \sim \frac{1}{\delta_0^{d-2}}, \qquad a_2 \sim \frac{1}{\delta_0^{d-4}}, \cdots \tag{2.2.6}$$

and so on. For odd $d$, the $O(R^0)$ term is not among those in (2.2.4) and thus should be finite. For even $d$, there can be a $\log \delta_0$ term at the order $O(R^0)$ and should come with $\log \frac{R}{\delta_0}$ in order to have to the right dimension. We thus conclude that for a scale invariant theory, the entanglement entropy across a scalable surface $\Sigma$ in the vacuum should have the form

$$S^{(\Sigma)} = \begin{cases} \frac{R^{d-2}}{\delta_0^{d-2}} + \cdots + \frac{R}{\delta_0} + (-1)^{\frac{d-1}{2}} s_d^{(\Sigma)} + \frac{\delta_0}{R} + \cdots & \text{odd d} \\ \frac{R^{d-2}}{\delta_0^{d-2}} + \cdots + \frac{R^2}{\delta_0^2} + (-1)^{\frac{d-2}{2}} s_d^{(\Sigma)} \log \frac{R}{\delta_0} + \text{const} + \frac{\delta_0^2}{R^2} + \cdots & \text{even d} \end{cases} \tag{2.2.7}$$

where for notational simplicity we have suppressed the coefficients of non-universal

terms. It is important to emphasize that $S$ does not contain any divergent terms with negative powers of $R$ in the limit $\delta_0 \to 0$. The form (2.2.7) was first predicted from holographic calculations in [22] for CFTs with a gravity dual. $s_d^{(\Sigma)}$ is an $R$-independent constant which gives the universal part of the entanglement entropy. The sign factors before $s_d^{(\Sigma)}$ in (2.2.7) are chosen for later convenience. As indicated by the superscript, $s_d^{(\Sigma)}$ in general depends on the shape of the surface.

For a general QFT, there could be other mass scales, which we will denote collectively as $\mu$. Now the coefficients $a_i$ in (2.2.4) can also depend on $\mu$, e.g., we can write $a_1$ as

$$a_1 = \frac{1}{\delta_0^{d-2}} h_1(\mu\delta_0) \tag{2.2.8}$$

and similarly for other coefficients. Note that by definition of $\delta_0$, we always have $\mu\delta_0 \ll 1$ and $h_1$ can be expanded in a power series of $\mu\delta_0$. Now for a renormalizable theory, the dependence on $\mu$ must come with a non-negative power, as when taking $\mu\delta_0 \to 0$, $a_1$ should not be singular and should recover the behavior of the UV fixed point. In other words, for a renormalizable theory, the scale(s) $\mu$ arises from some relevant operator at the UV fixed point, which implies that $\mu\delta_0$ should always come with a non-negative power in the limit $\mu\delta_0 \to 0$. This implies that the UV divergences of $a_i$ should be no worse than those in (2.2.6). In particular, there cannot be divergent terms with negative powers of $R$ for even $d$, and for odd $d$ the divergence should stop at order $O(R)$. These expectations will be confirmed by our study of holographic systems in Sec. 3.3.4 and 3.3.5 (see e.g. (3.3.41)), where we will find that $h_1(\mu\delta_0)$ has the expansion $h_1(\mu\delta_0) = c_0 + c_2(\mu\delta_0)^{2\alpha} + c_3(\mu\delta_0)^{3\alpha} + \cdots$, where $\alpha = d - \Delta$ with $\Delta$ the UV dimension of the leading relevant perturbation at the UV fixed point.

So far we have been considering the vacuum. The discussion of the structure of divergences should work also for systems at finite temperature or finite chemical potential. In such a mixed state, while (2.2.2) no longer holds, equation (2.2.3) should still apply as the short-distance physics should be insensitive to the presence of temperature or chemical potential. Also recall that for a Lorentz invariant system, there is an alternative argument for (2.2.4) which does not use (2.2.3).

### 2.2.2 Properties of $\mathcal{S}^{(\Sigma)}(R)$

Given the structure of divergent terms in $S^{(\Sigma)}(R)$ discussed in the previous subsection, one can then readily check that when acting on $S^{(\Sigma)}(R)$ with the differential operator in (1.2.4), all the UV divergent terms disappear and the resulting $\mathcal{S}_d^{(\Sigma)}(R)$ is finite in the continuum limit $\delta_0 \to 0$. In fact, what the differential operator does is to eliminate any term (including finite ones) in $S^{(\Sigma)}(R)$ which has the same $R$-dependence as the terms in (2.2.4). We believe, for the purpose of extracting long range correlations, it is sensible to also eliminate possible finite terms with the same $R$-dependence, as they are "contaminated" by short-distance correlations. In particular, in the continuum limit this makes $\mathcal{S}_d^{(\Sigma)}(R)$ invariant under any redefinitions of the UV cutoff $\delta_0$ which do not involve $R$.[3] With a finite $\delta_0$, $\mathcal{S}_d^{(\Sigma)}(R)$ does depend on $\delta_0$, but only very weakly, through inverses powers of $\frac{\delta_0}{R}$. This will be important in our discussion below.

In the rest of this section we show that the resulting $\mathcal{S}_d^{(\Sigma)}(R)$ is not only UV finite, but also have various desirable features. In this subsection we discuss its behavior in the vacuum, while in Sec. 2.2.3 discuss its properties at a finite temperature and chemical potential.

For a scale invariant theory, from (2.2.7) we find that for all $d$

$$\mathcal{S}_d^{(\Sigma)}(R) = s_d^{(\Sigma)} \tag{2.2.9}$$

is $R$-independent. The sign factors in (2.2.7) were chosen so that there is no sign factor in (2.2.9). Note that if we make a cutoff redefinition of the form $\delta_0 \to \delta_0 \left(1 + c_1 \mu \delta_0 + c_2 (\mu \delta_0)^2 + \cdots\right)$ where $\mu$ is some mass scale, for odd $d$ the UV finite term in (2.2.7) is modified. But $\mathcal{S}_d^{(\Sigma)}(R)$, and $s_d^{(\Sigma)}$ as defined from (2.2.9), is independent of this redefinition.

Let us now look at properties of $\mathcal{S}_d^{(\Sigma)}(R)$ for a general renormalizable QFT (i.e. with a well-defined UV fixed point). Below we will find it convenient to introduce a floating cutoff $\delta$, which we can adjust depending on scales of interests. At the new

[3]Since $R$ is the scale at which we probe the system, reparameterizations of the short-distance cutoff should not involve $R$.

cutoff $\delta$, the system is described by the Wilsonian effective action $I_{eff}(\delta;\delta_0)$, which is obtained by integrating out degrees of freedom from the bare cutoff $\delta_0$ to $\delta$. The entanglement entropy $S^{(\Sigma)}(R;\delta_0,\delta)$ calculated from $I_{eff}(\delta;\delta_0)$ with cutoff $\delta$ should be independent of choice of $\delta$. So should the resulting $\mathcal{S}_d^{(\Sigma)}(R)$. Below we will consider the continuum limit, i.e. with bare cutoff $\delta_0 \to 0$.

First consider the small $R$ limit, i.e. $R$ is much smaller than any other length scale of the system. Clearly as $R \to 0$, these other scales should not affect $S^{(\Sigma)}(R)$, which should be given by its expression at the UV fixed point. Accordingly, $\mathcal{S}_d^{(\Sigma)}(R)$ also reduces to that of the UV fixed point, i.e.

$$\mathcal{S}_d^{(\Sigma)}(R) \to s_d^{(\Sigma,\mathrm{UV})}, \quad R \to 0\ . \tag{2.2.10}$$

As we will see in Sec. 4.1.1, studies of holographic systems (with $\Sigma$ given by a sphere) predict that the leading small $R$ correction to (2.2.10) is given by

$$\mathcal{S}_d^{(\Sigma)}(R) = s_d^{(\Sigma,\mathrm{UV})} + O((\mu R)^{2\alpha}) \quad R \to 0 \tag{2.2.11}$$

where $\alpha = d - \Delta$ with $\Delta < d$ the UV dimension of the leading relevant scalar perturbation. Equation (2.2.11) has a simple interpretation that the leading contribution from a relevant operator comes at two-point level. We believe it can be derived in general, but will not pursue it here.

The story is more tricky in the large $R$ limit, as all degrees of freedom at scales between the bare UV cutoff $\delta_0$ and $R$ could contribute to the entanglement entropy $S^{(\Sigma)}(R)$ in this regime. Nevertheless, one can argue that

$$\mathcal{S}_d^{(\Sigma)}(R) \to s_d^{(\Sigma,\mathrm{IR})}, \quad R \to \infty \tag{2.2.12}$$

as follows. When $R$ becomes much larger than all other length scales of the system, we can choose a floating cutoff $\delta$ to be also much larger than all length scales of the

system while still much smaller than $R$, i.e.

$$\frac{1}{\mu_1}, \frac{1}{\mu_2}, \cdots \ll \delta \ll R \tag{2.2.13}$$

where $\mu_i, i = 1, 2, \cdots$ denote possible mass parameters of the system. Now the physics between $\delta$ and $R$ is controlled by the IR fixed point, i.e. we should be able to write $S^{(\Sigma)}(R)$ again as (2.2.7), but with $\delta_0$ replaced by $\delta$, and $s_d^{(\Sigma)}$ by $s_d^{(\Sigma,\mathrm{IR})}$. Then equation (2.2.12) immediately follows. In other words, while in terms of the bare cutoff $\delta_0$, the entanglement entropy $S^{(\Sigma)}(R) = S^{(\Sigma)}(\delta_0, R, \mu_1, \mu_2, \cdots)$ could be very complicated in the large $R$ regime, involving many different scales, there must exist a redefinition of short-distance cutoff $\delta_{\mathrm{IR}} = \delta_{\mathrm{IR}}(\delta, \mu_1, \mu_2, \cdots)$, in terms of which $S^{(\Sigma)}(R)$ reduces to the standard form (2.2.7) with $\delta$ replaced by $\delta_{\mathrm{IR}}$, and $s_d^{(\Sigma)}$ by $s_d^{(\Sigma,\mathrm{IR})}$. In fact, higher order terms in (2.2.7) with negative powers of $R$ also imply that generically we should expect the leading large $R$ corrections to (2.2.12) to have the form

$$\mathcal{S}_d^{(\Sigma)}(R) = s_d^{(\Sigma,\mathrm{IR})} + \begin{cases} O(\frac{1}{R}) & \text{odd d} \\ O(\frac{1}{R^2}) & \text{even d} \end{cases}, \quad R \to \infty \,. \tag{2.2.14}$$

This expectation is supported by theories of free massive scalar and Dirac fields as we will see in Sec. 3.2, and by holographic systems as we will see in Sec. 4.1.1. Holographic systems also predict an exception to (2.2.14) which happens when the flow away from the IR fixed point toward UV is generated by an irrelevant operator with IR dimension $\Delta_{\mathrm{IR}}$ sufficiently close to $d$, for which we have instead (see Sec. 4.1.1)[4]

$$\mathcal{S}_d^{(\Sigma)}(R) = s_d^{(\Sigma,\mathrm{IR})} + O\left(\frac{1}{(\tilde{\mu}R)^{2\tilde{\alpha}}}\right), \quad \text{for} \begin{cases} \tilde{\alpha} < \frac{1}{2} & \text{odd d} \\ \tilde{\alpha} < 1 & \text{even d} \end{cases}, \quad R \to \infty \,, \tag{2.2.15}$$

where $\tilde{\alpha} = \Delta_{\mathrm{IR}} - d$.

By adjusting the floating cutoff $\delta$, one can also argue that $\mathcal{S}_d^{(\Sigma)}(R)$ should be

[4]The expression below is derived in Sec. 4.1.1 for $\Sigma$ given by a sphere and closely separated UV/IR fixed points. We believe the result should be more general, applicable to generic systems and smooth $\Sigma$, but will not pursue a general proof here.

most sensitive to contributions from degrees of freedom around $R$. Consider e.g. a length scale $L_1$ which is much smaller than $R$. In computing $S^{(\Sigma)}(R)$, we can choose a floating short-distance cutoff $\delta$ which satisfies

$$L_1 \ll \delta \ll R \ . \tag{2.2.16}$$

As discussed at the beginning of this subsection, by design $\mathcal{S}_d^{(\Sigma)}(R)$ is insensitive to short-distance cutoff $\delta$ when $\delta \ll R$.[5] We thus conclude that $\mathcal{S}_d^{(\Sigma)}(R)$ should be insensitive to contributions of from d.o.f around $L_1$.

While our above discussion around and after (2.2.12) assumes a conformal IR fixed point, the discussion also applies to when the IR fixed point is a gapped phase, where there are some differences depending on the spacetime dimension. For odd $d$, using $d = 3$ as an illustration, the entanglement entropy for a smooth surface $\Sigma$ in a gapped phase has the form (see e.g. also [39])

$$S^{(\Sigma)}(R) = \alpha R - \gamma + O(R^{-1}) \tag{2.2.17}$$

where $\gamma$ is the topological entanglement entropy [40,41] . We then have

$$\mathcal{S}_3^{(\Sigma)}(R) \to \gamma, \qquad R \to \infty \ . \tag{2.2.18}$$

In gapped phases without topological order, $\gamma = 0$. Thus a nonzero $\mathcal{S}_3^{(\Sigma)}(R \to \infty)$ signals the system has long range entanglement, i.e. the system is either gapless or topological-ordered in the IR. The two cases can be distinguished in that for a topological ordered phase $\gamma$ should be shape-independent, but in a gapless case, $s_3^{(\Sigma,\mathrm{IR})}$ in (2.2.10) is shape-dependent.

For even $d$, in a gapped phase we expect that $S^{(\Sigma)}(R)$ does not have a term

[5] Of course ultimately as mentioned earlier $\mathcal{S}_d^{(\Sigma)}(R)$ should be independent of choice $\delta$, when one includes all possible dependence on $\delta$ including those in coupling constants. Here we are emphasizing that even explicit dependence on $\delta$ should be suppressed by negative powers of $\frac{\delta}{R}$.

proportional to $\log R$ for large $R$, and thus we should have

$$\mathcal{S}_{2n}^{(\Sigma)}(R) \to 0, \quad R \to \infty, \qquad n = 1, 2, \cdots . \tag{2.2.19}$$

Nevertheless, it has been argued in [39] that the size-independent part of the entanglement entropy contains topological entanglement entropy. Such a topological term could not be captured by $\mathcal{S}_d^{(\Sigma)}(R)$, as all terms in (1.2.4) contain derivatives with respect to $R$ for even $d$. This is not surprising, as in even $d$, the $R$-independent part of the entanglement entropy also contains a finite non-universal local part, as is clear from the discussion around (2.2.4). Thus it is not possible to separate the topological from the non-universal contribution using a single connected entangling surface, and one has to resort to constructions like those in [40, 41] to consider combination of certain regions in such a way that the local part cancels while the topological part remains [39].

### 2.2.3 Finite temperature and chemical potential

As discussed at the end of Sec. 2.2.1, we expect $\mathcal{S}_d^{(\Sigma)}(R)$ should also be UV finite in the continuum limit at a finite temperature or chemical potential. Here we briefly discuss its properties, and for simplicity will restrict to a scale invariant theory.[6]

For a scale invariant system at a finite temperature $T$, since there is no other scale in the system, $\mathcal{S}_d^{(\Sigma)}(R, T)$ must have a scaling form, i.e.

$$\mathcal{S}_d^{(\Sigma)}(R, T) = \mathcal{S}_d^{(\Sigma)}(RT) . \tag{2.2.20}$$

In particular, in the high temperature limit, i.e. $RT \gg 1$ it must be dominated by thermal entropy at leading order, while in the low temperature limit $RT \to 0$, it should reduce to $s_d^{(\Sigma)}$. For a scale invariant theory, the thermal entropy has the form $S_d^{\rm Th} = \eta_d T^{d-1} V_\Sigma \sim (TR)^{d-1}$, where $V_\Sigma$ is volume of the spatial region enclosed by $\Sigma$

[6] See also [42] regarding scaling behavior of the entanglement entropy at finite $T$. In ref. [42] considered the entanglement entropy itself with UV part subtracted manually.

and $\eta_d$ is some constant. Thus we should have

$$\mathcal{S}_d^{(\Sigma)}(RT) \to \begin{cases} S_d^{\rm Th} & \text{odd d} \\ \frac{(d-1)!!}{(d-2)!!} S_d^{\rm Th} & \text{even d} \end{cases}, \quad RT \to \infty \ . \tag{2.2.21}$$

More explicitly, for $d = 3$ we expect when $RT \gg 1$,

$$\mathcal{S}_d^{(\Sigma)}(RT) = \eta_d T^2 V_\Sigma + c_d^{(\Sigma)} + \cdots \tag{2.2.22}$$

where the first term is simply the thermal entropy, $\cdots$ denotes terms with negative powers of $RT$. The second term $c_d^{(\Sigma)}$ is a constant. It would be interesting to compute this constant for some explicitly examples to see whether some physical interpretation (or significance) can be attached to it.

Similarly, with a nonzero chemical potential $\mu$, as a generalization of (2.2.20) we expect that

$$\mathcal{S}_d^{(\Sigma)}(R, \mu, T) = \mathcal{S}_d^{(\Sigma)}\left(\frac{T}{\mu}, RT\right) \ . \tag{2.2.23}$$

## 2.3 Entanglement entropy of a (non)-Fermi liquid

In this section we show that the entanglement entropy of a (non)-Fermi liquids can be obtained by simple dimensional analysis.[7] Consider a $d$-dimensional system of a finite fermions density whose ground state is described by a Fermi surface of radius $k_F$. We have in mind a Fermi liquid, or a non-Fermi liquid described by the Fermi surface coupled to some gapless bosons (as e.g. in [47]). In either case, the low energy dynamics of the system involves fermionic excitations locally in momentum space near the Fermi surface, and different patches of the Fermi surface whose velocities are not parallel or anti-parallel to each other essentially decouple. In particular, $k_F$ drops out of the low energy effective action. In this picture the number of independent degrees of freedom is proportional to the area of the Fermi surface $A_{FS} \propto k_F^{d-2}$, which can be

[7] See also a recent discussion in [42] based on finite temperature scaling and crossover. See also [43–46] for recent discussion of logarithmic enhancement of holographic "non-Fermi liquids."

considered as the "volume" of the available phase space. We thus expect in the large $R$ limit, the "renormalized entanglement entropy" $\mathcal{S}_d^{(\Sigma)}(R)$ should be proportional to the area of the Fermi surface $A_{FS}$. Since there is no other scale in the system than $R$, $\mathcal{S}_d^{(\Sigma)}(R)$ should then have the form

$$\mathcal{S}_d^{(\Sigma)}(R) \propto k_F^{d-2} R^{d-2} \propto A_{FS} A_\Sigma, \qquad R \to \infty \,. \tag{2.3.1}$$

where $A_\Sigma$ denotes the area of the entangling surface $\Sigma$. In other words, our "renormalized entanglement entropy" should satisfy an "area law." Using (1.2.4) one can readily see that the area law (2.3.1) translates into the well-known *area law violating* behavior in the original entanglement entropy [48,49] (see also [50])

$$S^\Sigma(R) \propto k_F^{d-2} R^{d-2} \log(k_F R) + \cdots \propto A_{FS} A_\Sigma \log(A_{FS} A_\Sigma) + \cdots \,, \tag{2.3.2}$$

where $k_F$ in the logarithm is added on dimensional ground and $\cdots$ denotes other non-universal parts. We note that this result does not depend on whether the Fermi surface has quasi-particles or not, i.e. whether it is a Fermi or non-Fermi liquid, only depends on the expectation that $\mathcal{S}_d^{(\Sigma)}(R)$ is proportional to the area of the Fermi surface.

This analysis can also be immediately generalized to predict the qualitative behavior of the entanglement entropy of higher co-dimensional Fermi surfaces. For a co-dimensional $n$ Fermi surface we should have[8]

$$\mathcal{S}_d^{(\Sigma)}(R) \propto (k_F R)^{d-n} \tag{2.3.3}$$

which implies that in the entanglement entropy itself[9]

$$S^{(\Sigma)}(R) \propto \begin{cases} (k_F R)^{d-n} \log(k_F R) & \text{n even} \\ (k_F R)^{d-n} & \text{n odd} \end{cases} \,. \tag{2.3.4}$$

[8] We define the co-dimension with respect to the full spacetime dimension $d$.

[9] These results were also obtained by B. Swingle (unpublished).

Thus we find that there is a $\log R$ factor only for even co-dimensional Fermi surfaces. These results are again independent of whether there are quasi-particles. Note that for a Fermi point where $n = d$, equation (2.3.4) in consistent with one's expectation that for massless fermions there is a universal $\log R$ term only for even $d$. For general $n$, at least for free fermions, the alternating behavior of logarithmic enhancement in (2.3.4) may also be understood (by generalizing an argument of [50]) as follows: at each point of a co-dimensional $n$ Fermi surface, there is an $n$-dimensional free fermion CFT. The $\log R$ appearance in (2.3.4) is then consistent with the fact that for an $n$-dimensional CFT, there is a universal $\log R$ piece only for $n$ even.

It would be interesting to see whether our discussion may also be used to understand the logarithmic enhancement in the entanglement entropy of the critical spin liquids in [51] which are described by a projected Fermi sea state.

## 2.4 Renormalized Rényi entropies

The discussions of Sec. 2.2–Sec. 2.3 for the entanglement entropy can be applied almost without any change to Rényi entropies. The main results include:

1. The divergent pieces of $S_n^{(\Sigma)}$ should be expressible in terms of the local geometric invariants as in (2.2.1).

2. For a pure state, equations (2.2.2)–(2.2.3) apply to Rényi entropies. As a result the renormalized Rényi entropies $\mathcal{S}_{n,d}^{(\Sigma)}$, obtained by acting the differential operators in (1.2.4) to $S_n^{(\Sigma)}$, are UV finite.

3. For a CFT, the Rényi entropies $S_n^{(\Sigma)}$ have the same structure as (2.2.7), i.e.

$$S_n^{(\Sigma)}(R) = \begin{cases} \frac{R^{d-2}}{\delta_0^{d-2}} + \cdots + \frac{R}{\delta_0} + (-1)^{\frac{d-1}{2}} s_{n,d}^{(\Sigma)} + \frac{\delta_0}{R} + \cdots & \text{odd d} \\ \frac{R^{d-2}}{\delta_0^{d-2}} + \cdots + \frac{R^2}{\delta_0^2} + (-1)^{\frac{d-2}{2}} s_{n,d}^{(\Sigma)} \log \frac{R}{\delta_0} + \text{const} + \frac{\delta_0^2}{R^2} + \cdots & \text{even d} \end{cases} \tag{2.4.1}$$

with

$$\mathcal{S}_{n,d}^{(\Sigma)}(R) = s_{n,d}^{(\Sigma)} = \text{const} \ . \tag{2.4.2}$$

4. For a general (renormalizable) QFT $\mathcal{S}^{(\Sigma)}_{n,d}(R)$ interpolate between the values of the UV and IR fixed point

$$\mathcal{S}^{(\Sigma)}_{n,d}(R) \to \begin{cases} s^{(\Sigma,\mathrm{UV})}_{n,d} & R \to 0 \\ s^{(\Sigma,\mathrm{IR})}_{n,d} & R \to \infty \end{cases} , \tag{2.4.3}$$

and are most sensitive to the degrees of freedom at the scale $R$.

5. For a scale invariant theory at finite temperature and chemical potential, $\mathcal{S}^{(\Sigma)}_{n,d}$ should take the scaling form

$$\mathcal{S}^{(\Sigma)}_{n,d}(R,\mu,T) = \mathcal{S}^{(\Sigma)}_{n,d}\left(\frac{T}{\mu}, RT\right) . \tag{2.4.4}$$

Unlike for entanglement entropy we do not expect a simple relation with the thermal entropy in the high temperature limit.

6. All Rényi entropies contain logarithmic violations of the area law for a (non)-Fermi liquid

$$S^{(\Sigma)}_n(R) \propto A_{FS}A_\Sigma \log(A_{FS}A_\Sigma) + \cdots . \tag{2.4.5}$$

This generalizes a previous result for the free Fermi gas [52].

The key difference between entanglement entropy and the Rényi entropies is that strong subadditivity does not hold for the latter. In the following sections we discuss how entanglement entropy is related to the number of degrees of freedom. These relations do not appear to have obvious generalization to Rényi entropies.

## 2.5 Entanglement entropy as measure of number of degrees of freedom

For the rest of this chapter we will restrict our discussion to the renormalized entanglement entropy in the vacuum. In Sec. 2.2 we showed that in the vacuum $\mathcal{S}^{(\Sigma)}_d(R)$ introduced in (1.2.4) has various desirable features:

1. It has a well-defined continuum limit.

2. For a CFT, it is independent of $R$ and given by the universal part of the entanglement entropy (2.2.7)

$$\mathcal{S}_d^{(\Sigma)}(R) = s_d^{(\Sigma)} \ . \tag{2.5.1}$$

3. For a renormalizable quantum field theory, it interpolates between the values of UV and IR fixed points as $R$ is increased from zero to infinity.

$$\mathcal{S}_d^{(\Sigma)}(R) \to \begin{cases} s_d^{(\Sigma,\mathrm{UV})} & R \to 0 \\ s_d^{(\Sigma,\mathrm{IR})} & R \to \infty \end{cases} \ . \tag{2.5.2}$$

   It should be understood that in (2.5.2) if the IR fixed point is described by a gapped phase, then $s_d^{(\mathrm{IR})}$ is either given by the topological entanglement entropy (for odd $d$) or zero (for even $d$).

4. It is most sensitive to degrees of freedom at scale $R$.

Thus $\mathcal{S}_d^{(\Sigma)}(R)$ provides a set of observables which can be used to directly probe and characterize quantum entanglement at a given scale $R$. As discussed in the Introduction, these properties also imply that we may interpret the dependence on $R$ as a RG flow. A natural question which then arises is whether $\mathcal{S}_d^{(\Sigma)}(R)$ could also provide a scale-dependent measure of the number of degrees of freedom of a system. Given the physical intuition that RG leads to a loss of degrees of freedom, a necessary condition for this interpretation is then

$$R\frac{d\mathcal{S}_d^{(\Sigma)}(R)}{dR} < 0 \tag{2.5.3}$$

which in turn requires (given (2.5.2))

$$s_d^{(\Sigma,\mathrm{UV})} > s_d^{(\Sigma,\mathrm{IR})} \ . \tag{2.5.4}$$

Note that (2.5.4) alone is enough to establish $s_d^{(\Sigma)}$ as a measure of the number of degrees of freedom for CFTs, while establishing $\mathcal{S}_d^{(\Sigma)}(R)$ as a measure of degrees of

freedom for general QFTs requires a much stronger condition (2.5.3).

For $d = 2$, the entangled region becomes an interval (there is no shape difference) and equation (1.2.4) reduces to[10]

$$\mathcal{S}_2(R) = R\frac{dS}{dR}\,, \tag{2.5.5}$$

which for a CFT then gives [53–55]

$$\mathcal{S}_2 = \frac{c}{3} \tag{2.5.6}$$

where $c$ is the central charge. In this case, Zamolodchikov's $c$-theorem [8] ensures (2.5.4) and there exists a beautiful proof by Casini and Huerta [56,57] showing that $\mathcal{S}_2(R)$ is indeed monotonically decreasing for all Lorentz-invariant, unitary QFTs. Note that while there already exist an infinite number of $c$-functions [14] including Zamolodchikov's original one, $\mathcal{S}_2(R)$ has some special appeal, given that it also characterizes the entanglement of a system. We would like to propose that it gives a "preferred" $c$-function which best characterizes the number of d.o.f. of a system at scale $R$.

In higher dimensions, the shape of $\Sigma$ also matters. Could (2.5.3) and (2.5.4) apply to generic or only certain shapes? For this purpose, consider first the weaker condition (2.5.4).

For even $d \geq 4$, since $s_d^{(\Sigma)}$ appears as the coefficient of the divergent term $\log \delta_0$ in (2.2.7), it can be expressed in terms of integrals of the geometric invariants associated with $\Sigma$ (recall (2.2.1)), and in particular related to trace anomaly [22,58]. For example, for $d = 4$ [22,58]

$$s_4^{(\Sigma)} = 2a_4 \int_\Sigma d^2\sigma\sqrt{h}\, E_2 + c_4 \int_\Sigma d^2\sigma\sqrt{h}\, I_2 \tag{2.5.7}$$

[10]The function (2.5.5) has also been discussed e.g. in [7,32] as the universal part of the entanglement entropy in $d = 2$.

where $a_4$ and $c_4$ are coefficients of the trace anomaly and (below $K = K_{ab}h^{ab}$)

$$E_2 = \frac{1}{4\pi}\mathcal{R} = \frac{1}{4\pi}\left(K^2 - K_{ab}K^{ab}\right) \tag{2.5.8}$$

$$I_2 = \frac{1}{2\pi}\left(\frac{1}{2}K^2 - K_{ab}K^{ab}\right) . \tag{2.5.9}$$

In (2.5.8) $\mathcal{R}$ is the intrinsic curvature on $\Sigma$ and in the second equality of (2.5.8) we have used the Gauss-Codacci relation in flat space. $E_2$ is the Euler density for $d = 2$ and $\int_\Sigma d^2\sigma\sqrt{h}E_2$ is a topological invariant with value 2 for a surface with spherical topology. $I_2$ is a Weyl invariant and is zero for a sphere. For a sphere we then have

$$s_4^{(\text{sphere})} = 4a_4 \tag{2.5.10}$$

while for other shapes, $s_4^{(\Sigma)}$ will be a linear combination of $a_4$ and $c_4$. More than twenty years ago, Cardy conjectured that [16] $a_4$ and its higher dimensional generalizations obey the analogue of $c$-theorem. Only very recently was it proven for $d = 4$ [17, 18]. In addition, there are strong indications any combination of $a_4$ and $c_4$ (including $c_4$) will not satisfy such a condition citeKomargodski:2011vj,Komargodski:2011xv. Thus for $d = 4$ *only* for $\Sigma =$ sphere could the condition (2.5.4) be satisfied. For higher even dimensions the situation is less clear, but one again has [19–22][11]

$$s_d^{(\text{sphere})} = 4a_d . \tag{2.5.11}$$

For odd $d$, $s_d^{(\Sigma)}$ does not arise from local terms in (2.2.7), thus we do not expect that it can be expressed in terms of local geometric invariants on $\Sigma$. This is in contrast to the local shape dependence in the even dimensional case. It would be interesting to understand how $s_d^{(\Sigma)}$ depends on the shape of the entangling surface. It was found in [19] that for a sphere

$$s_d^{(\text{sphere})} = (\log Z)_{\text{finite}} \tag{2.5.12}$$

[11] In addition, the structure of (2.5.7) persists in higher even dimensions except that there are more Weyl invariants [20, 21, 59].

where $(\log Z)_{\text{finite}}$ is the finite part of the Euclidean partition for the CFT on $S^d$. Some support has been found that $s_d^{(\text{sphere})}$ (equivalently $(\log Z)_{\text{finite}}$) satisfies the condition (2.5.4) [20, 21, 23–25].

To summarize, for $\Sigma$ given by a sphere, there are (strong) indications that $s_d^{(\text{sphere})}$ could satisfy (2.5.4) and thus provide a measure of the number of degrees of freedom for CFTs in all dimension (including both odd and even) [19–21]. Below we will simply call $s_d^{(\text{sphere})}$ the central charge of a CFT. For $d \neq 4$, other shapes could still provide a similar measure, which will be left for future investigation. For the rest of the chapter we study the stronger condition (2.5.3) for $\Sigma$ = sphere in $d = 3$ and $d = 4$. For notational simplicity, we will drop the superscript "sphere" in various quantities and denote them simply as $S(R), \mathcal{S}_d(R)$ and $s_d$.

## 2.A Induced metric and extrinsic curvature for a scalable hypersurface

Denote the spherical coordinates in $\mathbb{R}^n$ as $(r, \theta_a)$ where $\theta_a, a = 1, \ldots n-1$ denote all the angular variables. Then a scalable hypersurface $\Sigma$ can be specified as

$$r = Rf(\theta_a) \ , \tag{2.A.1}$$

where $f(\theta_a)$ is a smooth function of the angular variables only and $R$ denotes the size. Clearly as we change $R$, the shape of the surface which is specified by $f$ does not change. Plugging (2.A.1) into the metric for $\mathbb{R}^n$ we find that the full flat space metric for $\mathbb{R}^n$ can be written as

$$ds^2 = (fdR + Rdf)^2 + R^2 f^2 d\Omega^2 = f^2 dR^2 + 2RdRfdf + ds_\Sigma^2, \tag{2.A.2}$$

where $d\Omega^2$ is the standard metric on a unit sphere and $ds_\Sigma^2$ is the induced metric on $\Sigma$

$$ds_\Sigma^2 = R^2 \left(f^2 d\Omega^2 + (df)^2\right) \equiv h_{ab} d\theta^a d\theta^b \ . \tag{2.A.3}$$

Note that since $R^2$ appears in $h_{ab}$ as an overall prefactor, the Christoffel symbol $\Gamma$ built from $h_{ab}$ is clearly independent of $R$, and thus the intrinsic covariant derivative $D_a = \partial_{\theta_a} + \Gamma$ on $\Sigma$ is independent of $R$. From (2.A.2) one can also read that the standard lapse function $N$ is independent of $R$, while the shift vector $N_a \propto R$. Thus the extrinsic curvature $K_{ab}$ which can be written as

$$K_{ab} = \frac{1}{2} N^{-1} \left( \partial_R h_{ab} - D_a N_b - D_b N_a \right) \propto R \, . \tag{2.A.4}$$

Thus we have established (2.2.5). Since in $F$ of (2.2.1) all indices have to contracted and there are an even number of $K_{ab}$, thus $F$ can only depend on $R$ through $R^{-2n}$ for $n$ some non-negative integer. This then establishes (2.2.4).[12] Note that $n = 2$ is a bit special as in this case, both the curvature $K$ and $h$ have only a single component, but the same conclusion applies.

For illustration, let us also give an example of a surface which is not scalable. Consider in $\mathbb{R}^2$ a curve specified by

$$x^2 + \frac{y^4}{b^2} = R^2 \tag{2.A.5}$$

whose shape clearly changes with $R$. For this curve there is an additional dimensional parameter $b$, and our previous discussion does not apply.

[12] For theories breaking parity it is possible to have terms with different powers from those indicated in (2.2.4) [39], but they have negative powers of $R$. From our discussion in the main text, they will not give rise to divergent terms.

# Chapter 3

# Monotonicity of renormalized entanglement entropy

## 3.1 Introduction

In this chapter we explore the properties of the renormalized entanglement entropies (REE) $\mathcal{S}_3$ and $\mathcal{S}_4$.[1] We test whether the REE satisfies the properties required from a measure of the number of degrees of freedom. We start by the study of REE in free theories, where the RG flow is between a UV massless fixed point and the empty theory in the IR. We then move on to field theories with holographic duals. After setting up the machinery, we perform a detailed study of a variety of RG flows.

These examples allow us to conjecture that in three dimensions REE is always non-negative and monotonic, and provides a measure of the number of degrees of freedom of a system at scale $R$. In four dimensions, however, we find examples in which it is neither monotonic nor non-negative.

## 3.2 Free massive scalar and Dirac fermions in $d = 3$

In this section we consider $\mathcal{S}_3(R)$ for a free massive scalar and Dirac field. For a free massive field, we expect that $\mathcal{S}_3(R)$ should approach that for a massless field as

[1] In Sec. 1.4.3 we have already showed that $\mathcal{S}_2$ is monotonic in any quantum field theory.

$R \to 0$, and 0 as $R \to \infty$. We would like to see whether it is monotonic and positive in between. Recently, in the limit of $mR \gg 1$, it was found in [7, 60] that ($\delta$ is a short-distance cutoff)

$$S_{\text{scalar}}(mR) = \#\frac{R}{\delta} - \frac{\pi}{6}mR - \frac{\pi}{240}\frac{1}{mR} + \cdots \tag{3.2.1}$$

$$S_{\text{Dirac}}(mR) = \#\frac{R}{\delta} - \frac{\pi}{6}mR - \frac{\pi}{40}\frac{1}{mR} + \cdots . \tag{3.2.2}$$

From (1.2.4) we thus find that

$$\mathcal{S}_{\text{scalar}}(mR) = +\frac{\pi}{120}\frac{1}{mR} + \cdots \tag{3.2.3}$$

$$\mathcal{S}_{\text{Dirac}}(mR) = +\frac{\pi}{20}\frac{1}{mR} + \cdots \tag{3.2.4}$$

which are indeed monotonically decreasing with $R$. Note that the $\frac{1}{mR}$ fall-off in the above expressions is also consistent with our earlier expectation (2.2.14).

We emphasize that if one simply subtracts the divergent part in (3.2.1), then the resulting

$$S^{(\text{finite})}_{\text{scalar}}(mR) = -\frac{\pi}{6}mR - \frac{\pi}{240}\frac{1}{mR} + \cdots \tag{3.2.5}$$

approaches minus infinity linearly as $R \to \infty$ and thus does *not* have a good asymptotic limit. The presence of such a linear term can be understood as a finite renormalization between the short distance cutoffs of the UV and IR fixed points, as discussed in Sec. 2.2. In contrast, $\mathcal{S}_3(R)$ approaches zero as $R \to \infty$ as one would expect of a system with a mass gap.

We have also calculated $\mathcal{S}_3(R)$ numerically for a massive scalar field[2] for a range of $mR$ as shown in Fig. 3-1 (see Appendix 3.A for details for the numerical calculation). The numerical result is consistent with our expectation of the limiting values of $\mathcal{S}_3(R)$ in the small and large $R$ limits, and also suggests that it is monotonic in between.

[2]Compared to that of a scalar, the computation for a Dirac fermion requires significantly more computer time to achieve the same accuracy. We will leave it for future investigation.

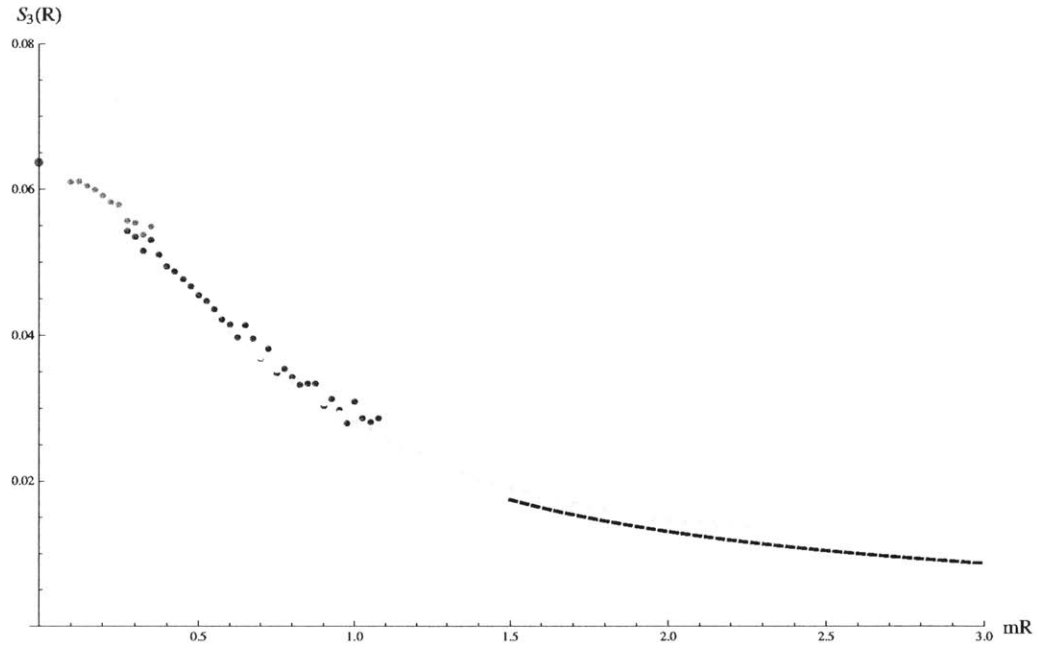


Figure 3-1: $\mathcal{S}_3(R)$ for a free massive scalar field: The red point is the value for $m = 0$. The black dashed line is the result of the asymptotic expansion (3.2.3). The numerical results are computed following the method of [5] with a radial lattice discretization. We choose the system size to be $L_{IR} = 200a$, where $a$ is the lattice spacing. To avoid boundary effects the restriction to $10a \leq R \leq 45a$ was made. To extend the range of $mR$ we obtained the results for $1/m = 20a,\ 40a,\ 120a$. In the plots, the orange dots are data points for $1/m = 120a$, the blue ones are for $1/m = 40a$, and the green ones are for $1/m = 20a$. As expected all our data points collapse into one curve as $\mathcal{S}_3(R)$ can only depend on $mR$ in the continuum limit. For more details see Appendix 3.A.

## 3.3 $\mathcal{S}_d(R)$ for Holographic flow systems

In this section we discuss properties of $\mathcal{S}_d(R)$ (defined for a sphere) for systems with a gravity dual using the proposal of [22,61] (see [62] for a review), which relates the entanglement entropy to the area of a minimal surface. Other recent discussion of entanglement entropy in holographic RG flow systems include [20,21,63–67]

We will restrict our discussion to $d \geq 3$. After a brief discussion of the general set-up, we derive a relation between $\mathcal{S}_d$ and the undetermined constant in the asymptotic expansion of the minimal surface. We then show that when the central charges of the IR and UV fixed points are close, for all dimensions, $\mathcal{S}_d$ is always monotonically

deceasing with $R$ at leading order in the expansion ot difference of central charges of the UV and IR fixed points. Thus for flows between two sufficiently closely separated fixed points, $\mathcal{S}(R)$ appears to provide a good central function.

### 3.3.1 Gravity set-up

We consider a bulk spacetime which describes a renormalization group flow in the boundary theory. We assume that the system is Lorentz invariant. The flow can be induced either by turning on the source for some relevant scalar operators or by certain scalar operators developing vacuum expectation values (without a source). Below we will refer to them as source and vev deformation respectively. We denote the corresponding bulk fields by $\phi_a$.

The bulk action can be written as

$$I = \frac{1}{2\kappa^2}\int d^{d+1}x\sqrt{-g}\left[R - \frac{1}{2}G_{ab}\partial\phi_a\partial\phi_b - V(\phi_a)\right] \tag{3.3.1}$$

where $G_{ab}$ is some positive-definite metric on the space of scalar fields. The spacetime metric can be written in a form

$$ds^2 = \frac{L^2}{z^2}\left(-dt^2 + d\rho^2 + \rho^2 d\Omega_{d-2}^2 + \frac{dz^2}{f(z)}\right) . \tag{3.3.2}$$

We assume that $V(\phi_a)$ has a critical point at $\phi_a = 0$ with $V(0) = -\frac{d(d-1)}{L^2}$, which corresponds to the UV fixed point. Near the boundary $z = 0$,

$$\phi_a(z) \to 0, \quad f(z) \to 1, \qquad z \to 0 \tag{3.3.3}$$

and the spacetime metric is that of $AdS_{d+1}$ with curvature radius $L$. Einstein equations and positive-definiteness of the kinetic term coefficients $G_{ab}$ require that the evolution of $f$ with $z$ should satisfy [68]

$$\partial_z f(z) > 0 \tag{3.3.4}$$

i.e. $f(z)$ is a monotonically increasing function. More generally, equation (3.3.4) follows from the null energy condition and Einstein equations, regardless of specific form of the scalar action.

At small $z$, $f(z)$ can be expanded as

$$f(z) = 1 + \mu^{2\alpha} z^{2\alpha} + \cdots , \qquad z \to 0 \tag{3.3.5}$$

where $\mu$ is some mass scale and $\alpha$ some positive constant. For a source deformation, $\alpha = d - \Delta$ with $\Delta$ the UV dimension of the *leading* relevant perturbating operator (i.e. the one with the smallest $\alpha$).[3] For a vev deformation we have $\alpha = \Delta$.[4]

In the IR, as $z \to \infty$, we can have the following possibilities:

1. Flow to an IR conformal fixed point. In this case $\phi_a$ approaches a neighboring critical point $\phi_a = \phi_a^{(0)}$ with $V(\phi^{(0)}) = -\frac{d(d-1)}{L_{IR}^2}$, and $V(\phi^{(0)}) < V(0)$, $L > L_{IR}$. The flow solution then describes a domain wall with the metric (3.3.2) interpolating between two $\mathrm{AdS}_{d+1}$ with curvature radius given by $L$ and $L_{IR}$ respectively, i.e.

$$f(z) \to \frac{L^2}{L_{IR}^2} \equiv f_\infty > 1, \qquad z \to +\infty . \tag{3.3.6}$$

   Near the IR fixed point, i.e. $z \to \infty$, $f$ can be expanded as

$$f(z) = f_\infty \left( 1 - \frac{1}{(\tilde{\mu} z)^{2\tilde{\alpha}}} + \cdots \right) , \tag{3.3.7}$$

   where $\tilde{\alpha} = \tilde{\Delta} - d$, with $\tilde{\Delta}$ being the dimension of the leading irrelevant perturbing operator at the IR fixed point, and $\tilde{\mu}$ is a mass scale characterizing irrelevant perturbations.

2. The spacetime becomes singular at $z = \infty$: since $f$ has to increase with $z$,

[3]Note that when $\Delta = \frac{d}{2}$ for which $\alpha = \frac{d}{2}$, we should replace the second term in (3.3.5) by $(\mu z)^d (\log \mu z)^2$.

[4]The above description is for the standard quantization. In the alternative quantization (which applies to $\frac{d}{2} - 1 < \Delta < \frac{d}{2}$), we have instead $\alpha = \Delta$ for a source deformation and $\alpha = d - \Delta$ for a vev deformation.

instead of approaching a constant as in (3.3.6), $f(z)$ can blow up as $z \to \infty$, e.g.

$$f(z) \propto z^n, \qquad n > 0 \,. \tag{3.3.8}$$

Given $n > 0$, the $z = \infty$ singularity in fact sits at a *finite proper distance* away. From the standard IR/UV connection the naive expectation is the corresponding IR phase should be gapped. As we will discuss later, it turns out this is only true for $n > 2$, an example of which is the GPPZ flow [69]. We also discuss the Coulomb branch flow that has $n = 2$ [70, 71] that can also be regarded as gapped.[5]

For $n < 2$, the story is more intricate and there exist gapless modes in the IR. Below we will refer to $n < 2$ geometries scaling geometries, examples of which include the near horizon geometries of D1, D2 and D4-branes. In these examples, the IR fixed point either does not have a good gravity description (like in the case of D1 or D4 branes) or the number of degrees of freedom at the IR fixed point scales with $N$ with a lower power than $N^2$ (like in the case of D2 branes, where the IR description is in terms of M2 branes giving $N^{3/2}$ degrees of freedom). Thus one should interpret the scaling region (3.3.8) as describing an intermediate scaling regime of the boundary theory before the true IR phase is reached. While one should be wary of such singular spacetimes, they appear to give sensible answers for correlation functions consistent with the interpretation of a gapped phase (see e.g. [72]).In this thesis we will assume such singular geometries make sense.

In our subsequent discussion we will assume that there exists a crossover scale $z_{CO}$ such that (3.3.7) or (3.3.8) is valid for

$$z \gg z_{CO} \,. \tag{3.3.9}$$

[5]In Coulomb branch flow [70,71] which describes a Higgs phase of the $\mathcal{N} = 4$ SYM theory, there is a single Goldstone mode corresponding to spontaneous breaking of conformal symmetry. In the large $N$ limit, the effect of such a gapless mode on observables like entanglement entropy can be neglected. We will thus still call it a "gapped" phase.

While in this chapter we will be focusing on vacuum solutions (i.e. with Lorentz symmetry), since the holographic computation of the entanglement entropy for a static system only depends on the spatial part of the metric [61], the techniques we develop in this chapter for calculating the large $R$ behavior of the REE also apply to a more general class of metrics of the form

$$ds^2 = \frac{L^2}{z^2}\left(-g(z)dt^2 + d\vec{x}^2 + \frac{dz^2}{f(z)}\right) . \tag{3.3.10}$$

This is in fact the most general metric describing a translational and rotational invariant boundary system including all finite temperature and finite chemical potential solutions. $g$ does not directly enters the computation of the REE. Its presence is felt in the more general behavior allowed for $f$; the null energy condition no longer requires $f$ to be monotonically increasing. For example, for a black hole solution $f$ decreases from the boundary value 1 to zero at the horizon. The null energy condition also allows $n < 0$ in (3.3.8) for certain $g$. One such example is the hyperscaling violating solution [43–45, 73, 74] (at $T = 0$), where the metric functions have the scaling form

$$g(z) = bz^m \qquad f(z) = az^n, \qquad z \to \infty . \tag{3.3.11}$$

We will discuss the black hole case in section 4.5.

### 3.3.2 Holographic Entanglement entropy: strip

We first discuss the holographic entanglement entropy of the strip region (4.1.11). It is obtained by minimizing the action:

$$S_{\text{strip}}(R) = \frac{L^{d-1}}{4G_N}\ell^{d-2}A \tag{3.3.12}$$

where $G_N$ is the bulk Newton constant and $A$ is the area functional [61, 75]. If the spacetime is singular, as in the case of (3.3.8), the minimal surface can become disconnected. In this case, the minimal surface consists of two disconnected straight planes $x(z) = \pm R$. The minimal surface area is independent from $R$ due to the

translational symmetry of the problem. If the surface is connected, its area is given by

$$A = \int_{-R}^{R} dx \frac{1}{z^{d-1}} \sqrt{1 + \frac{z'^2}{f(z)}} \ . \tag{3.3.13}$$

The shape of the entangling surface is specified by the boundary conditions

$$z(x = R) = 0, \qquad z'(x = 0) = 0 \ . \tag{3.3.14}$$

Since the action has no implicit dependence on $x$, we have an associated conserved quantity:

$$\frac{1}{z^{d-1}} \frac{1}{\sqrt{1 + \frac{z'^2}{f}}} = \text{const} \ . \tag{3.3.15}$$

This reduces the equation of motion to first order:

$$z' = -\frac{1}{z^{d-1}} \sqrt{f(z) \left( z_t^{2(d-1)} - z^{2(d-1)} \right)} \ , \tag{3.3.16}$$

where $z_t = z(x = 0)$ gives the tip of the minimal surface. $z_t$ is determined by requiring $z(R) = 0$. i.e.

$$R = \int_0^{z_t} du \, \frac{u^{d-1}}{\sqrt{f(u) \left( z_t^{2(d-1)} - u^{2(d-1)} \right)}} = z_t \int_0^1 dv \, \frac{v^{d-1}}{\sqrt{f(z_t v)(1 - v^{2(d-1)})}} \ . \tag{3.3.17}$$

Inverting this implicit equation gives the relation $z_t(R)$. Using (3.3.16) we can also write (3.3.13) as

$$A = \frac{2}{z_t^{d-2}} \int_{\frac{\delta}{z_t}}^1 \frac{dv}{v^{d-1}} \frac{1}{\sqrt{f(z_t v)(1 - v^{2(d-1)})}} \tag{3.3.18}$$

where $\delta$ is a UV cutoff.

Expanding (3.3.16) near the boundary $z = 0$, we find the expansion

$$x(z) = R - \frac{z^d}{d \, z_t^{d-1}} + \cdots \ . \tag{3.3.19}$$

Varying (3.3.13) with respect to $R$ and using (3.3.19), we find that

$$R^{d-1}\frac{dA}{dR} = 2\left(\frac{R}{z_t}\right)^{d-1} \tag{3.3.20}$$

which implies that $\mathcal{R}_d(R)$ defined in (4.1.13) is given by

$$\mathcal{R}_d = \frac{L^{d-1}}{2G_N}\left(\frac{R}{z_t}\right)^{d-1} . \tag{3.3.21}$$

Thus to find $\mathcal{R}_d$ it is enough to invert (3.3.17) to obtain $z_t(R)$. (3.3.21) was obtained before in [76].

### 3.3.3 Holographic Entanglement entropy: sphere

From the prescription of [61], the entanglement entropy for a spherical region of radius $R$ is obtained by

$$S(R) = \frac{2\pi L^{d-1}}{\kappa^2}\omega_{d-2}A = KA, \quad K \equiv \frac{2\pi L^{d-1}}{\kappa^2}\omega_{d-2} \tag{3.3.22}$$

where $\omega_{d-2}$ is the area of a unit $(d-2)$-dimensional sphere and $A$ is obtained by minimizing the surface area

$$A = \int_0^R d\rho\, \frac{\rho^{d-2}}{z^{d-1}}\sqrt{1+\frac{z'^2}{f(z)}} = \int_0^{z_m} dz\, \frac{\rho^{d-2}}{z^{d-1}}\sqrt{\rho'^2+\frac{1}{f(z)}} , \tag{3.3.23}$$

with the boundary condition at infinity

$$\rho(z=0) = R . \tag{3.3.24}$$

Depending on the spacetime metric, there can be two kinds of minimal surfaces as indicated in Fig. 3-2. For the disk type, the minimal surface ends at a finite $z_m$ with

$$\rho(z_m) = 0, \qquad \rho'(z_m) = \infty . \tag{3.3.25}$$

The cylinder type solution extends all the way to $z = \infty$ with

$$\rho(z) \to \rho_0, \quad \rho'(z) \to 0, \qquad z \to \infty \tag{3.3.26}$$

with $\rho_0$ a finite constant. When the IR geometry is given by another $AdS_{d+1}$ as in (3.3.6), the minimal surface is always of disk type. In Appendix 3.B we show that for singular IR geometries with (3.3.8), cylinder type solution can exist when the exponent $n > 2$. As also discussed in Appendix 3.B, for $n > 2$, there exists a critical minimal surface which closes off exactly at $z = \infty$, i.e. it can be viewed either as a surface of cylinder topology with $\rho_0 = 0$ or a surface of disk topology with $z_m = \infty$. This critical surface will be important for "second order phase transitions" in entanglement entropy we observe in some examples of Sec. 3.4.

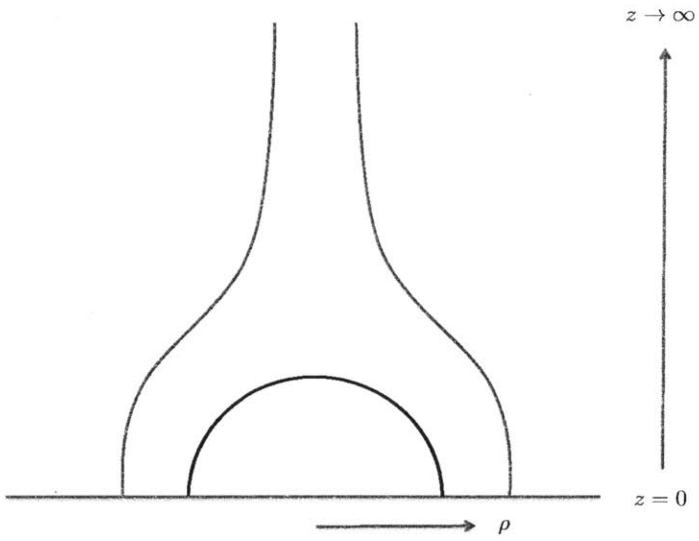


Figure 3-2: Cartoon of a minimal surface of disk topology (black) v.s. a minimal surface of cylinder topology (red). The cylinder type surface is possible only for (3.3.8) with $n > 2$.

The equation of motion can be written as

$$(d-2)\frac{1}{f} + (d-1)\frac{\rho\rho'}{z} = \rho\sqrt{\rho'^2 + \frac{1}{f}}\partial_z\left(\frac{\rho'}{\sqrt{\rho'^2 + \frac{1}{f}}}\right) \tag{3.3.27}$$

or

$$fz'' + \left(\frac{d-2}{\rho}z' + \frac{(d-1)f}{z}\right)\left(f + z'^2\right) - \frac{\partial_z f}{2}z'^2 = 0 \ . \tag{3.3.28}$$

At the UV fixed point, $f = 1$, the minimal surface is given by the hemisphere [22]

$$\rho_0(z) = \sqrt{R^2 - z^2}, \qquad z_{m0} = R \ . \tag{3.3.29}$$

Evaluating on (3.3.29), the action (3.3.23) is divergent near $z = 0$. We introduce a UV cutoff $z = \delta$ and the regularized action becomes

$$A = R\int_\delta^R dz\, \frac{(R^2 - z^2)^{\frac{d-3}{2}}}{z^{d-1}} \ . \tag{3.3.30}$$

One then finds the entanglement entropy has the form (2.2.7), with

$$\mathcal{S}_d^{(\mathrm{UV})} = s_d^{(\mathrm{UV})} = \frac{(d-3)!!}{(d-2)!!}K \ . \tag{3.3.31}$$

Similarly at the IR fixed point with $f = \frac{L^2}{L_{\mathrm{IR}}^2}$ we find

$$\mathcal{S}_d^{(\mathrm{IR})} = s_d^{(\mathrm{IR})} = \frac{(d-3)!!}{(d-2)!!}K_{\mathrm{IR}} \ , \quad K_{\mathrm{IR}} \equiv \frac{2\pi L_{\mathrm{IR}}^{d-1}}{\kappa^2}\omega_{d-2} \ . \tag{3.3.32}$$

### 3.3.4 $\mathcal{S}_d$ in terms of asymptotic data

We now derive a formula to relate $\mathcal{S}_d$ directly to a finite coefficient in the asymptotic expansion of the minimal surface solution near the boundary. For definiteness we will restrict our discussion to a single scalar field, but the conclusion is general.

Consider the action (3.3.23) with a cutoff at $z = \delta$,

$$A = \int_\delta^{z_m} dz\, \frac{\rho^{d-2}}{z^{d-1}}\sqrt{\rho'^2 + \frac{1}{f}} \equiv \int_\delta^{z_m} dz\, \mathcal{L} \tag{3.3.33}$$

with boundary conditions (3.3.24) and (3.3.25) (or (3.3.26) with $z_m = \infty$). In the above equation, varying $R$ with $\delta$ fixed, and using the standard Hamilton-Jacobi

method we find

$$\frac{dA}{dR} = -\mathcal{H}(z_m)\frac{dz_m}{dR} - \Pi\frac{d\rho}{dR}\bigg|_\delta = -\Pi(\delta)\frac{d\rho(\delta)}{dR} \tag{3.3.34}$$

where

$$\Pi = \frac{\partial\mathcal{L}}{\partial\rho'} = \frac{\rho^{d-2}}{z^{d-1}}\frac{\rho'}{\sqrt{\rho'^2+\frac{1}{f}}}, \qquad \mathcal{H} = \Pi\rho' - \mathcal{L} = -\frac{\rho^{d-2}}{z^{d-1}}\frac{1}{f\sqrt{\rho'^2+\frac{1}{f}}} \tag{3.3.35}$$

and we have used that $\mathcal{H}(z_m) = 0$ due to the boundary condition there (for both (3.3.25) and (3.3.26)). Equation (3.3.34) only depends on the local solution near infinity and can be evaluated using the asymptotic expansion there.

For small $z$, $f(z)$ has the expansion (see e.g. also [77])

$$f(z) = 1 + \sum_{n=0}^{\infty} f_n z^{d+n} + \sum_{m=2}^{\infty} c_n z^{m\alpha} \tag{3.3.36}$$

where $\alpha$ was introduced in (3.3.5). Note that here we are considering a flat boundary, so the first series of (3.3.36) starts only at order $O(z^d)$. The second series comes from the scalar contribution. Similarly, $\rho(z)$ can be expanded as [77–79][6]

$$\rho(z) = R - \frac{z^2}{2R} + \cdots + c_d(R)z^d + \cdots + \sum_{n=2,m=2}^{\infty} a_{nm}(R)z^{n+m\alpha}\,. \tag{3.3.37}$$

In (3.3.37), the first $\cdots$ contains only even powers of $z$ up to $z^d$ and the second $\cdots$ contains integer powers greater than $d$. Note that the structure of expansion in (3.3.37) excluding the last term follows from the standard Fefferman-Graham expansion applied to a submanifold in AdS [78], while the last term comes from the similar series in the expansion of $f$. In (3.3.37), $c_d$ is undetermined and all other coefficients can be determined in terms of coefficients in (3.3.36) and $c_d$ from local analysis of the minimal surface equation of motion near $z = 0$.

[6]There are also logarithmic terms when two series share common terms. For example, when $n + m\alpha = d$, there is a term proportional to $z^d \log \mu z$ with $\mu$ a mass scale associated with relevant perturbation. Presence of these additional logs will not affect our discussion. So below we will not make them explicit.

Plugging the expansion (3.3.37) into (3.3.34) we find that in the limit $\delta \to 0$

$$\frac{dA}{dR} = -dR^{d-2}c_d(R) - \frac{e_d}{R} + \left.\frac{dA}{dR}\right|_{\text{non-universal}} \tag{3.3.38}$$

where

$$e_d = \frac{1}{2}\left(1 + (-1)^d\right)\left(1 - (-1)^{\frac{d-2}{2}}\right)\frac{(d-3)!!}{(d-2)!!} \tag{3.3.39}$$

in non-vanishing only in $d = 4k, k = 1, 2, \cdots$ dimensions. The non-universal part has the form

$$\left.\frac{dA}{dR}\right|_{\text{non-universal}} = b_1(\delta)R^{d-3} + b_2(\delta)R^{d-5} + \cdots \tag{3.3.40}$$

with only terms of non-negative powers of $R$. $b_n$ can be expressed in terms of a divergent series of $\delta$, with $\delta^{2-d}$ the most divergent term in $b_1$, $\delta^{4-d}$ for $b_2$, and so on. More explicitly, introducing a dimensional parameter $\mu$ to characterize the dimension of $c_n$ (with $c_n \sim \mu^{n\alpha}$), then the series in $b_1$ can be schematically written as

$$b_1 \sim \frac{1}{\delta^{d-2}}\left(1 + (\mu\delta)^{2\alpha} + (\mu\delta)^{3\alpha} + \cdots\right) + \text{const}\ . \tag{3.3.41}$$

The structure of non-universal terms (3.3.40) are consistent with that argued in Sec. 2.2 (recall the discussion below (2.2.8)). They go away when acted with the differential operator in (1.2.4) and do not appear in $\mathcal{S}_d$.

As a result $\mathcal{S}_d(R)$ can be solely expressed in terms of $c_d(R)$. More explicitly, from (3.3.38) and (??) we find that for $d = 3$

$$\frac{1}{K}\mathcal{S}_3(R) = -3R^2c_3(R) + 3\int_0^R dR'\, R'c_3(R') + C \tag{3.3.42}$$

where $C$ is determined by requiring $\mathcal{S}_3(R = 0)$ reduces to the value at the UV fixed point. Also note

$$\frac{1}{K}\frac{d\mathcal{S}_3}{dR} = -3R\,\partial_R\left[Rc_3(R)\right]\ . \tag{3.3.43}$$

Similarly, for $d = 4$,

$$\frac{1}{K}\mathcal{S}_4 = 1 - 2R^3c_4(R) - 2R^4\frac{dc_4}{dR}\ . \tag{3.3.44}$$

### 3.3.5 Two closely separated fixed points

Let us now consider the situation in which the bulk cosmological constants of the UV and IR fixed points are close to each other, which translates into the boundary theory as that the central charges $s_d$ (3.3.31) of the UV and IR fixed points are close. In this case we have

$$f(z) = 1 + \epsilon g(z), \qquad \epsilon \equiv \frac{L^2}{L_{\rm IR}^2} - 1 \ll 1, \qquad g'(z) > 0, \qquad g(z) \to \begin{cases} 0 & z \to 0 \\ 1 & z \to \infty \end{cases} . \tag{3.3.45}$$

We expect the minimal surface to be close to that of a CFT, i.e.

$$\rho(z) = \rho_0(z) + \epsilon \rho_1(z) + \cdots \tag{3.3.46}$$

with $\rho_0$ given by (3.3.29), and

$$A = A_0 + \epsilon A_1 + \cdots . \tag{3.3.47}$$

Under variations of $f$, the variation of the cutoff action (3.3.33) can be written as

$$\delta A = \int_\delta^{z_m} dz \frac{\delta \mathcal{L}}{\delta f} \delta f - \mathcal{H}(z_m) \delta z_m - \Pi \delta \rho \big|_\delta \tag{3.3.48}$$

where $\mathcal{H}$ and $\Pi$ were introduced in (3.3.35) and $\delta z_m$ and $\delta\rho$ denote the induced variations due to $\delta f$. Now apply the above equation to (3.3.45)–(3.3.47), we find that

$$A_1 = \int_\delta^R dz \left. \frac{\delta \mathcal{L}}{\delta f} \right|_{\rho_0} g(z) + \Pi(\delta)\big|_{\rho_0} \rho_1(\delta) \tag{3.3.49}$$

where $\mathcal{H}(z_m)$ again vanishes due to the boundary condition (3.3.24) at $z_m$. $\rho_1(z)$ is obtained by solving the linearized equation following from (3.3.23) around (3.3.29). To find its value at the short-distance cutoff $\delta$, it is enough to use the leading order

expression (3.3.5) for $f$ (with $g(z) = (\mu z)^{2\alpha} + \cdots$), and we find that[7]

$$\rho_1(\delta) = c(\alpha)(\mu\delta)^{2\alpha}\frac{\delta^2}{\sqrt{R^2-\delta^2}} + \cdots , \qquad c(\alpha) = \frac{2+\alpha-d}{2(1+\alpha)(2+2\alpha-d)} . \tag{3.3.50}$$

Plugging the explicit form (3.3.29) of $\rho_0$ and (3.3.50) into (3.3.49), we find that

$$A_1 = -\frac{1}{2R}\int_\delta^R dz\,(R^2-z^2)^{\frac{d-1}{2}}\,z^{1-d}\,g(z) + c(\alpha)\frac{(R^2-\delta^2)^{\frac{d-3}{2}}}{R\delta^{d-4}}(\mu\delta)^{2\alpha} + \cdots . \tag{3.3.51}$$

The divergent terms in the above equation are again consistent with the structure described in Sec. 2.2.1 and thus will not contribute to $\mathcal{S}_d(R)$.[8]

Now applying (1.2.4) to (3.3.51) we find that, for odd $d$,

$$\mathcal{S}_d^{(1)}(R) = -\frac{(d-1)!!}{(d-2)!!}\frac{K}{2R}\int_0^R dz\,g(z) = -\frac{(d-1)!!}{(d-2)!!}\frac{K}{2}\int_0^1 dx\,g(xR) \tag{3.3.52}$$

and for even $d$

$$\mathcal{S}_d^{(1)}(R) = -\frac{(d-1)!!}{(d-2)!!}\frac{K}{2R}\int_0^R dz\,\frac{zg(z)}{\sqrt{R^2-z^2}} = -\frac{(d-1)!!}{(d-2)!!}\frac{K}{2}\int_0^1 dx\,\frac{xg(xR)}{\sqrt{1-x^2}} . \tag{3.3.53}$$

It is interesting to note that for a monotonic $g(z)$, both (3.3.52) and (3.3.53) are monotonic

$$\frac{d\mathcal{S}_d^{(1)}}{dR} < 0 . \tag{3.3.54}$$

Also note that in the limit $R \to \infty$, we can replace $g(xR)$ in both expressions by its value at infinity $g(\infty) = 1$, leading to

$$\mathcal{S}_d^{(1)}(R \to \infty) = -\frac{(d-1)!!}{(d-2)!!}\frac{K}{2} \tag{3.3.55}$$

which is precisely the expected difference between the values of the IR and UV fixed point (see (3.3.31) and (3.3.32)) expanded to first order in $\epsilon$. Thus to first order in $\epsilon$

[7]When $\alpha = \frac{d-2}{2}$, equation (3.3.50) becomes $\rho_1(\delta) = -\frac{d-2}{2d}(\mu\delta)^{d-2}\frac{\delta^2}{\sqrt{R^2-\delta^2}}\log\mu\delta$.

[8]Note that for some special values of $\alpha$, both terms in the above equation can lead to logarithmic terms which contain $\log\mu\delta$, as pointed out before in [7,77]. These terms are also consistent with the structure described in Sec. 2.2.

we have recovered

$$\mathcal{S}_d(R \to \infty) = \mathcal{S}_d^{(\mathrm{IR})} \ . \tag{3.3.56}$$

## 3.4 Some numerical studies

We now consider some specific holographic RG flows, including some "realistic" ones which describe known field theory flows at large $N$ and strong coupling. In these examples, the minimal surface cannot be found analytically and numerical calculations are needed. In some examples, the gravity solutions are only known numerically. In computing the entanglement entropy, one could to choose to evaluate (3.3.23) directly after obtaining the numerical solution for the minimal surface. The numerical integrations can sometimes be time-consuming. It is often more convenient to use (3.3.42) or (3.3.44) to obtain $\mathcal{S}_d$ directly from the coefficient $c_d(R)$ in the asymptotic expansion of the minimal surface solution near the boundary.

We will first consider $d = 3$, where we find that $\mathcal{S}_3(R)$ is always non-negative and monotonic. This is no longer the case for $d = 4$. The non-monotonic examples include the GPPZ flow [69] which describes the flow of the $\mathcal{N} = 4$ SYM theory to a confining phase under a mass deformation and the so-called Coulomb branch flow [70,71] which describes the $\mathcal{N} = 4$ SYM theory in a Higgs phase.

The two realistic examples below in Sec. 3.4.1 and 3.4.2 have also been considered recently in [67].

### 3.4.1 $d = 3$

#### A realistic flow

We first consider the holographic RG flow of [80] which describes the flow from M2 brane theory at UV to an $\mathcal{N} = 2$ superconformal theory with an $SU(3) \times U(1)$ global symmetry at IR. The flow involves two scalar operators whose UV and IR dimensions

are respectively

$$\Delta = (2,2), \qquad \Delta_{\rm IR} = \left(\frac{1}{2}(1+\sqrt{17}), \frac{1}{2}(5+\sqrt{17})\right) . \tag{3.4.1}$$

Thus in (3.3.5) and (3.3.7), $\alpha = 1$ and $\tilde{\alpha} = \frac{1}{2}(\sqrt{17}-1) \approx 1.562$. Also $\frac{L^2}{L_{UV}^2} = \frac{3^{\frac{3}{2}}}{4} \approx 1.299$. The numerical results are presented in Fig. 3-3. Clearly, $\mathcal{S}_3(R)$ is positive, and monotonic. Note that for this flow, $\epsilon$ in (3.3.45) is $\epsilon \approx 0.3$, and thus equation (3.3.52) should be a reasonable approximation, which is confirmed by numerical results. Since $\tilde{\alpha} > \frac{1}{2}$, from (4.1.27) we expect $\mathcal{S}_3(R)$ should fall off as $1/R$ for large $R$. This appears to fit the numerical data very well.

### A sharp domain wall: first order phase transition

The earlier example is a rather shallow domain wall. Let us now consider a sharp domain wall. Unfortunately, there appears no realistic example of this type. We will thus play with toy examples by coming up with various monotonic functions $f(z)$, a strategy which we will repeatedly use below. By scanning through various examples we find that even for $\frac{L}{L_{\rm IR}} \gg 1$, $\mathcal{S}_3(R)$ remains monotonic and approaches to the right asymptotic value. However, a new phenomenon arises when the domain wall becomes steep, as in the left plot of Fig. 3-4. In this case, the minimal surface action (3.3.23) can have more than one extrema for certain range of $R$, as indicated in the middle plot of Fig. 3-4. The minimal surface prescription instructs us to pick the one with the smallest area. While the entanglement entropy itself is continuous as a function of $R$, after taking derivative to obtain $\mathcal{S}_3(R)$, we find there is a discontinuous jump at some value $R_c$ as shown in the right plot of Fig. 3-4. In other words, there is a first-order "phase transition" in the entanglement entropy at $R_c$. Despite the jump, $\mathcal{S}_3$ is still monotonic and approaches the right asymptotic value.

### "Gapped" phases

We now consider some examples where the IR is described by a "gapped" phase. We are interested in systems with Lorentz symmetry, and thus are forced to consider

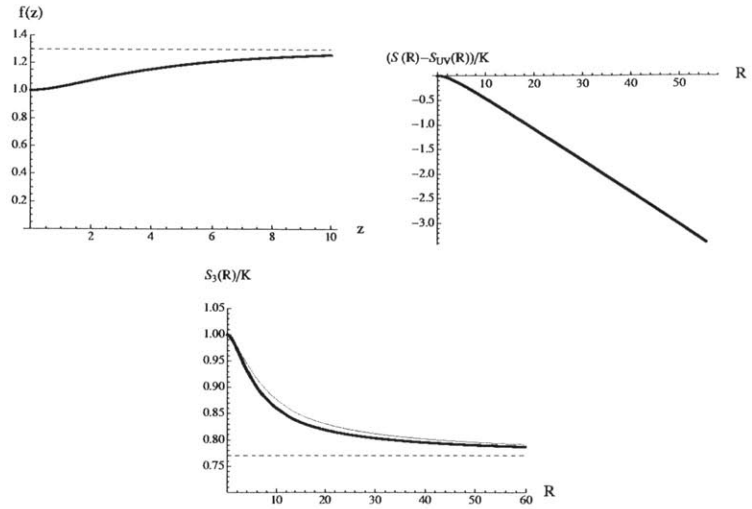


Figure 3-3: **Left:** $f(z)$ for the domain wall solution describing the flow of M2-brane theory to an IR fixed point preserving $\mathcal{N} = 2$ supersymmetry. **Middle:** plot of $S(R) - S_{\rm UV}(R)$ where $S_{\rm UV}$ denotes that at the UV fixed point. The UV divergences cancel when taking the difference, but the resulting expression does not have a well-defined large $R$ limit, with a linear $R$-dependence. As in the case of a free massive scalar and Dirac field of Sec. 3.2, the presence of such a linear term can be understood as a finite renormalization between the short distance cutoffs of the UV and IR fixed points, as discussed in Sec. 2.2. **Right:** $\mathcal{S}_3(R)$ for this flow. We normalize the value at UV to be 1. The horizontal dashed line denotes the expected value (3.3.32) for the IR fixed point. The black line (lower line) is obtained from numerical calculation by using (3.3.42). For this flow, $\epsilon$ in (3.3.45) is $\epsilon \approx 0.3$, and thus equation (3.3.52) should be a reasonable approximation, whose results are plotted using the red line (upper line). Note that the part linear in $R$ in $-S_{\rm finite}$ as seen in the second plot is automatically eliminated when considering $\mathcal{S}_3(R)$.

singular geometries discussed around (3.3.8). An example of gapped phase with a regular geometry is the AdS soliton [81]. But the corresponding boundary theory contains a circle direction. Our discussion of the divergence structure of the entanglement entropy in Sec. 2.2 thus does not apply, and one needs to modify the definition of $\mathcal{S}_d(R)$, which we will not pursue here. The holographic entanglement entropy for an AdS soliton was considered before in [82]. A first-order phase transition between minimal surfaces with disk and cylinder topology similar to our third example below (right plot of Fig. 3-5) was found there.

Again due to lack of simple explicit examples, we will consider some toy examples

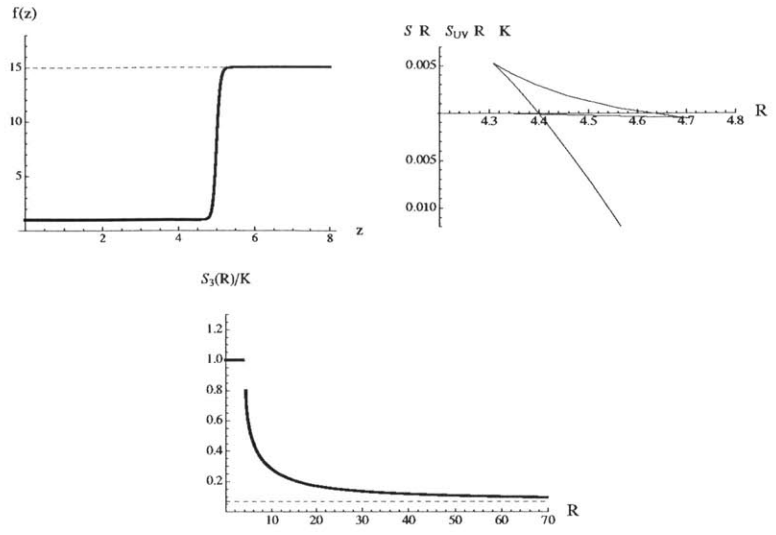


Figure 3-4: **Left:** a steep domain wall (toy example) with $f(z) = 1 + \frac{14z^{100}}{5^{100}+z^{100}}$. **Middle:** plot of $S(R) - S_{\text{conf}}(R)$ where $S_{\text{conf}}(R)$ denotes the entanglement entropy for the UV fixed point. The short-distance divergences cancel when taking the differences. For the indicated range of $R$, the action (3.3.23) has three extrema, all of disk type. The entanglement entropy of the system is given by the smallest of them. There is a first-order "phase transition" at $R_c = 4.4$. **Right:** $\mathcal{S}_3(R)$ has a discontinuous jump, which is indicated by the vertical green line. The dashed horizontal line is the expected asymptotic value for the IR fixed point.

by postulating certain $f(z)$. In Fig. 3-5, we consider three such examples which illustrate three possible scenarios.

In the left plot we consider $f(z) = 1 + z^2$. In this case since $f(z \to \infty) \sim z^2$ with an exponent 2, only minimal surface of disk topology is possible. There appears to be a unique minimal surface solution for all $R$, and $\mathcal{S}_3(R)$ is smooth.

The middle plot is for $f(z) = 1 + z^3$, in which case, when $R$ is sufficiently large, the minimal surface is of cylinder type (see discussion around (3.3.26) and Appendix 3.B). This is indicated in the plot by the red curve. The black curve for smaller $R$ values has minimal surface of disk type. $\mathcal{S}_3(R)$ appears to be continuous at the transition point where the minimal surface changes topology. Thus the entanglement entropy has a "second-order phase transition." Note that approaching the transition point from the smaller $R$ side, the end point $z_m$ of the disk-like surface approaches infinity, while from the larger $R$ side, $\rho_0$ for the cylinder-like surface approaches zero. The

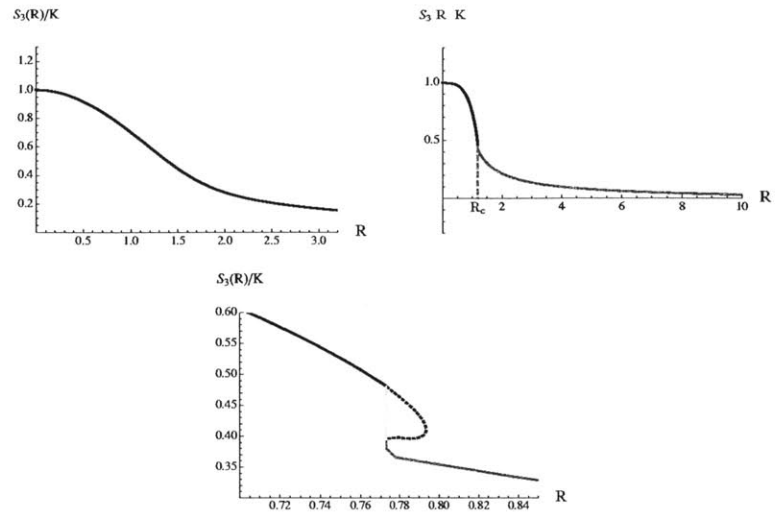


Figure 3-5: **Left:** $\mathcal{S}_3(R)$ for $f(z) = 1 + z^2$. **Middle:** $\mathcal{S}_3(R)$ for $f(z) = 1 + z^3$ which exhibits a "second-order phase transition" from minimal surface of disk topology (black curve) to cylindrical topology (red curve). **Right:** $\mathcal{S}_3(R)$ for $f(z) = (1 + z^2)^2$, which exhibits a "first-order phase transition" between the surfaces of two topologies. The dashed curve corresponds to other extrema of the minimal surface action. There is a discontinuous jump in $\mathcal{S}_3(R)$ which is indicated by the green vertical line.

two branches meet at the critical surface discussed in Appendix 3.B (see Fig. 3-6 for a cartoon). It may be interesting to understand the critical behavior of such a transition which we will leave for future study.

The right plot of Fig. 3-5 is for $f(z) = (1+z^2)^2$, which exhibits a "first-order phase transition." Again the red and black curves have minimal surface of cylinder-type and disk-type respectively. Now near the transition between the two topologies, the action (3.3.23) now has three extrema, with the non-minimal area extrema indicated in the plot by dotted lines. There is a discontinuous jump in $\mathcal{S}_3(R)$ at the transition point.

In all these examples, $\mathcal{S}_3(R)$ appears to approach zero at large $R$, although our numerics cannot go to too large $R$.

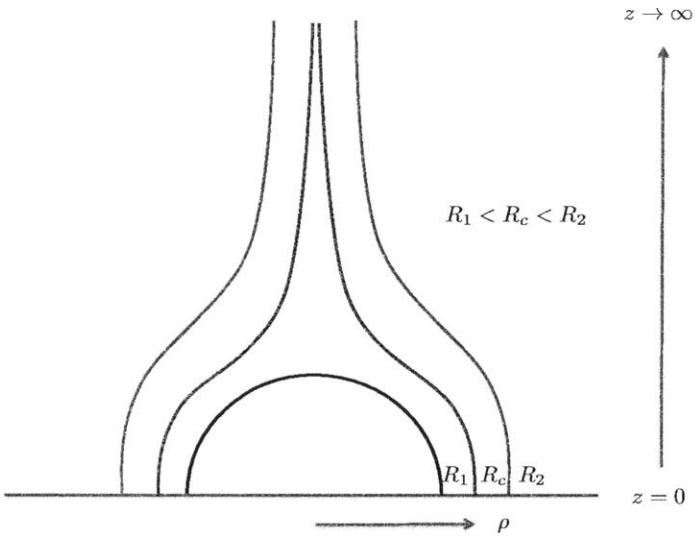


Figure 3-6: Cartoon of a "second-order phase transition" from a minimal surface of disk topology (black) to a minimal surface of cylinder topology (red) as we increase $R$. The surface (brown) at $R_c$ is the critical surface discussed in Appendix 3.B.

### Non-monotonic $f(z)$

Finally just for comparison, in Fig. 3-7 we show a toy model of $f$ which is not monotonic, neither is the corresponding $\mathcal{S}_3$. This toy example illustrates nicely several important aspects of the properties of $\mathcal{S}_3(R)$:

1. As mentioned earlier, the monotonicity of $f$ is tied to the imposing of null energy condition, which can be interpreted as the bulk reflection of boundary unitarity. This indicates that the monotonicity of $\mathcal{S}_3(R)$ is closely tied to unitarity of the boundary system.

2. The location in $R$ where the non-monotonicity of $\mathcal{S}_3(R)$ occurs appears to roughly scale with $z$. From the IR/UV connection, $z$ translats into a boundary length scale. That the non-monotonicity of $f(z)$ at certain $z$ directly translates into non-monotonicity of $\mathcal{S}_3(R)$ at certain $R$ which roughly scales with $z$ indicates that $\mathcal{S}_3(R)$ is most sensitive to contributions from degrees of freedom around scale $R$. In contrast, as shown in the figure the entanglement entropy itself is rather featureless as a function of $R$.

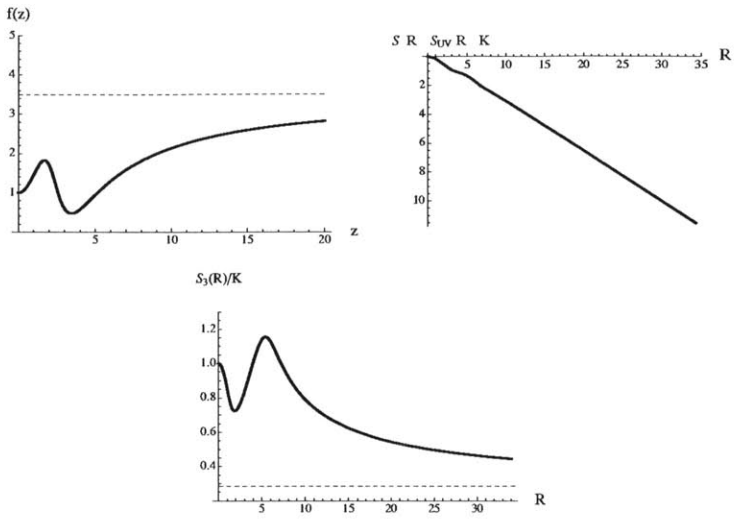


Figure 3-7: **Left:** A toy model of $f(z)$ which is non-monotonic. **Middle:** The entanglement entropy itself is not sensitive to the non-monotonic feature of $f$. **Right:** the corresponding $\mathcal{S}_3(R)$ is sensitive and also becomes non-monotonic.

### 3.4.2 $d = 4$

#### Leigh-Strassler flow

We first consider the flow from the $\mathcal{N} = 4$ SYM theory ($d = 4$) to an $\mathcal{N} = 1$ superconformal fixed point with $SU(2) \times U(1)$ global symmetry [68, 83]. The flow involves two scalar operators whose UV and IR dimensions are respectively

$$\Delta = (2, 3), \qquad \Delta_{\text{IR}} = \left(1 + \sqrt{7}, 3 + \sqrt{7}\right) . \tag{3.4.2}$$

Thus in (3.3.5) and (3.3.7), $\alpha = 1$ and $\tilde{\alpha} = \sqrt{7} - 1 \approx 1.646$. Also $\frac{L^2}{L_{UV}^2} = \frac{2^{\frac{10}{3}}}{9} \approx 1.12$. The numerical results are given in Fig. 3-8. $\mathcal{S}_4(R)$ is positive and monotonic. For this flow, $\epsilon$ in (3.3.45) is $\epsilon \approx 0.12$, and thus equation (3.3.53) should be a good approximation, which is confirmed by the numerical results. Since $\tilde{\alpha} > 1$, from (4.1.27) we expect $\mathcal{S}_4(R)$ should fall off as $1/R^2$ for large $R$. Our numerical data for large $R$ are not good enough to test this conclusively, but does not appear to directly contradict with it.

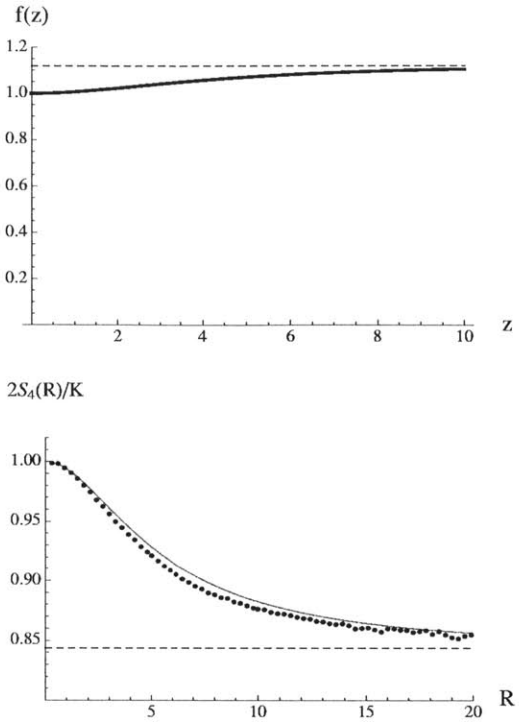


Figure 3-8: **Left:** $f(z)$ for the domain wall solution describing the Leigh-Strassler flow from $\mathcal{N} = 4$ SYM theory to an IR fixed point preserving $\mathcal{N} = 1$ supersymmetry. **Right:** $\mathcal{S}_4(R)$ for this flow. The horizontal line denotes the expected value for the IR theory. The dotted line is obtained from direct numerical calculation. For this flow, $\epsilon$ in (3.3.45) is $\epsilon \approx 0.12$, and thus equation (3.3.53) should be a good approximation, whose results are plotted using the solid line.

### A sharp domain wall

In the Leigh-Strassler flow discussed above, the central charges of the UV and IR fixed points are close. Our discussion in Sec. 3.3.5 indicates that in such a situation $\mathcal{S}_d(R)$ should be monotonic and positive. Now let us consider a toy example in which the domain wall is steep and the separation of central charges is large. As indicated in Fig. 3-9, $\mathcal{S}_4(R)$ is neither monotonic nor positive definite. In contrast to the $d = 3$ example of Sec. 3.4.1, there is no phase transition here.

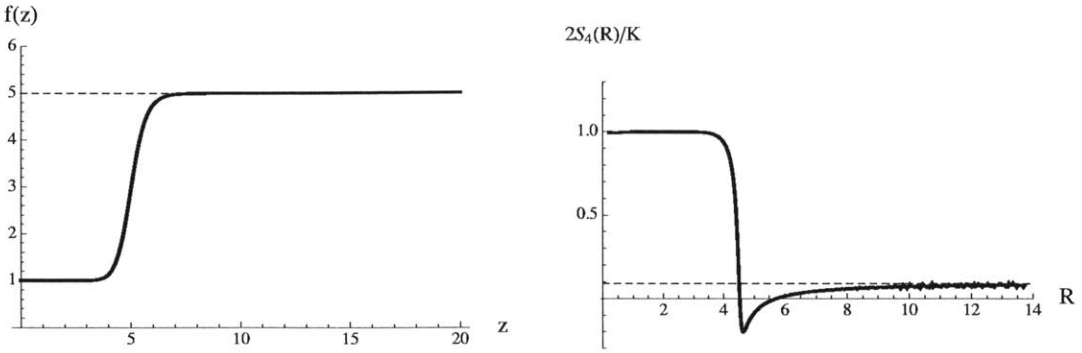


Figure 3-9: **Left:** A steep domain wall (toy example) in $d = 4$ with $f(z) = 1 + \frac{4z^{15}}{5^{15}+z^{15}}$. **Right:** In contrast to the example of Sec. 3.4.1 in $d = 3$, $\mathcal{S}_4(R)$ is smooth, but is neither monotonic nor positive definite. The dash line is the expected asymptotic value for the IR fixed point.

### Gapped phases I: GPPZ flow

We now consider the GPPZ flow [69] which describes the flow of the $\mathcal{N} = 4$ SYM theory to a confining theory under a mass deformation, which has UV dimension $\Delta = 3$. For this flow the metric is known analytically with

$$f(z) = \left(1 + \frac{z^2}{L^2}\right)^2 . \tag{3.4.3}$$

Note that as $z \to \infty$, $f \sim z^4 \to \infty$. Low energy excitations of this system have a discrete spectrum with a finite mass gap (see e.g. [72]). For such a gapped phase we expect $\mathcal{S}_4(R) \to 0$ for large $R$. Fig. 3-10 gives the entanglement entropy and $\mathcal{S}_4$ for this system. While the finite part of the entanglement entropy appears to grow linearly with $R$ at large $R$, $\mathcal{S}_4$ approaches zero from negative side. Similar to the $f(z) = 1 + z^3$ example in $d = 3$ discussed in Sec. 3.4.1, there is a "second order phase transition" from minimal surface of disk topology (black curve) to cylindrical topology (red curve), where $\mathcal{S}_4(R)$ remains continuous (as far as our numerics could tell). Again as in the discussion of $f(z) = 1 + z^3$ the transition goes through the critical surface of Appendix 3.B, as indicated in Fig. 3-6.

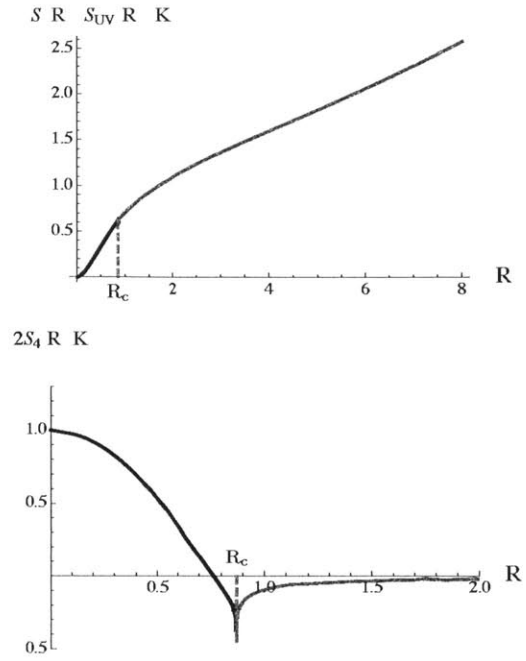


Figure 3-10: **Left:** plot of entanglement entropy $S(R) - S_{\rm UV}(R)$ for GPPZ flow where $S_{\rm UV}(R)$ denotes the entanglement entropy for the UV fixed point. The short-distance divergences cancel when taking the differences. **Right:** plot of $\mathcal{S}_4(R)$ for GPPZ flow, which is neither positive-definite nor monotonic. The system also exhibits a "second order phase transition" from minimal surface of disk topology (black curve) to cylindrical topology (red curve), where $\mathcal{S}_4(R)$ remains continuous (as far as our numerics could tell).

### Gapped phases II: Coulomb branch flow

The Coulomb branch flow describes the spontaneous breaking of the gauge symmetry (and also conformal symmetries) of the $\mathcal{N} = 4$ SYM by a vacuum expectation value for an operator which is bilinear in the fundamental scalars [70, 71]. Thus here there is no operator deformation, and the end point describes a point on the Coulomb Branch. It involves a scalar field of UV dimension $\Delta = 3$. The metric is also known analytically, although through an implicit function

$$z = \frac{1}{\mu}(1-v)^{\frac{1}{2}}v^{-\frac{1}{3}}, \qquad f = \frac{(v+2)^2}{9v^{\frac{2}{3}}} \tag{3.4.4}$$

with $\mu$ a mass scale characterizing the expectation values of the adjoint scalars of the $\mathcal{N} = 4$ theory. Near $z = 0$ (boundary),

$$f = 1 + \frac{2}{9}\mu^4 z^4 + \cdots , \tag{3.4.5}$$

and near $z = \infty$,

$$f = \frac{4}{9}\mu^2 z^2 + \cdots . \tag{3.4.6}$$

While the singularity $z = \infty$ lies at a finite proper distance away, but it takes a null geodesic an infinite time in $t$. The low energy excitations of the system include a massless Goldstone mode from spontaneous breaking of scaling symmetry, and a continuous spectrum above a finite mass gap (see e.g. [72]). Note that the single Goldstone mode will have a nontrivial $O(1)$ contribution to $\mathcal{S}_4$, but is not visible in the order $O(N^2)$ we are considering. So we expect $\mathcal{S}_4(R) \to 0$ for large $R$ as in a gapped phase. With large $z$ behavior given by (3.4.6), there can only be minimal surface with a disk topology. The numerical result is shown in Fig. 3-11, with a unique minimal surface solution for all $R$. However, $\mathcal{S}_4(R)$ is neither monotonic nor positive-definite.

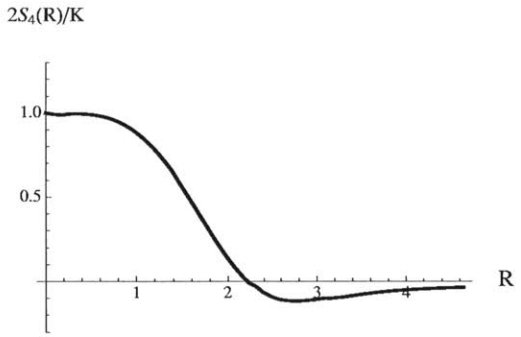


Figure 3-11: $\mathcal{S}_4(R)$ for the Coulomb branch flow.

### 3.4.3 Summary

To summarize, we find that in $d = 3$ all examples (which are Lorentz invariant and satisfy the null energy condition) have a monotonic and non-negative $\mathcal{S}_3(R)$, while this is no longer the case for $\mathcal{S}_4(R)$ in $d = 4$. We also find that the monotonicity of $\mathcal{S}_3(R)$ is tied very closely to the null energy condition, which can be interpreted as the bulk reflection of boundary unitarity. Thus it is tempting to conjecture it is always monotonic in the vacuum of a Lorentz-invariant, unitary QFT.

Note that although $\mathcal{S}_4(R)$ is not monotonic, given the relation (2.5.10) and the recently proved $a$-theorem [17, 18] for $d = 4$, we still always have $\mathcal{S}_4(R \to 0) > \mathcal{S}_4(R \to \infty)$.

Even if $\mathcal{S}_3(R)$ turns out to be monotonically decreasing in the vacuum we do not expect it to remain so at a finite temperature/chemical potential. As discussed in Sec. 2.2.3 at a finite temperature we expect $\mathcal{S}_d(R)$ to be proportional to the thermal entropy, i.e. proportional to the volume of the entangled region in the large $R$ limit with a positive coefficient. Similarly for a system with a Fermi surface (i.e. at a chemical potential), we argued in Sec. 2.3 that $\mathcal{S}_d(R)$ should be proportional to the area of the entangled region at large $R$. While our dimensional analysis could not determine the prefactor, we expect it to be positive on physical ground. Clearly the corresponding $\mathcal{S}_d(R)$ which starts as a constant for small $R$, cannot not be monotonically decreasing in either situation. In the holographic context, the function $f(z)$ in the spacetime metric for states of finite chemical potential or finite temperature does satisfy (3.3.4) (instead it decreases to zero at the horizon).

We also observe first-order and second-order "phase" transitions in $\mathcal{S}_d(R)$.[9] By first-order, we mean $\mathcal{S}_d(R)$ has a discontinuous jump, while in a second-order transition, $\mathcal{S}_d(R)$ is continuous, but not smooth. When the IR is described by a conformal fixed point (corresponding to a different AdS geometry), the phase transitions appear to be first-order and do not involve change of the topology of the minimal surface, as in a sharp domain wall in $d = 3$ discussed in Sec. 3.4.1. When the IR is described

[9]Note that "phase" transitions in the holographic entanglement entropy have also been observed in various other contexts [82, 84–88], but all appear to be the first-order.

by a "gapped" phase corresponding to certain singular bulk IR geometries, the phase transitions (which can be first- or second-order) appear to involve change of topology of the minimal surface. Second-order transitions appear to be controlled by the critical surface discussed in Appendix 3.B. Examples which exhibit a second-order transition include the GPPZ flow [69] which describes the flow of the $\mathcal{N} = 4$ SYM theory to a confining phase under a mass deformation.

Such phase transitions are interesting, as they signal drastic changes of some underlying physics. In the example of a sharp domain wall, the system transitions very quickly (i.e. in a very short range of scales) from the UV to IR regimes, thus it appears that the entanglement entropy does not have "time" to respond to that quick change, which results in a discontinuity. Similarly the phase transitions in the case where the IR is a gapped phase likely signal that the system is opening a gap. Similar first-order phase transitions have been observed before in [85–87] and were interpreted as a confinement/deconfinement transition.

## 3.5 Conclusions and discussion

We introduced a "renormalized entanglement entropy" $\mathcal{S}_d^{(\Sigma)}(R)$ which appears to capture only the "universal" part of the entanglement entropy. We illustrated the power of this construction by showing that the qualitative behavior of the entanglement entropy of a system with a Fermi surface could be obtained by simple dimensional analysis.

We also showed that (in the vacuum) $\mathcal{S}_d^{(\Sigma)}(R)$ has various nice features (as listed in the Introduction) which make it natural to interpret it as describing the RG flow of the entanglement entropy with distance scale. We were particularly interested in finding out whether it could be monotonic and provide a scale-dependent measure of the number of degrees of freedom of a quantum system. In $d = 3$ our studies of free theories and holographic systems support the conjecture that $\mathcal{S}_3(R)$ is non-negative and monotonic for Lorentz-invariant, unitary QFTs. In $d = 4$, this is no longer true. We find examples in which $\mathcal{S}_4(R)$ is neither monotonic nor positive-definite.

Let us now mention some future questions:

1. In our discussion $\mathcal{S}_d^{(\Sigma)}(R)$ was constructed by using the differential operator in (1.2.4) to strip shorter-distance correlations (including cutoff dependence) away from the entanglement entropy $S^{(\Sigma)}(R)$. In particular, to show its UV finiteness we had to examine the the specific structure of divergent terms in $S^{(\Sigma)}(R)$. It would be interesting to have an intrinsically finite way to define it. One possibility is that one may obtain it from certain limit of the mutual information (and their generalizations involving more than two regions).[10]

2. The monotonicity of $\mathcal{S}_3(R)$ would imply that

$$R\frac{d\mathcal{S}_3(R)}{dR} = R^2\frac{d^2S}{dR^2} < 0 \ , \tag{3.5.1}$$

   i.e. as a function $R$, $S(R)$ is a concave function. This feels like a relation that can perhaps arise from a clever use of the strong subadditivity condition of the entanglement entropy, which is also responsible for the monotonicity of $\mathcal{S}_2(R)$ in $d = 2$ [56, 57]. It is also important to examine more examples for further confirmation or counterexamples. In the holographic context, for example, it would be interesting to generalize our discussion to gravity theories with higher derivatives as in [20, 21, 59, 63–66, 91, 92] to test the robustness of the conjecture.

3. Suppose $\mathcal{S}_3(R)$ turns out to be monotonic, it is then rather curious this is no longer true for $\mathcal{S}_4(R)$ in $d = 4$.

   (a) One logical possibility is that $\mathcal{S}_4(R)$ is monotonic, but the holographic examples in which it is not are pathological.[11] The example of Sec. 3.4.2 is a toy model with a very sharp domain wall which is clearly artificial, while those of Sec. 3.4.2 and 3.4.2 involve singular geometries. It would be important to completely settle this using more examples.

[10] See e.g. [89, 90] for discussions mutual information in general quantum field theories and of possibility of a $c$-theorem from mutual information.

[11] Another possibility is that the holographic entanglement entropy formula needs to be modified in these cases.

(b) Now let us assume that $\mathcal{S}_4(R)$ is indeed not always monotonic. Then one possibility is that some modifications on the definition of $\mathcal{S}_4$ are needed in order to construct a central function out of the entanglement entropy on a sphere. Another possibility is that the $c$-theorem for $d = 4$ may require physical information which is not encoded in the entanglement entropy for a spherical region. One hint which points to this thinking is that for $d = 4$ or higher, the monotonicity of $\mathcal{S}_d(R)$ would involve more than two derivatives on $S(R)$, e.g. for $d = 4$, it amounts to

$$R^3\partial_R^3 S + R^2\partial_R^2 S < R\partial_R S \ , \tag{3.5.2}$$

while the strong subadditivity condition can only lead to the second derivative of $S(R)$ when applied to infinitesimally separated regions. From this perspective, it appears likely $\mathcal{S}_d(R)$ will also not be monotonic for $d \geq 5$. It would be good to check this explicitly. It would also be interesting to understand whether non-monotonic regions signal some interesting underlying physics at those distance scales.

4. All examples of this thesis have been on relativistic theories. It would be interesting to explore non-relativistic systems and also time-dependent systems.

5. We find in holographic systems that when the difference of the central charges of the UV and IR fixed points of a QFT is sufficiently small, then $\mathcal{S}_d$ is positive and monotonic for all $d$.

6. In both $d = 3$ and $d = 4$ we observed first-order and second-order "phase" transitions in $\mathcal{S}_d(R)$. For a first-order transition, $\mathcal{S}_d(R)$ has a discontinuous jump, while in a second-order transition, $\mathcal{S}_d(R)$ is continuous, but not smooth. It would be interesting to understand whether such "phase transitions" are due to artifacts of the the large $N$ approximation one is working with. Even if they are, their presence should still reflect some underlying features of the system at finite $N$. For example, as mentioned earlier, the transition in the GPPZ flow

may signal the opening of a gap of the system.

## 3.A Details of the numerical calculation of $\mathcal{S}_3(R)$ for a free massive scalar

We start with the Hamiltonian for a free massive scalar in $d = 3$

$$H = \frac{1}{2}\int d^2x \ \left[\Pi^2 + (\nabla\phi)^2 + m^2\phi^2\right] . \tag{3.A.1}$$

where $\Pi$ is canonical momentum for $\phi$. In terms of the Fourier transform of $\phi$ and $\Pi$ in the angular $\theta$ direction

$$\begin{aligned} \phi_0 &= \sqrt{\frac{r}{2\pi}}\int d\theta\ \phi(\theta,r), \qquad \phi_l + i\phi_{-l} = \sqrt{\frac{r}{\pi}}\int d\theta\ e^{il\theta}\phi(\theta,r), \quad l>0 \\ \Pi_0 &= \sqrt{\frac{r}{2\pi}}\int d\theta\ \Pi(\theta,r), \qquad \Pi_l + i\Pi_{-l} = \sqrt{\frac{r}{\pi}}\int d\theta\ e^{il\theta}\Pi(\theta,r), \quad l>0 \end{aligned} \tag{3.A.2}$$

the Hamiltonian then can be written as $H = \sum_{l=-\infty}^{\infty} H_l$ with

$$H_l = \frac{1}{2}\int_0^\infty dr \ \left[\Pi_l^2 + r\partial_r\left(\frac{\phi_l}{\sqrt{r}}\right)^2 + m^2\phi_l^2 + \frac{l^2}{r^2}\phi_l^2\right] . \tag{3.A.3}$$

Also note that $\phi_l, \Pi_l$ satisfy the canonical commutation relation

$$[\phi_l(r), \Pi_{l'}(r')] = i\delta_{ll'}\delta(r-r') . \tag{3.A.4}$$

We discretize (3.A.3) with a uniform lattice in the radial direction:

$$H_l = \frac{1}{2a}\sum_{j=1}^{N}\left[\Pi_l(j)^2 + \left(j+\frac{1}{2}\right)\left[\frac{\phi_l(j)}{\sqrt{j}} - \frac{\phi_l(j+1)}{\sqrt{j+1}}\right]^2 + m^2\phi_l^2(j) + \frac{l^2}{j^2}\phi_l(j)^2\right] , \tag{3.A.5}$$

where $a$ is the lattice spacing and $r = ja$ and we introduced an IR cutoff $\Lambda_{IR} = Na$. The radius of the disk is taken to be:

$$R = \left(n + \frac{1}{2}\right) a \ . \tag{3.A.6}$$

The Hamiltonians (3.A.5) can be written in a general form

$$H = \frac{1}{2}\sum_{i=1}^{N} \Pi_i^2 + \frac{1}{2}\sum_{ij=1}^{N} \phi_i K_{ij} \phi_j \ , \tag{3.A.7}$$

and we are interested in the entanglement entropy $S(n, N)$ for the subset of degrees of freedom $\phi_\alpha, \alpha = 1, 2, \cdots n < N$ when the system is in the vacuum. The problem was solved in [5] and the result can be written as follows. Decompose $\Omega \equiv \sqrt{K}$ as

$$\Omega = \begin{pmatrix} A & B \\ B^T & C \end{pmatrix} \tag{3.A.8}$$

where $A$ has rank $n$ and let

$$\beta = \frac{1}{2} B^T A^{-1} B \, , \qquad \beta' = \frac{1}{\sqrt{C - \beta}} \beta \frac{1}{\sqrt{C - \beta}} \, , \qquad \Xi = \frac{\beta'}{1 + \sqrt{1 - \beta'^2}} \, . \tag{3.A.9}$$

Then, $S(n, N)$ can be written in terms of the $(N - n) \times (N - n)$ matrix $\Xi$ as

$$S(n, N) = -\ \mathrm{tr} \left[ \log(1 - \Xi) + \frac{\Xi}{1 - \Xi} \log \Xi \right] \ . \tag{3.A.10}$$

For our case:

$$\begin{aligned} K_l^{11} &= \frac{3}{2} + j^2 + m^2 \, , \\ K_l^{jj} &= 2 + \frac{l^2}{j^2} + m^2 \, , \\ K_l^{j,j+1} &= -\frac{j + 1/2}{\sqrt{j(j+1)}} = K_n^{j+1,j} \end{aligned} \tag{3.A.11}$$

and the entanglement entropy for a spherical region of radius $R$ can then be written as

$$S(R) = \sum_{l=-\infty}^{\infty} S_l(n, N) \tag{3.A.12}$$

where $S_l(n, N)$ is given by (3.A.10) with $\Xi_l$ obtained from (3.A.11) via (3.A.9) for each $l$.

To get $S_l(n, N)$ we need the eigenvalues of $\Xi_l$. It can be checked that all square roots and inversions are well defined, and all the eigenvalues of $\Xi_l$ lie between 0 and 1. One can also show that the sum over $l$ converges at fixed $n$, $N$.

For $m = 0$, $S(R)$ entropy should have the form

$$S(R) = c_1 \frac{R}{a} - s_3 + O\left(\frac{a}{R}, \frac{R}{\Lambda_{IR}}\right) \tag{3.A.13}$$

where $s_3$ is known analytically [93]

$$s_3 = \frac{1}{16}\left(2\log 2 - \frac{3\zeta(3)}{\pi^2}\right) \approx 0.0638\ . \tag{3.A.14}$$

From our numerical calculations we get for $m = 0$

$$c_1 = 0.4643821 \qquad s_3 = 0.0635 \pm 0.0004 \tag{3.A.15}$$

The calculations were performed with the choice of IR cutoff $N = 200$. To avoid the boundary effects from both the UV (small $n$) and IR (large $n$) cutoffs, we needed to restrict to the range $10 \leq n \leq 45$. We require $10^{-6}$ absolute accuracy for the result of the entropy calculation in order to be able to extract $\mathcal{S}_3(R)$ with satisfactory precision. To achieve this we followed the analysis of [94] which shows that the finite volume corrections (accounting for a finite $N$) go as $N^{-(2l+2)}$. With our choice $N = 200$, they are thus negligible for $l \geq 3$. For $l < 3$ we determine the coefficient of the correction by doing the calculation for several choices of $N > 200$ and extrapolate to infinite $N$. We refer the reader to [94] for details.

At finite $m$, given the limited range of $10 \leq n \leq 45$ (thus limited range of $R$) for

which we can do calculations for a given $m$, we extend the range of $mR$ by working with different choices of $m$ in lattice units. Since $\mathcal{S}_3(R)$ can only depend on $mR$ in the continuum limit, data points from different choices of $m$ should collapse into a single curve, and they indeed do. The results are shown in Fig. 3-1 of Sec. 3.2. Choosing $1/m = 20a$ enabled us to cover the range $0.55 < mR < 2.25$, while $1/m = 40a,\ 120a$ cover the range $0.275 < mR < 1.125$ and $0.09 < mR < 0.375$ respectively. In Fig. 3-1 one can see that in the overlapping regimes the data points agree, justifying the continuum extrapolation of the lattice results, i.e. the $\mathcal{S}_3(mR)$ determined here is independent of the discretization.

## 3.B Cylinder-like solutions

In this Appendix we discuss when a cylinder-like solution minimal surface could appear. We will show that for a bounded $f$, the minimal surface solution is always disk-like, while when $f(z) \sim z^n$ for large $z$, a cylinder-like solution can appear only when $n > 2$.

Extremizing the minimal surface action (3.3.23) leads to the equation of motion

$$(d-2)\frac{1}{f} + (d-1)\frac{\rho\rho'}{z} = \rho\sqrt{\rho'^2 + \frac{1}{f}}\,\partial_z\left(\frac{\rho'}{\sqrt{\rho'^2 + \frac{1}{f}}}\right) . \tag{3.B.1}$$

Let us first consider a bounded $f$, i.e. with asymptotic behavior

$$f(z) = f_0 + f_1 z^{-m} + \cdots , \quad m > 0, \quad z \to \infty . \tag{3.B.2}$$

Then with a cylinder-like solution

$$\rho(z) = \rho_0 + \rho_1 z^{\alpha} + \cdots , \quad \alpha < 0, \quad z \to \infty , \tag{3.B.3}$$

in the equation of motion (3.B.1), the leading term on the left hand side (LHS) is of order $O(1)$ while that on the right hand (RHS) is of order $O(z^{\alpha-2})$, and thus a

solution is not possible.

Now let us consider an unbounded $f(z)$ with the large $z$ behavior

$$f^{-1} = az^{-n}(1 + \cdots), \qquad n > 0, \quad z \to \infty . \tag{3.B.4}$$

With (3.B.3), in the equation of motion (3.B.1), the leading term on the left hand side is

$$\text{LHS} = (d-2)az^{-n} + (d-1)\rho_0\rho_1\alpha z^{\alpha-2} + \cdots . \tag{3.B.5}$$

The leading behavior on the RHS is given by

$$\text{RHS} = \begin{cases} -\frac{1}{2}\rho_0\rho_1\alpha(2-n-2\alpha)z^{-n-\alpha} & \alpha > 1 - \frac{n}{2} \\ \frac{1}{2}\rho_0\rho_1\alpha(n+2\alpha-2)z^{\alpha-2} & \alpha < 1 - \frac{n}{2} \\ \sim z^{-\beta}, \quad \beta > \frac{n}{2} + 1 & \alpha = 1 - \frac{n}{2} \end{cases} \tag{3.B.6}$$

Comparing (3.B.5) and (3.B.6) we find that the leading order equation can only be satisfied for the case of the second line of (3.B.6) with

$$\alpha = 2 - n . \tag{3.B.7}$$

Note that since $\alpha < 0$, this requires $n > 2$. We also find that the equation of motion requires

$$\rho_1 = \frac{2(d-2)a}{\rho_0(n-2)(n+2d-4)} . \tag{3.B.8}$$

We thus conclude that for $n > 2$, a cylinder-like solution could exist with the large $z$ behavior given by

$$\rho(z) = \rho_0 + \frac{2(d-2)a}{\rho_0(n-2)(n+2d-4)} z^{2-n} + \cdots, \quad z \to \infty . \tag{3.B.9}$$

We notice that in (3.B.9) the coefficient before the second term becomes singular when $\rho_0 \to 0$. This implies if there is a solution with $\rho_0 = 0$ it should comes with a larger power than (3.B.7). Writing for large $z$, $\rho(z) = \rho_1' z^{\alpha'} + \cdots$ with $\alpha' < 0$, we

again find that a solution is possible only for $n > 2$, for which the leading behavior of the solution is given by

$$\rho(z) = \sqrt{\frac{2(d-2)a}{(d-1)(n-2)}} z^{1-\frac{n}{2}} (1 + \cdots) \ . \tag{3.B.10}$$

Equation (3.B.10) describes a solution in which the minimal surface just closes off at $z = \infty$. Note that (3.B.10) can be considered as the $\rho_0 \to 0$ limit of (3.B.9) in the following sense. Equation (3.B.9) was derived assuming that the second term is much smaller than the first term, i.e. for

$$z^{n-2} \gg \frac{1}{\rho_0^2} \frac{2(d-2)a}{(n-2)(n+2d-4)} \equiv z_0^{n-2} \ . \tag{3.B.11}$$

When $\rho_0^2 \ll a$, equation (3.B.10) is valid in the region $1 \ll z < z_0$, while one has (3.B.9) for $z \gg z_0$. In the limit $\rho_0 \to 0$, $z_0 \to \infty$, and thus (3.B.10) becomes valid in the full large $z$ region.

The solution (3.B.10) can be considered as the critical surface lying at the boundary between the spaces of disk-like and cylinder-like solutions. As discussed in Sec. 3.4, indeed it appears to control the transition point of certain "second order phase transitions" from minimal surface of disk topology to cylindrical topology.

# Chapter 4

# Renormalized entanglement entropy in the vicinity of fixed points

## 4.1 Introduction and summary

For a general quantum field theory the REE can be interpreted as characterizing entanglement at scale $R$. In particular, the $R$-dependence can be interpreted as describing the renormalization group (RG) flow of entanglement entropy with distance scale. In [6], it was conjectured that in three spacetime dimension the REE for a sphere $\mathcal{S}_3^{\text{sphere}}$ is monotonically decreasing and non-negative for the vacuum of Lorentz invariant, unitary QFTs, providing a central function for the F-theorem conjectured previously in [20,21,23–25]. The monotonic nature of $\mathcal{S}_3^{\text{sphere}}$, and thus the F-theorem, was subsequently proved in [28]. In $(1+1)$-dimension, $\mathcal{S}_2$ reduces to an expression previously considered in [56, 57], where its monotonicity was also established. There are, however, some indications [6] that in four spacetime dimensions $\mathcal{S}_4^{\text{sphere}}$ is neither monotonic nor non-negative.

More generally, regardless of whether it is monotonic, REE provides a new set of

observables to probe RG flows.[1] From REE, one can introduce an "entropic function" defined in the space of couplings (or in other words the space of theories)

$$\mathcal{C}^{(\Sigma)}(g^a(\Lambda)) \equiv \mathcal{S}^{(\Sigma)}\left(R\Lambda, g^a(\Lambda)\right)\Big|_{R=\frac{1}{\Lambda}} = \mathcal{S}^{(\Sigma)}\left(1, g^a(\Lambda)\right) \tag{4.1.1}$$

where $g^a(\Lambda)$ denotes collectively all couplings and $\Lambda$ is the RG energy scale. Given that $\mathcal{S}^{(\Sigma)}$ is a measurable quantity, it should satisfy the Callan-Symanzik equation

$$\Lambda \frac{d\mathcal{S}^{(\Sigma)}\left(R\Lambda, g^a(\Lambda)\right)}{d\Lambda} = 0\ , \tag{4.1.2}$$

which leads to

$$\Lambda \frac{d\mathcal{C}^{(\Sigma)}(g^a(\Lambda))}{d\Lambda} = -R \frac{d\mathcal{S}^{(\Sigma)}\left(R\Lambda, g^a(\Lambda)\right)}{dR}\Big|_{R=\frac{1}{\Lambda}}\ . \tag{4.1.3}$$

The $R$-dependence of $\mathcal{S}^{(\Sigma)}$ is translated into the running of $\mathcal{C}^{(\Sigma)}(g(\Lambda))$ in the space of couplings, with $R \to 0$ and $R \to \infty$ limits correspond to approaching UV and IR fixed points of RG flows. At a fixed point $g_*$, $\mathcal{C}^{(\Sigma)}(g_*) = s_d^{(\Sigma)}$ and the monotonicity of $\mathcal{S}^{(\Sigma)}$ with respect to $R$ translates to the monotonicity of $\mathcal{C}^{(\Sigma)}$ with respect to $\Lambda$.

For $\Sigma$ being a sphere, some partial results were obtained earlier in [6, 33] for the small and large $R$ behavior of REE (or equivalently for $\mathcal{C}$ near a UV and IR fixed point) in holographic theories. From now on we will focus on a spherical region and suppress the superscript $(\Sigma)$ on $\mathcal{S}$ and $\mathcal{C}$. For a (UV) fixed point perturbed by a relevant operator of dimension $\Delta < d$, it was found that

$$\mathcal{S}_d(R) = s_d^{(\mathrm{UV})} - A(\Delta)(\mu R)^{2(d-\Delta)} + \cdots\ , \quad R \to 0 \tag{4.1.4}$$

where $\mu$ is a mass scale with the relevant (dimensional) coupling given by $g = \mu^{d-\Delta}$, and $A(\Delta)$ is some *positive* constant. The above equation leads to an entropic function given by

$$\mathcal{C}_d(g) = s_d^{(\mathrm{UV})} - A(\Delta) g_{eff}^2(\Lambda), \qquad \Lambda \to \infty \tag{4.1.5}$$

where $g_{eff}(\Lambda) = g\Lambda^{\Delta-d}$ is the effective dimensionless coupling at scale $\Lambda$. Equa-

[1] See [95, 96] for other ideas for probing RG flows using entanglement entropy.

tion (4.1.5) has a simple interpretation that the leading UV behavior of the entropic function is controlled by the two-point correlation function of the corresponding relevant operator. We expect this result to be valid also outside holographic systems. This appears to be also consistent with general arguments from conformal perturbation theory [97]. It is curious, however, that low dimensional free theories defy this expectation. For example in $d = 2$, as $R \to 0$ [30–32]

$$\text{free scalar}: \qquad \mathcal{S}_2(R) = \frac{1}{3} + \frac{1}{\log\left(m^2R^2\right)} + \cdots \tag{4.1.6}$$

$$\text{Dirac fermion}: \qquad \mathcal{S}_2(R) = \frac{1}{3} - 4m^2R^2\,\log^2\left(m^2R^2\right) + \cdots\,, \tag{4.1.7}$$

while for a $d = 3$ free massive scalar [98] ruled out the $m^4R^4$ short distance behavior based on numerics.[2] It is interesting that the logarithmic terms in (4.1.6), (4.1.7) do not appear in holographic theories. The physical origin of these terms is not fully understood, and it would be desirable to have a field theory computation that reproduces both (4.1.4) and (4.1.6), (4.1.7).

Near an IR fixed point, it was argued in [6] that the large $R$ behavior of $\mathcal{S}(R)$ should have the form

$$\begin{aligned}\mathcal{S}_d(R) &= s_d^{(\mathrm{IR})} + \frac{B(\tilde{\Delta})}{(\tilde{\mu}R)^{2(\tilde{\Delta}-d)}} + \cdots \\ &\quad + \begin{cases} \frac{s_1}{\tilde{\mu}R} + \frac{s_3}{(\tilde{\mu}R)^3} + \cdots & \text{odd } d \\ \frac{s_2}{(\tilde{\mu}R)^2} + \frac{s_4}{(\tilde{\mu}R)^4} + \cdots & \text{even } d \end{cases}, \quad R \to \infty\,,\end{aligned} \tag{4.1.8}$$

where $\tilde{\Delta} > d$ is the dimension of the leading irrelevant operator, $\tilde{\mu}$ is a mass scale characterizing the irrelevant perturbation, and $B(\tilde{\Delta})$ is a constant. The first line, similar to (4.1.4), has a natural interpretation in terms of conformal perturbations of the IR fixed point. The coefficient $B(\tilde{\Delta})$ is expected to depend only on physics of the IR fixed point. In terms of irrelevant coupling $\tilde{g} = \tilde{\mu}^{d-\Delta}$ corresponding to the leading

[2]Note that the relevant deformation of the massless scalar UV fixed point, $\phi^2$ has dimension $\Delta = 1$, hence (4.1.4) would predict an $m^4R^4$ behavior.

irrelevant operator, equation (4.1.8) leads to

$$\begin{aligned} C(\Lambda) &= s_d^{(\mathrm{IR})} + B(\tilde{\Delta})\tilde{g}_{eff}^2(\Lambda) + \cdots \\ &\quad + \begin{cases} s_1 \tilde{g}_{eff}^{\frac{1}{\tilde{\Delta}-d}}(\Lambda) + \cdots & \text{odd } d \\ s_2 \tilde{g}_{eff}^{\frac{2}{\tilde{\Delta}-d}}(\Lambda) + \cdots & \text{even } d \end{cases}, \quad \Lambda \to \infty \,, \end{aligned} \tag{4.1.9}$$

where $\tilde{g}_{eff}(\Lambda) = \tilde{g}\Lambda^{\tilde{\Delta}-d}$ is the effective dimensionless coupling at scale $\Lambda$. It is amusing that the "analytic" contributions in $1/R$ in (4.1.8) lead to non-analytic dependence on the coupling while non-analytic contributions in $1/R$ lead to analytic dependence on the coupling. Note the first line dominates for

$$\tilde{\Delta} < \begin{cases} d + \frac{1}{2} & \text{odd } d \\ d + 1 & \text{even } d \end{cases} \tag{4.1.10}$$

i.e. if the leading irrelevant operator is not too irrelevant. Note in this range $B(\tilde{\Delta}) > 0$. The second line of (4.1.8)-(4.1.9) can be expected from (2.2.4): the contributions of any degrees of freedom at some lengths scale $\ell \ll R$ should have an expansion of the form (2.2.4). Thus the coefficients $s_n$ are expected to depend on the RG trajectory from the cutoff scale $\delta$ to $R$.[3]

Support for (4.1.8) was provided in [6] by examining holographic RG flows between two closely separated fixed points. In this chapter we prove (4.1.8) for all Lorentz invariant holographic flows with an IR conformal fixed point, which is described on the gravity side by a domain wall geometry interpolating between two AdS spacetimes of different cosmological constant. In particular, we show that $B(\tilde{\Delta})$ is the same as that obtained earlier for RG flows between two closely separated fixed points; this is consistent with the expectation that it should only depend on the physics at the IR fixed point. We obtain a general expression for $s_1$ in $d = 3$ in terms of an integral of the spacetime metric over the full spacetime. With more diligence, other coefficients in generic $d$ dimensions can be straightforwardly obtained using our techniques, although

[3]Since here we consider the $R \to \infty$ limit $s_n$ should thus depend on the full RG trajectory from $\delta$ to $\infty$.

we will not determine them here.

In addition to domain wall geometries, we also consider a class of geometries, which are singular in the IR. These correspond to either gapped systems, or systems whose IR fixed point does not have a gravity description (or has degrees of freedom smaller than $O(N^2)$). We will see that for these geometries the asymptotic behavior of REE provides a simple diagnostic of IR gapless degrees of freedom.

While in this chapter we focus on the vacuum flows, the techniques we develop can be used to obtain the large $R$ expansion of the entanglement entropy for generic static holographic geometries, including nonzero temperature and chemical potential. As an illustration we study the behavior of extremal surfaces in a general black hole geometry in the large size limit. We also show that, in this limit, for *any shape* of the entangling surface the leading behavior of the EE is the thermal entropy. While this result is anticipated, a general holographic proof appears to be lacking so far.

For $d = 2, 3$, the monotonicity of $\mathcal{S}_d$ in $R$ leads to a monotonic $\mathcal{C}_d$ in coupling space, i.e. $\mathcal{C}_d$ is a c-function. Equations (4.1.6)–(4.1.7) show that for a free massive field, $\mathcal{C}_2$ is not stationary near the UV fixed point, and neither is $\mathcal{C}_3$ for a free massive scalar field, as pointed out in [98]. From (4.1.9) we see that $\mathcal{C}_d$ is in fact generically non-stationary near an IR fixed point for $\tilde{\Delta} - d > \frac{1}{2}$ ($\tilde{\Delta} - d > 1$) for odd (even) dimensions. The physical reason behind the non-stationarity is simple: while the contribution from degrees of freedom at short length scales are suppressed in $\mathcal{S}_d$, they are only suppressed as a fixed inverse power of $R$, and are the dominant subleading contribution, when the leading irrelevant operator is sufficiently irrelevant. The non-stationarity of $\mathcal{S}$ (or $\mathcal{C}$) is independent of the monotonic nature of $\mathcal{S}$ (or $\mathcal{C}$) and should not affect the validity of c- or F-theorems. In contrast to the Zamolodchikov c-function [8], which is stationary, in our opinion, the non-stationarity of $\mathcal{C}$ should be considered as an advantage, as it provides a more sensitive probe of RG flows. For example, from (4.1.9) by merely examining the leading approach to an IR fixed point, one could put constraints on the dimension of the leading irrelevant operator.

While in this chapter we will be mainly interested in taking the entangling surface to be a sphere of radius $R$, for comparison we also examine the IR behavior for a

strip. Since the boundary of a strip is not scalable, the definition (1.2.4) has to be modified. Consider a strip

$$x_1 \in (-R, R), \quad x_i \in (0, \ell), \quad i = 2, \cdots, d-1 \tag{4.1.11}$$

where for convenience we have put other spatial directions to have a finite size $\ell \to \infty$. Note that due to translational symmetries of the entangled region in $x_i$ directions, the EE should have an extensive dependence on $\ell$, i.e. it should be proportional to $\ell^{d-2}$. Furthermore, for the boundary of a strip the extrinsic curvature and all tangential derivatives vanish. Hence we conclude that the only divergence is the area term

$$S_{\text{strip}}(R) = \ell^{d-2} \left( \frac{\#}{\delta^{d-2}} + \text{finite} \right) . \tag{4.1.12}$$

In particular, the divergent term should be $R$-independent. This thus motivates us to consider $R\frac{dS}{dR}$, which should be finite and devoid of any cutoff dependent ambiguities. Given that all the dependence in $S$ on $\ell$ comes from the over factor $\ell^{d-2}$, it is convenient to introduce dimensionless quantity $\mathcal{R}_d$ defined by

$$R\frac{dS}{dR} \equiv \frac{\ell^{d-2}}{R^{d-2}} \mathcal{R}_d(R) . \tag{4.1.13}$$

This quantity was considered earlier in [22,76]. For a CFT there is no scale other than $R$, hence $\mathcal{R}_d$ should be a $R$-independent constant, which can be readily extracted from expressions in [22,61]. For a general QFT, $\mathcal{R}_d$ should be a dimensionless combination of $R$ and other possible mass scales of the system.

Calculating $\mathcal{R}_d$ for a domain wall geometry describing flows among two conformal fixed points, we find an interesting surprise. The second line of (4.1.8) can be understood from a local curvature expansion associated with a spherical entangling surface. Such curvature invariants altogether vanish for a strip and thus one may expect that for a strip only the first line of (4.1.8) should be present. We find instead find that

$\mathcal{R}_d$ has the large $R$ behavior

$$\begin{aligned}\mathcal{R}_d(R) &= \mathcal{R}_d^{(IR)} + c(\tilde{\Delta})(\tilde{\mu}R)^{-2(\tilde{\Delta}-d)} + \dots \\ &\quad + t_d(\tilde{\mu}R)^{-d} + \dots \ , \end{aligned} \tag{4.1.14}$$

where $\mathcal{R}_d^{(IR)}$ is $R$-independent constant characterizing the IR fixed point, $c(\tilde{\Delta})$ is a constant which depends only on the IR data, while the constant $t_d$ involves an integral over the whole radial direction, signaling that this term receives contributions from degrees of freedom of all length scales. Note that similarly to the sphere case, the terms in the second line is the leading approach to the IR fixed point value for $\tilde{\Delta} > 3d/2$. Note that the terms we find come from the following terms in $S_{\text{strip}}(R)$:

$$\begin{aligned}S_{\text{strip}}(R) &= \ell^{d-2}\left(\frac{\#}{\delta^{d-2}} - \frac{\mathcal{R}_d^{(IR)}}{(d-2)\,R^{d-2}} - \frac{c(\tilde{\Delta})}{(2\tilde{\Delta}-d-2)\tilde{\mu}^{2(\tilde{\Delta}-d)}}\,R^{-(2\tilde{\Delta}-d-2)} + \dots \right. \\ &\quad \left. - \frac{t_d}{2(d-1)\tilde{\mu}^d}(\tilde{\mu}R)^{-2(d-1)} + \dots\right) \ . \end{aligned} \tag{4.1.15}$$

It would be interesting to see, whether it is possible to identify a geometric origin for the terms in the second line.

The chapter is organized as follows. In Sec. 3.3.1 we discuss the holographic geometries to be considered, and outline a general strategy to obtain the large $R$ expansion of REE for a spherical region for generic holographic geometries. In Sec. 4.2 we consider holographic theories which are gapped or whose IR fixed point does not have a good gravity description. In Sec. 4.3 we elaborate more on the physical interpretation of such geometries and consider some explicit examples. In Sec. 4.4 we consider domain wall geometries with an IR conformal fixed point. We conclude in Sec. 4.5 with some applications of the formalism to the black hole geometry.

### 4.1.1 Leading small $R$ dependence

In this section we examine the leading small and large $R$-dependence of $\mathcal{S}_d(R)$.

When $R$ is small, the range of $z$ covered by the minimal surface is also small. Thus we can use the asymptotic form (3.3.5) of the function $f(z) = 1 + \delta f + \cdots$

with $\delta f = (\mu z)^{2\alpha}$, and treat the deviation from pure AdS as a small perturbation. To first order in $\delta f$, equation (4.D.6) then again applies with $g$ there replaced by $\delta f$. The calculation then becomes very similar to that of section 3.3.5, and we find the following leading behavior

$$\mathcal{S}_d(R) = \mathcal{S}_d^{(\mathrm{UV})} - \frac{(d-1)!!}{(d-2)!!}\frac{K}{2}a(\alpha)(\mu R)^{2\alpha} + \cdots, \quad R \to 0 \tag{4.1.16}$$

with $\mathcal{S}_d^{(\mathrm{UV})}$ given by (3.3.31) and $a(\alpha)$ is given by

$$a(\alpha) = \begin{cases} \frac{1}{1+2\alpha} & \text{d odd} \\ \frac{\sqrt{\pi}\Gamma(1+\alpha)}{2\Gamma\left(\frac{3}{2}+\alpha\right)} & \text{d even} \end{cases} . \tag{4.1.17}$$

Recall that for a source deformation $\alpha = d - \Delta$ where $\Delta$ is the UV dimension of the leading relevant operator. Equation (4.1.4) has a simple interpretation that the leading contribution from a relevant operator comes at two-point level, and should be valid also outside holographic systems. Also note that the sign of the numerical coefficient in (4.1.16) is such that at this order $\mathcal{S}_d(R)$ is monotonically decreasing with $R$.

### 4.1.2 Leading large $R$ dependence for closely separated fixpoints

In the large $R$ limit, estimating the leading $R$-dependent correction to the asymptotic value $\mathcal{S}_d(R \to \infty) = \mathcal{S}_d^{(\mathrm{IR})}$ for a general holographic system becomes more challenging. Here we will consider the case of two closely separated fixed points discussed in the last subsection where we can take advantage of the closed expressions (3.3.52) and (3.3.53). At large $R$, the argument $xR$ for $g(xR)$ is large except near $x = 0$, thus we should be able to use the asymptotic expansion of $g(z)$ for large $z$ (from (3.3.7) and (3.3.45)),

$$g(z) = 1 - (\tilde{\mu} z)^{-2\tilde{\alpha}} + \cdots . \tag{4.1.18}$$

Recall that $\tilde{\alpha} = \Delta_{\rm IR} - d$ where $\Delta_{\rm IR}$ is the IR scaling dimension of the leading irrelevant operator at the IR fixed point. Plugging (4.1.18) into (3.3.52) and (3.3.53), the 1 in (4.1.18) will give (3.3.55). To to first order in $\epsilon$ we can write

$$\mathcal{S}_d(R) = \mathcal{S}_d^{(\rm IR)} + I_d(R) + O(\epsilon^2) \tag{4.1.19}$$

where

$$I_d(R) = \frac{(d-1)!!}{(d-2)!!}\frac{\epsilon K}{2}\int_0^1 dx \frac{1}{(\tilde{\mu}Rx)^{2\tilde{\alpha}}} \begin{cases} 1 + \cdots & \text{odd d} \\ \frac{x}{\sqrt{1-x^2}} + \cdots & \text{even d} \end{cases} . \tag{4.1.20}$$

In (4.1.20) the $\cdots$ denotes contributions from higher order terms in (4.1.18) (represented by $\cdots$ there). Now notice that the integral in (4.1.20) becomes divergent when $\tilde{\alpha} \geq \frac{1}{2}$ for odd $d$ and $\tilde{\alpha} \geq 1$ for even $d$. In fact, even if the leading term in (4.1.20) is convergent, higher order terms in (4.1.18) will still eventually lead to divergent integrals (and will be more and more divergent). Physically such divergences reflect that higher order terms in the expansion of $g$ are more irrelevant and thus are more sensitive to the short-distance structure near $x = 0$.

When (4.1.20) is convergent we find

$$I_d(R) = \frac{(d-1)!!}{(d-2)!!}\frac{\epsilon K}{2}\frac{b(\tilde{\alpha})}{(\tilde{\mu}R)^{2\tilde{\alpha}}} + \cdots \tag{4.1.21}$$

with

$$b(\tilde{\alpha}) = \begin{cases} \frac{1}{1-2\tilde{\alpha}} & \tilde{\alpha} < \frac{1}{2}, \quad \text{d odd} \\ \frac{\sqrt{\pi}\Gamma(1-\tilde{\alpha})}{2\Gamma(\frac{3}{2}-\tilde{\alpha})} & \tilde{\alpha} < 1, \quad \text{d even} \end{cases} . \tag{4.1.22}$$

Now using odd $d$ for illustration, consider $\tilde{\alpha} > \frac{1}{2}$. Since the large $R$ expansion of $g$ assumes that $\tilde{\mu}z \gg 1$, we should split the integral at $x \sim \frac{1}{\tilde{\mu}R}$, i.e.

$$\int_0^1 dx\, g(xR) = \int_0^{\frac{1}{\tilde{\mu}R}} g(xR) + \int_{\frac{1}{\tilde{\mu}R}}^1 dx g(xR) . \tag{4.1.23}$$

Since $g(z)$ is well defined near $z = 0$, the first term in the above is convergent and

is of order $O(\frac{1}{\tilde{\mu}R})$. Now plugging the large $R$ expansion of $g$ into the second term of (4.1.23) we find the previously divergent term becomes

$$\frac{1}{(\tilde{\mu}R)^{2\tilde{\alpha}}}\int_{\frac{1}{\tilde{\mu}R}}^{1} dx\, x^{-2\tilde{\alpha}} \sim \frac{1}{\tilde{\mu}R} + \cdots \,. \tag{4.1.24}$$

Similarly, the leading contribution of a term of the form $z^{-n}$ with $n > 1$ in the large $z$ expansion of $g(z)$ will always be of order $O(R^{-1})$ regardless of the value of $n$. We thus conclude that for $\tilde{\alpha} > \frac{1}{2}$

$$I_d(R,\tilde{\alpha}) \sim \frac{1}{\tilde{\mu}R} \tag{4.1.25}$$

where the numerical coefficient now receives the contribution from all orders of the large $z$ expansion of $g(z)$. We treat this problem with the technique of subtractions in Appendix 4.E, and determine the prefactor of the $\frac{1}{\tilde{\mu}R}$ term. When $\tilde{\alpha} < \frac{1}{2}$, then the leading dependence is given by (4.1.21) as potentially divergent higher order terms give only a contribution which is of order $O(\frac{1}{\tilde{\mu}R})$ and is subleading compared to (4.1.21).

Exactly the same can be said regarding (3.3.53) for even $d$ except that the range becomes $\tilde{\alpha} > 1$ and the leading order contribution becomes of order $O(R^{-2})$.

We thus conclude that

$$\mathcal{S}_d(R) = \mathcal{S}_d^{(\mathrm{IR})} + \frac{(d-1)!!}{(d-2)!!}\frac{\epsilon K}{2}\frac{b(\tilde{\alpha})}{(\tilde{\mu}R)^{2\tilde{\alpha}}} + O(\epsilon^2), \quad \tilde{\alpha} < \begin{cases} \frac{1}{2} & \text{d odd} \\ 1 & \text{d even} \end{cases} \tag{4.1.26}$$

with $b(\tilde{\alpha})$ given by (4.1.22), and

$$\mathcal{S}_d(R) = \mathcal{S}_d^{(\mathrm{IR})} + \epsilon K \begin{cases} \frac{s_1}{\tilde{\mu}R} & \tilde{\alpha} > \frac{1}{2} \text{ (odd d)} \\ \frac{s_2}{(\tilde{\mu}R)^2} & \tilde{\alpha} > 1 \text{ (even d)} \end{cases} + O(\epsilon^2)\,, \tag{4.1.27}$$

where $s_1$ and $s_2$ are a functional of $g(z)$:

$$\begin{aligned} s_1 &= \frac{(d-1)!!\,\tilde{\mu}}{2(d-2)!!}\int_0^\infty dz\ z g'(z)\ , \\ s_2 &= \frac{(d-1)!!\,\tilde{\mu}^2}{4(d-2)!!}\int_0^\infty dz\ z^2 g'(z)\ , \end{aligned} \tag{4.1.28}$$

where the integrals are convergent for $\tilde{\alpha} > \frac{1}{2}$ and $\tilde{\alpha} > 1$ respectively. In Appendix 4.E we also determine the result, when $\tilde{\alpha}$ is outside of these ranges.

Note that equations (4.1.27) agree with the general expectation (2.2.14) of Sec. 2.2. Here we find that when the IR dimension of the involved irrelevant operator is not too large one should instead have (4.1.26), which can be considered as predictions from the holographic duality.

Finally when $\tilde{\alpha} = \frac{1}{2}$ for odd $d$ and $\tilde{\alpha} = 1$ for even $d$, similar argument leads to

$$\mathcal{S}_d(R) = \mathcal{S}_d^{(\mathrm{IR})} + \frac{(d-1)!!}{(d-2)!!}\frac{cK}{2}\begin{cases} \frac{\log\tilde{\mu}R}{\tilde{\mu}R} & \tilde{\alpha} = \frac{1}{2}\ (\text{odd d}) \\ \frac{\log\tilde{\mu}R}{(\tilde{\mu}R)^2} & \tilde{\alpha} = 1\ (\text{even d}) \end{cases} + \cdots\ . \tag{4.1.29}$$

### 4.1.3 Strategy for obtaining the entanglement entropy for a sphere

In general it is not possible to solve (3.3.27) or (3.3.28) exactly. Here we outline a strategy to obtain the large $R$ expansion of $S(R)$ (or $\mathcal{S}_d(R)$) via a matching procedure:

1. Expand $\rho(R)$ in (3.3.27) in $1/R$ as

$$\rho(z) = R - \frac{\rho_1(z)}{R} - \frac{\rho_3(z)}{R^3} + \cdots - \frac{\hat{\rho}(z)}{R^\nu} + \dots\ . \tag{4.1.30}$$

Note that the above expansion applies to the vacuum. For a black hole geometry one should include all integer powers of $1/R$ as we will discuss in more detail in section 4.5. The expansion (4.1.30) should be considered as an ansatz, motived by (4.1.8) one wants to show, but should be ultimately confirmed by the mathematical consistency of the expansion itself (and the matching described

below).

Depending on the IR behavior of a system, the large $R$ expansion (4.1.30) can contain terms which are not odd powers of $1/R$. We have denoted the exponent of the first such term in (4.1.30) as $\nu$, whose value will be determined later. The expansion is valid for $\rho(z)$ close to $R$, i.e. $\frac{\rho_1}{R} \ll R$ etc. It is clearly valid near the boundary (i.e. small $z$ where (3.3.37) applies), but depending on the configuration of the minimal surface it may also apply to regions, where $z$ is not small, as far as higher order terms in (4.1.30) remain small compared to $R$.

2. Determine the IR part (i.e. in the region where (3.3.6) or (3.3.8) applies) of the minimal surface in a large $R$ expansion. This has to be done case by case, as the IR expansions are different for different IR geometries.

3. Match the two solutions in the appropriate matching region. At the end of the matching procedure all free constants get determined including $c_d(R)$ of (3.3.37).

See Fig. 4-1 for an illustration of the matching procedure and in Fig. 4-2 we show how the minimal surfaces look for different IR geometries.

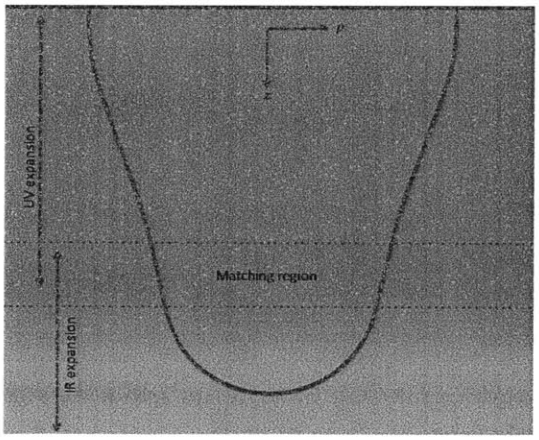


Figure 4-1: Sketch of the $R \to \infty$ minimal surface in a domain wall geometry (3.3.2)–(3.3.6). The violet and red regions represent the UV and IR regions of the expansion. The UV and IR solutions overlap in the matching region, which is used to determine the parameters of the two expansions.

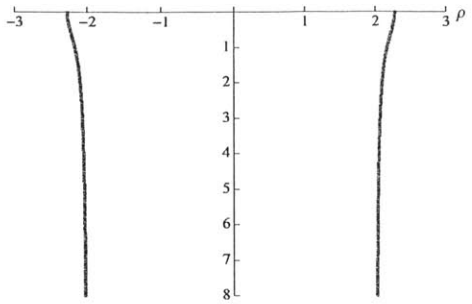


(a) Minimal surface for a gapped geometry (3.3.8) with $n > 2$.

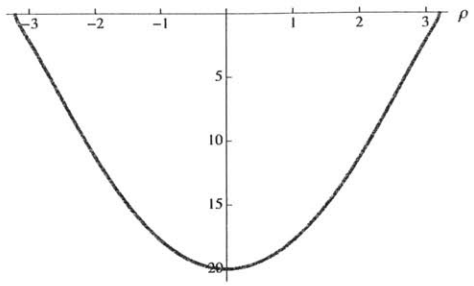


(b) Minimal surface for a scaling geometry with $0 < n < 2$.

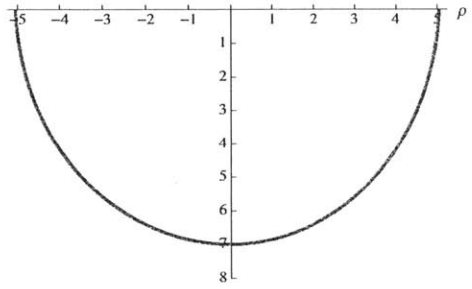


(c) Minimal surface for a domain wall geometry with IR geometry given by (3.3.6).

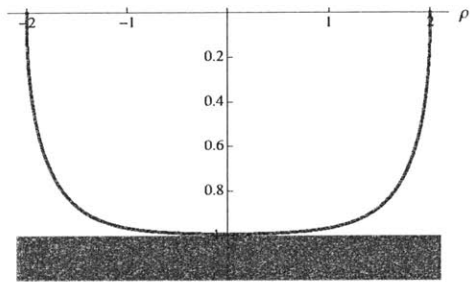


(d) Minimal surface for a Schwarzshild black hole. The beyond the horizon region is marked by gray.

Figure 4-2: Samples of minimal surfaces for IR geometries that fall into four different categories.

From (4.1.30) we see that $c_d(R)$ in (3.3.37) takes the following expansion

$$c_d(R) = -\frac{b_1}{dR} - \frac{b_3}{dR^3} + \cdots - \frac{\hat{b}}{dR^\nu} + \cdots , \tag{4.1.31}$$

where $b_n$ and $\hat{b}$ are some $R$-independent constants. It follows from (3.3.38) and (1.2.4) that a term proportional to $1/R^n$ in (4.1.31) contributes to $\mathcal{S}_d$ a term of order $1/R^{n-d+1}$, whose coefficient contains a factor $(n-1)(n-3)\cdots(n-(d-2))$ for odd $d$, or $(n-1)(n-3)\cdots(n-(d-3))$ for even $d$. Thus, among the integer powers of $1/R$ in (4.1.31), in odd $d$ the first possible nonvanishing contribution to $\mathcal{S}_d$ comes from $b_d$ giving a term proportional to $1/R$, and in even $d$ the first possible nonvanishing contribution comes from $b_{d-1}$ giving a term of order $O(R^0)$. Furthermore, the terms in (4.1.31) with odd integer powers will only give rise to odd inverse powers of $R$ in

odd dimensions and even inverse powers in even dimensions, as in the second line of (4.1.8). Finally from (3.3.38) and (1.2.4), a term proportional to $R^{-\nu}$ in (4.1.31) gives a contribution

$$\mathcal{S}_d(R) = \cdots + R^{d-1-\nu} \frac{K\,\hat{b}}{(d-1-\nu)\,\Gamma(\frac{1-\nu}{2})\,\Gamma(\frac{d}{2})} \begin{cases} \sqrt{\pi}\,\Gamma(\frac{d-\nu}{2}) & \text{odd } d \\ 2\,\Gamma(\frac{d+1-\nu}{2}) & \text{even } d \end{cases} + \cdots \ . \tag{4.1.32}$$

### 4.1.4 UV expansion

We now examine more explicitly the UV expansion (4.1.30) for the sphere, which is the same for all geometries of the form (3.3.2). The IR expansion and matching will be discussed in later sections case by case.

The equation for $\rho_i(z)$ can be written as

$$\frac{z^{d-1}}{\sqrt{f}} \left( \frac{\sqrt{f}}{z^{d-1}} \rho_i' \right)' = s_i \ , \tag{4.1.33}$$

where $s_i$ denotes a source from lower order terms with, for example,

$$s_1 = -\frac{d-2}{f} \ . \tag{4.1.34}$$

The equation for $\rho_1$ can be readily integrated to give

$$\rho_1(z) = b_1 \rho_{hom}(z) - (d-2) \int_0^z du\, \frac{u^{d-1}}{\sqrt{f(u)}} \int_\infty^u dv\, \frac{1}{v^{d-1}\sqrt{f(v)}} \ , \tag{4.1.35}$$

where $b_1$ is an integration constant and $\rho_{hom}$ is the homogenous solution to (4.1.33)

$$\rho_{hom}(z) = \int_0^z du\, \frac{u^{d-1}}{\sqrt{f(u)}} \ . \tag{4.1.36}$$

In particular because its unique $R$-dependence there are no source terms for $\hat{\rho}(z)$, thus it takes the form:

$$\hat{\rho}(z) = \hat{b}\rho_{hom}(z) \ . \tag{4.1.37}$$

As $z \to 0$, $\rho_1$ and $\hat{\rho}$ has the leading behavior (for $d \geq 2$)

$$\rho_1(z) = O(z^2), \qquad \hat{\rho}(z) = \frac{\hat{b}}{d} z^d + \cdots . \tag{4.1.38}$$

Note that the normalization of $\rho_{hom}$ in (4.1.37) was chosen such that the contribution to $c_d(R)$, read off from (4.1.38), gives the term appearing in (4.1.31).

## 4.2 Gapped and scaling geometries

In this section we consider the large $R$ behavior of the REE for holographic systems, whose IR geometry is described by (3.3.8). As mentioned below (3.3.8) there is an important difference between $n > 2$ and $n \leq 2$, to which we refer as gapped and scaling geometries respectively. For comparison we will treat them side by side. We will first consider the strip and then the sphere case.

### 4.2.1 Strip

In (3.3.17) to leading order in large $z_t$, we can replace $f(z)$ in the integrand by its large $z$ behavior $f(z) = az^n$, leading to

$$R(z_t) = z_t \left[ \int_0^1 dv \, \frac{v^{d-1}}{\sqrt{a(z_t v)^n (1 - v^{2(d-1)})}} + \cdots \right] = \frac{\alpha}{\sqrt{a}} z_t^{1-\frac{n}{2}} + \cdots , \quad z_t \to \infty \tag{4.2.1}$$

with

$$\alpha = \frac{2\sqrt{\pi}\,\Gamma\left(\frac{1}{2} + \frac{\eta}{4}\right)}{(2-n)\,\Gamma\left(\frac{\eta}{4}\right)}, \qquad \eta \equiv \frac{2-n}{d-1} . \tag{4.2.2}$$

For small $z_t$ we can replace $f(z_t v)$ in (3.3.17) by 1 and thus

$$R(z_t) = \frac{z_t}{d} + \cdots , \qquad z_t \to 0 . \tag{4.2.3}$$

For $n > 2$, the function $R(z_t)$ then goes to zero for both $z_t \to 0$ and $z_t \to \infty$, and

thus must have a maximum in between at some $z_t^{(max)}$. Introducing

$$R_{max} = z_t^{(max)} \int_0^1 dv \, \frac{v^{d-1}}{\sqrt{f(z_t^{(max)} v)(1 - v^{2(d-1)})}} \tag{4.2.4}$$

we conclude that for $R > R_{max}$ there is no minimal surface with strip topology. Instead, the minimal surface is just two disconnected straight planes $x(z) = \pm R$. The minimal surface area is independent from $R$ due to the translational symmetry of the problem. We conclude that for $n > 2$ in the $R \to \infty$ limit $S$ becomes independent of $R$, hence $\mathcal{R}_d(R > R_{max}) = 0$. For $n = 2$, $R(z_t) \to$ const at large $z_t$, and again in this case there is no minimal surface of strip topology and $\mathcal{R}_d(R > R_{max}) = 0$.

For $n < 2$, inserting (4.2.1) into (3.3.21) we find that

$$\mathcal{R}_d = \frac{L^{d-1}}{2G_N} \left( \frac{\alpha^2}{aR^n} \right)^{\frac{1}{\eta}} + \cdots \propto R^{-\beta} \,, \quad 0 < n < 2 \tag{4.2.5}$$

with

$$\beta = n \frac{d-1}{2-n} = \frac{n}{\eta} \,. \tag{4.2.6}$$

This result also applies to a hyperscaling violating geometry (3.3.11), and agrees with the scaling derived in [74].

### 4.2.2 Sphere

Since for $d = 2$, the sphere and strip coincide (the answer is then given by (4.2.5)), we will restrict our discussion below to $d \geq 3$.

#### IR expansion

We first consider the behavior of the minimal surface in the IR geometry (3.3.8). Plugging $f(z) = az^n$ into (3.3.27) we notice that if $\bar{\rho}(z)$ satisfies the resulting equation with $a = 1$, then

$$\rho(z) = \bar{\rho}\left( a^{-\frac{1}{2-n}} z \right) \tag{4.2.7}$$

satisfies (3.3.27) for any $a$. Furthermore, equation (3.3.27) is invariant under the scaling

$$\rho \to \lambda^{\frac{2-n}{2}} \rho \ , \qquad z \to \lambda z \ , \tag{4.2.8}$$

which implies that if $\rho(z)$ is a solution to (3.3.27), so is $\rho_\lambda(z) = \lambda^{\frac{2-n}{2}} \rho(\lambda^{-1} z)$.

Solutions of two different topologies are possible. As discussed in [6], for $n > 2$, in the large $R$ limit the minimal surface has the topology of a cylinder, while for $n \leq 2$, the minimal surface has the topology of a disk. See Fig. 4-2a and Fig. 4-2b.

For a solution of cylinder topology (i.e. for $n > 2$) the IR solution satisfies

$$\rho(z) \to \rho_0, \quad \Rightarrow \quad \rho_\lambda(z) \to \lambda^{\frac{2-n}{2}} \rho_0, \qquad z \to \infty \ . \tag{4.2.9}$$

Introducing a solution $\bar{\rho}_c(z)$ to (3.3.27) with $a = 1$, which satisfies the condition

$$\bar{\rho}_c(z \to \infty) = 1 \ , \tag{4.2.10}$$

we can write a general $\rho(z)$ in a scaling form

$$\rho(z) = \rho_0 \bar{\rho}_c(v), \qquad v \equiv (\rho_0^2 a)^{\frac{1}{n-2}} z \ . \tag{4.2.11}$$

From (3.3.27), $\rho(z)$ has the large $z$ expansion (see also Appendix C of [6])

$$\rho(z) = \rho_0 + \frac{2(d-2)}{\rho_0 a (n-2)(n+2d-4)} z^{2-n} + \cdots , \quad z \to \infty, \quad n > 2 \ . \tag{4.2.12}$$

For a solution of disk topology (i.e. for $n \leq 2$), there should exist a $z_t < \infty$, where

$$z_t = z(\rho = 0) \quad \text{or} \quad \rho(z_t) = 0 \ . \tag{4.2.13}$$

Now introducing a solution $\bar{\rho}_d(z)$ to (3.3.27) with $a = 1$, which satisfies the boundary condition $\bar{\rho}_d(1) = 0$, we can write $\rho(z)$ in a scaling form

$$\rho(z) = \frac{z_t^{(2-n)/2}}{\sqrt{a}} \bar{\rho}_d(u) , \quad \text{with} \quad u \equiv \frac{z}{z_t}, \quad \bar{\rho}_d(u = 1) = 0 \ . \tag{4.2.14}$$

Note that by taking $z_t$ sufficiently large, $u$ can be small even for $z \gg z_{CO}$, where (3.3.8) applies. Expanding $\bar{\rho}_d$ in *small* $u$ one finds that

$$\begin{aligned} \bar{\rho}_d(u) &= \bar{\alpha}_0 + \frac{\alpha_1}{\bar{\alpha}_0} u^{2-n} + \frac{\alpha_2}{\bar{\alpha}_0^3} u^{2(2-n)} + \cdots \\ &+ \frac{\bar{h}}{\bar{\alpha}_0^{\frac{2}{\eta}}} u^{d-n/2} + \cdots , \quad u \to 0 , \end{aligned} \tag{4.2.15}$$

where $\eta$ was introduced in (4.2.2) and

$$\alpha_1 = -\frac{2(d-2)}{(2-n)(2d-4+n)} , \quad \cdots . \tag{4.2.16}$$

$\bar{\alpha}_0$ and $\bar{h}$ are numerical constants that can be obtained by numerically solving the equation of motion. Using (4.2.15), we then get the expansion for $\rho(z)$:

$$\begin{aligned} \rho(z) &= \alpha_0 + \frac{\alpha_1}{a\alpha_0} z^{2-n} + \frac{\alpha_2}{a^2\alpha_0^3} z^{2(2-n)} + \cdots \\ &+ \frac{\bar{h}}{a^{\frac{1}{\eta}+\frac{1}{2}} \alpha_0^{\frac{2}{\eta}}} z^{d-n/2} + \cdots \end{aligned} \tag{4.2.17}$$

with

$$\alpha_0 \equiv \frac{\bar{\alpha}_0 \, z_t^{(2-n)/2}}{\sqrt{a}} . \tag{4.2.18}$$

This is all the information we need about the IR solution. Note that the above expansion applies to the range of $z$, which satisfies

$$z \gg z_{CO}, \qquad \frac{z}{z_t} \ll 1 . \tag{4.2.19}$$

The small $u$ expansion (4.2.15) is singular for $n = 2$, as can be seen from (4.2.16). Hence the $n = 2$ case should be treated separately, see Appendix 4.A.

**Matching**

We first examine the UV solutions (4.1.35) and (4.1.37) for a sufficiently large $z$ so that (3.3.8) applies. At leading order in large $z$, we then find that

$$\begin{aligned}\rho_1(z) &= \int_0^z du\, \frac{u^{d-1}}{\sqrt{f(u)}} \left( b_1 + (d-2) \int_u^\infty dv\, \frac{1}{v^{d-1}\sqrt{f(v)}} \right) \\ &= \frac{b_1}{\sqrt{a}} \frac{z^{d-n/2}}{d-n/2} (1+\ldots) + \frac{2(d-2)}{(2-n)(2d-4+n)\,a}\, z^{2-n} (1+\ldots) \quad (4.2.20) \\ \hat{\rho}(z) &= \frac{\hat{b}}{\sqrt{a}} \frac{z^{d-n/2}}{d-n/2} (1+\ldots)\ . \quad (4.2.21)\end{aligned}$$

Plugging (4.2.20) and (4.2.21) into (4.1.30), we see that to match the UV expansion with the $n > 2$ solution (4.2.12) at large $z$, we require

$$b_1 = \hat{b} = 0, \qquad \rho_0 = R\ . \quad (4.2.22)$$

We see that the UV expansion in fact directly matches to the behavior at $z \to \infty$ without the need of an intermediate matching region. Thus in this case the UV expansion (4.1.30) can be extended to arbitrary $z$ without breaking down, which can be verified by showing that higher order terms are all finite for any $z$. This is also intuitively clear from Fig. 4-2a where for large $R$ the minimal surface has a large radius at any $z$. Note that, since $\hat{b} = 0$, the non-integer $\nu$ term in (4.1.30) is not present.

For $n < 2$, where the minimal surface has the topology of a disk, the UV expansion is destined to break down at certain point before the tip of the minimal surface is reached. In the region (4.2.19) both the IR and UV expansions apply, and by comparing (4.2.20) and (4.2.21) with (4.2.17), we find that they match precisely provided that

$$\alpha_0 = R, \qquad b_1 = 0, \qquad \hat{b} = -\left(d - \frac{n}{2}\right) \bar{h} a^{-\frac{1}{\eta}}, \qquad \nu = \frac{2}{\eta}\ . \quad (4.2.23)$$

From (4.2.18) we conclude that $z_t$ scales with $R$ as

$$z_t \sim R^{\frac{2}{2-n}}, \qquad R \to \infty \,. \tag{4.2.24}$$

Again, the story for $n = 2$ is discussed in Appendix 4.A with equation (4.2.24) replaced by

$$z_t \sim \exp\left(-\frac{(d-1)^2 a}{2(d-2)} R^2\right) \,. \tag{4.2.25}$$

**Asymptotic expansion of the REE**

We will now obtain the leading order behavior of the REE in the large $R$ limit.

**1.** $n > 2$

Let us first consider $n > 2$. From the discussion below (4.1.31), we expect the leading order term for odd $d$ to be proportional to $1/R$, which comes from the $1/R^d$ term in the expansion of $c_d$. For even $d$, the leading term can in principle be $1/R^0$, which comes from the $1/R^{d-1}$ term in the expansion of $c_d$. Note, however, since this a gapped system, we expect the order $1/R^0$ term to vanish. So, for even $d$, the leading term should come from the $1/R^{d+1}$ term.

Since even for $d = 3$ we would need to know $c_3(R)$ to $1/R^3$ order, and we only worked out $\rho_1$ (which only determines $c_3(R)$ to $1/R$), our results seem insufficient to determine the $1/R$ contribution to $\mathcal{S}_3$. However, the $1/R$ contribution to $\mathcal{S}_3$ can be obtained by directly evaluating the on-shell action [33], as the $1/R$ piece is the next to leading term in the large $R$ expansion of $S$. For $d = 4$, we can use $\rho_1$ to verify that the $1/R^0$ term (in the REE) vanishes as expected for a gapped system. With due diligence, it is straightforward to work out higher order terms, but will not be attempted here.

For $d = 3$, plugging (4.1.30) into (3.3.23) we have the expansion

$$\begin{aligned} A &= R\int_\delta^\infty dz \frac{1}{z^2\sqrt{f(z)}} + \frac{1}{R}\int_0^\infty dz \left[\frac{\sqrt{f(z)}}{2z^2}\rho_1'(z)^2 - \frac{\rho_1(z)}{z^2\sqrt{f(z)}}\right] + O\left(\frac{1}{R^3}\right) \\ &= \#\, R + \frac{1}{R}\int_0^\infty dz \left[\frac{\sqrt{f(z)}}{2z^2}\rho_1'(z)^2 + \rho_1(z)\left(\frac{\sqrt{f}\rho_1'}{z^2}\right)'\right] + O\left(\frac{1}{R^3}\right) \,, \end{aligned} \tag{4.2.26}$$

where in the second line we have used (4.1.33). Integrating by parts the second term in the integrand we find that

$$A = \#R - \frac{1}{R}\int_0^\infty dz\ \frac{\sqrt{f(z)}}{2z^2}\rho_1'(z)^2\ , \tag{4.2.27}$$

where the boundary terms vanishe due to (4.1.38) and (4.2.12). We thus find that

$$A = \#\,R - \frac{a_1}{2R} + \cdots\ , \quad a_1 = \int_0^\infty dz\ \frac{z^2}{\sqrt{f(z)}}\left[\int_z^\infty dv\ \frac{1}{v^2\sqrt{f(v)}}\right]^2\ . \tag{4.2.28}$$

It is desirable to make work with dimensionless coefficients that only depend on ratios of scales. We can use

$$\tilde{\mu} \equiv a^{1/n} \tag{4.2.29}$$

as an energy scale and define the dimensionless coefficient

$$s_1 \equiv \tilde{\mu}\, a_1 = \int_0^\infty dz\ \frac{z^2}{\sqrt{f(z/\tilde{\mu})}}\left[\int_z^\infty dv\ \frac{1}{v^2\sqrt{f(v/\tilde{\mu})}}\right]^2\ , \tag{4.2.30}$$

where all integration variables are dimensionless, and $s_1$ only depends on ratios of scales, e.g. $(\tilde{\mu}\, z_{CO})$. Finally, we obtain

$$\mathcal{S}_3 = \frac{s_1 K}{\tilde{\mu} R} + \cdots\ , \qquad n > 2\ . \tag{4.2.31}$$

This result agrees with those in [33]. It is interesting to note that the coefficient of $1/R$ term depends on the full spacetime metric, i.e. in terms of the boundary theory, the full RG trajectory.

For $d = 4$, the expansion of $A$ has the form

$$A = a_0 R^2 + a_2 + O(1/R^2) \tag{4.2.32}$$

where

$$a_0 = \int_\delta^\infty dz \frac{1}{z^3\sqrt{f(z)}}, \qquad a_2 = \int_\delta^\infty dz \frac{f(z)\rho_1'(z)^2 - 4\rho_1(z)}{2z^3\sqrt{f(z)}} \tag{4.2.33}$$

with $\delta$ a UV cutoff. Neither of the first two terms indicated in (4.2.32) will contribute to $\mathcal{S}_4$ after differentiations in (1.2.4). As expected, $a_0 \sim 1/\delta^2$ is UV divergent. $a_2$ contains a logarithmic UV divergence $\log \delta\mu$, where $\mu$ is mass scale controlling the leading relevant perturbation from the UV fixed point. At large $z$, from (4.2.20) and (4.2.22) $\rho_1 \sim z^{2-n}$, hence the integrand for $a_2$ goes as $\sim z^{-1-3n/2}$, and the integral is convergent at the IR end. An IR divergent $a_2$ would signal a possible $\log R$ term. Thus we conclude that the leading order contribution for $d = 4$ is of order $1/R^2$, consistent with our expectation that the system is gapped.

**2.** $n \leq 2$

For $n < 2$, $\hat{b}$ in (4.1.31) is nonzero and its contribution to $\mathcal{S}_d$ can be directly written down from (4.2.23)

$$\mathcal{S}_d = e_n \frac{K}{a^{\frac{1}{\eta}} R^\beta} + \begin{cases} O(R^{-1}) & d \text{ odd} \\ O(R^{-2}) & d \text{ even} \end{cases}, \tag{4.2.34}$$

where $\eta$ and $\beta$ were defined in (4.2.2) and (4.2.6) respectively, and

$$e_n = \frac{d - n/2}{n} \frac{\eta \bar{h}}{\Gamma\left(\frac{d}{2}\right)\Gamma\left(\frac{1}{2} - \frac{1}{\eta}\right)} \times \begin{cases} \sqrt{\pi}\Gamma\left(\frac{1}{2} - \frac{n}{2\eta}\right) & d \text{ odd} \\ 2\Gamma\left(1 - \frac{n}{2\eta}\right) & d \text{ even} \end{cases}. \tag{4.2.35}$$

For $n = 2$ the first term in (4.2.34) should be replaced by (see (4.A.9) and Appendix 4.A)

$$\mathcal{S}_d^{(\text{non-analytic})} \propto \left(a\, R^2\right)^t \exp\left(-\frac{(d-1)^2 a}{2(d-2)} R^2\right) \qquad t \equiv \frac{d-3}{2} + \left[\frac{d}{2}\right]. \tag{4.2.36}$$

Below for convenience we will refer to the first term in (4.2.34) (or (4.2.39)) as "non-analytic", while terms of inverse odd powers in odd dimensions (and even inverse

powers in even dimensions) as "analytic." Note that the non-analytic term is the leading contribution in the large $R$ limit when

$$n < n_c \equiv \begin{cases} \frac{2}{d} & d \text{ odd} \\ \frac{4}{d+1} & d \text{ even} \end{cases} , \tag{4.2.37}$$

in which case one can check that the coefficient $e_n$ is positive. In Fig. 4-3 we plotted $e_n$ for $d = 2, 3$ and 4. Note that for odd $d$, $e_n$ diverges as $n \to n_c$, while for even $d$ it stays finite.[4] Despite appearances the numerical factors multiplying $\bar{h}$ in (4.2.35) do not diverge at $n = n_c$, hence the features described in Fig. 4-3 are caused by $\bar{h}$.

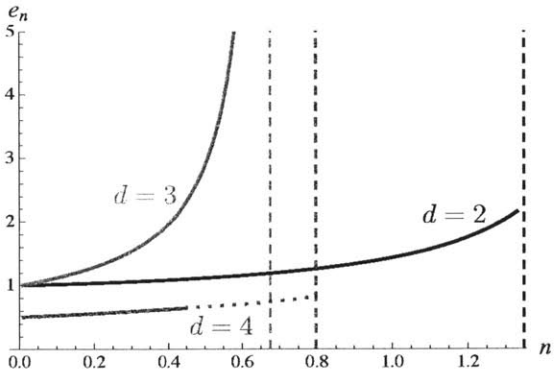


Figure 4-3: $e_n$ plotted as a function of $n$ for $d = 2, 3$ and 4. The vertical dashed lines indicate $n_c$. (4.2.35) consists of numerical factors and $\bar{h}$, which is a constant determined by the IR solution, $\bar{\rho}_d$. $\bar{h}$ was obtained by numerically determining $\bar{\rho}_d$ and fitting the small $u$ expansion (4.2.15). For $d = 2$ we know the exact answer from (4.2.5); the data points lie exactly on the analytically determined curve. For $d = 4$ the dotted part of the line is an extrapolation of the solid line; we do not have reliable numerical results in that region for $\bar{h}$.

Let us consider the $n \to n_c$ limit of (4.2.34) for odd $d$. Because $e_n$ diverges as $n \to n_c$, in order for (4.2.34) to have a smooth limit, we expect the coefficient of the $1/R$ term in (4.2.34) to diverge too, in a way that the divergences cancel resulting in a logarithmic term

$$\mathcal{S}_d = \#\frac{\log R}{R} + \cdots , \qquad n = \frac{2}{d}, \quad d \text{ odd} . \tag{4.2.38}$$

[4]For $d = 2$ apart from the numerical results, we can analyze the analytic answer given in (4.2.5).

The coefficient of the logarithmic term is given by the residue of (4.2.35) in the limit $n \to n_c$. In contrast, for even $d$, $e_n$ is finite at $n = n_c$. Thus, the leading term will simply be of order $1/R^2$ with no logarithmic enhancement (there can still be logarithmic terms at higher orders).

For $d = 3$ one can calculate the coefficient of $1/R$ term in (4.2.34) similar to $n > 2$ case discussed. See Appendix 4.B for a derivation. One finds

$$\mathcal{S}_3(R) = e_n \frac{K}{(\tilde{\mu}R)^{\frac{2n}{2-n}}} + \frac{K s_1}{\tilde{\mu}R} + \cdots , \tag{4.2.39}$$

where $s_1$ is given by (4.2.28) for $n > \frac{2}{3}$, and for $n < \frac{2}{3}$ by

$$s_1 = \int_0^\infty dz \left( \frac{z^2}{\sqrt{f(z/\tilde{\mu})}} \left[ \int_z^\infty dv \, \frac{1}{v^2 \sqrt{f(v/\tilde{\mu})}} \right]^2 - \frac{4}{(2+n)^2} \frac{1}{z^{3n/2}} \right) . \tag{4.2.40}$$

In this case, we can work out explicitly how the divergence in the limit $n \to n_c$ cancels between the coefficients of the analytic and non-analytic pieces. Note that the divergence in $s_1$ comes from the second term in the integrand in (4.2.40)[5]

$$s_1 = -\frac{3}{8\,(2/3 - n)} + \ldots . \tag{4.2.41}$$

The numerical results presented in Fig. 4-3 are consistent with the behavior

$$e_n = \frac{3}{8\,(2/3 - n)} + \ldots , \tag{4.2.42}$$

to 1% precision. Plugging into (4.2.39) then gives

$$\mathcal{S}_3(R) = K \frac{27}{32} \frac{\log \tilde{\mu}R}{\tilde{\mu}R} + \frac{\#}{R} + \cdots . \tag{4.2.43}$$

We can perform the same calculation with $n = 2/3$ fixed from the beginning, and we get the same result, see (4.B.14).

[5]At first sight it seems puzzling that the divergence comes from the UV region, $z = 0$. However, this is just an artifact of the subtraction we chose.

### 4.2.3 Discussion

We now briefly summarize the results by comparing between the strip and the sphere, and between $n < 2$, $n > 2$ and $n = 2$ geometries.

The presence of analytic terms for the sphere can be expected from the general structure of local contributions to the entanglement entropy [6, 39], which implies the existence of terms of the form $1/R + 1/R^3 + \cdots$ for odd dimensions and $1/R^2 + 1/R^4 + \cdots$ for even dimensions. Note the coefficient (4.2.28), (4.2.40) of the $1/R$ term in (4.2.31) and (4.2.39) depend on the full spacetime metric and thus the full RG trajectory. This is consistent with the physical interpretation that such coefficients encode the contributions from degrees of freedom at all shorter length scales compared to $R$.[6] For a strip, other than the area, all curvature invariants associated with the entangling surface vanish, and thus the analytic terms are altogether absent.

For $n < 2$ geometries, non-analytic terms are present for both the strip and the sphere, and have the same scaling. We note that the non-analytic terms (including the coefficients) are solely determined by the IR geometry. From the boundary perspective they can be interpreted as being determined by the IR physics. The presence of these non-analytic terms (despite the fact that they could be subleading compared to analytic terms) imply that the IR phase described by (3.3.8) is not fully gapped, and some IR gapless degrees of freedom are likely responsible for the non-analytic scaling behavior. For this reason we refer to such geometries as scaling geometries. Note that due to the singularity at $z = \infty$, we should view the region (3.3.8) as describing an intermediate scaling regime. It likely does not describe the genuine IR phase, which depends on how the singularity is resolved. Thus our discussion above should be interpreted as giving the behavior of $\mathcal{S}(R)$ for an intermediate regime. We will see some explicit examples in the next section.

In contrast for $n > 2$, there is no non-analytic term and we expect the dual system to be fully gapped in the IR.

For $n = 2$ the strip and sphere entanglement entropies show different behaviors as emphasized recently by [99]. For $R \to \infty$ the minimal surface for a strip is discon-

[6] In (4.2.28), (4.2.40) the upper limits of the integrals are $\infty$, as we are considering $R \to \infty$ limit.

nected, and hence there is no non-analytic term in the expansion of $\mathcal{R}_d$. However, for a spherical entangling surface the topology of the minimal surface is a disc, and $\mathcal{S}_d$ contains an exponentially small term (4.2.36). In next section, by examining the spectral function of a scalar operator, we argue that an $n = 2$ geometry describes a gapped phase, but with a continuous spectrum above the gap.

## 4.3 More on scaling geometries

In this section, we discuss further the properties of a scaling geometry with $n \leq 2$ by examining the behavior of a probe scalar field. We show that the system has gapless excitations in the IR. We emphasize that here the term IR is used in a relative sense, i.e. IR relative to the UV fixed point. The understanding of "genuine" IR phase of the system depends on how the singularity at $z = \infty$ is resolved. In this sense, the scaling region (3.3.8) should be considered as characterizing an intermediate regime, and our discussion of the entanglement entropy of the last section and correlation functions below should be considered as applying only to this intermediate regime. In the second part of this section we consider some explicit examples, where a scaling geometry arises as an intermediate phase.

### 4.3.1 Correlation functions

Consider a probe scalar field in a spacetime (3.3.2) with (3.3.8). A similar analysis was done in [72] for two specific flows in $d = 4$ dimensions with $n = 3$ and $n = 2$ respectively,[7] and more recently in [74] in the context of hyperscaling violating geometries.

The field equation for a minimally coupled scalar in momentum space can be written as

$$\phi''(z) + \left(\frac{f'(z)}{2f(z)} - \frac{d-1}{z}\right)\phi'(z) - \frac{m^2 + k^2 z^2}{z^2 f(z)}\phi(z) = 0 \,, \tag{4.3.1}$$

[7]There the scalar fields of interest mixed with the metric, here we assume no mixing.

where $k^\mu$ is the energy-momentum along the boundary spacetime directions and $k^2 = \eta_{\mu\nu}k^\mu k^\nu$.

First, consider the gapped case, corresponding to $n > 2$. For $z \to \infty$ the two allowed behaviors for the scalar field are:

$$\phi_+ = 1 - \frac{2k^2}{(n-2)(2d+n-4)} z^{-(n-2)} + \cdots \tag{4.3.2}$$

$$\phi_- = z^{d-n/2} - \frac{2k^2}{(4+2d-3n)(-2+n)} z^{d-n/2-(n-2)} + \cdots , \tag{4.3.3}$$

where we have set $a = 1$ for simplicity of notation. The null energy condition requires that $n/2 < d$ [74], hence only $\phi_+$ is regular. Near $z \to 0$, the normalizable solution $\phi_{\text{norm}}(z)$ can be written as a linear superposition of $\phi_\pm$, i.e. $\phi_{\text{norm}}(z) = A_+(k)\phi_+ + A_-(k)\phi_-$ where $A_\pm(k)$ are some functions of $k^2$. Requiring both regularity at $z \to \infty$ and normalizability at the boundary then leads to $A_-(k) = 0$, which implies that the system has a discrete spectrum. This is in agreement with the findings of [72] in specific examples, and is consistent with our discussion at the end of last section that such a geometry should be describe a gapped theory.

For $n = 2$, in the scaling region (4.3.1) can be solved analytically

$$\phi_\pm = \left(\frac{m}{z}\right)^{-(d-1)/2} I_{\pm\nu}\left(\frac{m}{z}\right) \qquad \nu = \sqrt{\left(\frac{d-1}{2}\right)^2 + k^2} , \tag{4.3.4}$$

where $I$ is the modified Bessel function of the first kind. For $k^2 < -\Delta^2$, $\nu$ is imaginary and $\phi_\pm$ behave as plane waves near $z \to \infty$. Then following the standard story [100], choosing an infalling solution leads to a complex retarded Green function and a nonzero spectral function. We thus conclude that in this case, there is nonzero gap $\Delta = \frac{d-1}{2}$ and the system has a continuous spectrum above the gap. The presence of a continuum above a gap is presumably responsible for the exponential behavior (4.2.36) in the entanglement entropy.

Now we consider $n < 2$. For $k^2 < 0$ and $z \to \infty$, the solutions to (4.3.1) have the

"plane wave" form

$$\phi_{\pm} \to z^{(d-1)/2} \exp\left[\mp i \frac{2\sqrt{-k^2}}{2-n} z^{(2-n)/2}\right] . \tag{4.3.5}$$

Thus in this case one finds a continuous spectrum all the way to $k^2 \to 0_-$. The corresponding spectral function can be extracted from [74]

$$\rho(k^2) = \mathrm{Im}\, G_R(k^2) \propto (\sqrt{-k^2})^{\gamma}, \qquad \gamma = \frac{2d-n}{2-n} . \tag{4.3.6}$$

This continuous spectrum should be the origin of the "non-analytic" behavior in (4.2.34) for a sphere and (4.2.5) for a strip. It is also interesting to note that the exponents $\beta$ in (4.2.5), (4.2.34) and $\gamma$ in (4.3.6) satisfy a simple relation

$$\gamma = \beta + d . \tag{4.3.7}$$

It would be interesting to understand further the origin of such a relation.

### 4.3.2 Explicit examples: near horizon D$p$-brane geometries

We now consider the near-horizon Dp-brane geometries [101], which exhibit the scaling geometry (3.3.8) in some intermediate regime. EE in these geometries was analyzed previously in [74]. While these geometries are not asymptotically AdS, our earlier result for the non-analytic term in (4.2.34) is nevertheless valid, since it only relies on the geometry of the scaling region. We will focus on this leading non-analytic contribution in $1/R$.

The near horizon extremal black $p$-brane metric in the string frame can be written as

$$\begin{aligned} ds^2_{string,10} &= \frac{1}{\sqrt{gN}} \left(\frac{r}{l_s}\right)^{(7-p)/2} (dx^{\mu})^2 + \sqrt{gN} \left(\frac{r}{l_s}\right)^{-(7-p)/2} \left[dr^2 + r^2 d\Omega^2_{8-p}\right] \\ e^{\phi_{10}} &= g\,(gN)^{-(p-3)/4} \left(\frac{r}{l_s}\right)^{(p-3)(7-p)/4} , \end{aligned} \tag{4.3.8, 4.3.9}$$

where $g$ and $l_s$ are the string coupling and string length respectively. As we will only be interested in the qualitative dependence on $R$ and couplings, here and below we omit all numerical factors. We will restrict our discussion to $p \leq 5$, for which a field theory dual exists. After dimensional reduction and going to the Einstein frame, the metric can be written as (see also [74])

$$ds^2_{Einstein,p+2} = \frac{(gN)^{\frac{1}{p}} l_s^2}{z^2} \left[ (dx^\mu)^2 + gN \frac{dz^2}{(z/l_s)^{2(p-3)^2/(9-p)}} \right] , \tag{4.3.10}$$

which is of the same form as (3.3.2) and (3.3.8) with

$$n = \frac{2(p-3)^2}{(9-p)} = \begin{cases} 1 & p=1 \\ \frac{2}{7} & p=2 \\ 0 & p=3 \\ \frac{2}{5} & p=4 \\ 2 & p=5 \end{cases} , \qquad a = \frac{1}{gN l_s^n} . \tag{4.3.11}$$

In our convention, the bulk Newton constant is $G_N = g^2 l_s^{d-1} = N^{-2}(gN)^2 l_s^{d-1}$. The metric (4.3.10) is valid in the range [101]

$$(gN)^{-(9-p)/2p} \ll \left(\frac{z}{l_s}\right)^{3-p} \ll \left(gN^{\frac{3-p}{7-p}}\right)^{-(9-p)/2p} . \tag{4.3.12}$$

The LHS condition comes from the requirement of small curvature, while the RHS imposes small sting coupling (dilaton). For $p = 1, 2$ as $z$ is increased the system eventually settles into a CFT with degrees of freedom of order $O(N)$ and $O(N^{\frac{3}{2}})$ respectively, while for $p = 4, 5$ the system is eventually described by the free $U(N)$ Yang-Mills theory (i.e. with $O(N^2)$ degrees of freedom) as $z \to \infty$.

For our analysis of the previous section to be valid, $z_t$ should lie inside the region (4.3.12). For both strip (4.2.1) and sphere (4.2.24) we have $z_t \sim (\sqrt{a}\, R)^{\frac{2}{2-n}}$ which then leads to

$$\frac{1}{gN} \ll \left(\frac{R}{l_s}\right)^{3-p} \ll \frac{N^{\frac{2(5-p)}{7-p}}}{gN} . \tag{4.3.13}$$

Now plugging (4.3.11) into the "non-analytic" term in (4.2.34) for sphere (or similarly (4.2.5) for strip) we find that

$$\mathcal{S} \propto N^2 \lambda_{eff}^{\frac{p-3}{5-p}}(R) \tag{4.3.14}$$

where $\lambda_{eff}(R)$ is the effective dimensionless t' Hooft coupling at scale $R$,

$$\lambda_{eff}(R) = gN \left(\frac{R}{l_s}\right)^{3-p} . \tag{4.3.15}$$

In terms of $\lambda_{eff}$ equation (4.3.13) can also be written as

$$1 \ll \lambda_{eff}(R) \ll N^{\frac{2(5-p)}{7-p}} . \tag{4.3.16}$$

For $p = 1, 2$, $\lambda_{eff}$ increases with $R$ but appears in $\mathcal{S}$ with a negative power. For $p = 4$, the opposite happens. In all cases $\mathcal{S}$ decreases with $R$. The $p = 5$ case, for which $n = 2$, has to be treated differently and one finds from (4.2.36)

$$\mathcal{S} \propto \frac{N^2}{(gN)^{3/2}\, \lambda_{eff}(R)^{9/2}} \exp\left(-\frac{25}{8\lambda_{eff}(R)}\right) . \tag{4.3.17}$$

## 4.4 Domain wall geometry

We now consider the large $R$ behavior of the REE for holographic systems, whose IR geometry is described by (3.3.6), i.e. the system flows to a conformal IR fixed point. We will again consider the strip story first.

### 4.4.1 Strip

Again we start with (3.3.17) which can be written as

$$R(z_t) = \frac{z_t}{\sqrt{f_\infty}} \left[ a_d + \int_0^1 dv \, \frac{v^{d-1}}{\sqrt{(1 - v^{2(d-1)})}} \left( \sqrt{\frac{f_\infty}{f(z_t v)}} - 1 \right) \right] \tag{4.4.1}$$

with

$$a_d = \frac{\sqrt{\pi}\,\Gamma\left(\frac{d}{2(d-1)}\right)}{\Gamma\left(\frac{1}{2(d-1)}\right)} \,. \tag{4.4.2}$$

The leading behavior in large $z_t$ limit of the integral in (4.4.1) depends on the value of

$$\tilde{\alpha} \equiv \tilde{\Delta} - d \,. \tag{4.4.3}$$

For $\tilde{\alpha} < \frac{d}{2}$ we can directly expand $f(z_t v)$ using (3.3.7)

$$\sqrt{\frac{f_\infty}{f(z_t v)}} - 1 = \frac{1}{2 f_\infty (\tilde{\mu} z_t v)^{2\tilde{\alpha}}} + \cdots \tag{4.4.4}$$

and find

$$R(z_t) = \frac{z_t}{\sqrt{f_\infty}} \left[ a_d + \frac{\tilde{b}_d}{(\tilde{\mu} z_t)^{2\tilde{\alpha}}} + \cdots \right] \tag{4.4.5}$$

with

$$\tilde{b}_d = \frac{\sqrt{\pi}\,\Gamma\left(\frac{d-2\tilde{\alpha}}{2(d-1)}\right)}{2 f_\infty (1-2\tilde{\alpha})\,\Gamma\left(\frac{1-2\tilde{\alpha}}{2(d-1)}\right)} \,. \tag{4.4.6}$$

Note that $\tilde{b}_d$ is positive for any $d > 1$. For $\tilde{\alpha} \geq \frac{d}{2}$, the term on RHS of (4.4.4) leads to a divergence in (4.4.1) near $v = 0$ and should be treated differently.[8] In particular, the divergence indicates that the leading contribution should come from the integration region $v \ll 1$. We will thus approximate the factor $1/\sqrt{1 - v^{2(d-1)}}$ in the integrand of (4.4.1) by 1, leading to

$$R(z_t) = \frac{z_t}{\sqrt{f_\infty}} \left( a_d + \frac{b_d}{z_t^d} + \cdots \right) \tag{4.4.7}$$

where

$$b_d = \int_0^\infty du\; u^{d-1} \left( \sqrt{\frac{f_\infty}{f(u)}} - 1 \right) \,. \tag{4.4.8}$$

[8] Note that even for $\tilde{\alpha} < \frac{d}{2}$, higher order terms in the expansion on the RHS of (4.4.4) can similarly lead to divergences. They can be treated similarly as for $\tilde{\alpha} \geq \frac{d}{2}$, and give rise to higher order terms compared to the second term of (4.4.5).

Inverting (4.4.5) and (4.4.7) we find from (3.3.21)

$$\mathcal{R}_d = \frac{L^{d-1}}{2G_N}\left(\frac{a_d}{\sqrt{f_\infty}}\right)^{d-1} \times \begin{cases} 1+(d-1)\frac{\tilde{b}_d}{a_d}\left(\frac{\tilde{\mu}\sqrt{f_\infty}R}{a_d}\right)^{-2\tilde{\alpha}}+\cdots & (\tilde{\alpha}<\frac{d}{2}) \\ 1+(d-1)\frac{b_d}{a_d}\left(\frac{\sqrt{f_\infty}R}{a_d}\right)^{-d}+\cdots & (\tilde{\alpha}\geq\frac{d}{2}) \end{cases} . \tag{4.4.9}$$

We discuss the physical implication of this result in Sec. 4.4.3.

### 4.4.2 Sphere

With (3.3.6) as $z \to \infty$ the system flows to a CFT in the IR, and, as discussed in [6], to leading order in the large $R$ expansion the REE $\mathcal{S}_d$ approaches a constant, that of the IR CFT. Here we confirm that the subleading terms have the structure given in (4.1.8).

#### IR expansion

Since the IR geometries approaches AdS, in the large $R$ limit the IR part of the minimal surface should approach that in pure AdS. In particular, in the limit $R \to \infty$, we expect most part of the minimal surface to lie in the IR AdS region, hence the IR solution $z(\rho)$ can be written as

$$z(\rho) = z_0(\rho) + z_1(\rho) + \cdots , \qquad z_0(\rho) = \sqrt{f_\infty\,(R^2-\rho^2)} . \tag{4.4.10}$$

$z_0(\rho)$ is the minimal surface with boundary radius $R$ in a pure AdS with $f = f_\infty$. $z_1$ and $\cdots$ in (4.4.10) denote subleading corrections which are suppressed compared with $z_0$ by some inverse powers of $R$. Below we will determine the leading correction $z_1(\rho)$ by matching with the UV solution.

Plugging (4.4.10) into (3.3.27), and expanding to linear order in $z_1$, we find that

$$z_1'' + \frac{(d-2)R^2-2\rho^2}{\rho(R^2-\rho^2)}z_1' - \frac{(d-1)R^2}{(R^2-\rho^2)^2}z_1 = s(\rho) , \tag{4.4.11}$$

where the source term $s(\rho)$ is given by

$$s(\rho) = \frac{f_\infty^{\frac{1}{2}-\tilde{\alpha}}}{\tilde{\mu}^{2\tilde{\alpha}}} \frac{(d-1)R^2 + (\tilde{\alpha}-1)\rho^2}{(R^2-\rho^2)^{3/2+\tilde{\alpha}}} \ . \tag{4.4.12}$$

The homogenous equation, obtained by setting $s(\rho)$ to zero in (4.4.11), has the following linearly independent solutions

$$\phi_1 = \frac{R}{\sqrt{R^2-\rho^2}} \tag{4.4.13}$$

$$\phi_2 = \begin{cases} \frac{3}{2}\left[-1 + \frac{R}{\sqrt{R^2-\rho^2}} \operatorname{arctanh}\left(\frac{\sqrt{R^2-\rho^2}}{R}\right)\right] & (d=3) \\ \frac{(R-\rho)^2}{\sqrt{2}\rho\sqrt{R^2-\rho^2}} & (d=4) \\ \frac{5(R^2+2\rho^2)}{8\rho^2} - \frac{15}{8}\frac{R}{\sqrt{R^2-\rho^2}} \operatorname{arctanh}\left(\frac{\sqrt{R^2-\rho^2}}{R}\right) & (d=5) \end{cases} \tag{4.4.14}$$

$$W(\phi_1,\phi_2) \equiv \phi_1\phi_2' - \phi_1'\phi_2 = \begin{cases} -\frac{3R}{2\rho\sqrt{R^2-\rho^2}} & (d=3) \\ -\frac{R}{\sqrt{2}\rho^2} & (d=4) \\ -\frac{5R\sqrt{R^2-\rho^2}}{4\rho^3} & (d=5) \end{cases} \ . \tag{4.4.15}$$

Note that there is an expression for $\phi_2$ in terms of hypergeometric functions for all dimensions, but we find it more instructive to display explicit expressions in various dimensions. The final results will be written down in general $d$. $\phi_1$ is singular at $\rho = R$, while $\phi_2 \sim \frac{R^{d-3}}{\rho^{d-3}}$ is singular as $\rho \to 0$ (for $d = 3$, there is a logarithmic divergence) with $W \to -\frac{R^{d-3}}{\rho^{d-2}} + \cdots$. Also note that

$$\phi_2 \to \delta^{\frac{d-1}{2}}, \qquad W \to -\frac{d}{\sqrt{8}}\frac{\delta^{\frac{d-4}{2}}}{R}, \qquad \delta \equiv \frac{R-\rho}{R} \ll 1 \ . \tag{4.4.16}$$

In order for $z(\rho)$ to be regular at $\rho = 0$, $z_1$ should be regular there, and can be written as

$$z_1(\rho) = cR\phi_1(\rho) + \phi_1(\rho)\int_\rho^R dr\ \frac{\phi_2(r)}{W(r)}s(r) + \phi_2(\rho)\int_0^\rho dr\ \frac{\phi_1(r)}{W(r)}s(r) \ , \tag{4.4.17}$$

where $c$ is an integration constant. Note that the first integral above is convergent in the upper integration limit only for $\tilde{\alpha} < 1$. For $\tilde{\alpha} \geq 1$ some additional manipulations are required. For example for $1 < \tilde{\alpha} < 2$, we should replace the first integral by

$$\phi_1(\rho) \left[ \int_\rho^R dr \left( \frac{\phi_2(r)}{W(r)} s(r) - \frac{c_1}{\tilde{\mu}^{2\tilde{\alpha}} R^{\tilde{\alpha}} (R-r)^{\tilde{\alpha}}} \right) + \frac{c_1 R}{(\tilde{\alpha}-1)(\tilde{\mu}R)^{2\tilde{\alpha}}} \frac{1}{\delta^{\tilde{\alpha}-1}} \right] \tag{4.4.18}$$

where $c_1$ is the numerical constant appearing in the limit $\frac{\phi_2(r)}{W(r)} s(r) \to \frac{c_1}{\tilde{\mu}^{2\tilde{\alpha}} R^{\tilde{\alpha}} (R-r)^{\tilde{\alpha}}} + \cdots$ as $r \to R$, and is given by

$$c_1 = -\frac{2^{-\tilde{\alpha}} f_\infty^{1/2-\tilde{\alpha}} (-2 + d + \tilde{\alpha})}{d} \,. \tag{4.4.19}$$

For $\tilde{\alpha} > 2$ further subtractions may be needed. We will not write these separately, as they are irrelevant for our discussion below.

### Matching

The IR expansion (4.4.10) and (4.4.17) is valid for $z \gg z_{CO}$, where (3.3.7) applies. For sufficiently large $R$, this includes the region where

$$\delta \equiv \frac{R-\rho}{R} \ll 1, \qquad R\sqrt{\delta} \gg z_{CO}, \tilde{\mu}^{-1}, \cdots \tag{4.4.20}$$

where the $\cdots$ on the right hand side of the second inequality includes all other scales of the system. The UV expansion we discussed earlier in Sec. 4.1.4 applies to the region $\delta \ll 1$. Thus the IR and UV expansions can be matched for $\rho$ satisfying (4.4.20).

Let us now consider the behavior of (4.4.17) in the overlapping region (4.4.20). The first integral gives

$$\phi_1(\rho) \int_\rho^R dr \, \frac{\phi_2(r)}{W(r)} s(r) = d_1 R \frac{\delta^{1/2-\tilde{\alpha}}}{(\tilde{\mu}R)^{2\tilde{\alpha}}} \left(1 + O(\delta)\right) \,, \tag{4.4.21}$$

where for all $\tilde{\alpha}$

$$d_1 = -\frac{(d - 2 + \tilde{\alpha}) \, (2 f_\infty)^{1/2-\tilde{\alpha}}}{2(1-\tilde{\alpha})d} \,. \tag{4.4.22}$$

The second integral in (4.4.17) gives

$$\phi_2(\rho)\int_0^\rho dr\ \frac{\phi_1(r)}{W(r)}s(r) = d_2 R\frac{\delta^{1/2-\tilde{\alpha}}}{(\tilde{\mu}R)^{2\tilde{\alpha}}}\left(1+O(\delta)\right) + hR\frac{\delta^{\frac{d-1}{2}}}{(\tilde{\mu}R)^{2\tilde{\alpha}}}\left(1+O(\delta)\right)\ , \quad (4.4.23)$$

where

$$d_2 = -\frac{d-2+\tilde{\alpha}}{d(d-2+2\tilde{\alpha})}\left(2f_\infty\right)^{1/2-\tilde{\alpha}}, \quad h = f_\infty^{1/2-\tilde{\alpha}}\frac{2^{(d-3)/2}\pi\tilde{\alpha}\,\Gamma\left(\frac{d+1}{2}\right)}{d\sin\left(\frac{\pi}{2}(d+2\tilde{\alpha})\right)\Gamma\left(\frac{3}{2}-\tilde{\alpha}\right)\Gamma\left(\frac{d}{2}+\tilde{\alpha}\right)}\ . \quad (4.4.24)$$

Putting the two expansions together we get:

$$z_1(\rho) = \frac{cR}{\sqrt{2\delta}} + d_3 R\frac{\delta^{1/2-\tilde{\alpha}}}{(\tilde{\mu}R)^{2\tilde{\alpha}}}\left(1+O(\delta)\right) + hR\frac{\delta^{\frac{d-1}{2}}}{(\tilde{\mu}R)^{2\tilde{\alpha}}}\left(1+O(\delta)\right)\ , \quad (4.4.25)$$

where

$$d_3 = -\frac{d-2+\tilde{\alpha}}{2(1-\tilde{\alpha})(d-2+2\tilde{\alpha})}\left(2f_\infty\right)^{1/2-\tilde{\alpha}}\ . \quad (4.4.26)$$

One could consider the next order in the IR expansion, i.e. including a $z_2$ in (4.4.10). The equation for $z_2$ only differs from (4.4.11) by having a different source term, and the corresponding terms in (4.4.25) coming from the source will be proportional to $(\tilde{\mu}R)^{-4\tilde{\alpha}}$. Similarly, the corresponding terms at the $n$th order are proportional $(\tilde{\mu}R)^{-2n\tilde{\alpha}}$.

Now including $z_0$ in the region (4.4.20), we have the expansion

$$\frac{z(\rho)}{R} = \sqrt{2f_\infty\,\delta}\left[1+\frac{c}{\sqrt{4f_\infty\,\delta}} + \frac{d_3}{\sqrt{2f_\infty}}\frac{1}{(\tilde{\mu}R\sqrt{\delta})^{2\tilde{\alpha}}} + \frac{h}{\sqrt{2f_\infty}}\frac{\delta^{(d+2\tilde{\alpha}-2)/2}}{(\tilde{\mu}R\sqrt{\delta})^{2\tilde{\alpha}}} + \cdots\right]\ . \quad (4.4.27)$$

Clearly we have a double expansion in terms of $\delta$ and inverse powers of $\tilde{\mu}R\sqrt{\delta}$. The consistency of the expansion also requires that the constant $c$ have the scaling

$$c = \frac{\tilde{c}}{(\tilde{\mu}R)^2} \quad (4.4.28)$$

with $\tilde{c}$ now an $O(R^0)$ constant. Now inverting (4.4.27) we find that

$$\delta = \frac{z^2}{2f_\infty R^2} - \frac{\tilde{c}}{\sqrt{f_\infty}(\tilde{\mu}R)^2} + \frac{d_4}{2f_\infty}\frac{z^2}{R^2}\frac{1}{(\tilde{\mu}z)^{2\tilde{\alpha}}} - \tilde{h}\frac{z^d}{\tilde{\mu}^{2\tilde{\alpha}}R^{d+2\tilde{\alpha}}} + \cdots , \tag{4.4.29}$$

which can be considered as a double expansion in $z/R$ and $1/(\tilde{\mu}z)$ and

$$d_4 = \frac{d-2+\tilde{\alpha}}{(1-\tilde{\alpha})(d-2+2\tilde{\alpha})} , \qquad \tilde{h} = 2h(2f_\infty)^{-\frac{d+1}{2}} . \tag{4.4.30}$$

Now consider (4.1.35) with $z$ large, with $f(z)$ given by (3.3.7). We find that $\rho_1$ can be expanded as (see Appendix 4.C for details)

$$\rho_1(z) = \frac{b_1}{d\sqrt{f_\infty}}z^d(1+\cdots) + \frac{z^2}{2f_\infty} + \gamma + \frac{z^2}{2f_\infty}a(\tilde{\mu}z)^{-2\tilde{\alpha}} + O\left(\frac{z^2}{(\tilde{\mu}z)^{4\tilde{\alpha}}}\right) . \tag{4.4.31}$$

Note the above equation applies to all $\tilde{\alpha}$, but the expression for constant $\gamma$ depends on the range of $\tilde{\alpha}$. For example, for $\tilde{\alpha} > 1$,

$$\gamma = \int_0^\infty du \left[(d-2)\frac{u^{d-1}}{\sqrt{f(u)}}\int_u^\infty dv \frac{1}{v^{d-1}\sqrt{f(v)}} - \frac{u}{f_\infty}\right] . \tag{4.4.32}$$

At higher orders in $1/R$, it suffices to determine the leading term:

$$\rho_n(z) = \frac{b_n}{d\sqrt{f_\infty}}z^d + \cdots \qquad \hat{\rho}(z) = \frac{\hat{b}}{d\sqrt{f_\infty}}z^d + \cdots . \tag{4.4.33}$$

Using (4.4.31) and (4.4.33) in (4.1.30) we find that

$$\delta = \frac{b_1}{d\sqrt{f_\infty}R^2}z^d(1+\cdots) + \frac{z^2}{2f_\infty R^2}\left(1 + a(\tilde{\mu}z)^{-2\tilde{\alpha}} + \cdots\right) + \frac{\gamma}{R^2} + \cdots + \frac{\hat{b}}{d\sqrt{f_\infty}}\frac{z^d}{R^\nu} + \cdots . \tag{4.4.34}$$

Comparing (4.4.34) with (4.4.29) we find they match provided that

$$b_1 = 0, \qquad \tilde{c} = -\sqrt{f_\infty}\tilde{\mu}^2\gamma, \qquad \hat{b} = -d\sqrt{f_\infty}\frac{\tilde{h}}{\tilde{\mu}^{2\tilde{\alpha}}}, \qquad \nu = d + 2\tilde{\alpha} - 1 . \tag{4.4.35}$$

**Asymptotic expansion of REE**

With $\hat{b}$ and $\nu$ given by (4.4.35), from (4.1.32) we find the leading "non-analytic" contribution in $\mathcal{S}_d$ is given by

$$\mathcal{S}_d = \cdots + \frac{1}{2} K_{IR} \frac{(d-1)!!}{(d-2)!!} b(\tilde{\alpha}) \frac{f_\infty^{-\tilde{\alpha}}}{(\tilde{\mu} R)^{2\tilde{\alpha}}} + \cdots \tag{4.4.36}$$

with

$$K_{IR} \equiv K f_\infty^{-(d-1)/2}, \qquad b(\tilde{\alpha}) = \begin{cases} \frac{1}{1-2\tilde{\alpha}} & d \text{ odd} \\ \frac{\sqrt{\pi}\,\Gamma(1-\tilde{\alpha})}{2\Gamma\left(\frac{3}{2}-\tilde{\alpha}\right)} & d \text{ even} \end{cases} . \tag{4.4.37}$$

This above expression agrees with that obtained in [6] for two closely separated fixed points, which we review and extend in Appendix 4.E. As discussed in the Introduction this can be anticipated on the grounds that the coefficient of the non-analytic term should depend only on the physics at the IR fixed point.

As discussed earlier our UV expansion (4.1.30) was designed to produce the second line of (4.1.8), and the fact that the UV expansion is consistent with the IR expansion confirms the second line of (4.1.8).

In $d = 3$ using $\rho_1$ and $z_1$ obtained in last subsection we can obtain the coefficient of $1/R$ term by directly evaluating the action as we have done for the gapped and scaling geometries. The calculation is given in Appendix 4.D. The final answer is:

$$\mathcal{S}_3 = \mathcal{S}_3^{(IR)} + K_{IR} \frac{f_\infty^{-\tilde{\alpha}}}{(1-2\tilde{\alpha})(\tilde{\mu} R)^{2\tilde{\alpha}}} + \frac{K s_1}{\tilde{\mu} R} + \ldots , \tag{4.4.38}$$

where $s_1$ is given by (4.D.11):

$$s_1 = \begin{cases} \int_0^\infty dz \left[ \frac{z^2}{\sqrt{f(z/\tilde{\mu})}} \left[ \int_z^\infty dv \, \frac{1}{v^2 \sqrt{f(v/\tilde{\mu})}} \right]^2 - \frac{1}{f_\infty^{3/2}} \right] & \left(\frac{1}{2} < \tilde{\alpha}\right) \\ \int_0^\infty dz \left[ \frac{z^2}{\sqrt{f(z/\tilde{\mu})}} \left[ \int_z^\infty dv \, \frac{1}{v^2 \sqrt{f(v/\tilde{\mu})}} \right]^2 - \frac{1}{f_\infty^{3/2}} \left(1 + \frac{3+2\tilde{\alpha}}{2(1+2\tilde{\alpha})} \frac{1}{z^{2\tilde{\alpha}}}\right) \right] & \left(\frac{1}{4} < \tilde{\alpha} < \frac{1}{2}\right) \end{cases} \tag{4.4.39}$$

The expressions for smaller values of $\tilde{\alpha}$ are similar but require more subtractions. $s_1$

(and the integration variables, $z$ and $v$) is dimensionless, hence only depends on ratios of RG scales.

Our results are compatible with the F-theorem; for $\tilde{\alpha} < \frac{1}{2}$ the non-analytic term dominates in (4.4.38), and $b(\tilde{\alpha}) > 0$ in this range (4.4.37). For $\frac{1}{2} < \tilde{\alpha}$, where the $1/R$ term dominates over the non-analytic term, $s_1 > 0$ follows from (4.4.39).

As a consistency check, we apply these formulae to closely separated fixed points in Appendix 4.E. We recover (4.E.6) that is obtained using different methods. Another consistency check is that the $f_\infty \to \infty$ limit of (4.4.39) recovers $s_1$ for the scaling geometries (4.2.40). This had to be the case, as a scaling geometry can be viewed as a limit of domain walls with increasing $f_\infty$.

### 4.4.3 Discussion

We conclude this section making a comparison between the result for the strip (4.1.14), (4.4.9) and that for the sphere (4.1.8).

First, let us look at the strip result (4.4.9). When $\tilde{\alpha} < \frac{d}{2}$, $\mathcal{R}_d$ can be written in terms of an effective dimensionless irrelevant coupling $g_{eff}(R) = (\tilde{\mu}R)^{-\tilde{\alpha}}$ as

$$\mathcal{R}_d = \mathcal{R}_d^{(IR)} + \#g_{eff}^2(R) + \cdots \tag{4.4.40}$$

with a coefficient $\#$ only depending on the data at the IR fixed point. As for the sphere case (4.1.9), such a term can be expected from conformal perturbations around a fixed point. For $\tilde{\alpha} > \frac{d}{2}$, we see that the leading approach to the IR value saturates at $R^{-d}$ no matter what the dimension of the leading irrelevant operator is. In particular, the coefficient $b_d$ (4.4.8) involves an integral over all spacetime, suggesting this term receives contributions from degrees of freedom at all length scales (not merely IR degrees of freedom). This term may be considered as the counterpart for a strip of the second line in (4.1.8). But note that for a sphere the second line of (4.1.8) can be associated with a curvature expansion of a spherical entangling surface, while for a strip all such curvature terms are absent.

## 4.5 Black holes

In this section we consider the large $R$ expansion of the entanglement entropy for strip and sphere for a holographic system at a finite temperature/chemical potential, which is described by a black hole on the gravity side. Compared with examples of earlier sections, there are some new elements in the UV and IR expansions. The setup is exactly the same as discussed in Sec. 3.3.2 and Sec. 3.3.3 except that now the function $f(z)$ has a zero at some $z = z_h$:

$$f(z_h) = 0, \qquad f(z) = f_1(z_h - z) + f_2(z - z_h)^2 + \cdots , \quad z \to z_h \ . \tag{4.5.1}$$

In our discussion below, we will assume $f_1$ is nonzero. For an extremal black hole, $f_1$ vanishes, which requires a separate treatment and will be given elsewhere. For notational simplicity, we will set $z_h = 1$ below, which can be easily reinstated on dimensional grounds. We also introduce

$$\gamma \equiv \sqrt{\frac{(d-1)f_1 z_h}{2}} \ , \tag{4.5.2}$$

which will appear in many places below.

### 4.5.1 Strip

We again look at the strip first. As $R \to \infty$ we expect the tip of the minimal surface $z_t$ to approach the horizon $z_h = 1$. This can be seen immediately from equation (3.3.17): with $z_t = 1$, due to $f(1) = 0$, the integrand develops a double pole and the integral becomes divergent. To obtain the large $R$ behavior, we thus take

$$z_t = 1 - \epsilon, \qquad \epsilon \ll 1 \ , \tag{4.5.3}$$

and expand the integral in $\epsilon$. From (3.3.17) we find that

$$R = -\frac{1}{2\gamma} \log \frac{\epsilon}{4} + b_0 + O(\epsilon \log \epsilon) \ , \tag{4.5.4}$$

where $\gamma$ was introduced in (4.5.2) and

$$b_0 = \int_0^1 dv \left[ \frac{v^{d-1}}{\sqrt{f(v)\left(1-v^{2(d-1)}\right)}} - \frac{1}{2\gamma}\frac{1}{(1-v)} \right] . \tag{4.5.5}$$

Then we can express $\epsilon$ as a function of $R$:

$$\epsilon = 4e^{2\gamma b_0} e^{-2\gamma R}\left(1 + O(Re^{-2\gamma R})\right) . \tag{4.5.6}$$

Reinstating $z_h$, from (3.3.21)

$$\mathcal{R}_d = \frac{L^{d-1}}{2G_N}\left(\frac{R}{z_h}\right)^{d-1}(1 + (d-1)\epsilon + \cdots) . \tag{4.5.7}$$

The entanglement entropy itself can be written as

$$S_{\text{strip}} = \frac{L^{d-1}}{4G_N}\frac{2R\,l^{d-2}}{z_h^{d-1}}\left(1 - \frac{2(d-1)z_h}{\gamma R}e^{2\gamma b_0}e^{-\frac{2\gamma R}{z_h}} + \cdots\right) , \tag{4.5.8}$$

which is given by the Bekenstein-Hawking entropy with exponential corrections. For the $d = 2$ BTZ black hole one simply recovers the well known expression for a 2d thermal CFT by evalutaing (3.3.17) exactly.

### 4.5.2 Sphere

#### UV expansion

Anticipating a volume term and possibly other subleading terms in the entanglement entropy, we modify the UV expansion (4.1.30) to include terms of all integer powers in $1/R$, i.e.

$$\rho(z) = R - \rho_0(z) - \frac{\rho_1(z)}{R} + \cdots . \tag{4.5.9}$$

At finite temperature, we do not expect non-integer power law terms in $1/R$ in (4.5.9), except exponentially small terms. Here will focus on the lowest two terms in (4.5.9).

The equations for $\rho_0$ and $\rho_1$ are

$$\begin{aligned}
&\rho_0'' + \frac{f'}{2f}\rho_0' - \frac{d-1}{z}\rho_0'(1+f\rho_0'^2) = 0 \\
&\rho_1'' + \left(\frac{f'}{2f} - \frac{(d-1)(1+3f\rho_0'^2)}{z}\right)\rho_1' + \frac{d-2}{f}(1+f\rho_0'^2) = 0\ ,
\end{aligned} \tag{4.5.10}$$

which can be solved by

$$\rho_0 = \int_0^z dy\, \frac{y^{d-1}}{f^{\frac{1}{2}}\sqrt{a^{-1}-y^{2(d-1)}}} \tag{4.5.11}$$

and

$$\rho_1(z) = \int_0^z dz\, \frac{z^{d-1}}{f^{\frac{1}{2}}\left(1-az^{2(d-1)}\right)^{\frac{3}{2}}}\left(b + (d-2)\int_z^1 dy\, \frac{\sqrt{1-ay^{2(d-1)}}}{f^{\frac{1}{2}}y^{d-1}}\right) \tag{4.5.12}$$

with $a$ and $b$ integration constants.

The expansion (4.5.9) should break down for small $\rho$ when $\rho_0$ or higher order terms become comparable to $R$. As in the strip case we again expect that the tip of the surface $z(\rho=0) \equiv z_t$ approaches the horizon $z=1$, when $R$ is large. We thus expect the UV expansion to break down near the horizon. This indicates that we should choose

$$a = 1\ . \tag{4.5.13}$$

An immediate consequence of the above equation is that the expansion of $\rho_0$ near the boundary has the form

$$\rho_0 = \frac{1}{d}z^d + \cdots \quad \rightarrow \quad c_d(R) = -\frac{1}{d} + \cdots\ , \tag{4.5.14}$$

which from (3.3.38) immediately gives

$$S = \frac{L^{d-1}}{4G_N}\frac{\omega_{d-2}}{d-1}\frac{R^{d-1}}{z_h^{d-1}} + \cdots = \frac{L^{d-1}}{4G_N}\frac{V_{\text{sphere}}}{z_h^{d-1}} + \cdots\ , \tag{4.5.15}$$

where $V_{\text{sphere}}$ is the volume of the sphere and we have reinstated $z_h$. In Sec. 4.5.4 we generalize this result to an arbitrary shape.

**IR expansion**

It is clear both from general arguments and the numerical solution shown in Fig. 4-2 that the IR part of the minimal surface is very flat and stays in the near horizon region for a large range of $\rho$. This motivates us again to write

$$z_t = 1 - \epsilon \qquad \epsilon \to 0 \ . \tag{4.5.16}$$

The part of minimal surface near the horizon can then be expanded in terms of $\epsilon$

$$z(\rho) = 1 - \epsilon z_1(\rho) - \epsilon^2 z_2(\rho) + \cdots \tag{4.5.17}$$

with boundary conditions

$$z_1(0) = 1, \qquad z_m(0) = 0, \ \ m \geq 2, \qquad z_n'(0) = 0, \ \ n \geq 1 \ . \tag{4.5.18}$$

Below we will relate $\epsilon$ to $R$ by matching (4.5.17) with the UV expansion (4.5.9).

Plugging (4.5.17) into the equation of motion (3.3.28) we find that $z_1$ satisfies the equation

$$\frac{z_1''}{z_1} - \frac{1}{2}\frac{z_1'^2}{z_1^2} + \frac{d-2}{\rho}\frac{z_1'}{z_1} - \frac{\gamma^2}{2} = 0 \ , \tag{4.5.19}$$

where $\gamma$ was introduced in (4.5.2). Setting $z_1 = h^2$, one finds that $h$ satisfies the Bessel equation which then leads to

$$z_1 = \Gamma^2\left(\frac{d-1}{2}\right)\left(\frac{\gamma\rho}{2}\right)^{3-d} I^2_{\frac{d-3}{2}}(\gamma\rho) \ , \tag{4.5.20}$$

where we have imposed the boundary condition at $\rho = 0$. At large $\rho$ we then find that

$$z_1 = \Gamma^2\left(\frac{d-1}{2}\right)\left(\frac{\gamma\rho}{2}\right)^{3-d} \frac{e^{2\gamma\rho}}{2\pi\gamma\rho}\left(1 + O(\rho^{-2})\right) \ . \tag{4.5.21}$$

**Matching**

We now try to match the two sets of expansions in their overlapping region with

$$1 \ll \sigma \equiv R - \rho \ll R, \qquad \epsilon \ll u \equiv 1 - z \ll 1 \ . \tag{4.5.22}$$

In the above region equation (4.5.21) can be expanded in large $R$ as

$$z_1 = \Lambda e^{-2\gamma\sigma}\left(1 + \frac{c_{11}(\sigma)}{R} + \frac{c_{12}(\sigma)}{R^2} + \cdots\right) \equiv C_1(\sigma)\Lambda e^{-2\gamma\sigma} \tag{4.5.23}$$

with

$$\Lambda = \Gamma^2\left(\frac{d-1}{2}\right)\frac{2^{d-4}}{\pi\gamma^{d-2}}\frac{e^{2\gamma R}}{R^{d-2}} \qquad c_{11}(\sigma) = (d-2)\sigma, \qquad \cdots \ . \tag{4.5.24}$$

One can show that $z_2$ has a similar structure, i.e.

$$z_2 = \Lambda^2 e^{-4\gamma\sigma} c_{20}\left(1 + \frac{c_{21}(\sigma)}{R} + \frac{c_{22}(\sigma)}{R^2} + \cdots\right) \equiv \Lambda^2 e^{-4\gamma\sigma} C_2(\sigma) \ . \tag{4.5.25}$$

We thus have

$$u = \epsilon z_1 + \epsilon^2 z_2 + \cdots = \epsilon\Lambda C_1(\sigma)e^{-2\gamma\sigma} + (\epsilon\Lambda)^2 C_2(\sigma)e^{-4\gamma\sigma} + \cdots \ . \tag{4.5.26}$$

One now expands $\rho_0$ and $\rho_1$ for small $u$

$$\rho_0 = -\frac{1}{2\gamma}\log u + b_0 + b_{01}u + \cdots , \tag{4.5.27}$$

$$\rho_1 = \frac{b}{4\gamma(d-1)}\frac{1}{u} - b_{\log}\log u + b_{10} + b_{11}u + \cdots \tag{4.5.28}$$

where various coefficients $b_0, b_{01}, \cdots$ can be found explicitly from (4.5.11)–(4.5.12). In particular $b_0$ is given by (4.5.5). Using (4.5.27)–(4.5.28) in (4.5.9) we then find that

$$\sigma = \rho_0 + \frac{\rho_1}{R} + \cdots = \frac{b}{4\gamma(d-1)}\frac{1}{u} - \frac{1}{2\gamma}B_c(R)\log u + B_0(R) + B_1(R)u + \cdots \ , \tag{4.5.29}$$

where

$$B_c(R) = 1 + \frac{2\gamma b_{\log}}{R} + O(R^{-2}), \qquad B_0(R) = b_0 + \frac{b_{10}}{R} + O(R^{-2}), \qquad \cdots . \quad (4.5.30)$$

Now matching (4.5.26) and (4.5.29) we find they precisely match provided that $b = 0$ and

$$\epsilon = \epsilon_0 \left(1 + \frac{d_1}{R} + \frac{d_2}{R^2} + \cdots\right) \quad (4.5.31)$$

with

$$\epsilon_0 = e^{2\gamma b_0}\Lambda^{-1} = \left(\Gamma^2\left(\frac{d-1}{2}\right)\frac{2^{d-4}}{\pi\gamma^{d-2}}\frac{e^{2\gamma R}}{R^{d-2}}\right)^{-1} e^{2\gamma b_0}, \qquad d_1 = 2\gamma b_{10} - (d-2)b_0, \quad \cdots . \quad (4.5.32)$$

### 4.5.3 Large $R$ behavior of the entanglement entropy

By carrying out the procedure outlined above one could in principle obtain the large $R$ expansion for the entanglement entropy to any desired order. As an illustration we now calculate the constant term (i.e. $R$-independent term) in $S$ for $d = 3$.

We divide the area functional (3.3.23) into a UV and IR piece and calculate to $O(R^0)$:

$$A \equiv A_{UV} + A_{IR} \quad (4.5.33)$$

$$A_{UV} = \int_\delta^{z_*} dz\, \frac{\rho}{z^2}\sqrt{\rho'(z)^2 + \frac{1}{f(z)}} \quad (4.5.34)$$

$$A_{IR} = \int_0^{\rho_*} d\rho\, \frac{\rho}{z^2}\sqrt{1 + \frac{z'(\rho)^2}{f(z)}}\,, \quad (4.5.35)$$

where $z_*$ is an arbitrary point in the matching region and $\rho(z_*) = \rho_*$ and $\delta$ is a UV cutoff. Plugging in the UV expansion (4.5.9) and (4.5.11) into $A_{UV}$ we get:

$$A_{UV} = \int_\delta^{z_*} dz\, \frac{R - \rho_0(z)}{z^2\sqrt{f(z)(1-z^4)}} + \rho_1(z_*) + O\left(\frac{1}{R}\right) \quad (4.5.36)$$

This has an expression for small $u_* = 1 - z_*$:

$$A_{UV} = -\frac{1}{8\gamma^2}\log^2 u_* + \frac{R-b_0}{2\gamma}\log u_* + \rho_1(u_*) + \frac{R}{\delta} + a_{UV} + O(u_*) \ , \quad (4.5.37)$$

$$a_{UV} \equiv -R + \int_0^1 dz \left[\frac{R-\rho_0(z)}{z^2\sqrt{f(z)(1-z^4)}} - \frac{R}{z^2} - \frac{1}{4\gamma^2}\frac{\log(1-z)}{(1-z)} - \frac{1}{2\gamma}\frac{R-b_{00}}{1-z}\right] . \quad (4.5.38)$$

Note that $\rho_1(u_*)$ contains $\log u_*$ and constant terms, but we chose not to expand it for later convenience. We isolated all $u_*$ and $\delta$ dependence, hence $a_{UV}$ is a finite term independent of $u_*$. It includes finite area law terms. $A_{IR}$ is given by

$$A_{IR} = \int_0^{\rho_*} d\rho \left[\rho + c\,\rho\left(2z_1(\rho) + \frac{z_1'(\rho)^2}{2\gamma^2 z_1(\rho)}\right) + O(c^2)\right] . \quad (4.5.39)$$

Plugging in the results of the IR expansion we find

$$\begin{aligned} A_{IR} &= \frac{\rho_*^2}{2} + O(u_*) = \frac{R^2}{2} - R\rho_0(u_*) + \frac{\rho_0(u_*)^2}{2} - \rho_1(u_*) + O(u_*) \\ &= \frac{R^2}{2} + \frac{1}{8\gamma^2}\log^2 u_* - \frac{R-b_0}{2\gamma}\log u_* + \frac{b_0^2}{2} - \rho_1(u_*) \ . \end{aligned} \quad (4.5.40)$$

Adding together (4.5.37) and (4.5.40), we find that the $u_*$ dependence cancels which provides a nontrivial consistency check, and the final result is

$$A = \#\frac{R^2}{2} + (\text{area law terms}) + a \ , \quad (4.5.41)$$

$$a = \frac{b_0^2}{2} - \int_0^1 dz \left[\frac{\rho_0(z)}{z^2\sqrt{f(z)(1-z^4)}} - \frac{1}{2\gamma}\frac{-\frac{1}{2\gamma}\log(1-z) + b_0}{(1-z)}\right] . \quad (4.5.42)$$

$b_0$ is the constant term in the expansion (4.5.27) of $\rho_0$, and it is given by (4.5.5).

### 4.5.4 Leading order result for an arbitrary shape

For arbitrary shape we cannot go into as much detail as for the sphere case. Here we demonstrate that at leading order in the large size limit the entanglement entropy goes to thethermal entropy in an explicit calculation. To the best of our knowledge

this is the first demonstration using the holographic approach, although the result is widely expected.

We choose spherical coordinates on each $z$ slice of the spacetime:

$$ds^2|_{t=0} = \frac{L^2}{z^2}\left(\left[d\rho^2 + \rho^2 d\Omega_{d-2}^2\right] + \frac{dz^2}{f(z)}\right) , \tag{4.5.43}$$

$$d\Omega_{d-2}^2 = \sum_{i=1}^{d-2} g_i \, d\theta_i^2 , \tag{4.5.44}$$

where $g_i$ are just the conventional metric components:

$$g_1 = 1 , \qquad g_2 = \sin^2\theta_1 , \qquad g_3 = \sin^2\theta_1 \sin^2\theta_2 , \ldots . \tag{4.5.45}$$

We will use the notation

$$(\partial_\Omega F)^2 \equiv \sum_{i=1}^{d-2} \frac{1}{g_i}\left(\frac{\partial F}{\partial \theta_i}\right)^2 , \tag{4.5.46}$$

and denote the set of $\theta_i$'s as $\Omega$.

We parametrize the entangling surface in polar coordinates as

$$\rho = R\, r(\Omega) \tag{4.5.47}$$

where $r(\Omega)$ specifies the shape of the surface, while $R$ gives its size. The minimal surface $\rho(z, \Omega)$ then satisfies the boundary condition $\rho(z = 0, \Omega) = R\, r(\Omega)$.

The entanglement entropy is given by the minimal surface area:

$$S(R) = \frac{2\pi L^{d-1}}{\kappa^2} A = K' A, \quad K' \equiv \frac{2\pi L^{d-1}}{\kappa^2} , \tag{4.5.48}$$

where

$$A = \int_0^{z_t} dz \int d\Omega_{d-2} \, \frac{\rho^{d-2}}{z^{d-1}} \sqrt{(\partial_z \rho)^2 + \frac{1}{f(z)}\left(1 + \frac{(\partial_\Omega \rho)^2}{\rho^2}\right)} = \int_0^{z_t} dz \int d\Omega \, \mathcal{L} . \tag{4.5.49}$$

One can go through the same steps as for the sphere case, where $r(\Omega) = 1$, to

obtain the near boundary expansion:

$$\rho(z,\Omega) = Rr(\Omega) - \frac{z^2}{2R}\tilde{r}(\Omega) + \cdots + c_d(R,\Omega)z^d + \cdots + \sum_{n=2,m=2}^{\infty} a_{nm}(R,\Omega)z^{n+m\alpha} \ . \quad (4.5.50)$$

$\tilde{r}(\Omega)$ and the functions appearing in higher orders can be determined by solving algebraic equations only involving $r(\Omega)$ and its derivatives. One can use the asymptotic data, $c_d(R,\Omega)$ to obtain $dA/dR$, by using the Hamilton-Jacobi formalism [6]. We take $z$ to be time, and introduce the canonical momentum and Hamiltonian

$$\Pi = \int d\Omega \frac{\partial \mathcal{L}}{\partial(\partial_z \rho)} = \int d\Omega \frac{\rho^{d-2}}{z^{d-1}} \frac{\rho'}{\sqrt{(\partial_z\rho)^2 + \frac{1}{f(z)}\left(1 + \frac{(\partial_\Omega \rho)^2}{\rho^2}\right)}} \ , \quad (4.5.51)$$

$$\mathcal{H} = \Pi\rho' - \mathcal{L} = -\int d\Omega \frac{\rho^{d-2}}{z^{d-1}} \frac{1 + \frac{(\partial_\Omega\rho)^2}{\rho^2}}{\sqrt{(\partial_z\rho)^2 + \frac{1}{f(z)}\left(1 + \frac{(\partial_\Omega\rho)^2}{\rho^2}\right)}} \ . \quad (4.5.52)$$

One can show that

$$\frac{dA}{dR} = -dR^{d-2}\, c_d(R) - \frac{\tilde{e}_d}{R} + \dots \ , \quad (4.5.53)$$

where $\tilde{e}_d$ is proportional to $e_d$ in (3.3.38), dots denote non-universal terms that drop out when acted on with the differential operator (1.2.4), and

$$c_d(R) \equiv \int d\Omega \frac{r(\Omega)^{d-1}}{\sqrt{1 + \frac{(\partial_\theta r(\theta_i))^2}{r(\Omega)^2}}} c_d(R,\Omega) \ . \quad (4.5.54)$$

As a result $\mathcal{S}_d(R)$ can be solely expressed in terms of $c_d(R)$, and the same formulae apply as in section 3.3.3.

In the large $R$ limit we consider the expansion

$$\rho(z,\theta_i) = Rr(\Omega) - \rho_0(z,\Omega) + \cdots \ . \quad (4.5.55)$$

Plugging in the above expression into the equation of motions we can readily solve $\rho_0$

$$\rho_0(z,\Omega) = \int_0^z dz \frac{z^{d-1}}{f^{\frac{1}{2}}\sqrt{a(\Omega)^{-1} - z^{2(d-1)}}} \sqrt{1 + \frac{(\partial_i r(\Omega))^2}{r^2(\Omega}} \ , \tag{4.5.56}$$

where $a(\Omega)$ is an integration "constant" to be determined. As in (4.5.13), considering that the UV expansion (4.5.55) should break down precisely at the horizon, we require that

$$a(\Omega) = 1 \ . \tag{4.5.57}$$

Then $\rho_0$ factorizes and we obtain:

$$\rho_0(z,\Omega) = \sqrt{1 + \frac{(\partial_\Omega r(\Omega))^2}{r^2(\Omega)}}\, \rho_0^{(S)} = \sqrt{1 + \frac{(\partial_\Omega r(\Omega))^2}{r^2(\Omega)}} \int_0^z dy \, \frac{y^{d-1}}{f^{\frac{1}{2}}\sqrt{1 - y^{2(d-1)}}} \ , \tag{4.5.58}$$

where $\rho_0^{(S)}$ is the sphere result given in (4.5.11). We readily obtain:

$$c_d(R,\Omega) = -\frac{1}{d}\sqrt{1 + \frac{(\partial_\Omega r(\Omega))^2}{r(\Omega)^2}} \ , \tag{4.5.59}$$

$$c_d(R) = \int d\Omega \, \frac{r(\Omega)^{d-1}}{\sqrt{1 + \frac{(\partial_\Omega r(\Omega))^2}{r(\Omega)^2}}}\, c_d(R,\Omega) = -\frac{1}{d}\int d\Omega \, r(\Omega)^{d-1} = -\frac{(d-1)\, V_\Sigma}{d\, R^{d-1}} \ , \tag{4.5.60}$$

where $V_\Sigma$ is the volume enclosed by $\Sigma$. Plugging into (3.3.37) yields the result

$$S^{(\Sigma)} = K' V_\Sigma + \cdots \ . \tag{4.5.61}$$

## 4.A The $n = 2$ case

In the $n = 2$ case the minimal surface ending on the boundary theory sphere has disk topology. This was seen before in [6], where the Coulomb branch flow of $d = 4$ MSYM [70] was analyzed.

Firstly, we analyze the IR region. In section 4.2.2 we saw that the small $u$ expansion (4.2.15) of the reference solution $\bar{\rho}_d$ was singular for $n = 2$. Unlike in the $n < 2$

case, the expansion does not start with a constant term:

$$\bar{\rho}_d(u) = \sqrt{\frac{2(d-2)}{d-1}}\sqrt{\log\frac{u_0}{u}} + \cdots + \frac{\bar{h}}{u_0^{d-1}}\,u^{d-1} + \ldots \qquad (u \to 0)\ . \tag{4.A.1}$$

(4.2.14) then implies that $\rho(z)$ has the small $z/z_t$ expansion valid in the region (4.2.19):

$$\begin{aligned}\rho(z) &= \sqrt{\frac{2(d-2)}{(d-1)a}}\sqrt{\log\frac{u_0\,z_t}{z}} + \cdots + \frac{\bar{h}}{\sqrt{a}\,(u_0\,z_t)^{d-1}}\,z^{d-1} + \ldots \\ &= \sqrt{\frac{2(d-2)}{(d-1)a}}\sqrt{\log(\sqrt{a}\,u_0\,z_t)}\left[1 - \frac{1}{2}\,\frac{\log(\sqrt{a}\,z)}{\log(\sqrt{a}\,u_0\,z_t)} + \ldots\right] \\ &+ \frac{\bar{h}}{\sqrt{a}\,(u_0\,z_t)^{d-1}}\,z^{d-1} + \ldots\ .\end{aligned} \tag{4.A.2}$$

Let us turn our attention to the UV expansion (4.1.30). We have to modify it so that $\hat{\rho}$ is multiplied by a general function $F(R)$, not $R^{-\nu}$. To obtain the large $z$ behavior of $\rho_1(z)$ we go through the same steps as in (4.2.20) to get:

$$\rho_1(z) = \frac{b_1}{(d-1)\sqrt{a}}\,z^{d-1}(1+\ldots) + \frac{d-2}{(d-1)a}\log z\,(1+\ldots)\ . \tag{4.A.3}$$

We note that taking the $n \to 2$ limit of (4.2.20) can also give us this result. Plugging in $n = 2$ into (4.2.21), and combining all this together in (4.1.30) gives:

$$\rho(z) = R - \frac{1}{(d-1)\sqrt{a}}\left(\frac{b_1}{R} + \cdots + \hat{b}\,F(R)\right)z^{d-1} - \frac{d-2}{(d-1)a\,R}\log z + \ldots\ . \tag{4.A.4}$$

Matching this expansion to the IR solution (4.A.2) determines

$$R = \sqrt{\frac{2(d-2)}{(d-1)a}}\sqrt{\log(\sqrt{a}\,u_0\,z_t)} \tag{4.A.5}$$

$$b = 0 \tag{4.A.6}$$

$$\hat{b} = -(d-1)\,\bar{h} \tag{4.A.7}$$

$$F(R) = a^{(d-1)/2}\exp\left(-\frac{(d-1)^2\,a}{2(d-2)}\,R^2\right)\ . \tag{4.A.8}$$

It would be very interesting where exponential behavior comes from in field theory.

The non-analytic contribution to $\mathcal{S}_d$ is also exponentially small for $n = 2$. Using (3.3.38) and (4.1.31) the leading large $R$ contribution we get for $\mathcal{S}_d$ is

$$\mathcal{S}_d^{(\text{non-analytic})} \propto (a\,R^2)^t \exp\left(-\frac{(d-1)^2\,a}{2(d-2)}\,R^2\right) \qquad t \equiv \frac{d-3}{2} + \left[\frac{d}{2}\right] . \tag{4.A.9}$$

## 4.B $1/R$ term in the $d = 3$ scaling geometries

Let us divide the area func an IR part and let $z_*$ be some $z$ in the matching region that divides between the two regions. It is clear that the result should not depend on $z_*$.

$$A \equiv A_{UV} + A_{IR} = \int_0^{z_*} dz\,\frac{\rho}{z^2}\sqrt{\rho'(z)^2 + \frac{1}{f(z)}} + \int_{z_*}^{z_t} dz\,\frac{\rho}{z^2}\sqrt{\rho'(z)^2 + \frac{1}{f(z)}} \ . \tag{4.B.1}$$

For $A_{UV}$, we can go through the same steps leading to (4.2.27). We obtain

$$A_{UV} = \#\,R + \frac{1}{R}\int_0^{z_*} dz\,\left[\frac{\sqrt{f(z)}}{2z^2}\rho_1'(z)^2 - \frac{\rho_1(z)}{z^2}\right] + O\left(\frac{1}{R^3}\right) \ . \tag{4.B.2}$$

Because the integrand for $A_{UV}$ is the same as in the first line of (4.2.26), and only the upper limit of the integral differs, in analogy with (4.2.26) and (4.2.27), we obtain

$$A_{UV} = \#\,R + \frac{1}{R}\left[-\frac{1}{2}\int_0^{z_*} dz\,\frac{z^2}{\sqrt{f(z)}}\left[\int_z^\infty dv\,\frac{1}{v^2\sqrt{f(v)}}\right]^2 + \frac{\sqrt{f(z)}}{z^2}\rho_1'(z)\rho_1(z)\Big|_{z=z_*}\right] + \dots \ , \tag{4.B.3}$$

where the last term is a boundary term that vanished in (4.2.27); here it will play an important role.

For $z > z_{CO}$ we will assume for simplicity that $f(z) = a\,z^n$ exactly. We set $a = 1$ to avoid clutter. Corrections to $f(z)$ can be understood in a perturbative setup, and for fast enough convergence to the asymptotic behavior, the results obtained below should hold. In Appendix 4.D, we show how to incorporate subleading terms in $f(z)$

for domain wall flows. Because we have the full scaling symmetry in the IR, we can evaluate the IR on-shell action by using the solution $\bar{\rho}_d(z)$ introduced in (4.2.14).

$$A_{IR} = \int_{z_*}^{z_t} dz\, \frac{\rho}{z^2}\sqrt{\rho'(z)^2 + \frac{1}{f(z)}} = \frac{1}{z_t^n}\int_{z_*/z_t}^{1} du\, \frac{\bar{\rho}_d(u)}{u^2}\sqrt{\bar{\rho}_d'(u)^2 + \frac{1}{u^n}}\,. \qquad (4.B.4)$$

For small $u$ we can plug in the UV expansion (4.2.15) of $\bar{\rho}_d(z)$ into the integral to obtain the leading behavior of the integrand

$$\begin{aligned}\frac{\bar{\rho}_d(u)}{u^2}\sqrt{\bar{\rho}_d'(u)^2 + \frac{1}{u^n}} \;=\; & \frac{\bar{\alpha}_0}{u^{2+n/2}} + \frac{\alpha_1 + \frac{(2-n)^2}{2}\alpha_1^2}{\bar{\alpha}_0\, u^{3n/2}} + \ldots \\ & + \frac{\bar{h}\left(1 + \left(\frac{2}{n} - 1\right)\left(\frac{6}{n} - 1\right)\alpha_1\right)}{\bar{\alpha}_0^{\frac{2}{n}}}\, u^{1-n/2} + \ldots\,. \qquad (4.B.5)\end{aligned}$$

We have to subtract the divergences from the integrand coming from the first line of (4.B.5), in order to be able to obtain the $1/R$ expansion of $A_{IR}$. Note that for $n < 2/3$, only the first term gives a divergence. For $2/3 < n < 4/5$, only the first two terms give a divergence, and so on. It does not hurt to subtract arbitrary regular terms from the integrand, so we can proceed by subtracting the first few terms in the first line of (4.B.5). Finally, we can write down the result for $A_{IR}$

$$\begin{aligned}A_{IR} \;=\; & \frac{1}{z_t^n}\int_{z_*/z_t}^{1} du\, \left[\frac{\bar{\rho}_d(u)}{u^2}\sqrt{\bar{\rho}_d'(u)^2 + \frac{1}{u^n}} - \frac{\bar{\alpha}_0}{u^{2+n/2}} - \frac{\alpha_1 + \frac{(2-n)^2}{2}\alpha_1^2}{\bar{\alpha}_0\, u^{3n/2}} + \ldots\right] \\ & + \frac{1}{z_t^n}\left[-\frac{\bar{\alpha}_0}{\left(1 + \frac{n}{2}\right) u^{1+n/2}} - \frac{\alpha_1 + \frac{(2-n)^2}{2}\alpha_1^2}{\left(\frac{3n}{2} - 1\right)\bar{\alpha}_0\, u^{3n/2-1}} + \ldots\right]_{u=z_*/z_t}^{u=1}\,. \qquad (4.B.6)\end{aligned}$$

For $n = 2/3$ the above equation is replaced by

$$\begin{aligned}A_{IR} \;=\; & \frac{1}{z_t^{2/3}}\int_{z_*/z_t}^{1} du\, \left[\frac{\bar{\rho}_d(u)}{u^2}\sqrt{\bar{\rho}_d'(u)^2 + \frac{1}{u^{2/3}}} - \frac{\bar{\alpha}_0}{u^{7/3}} - \frac{\alpha_1 + \frac{8}{9}\alpha_1^2}{\bar{\alpha}_0\, u}\right] \\ & + \frac{1}{z_t^{2/3}}\left[-\frac{\bar{\alpha}_0}{\frac{4}{3}u^{4/3}} + \frac{\alpha_1 + \frac{8}{9}\alpha_1^2}{\bar{\alpha}_0}\log u\right]_{u=z_*/z_t}^{u=1}\,. \qquad (4.B.7)\end{aligned}$$

The lower limit of the integral in the first line can be sent to zero without encountering

divergences. Using (4.2.18) we can trade $z_t$ for $R$

$$z_t = \left(\frac{R}{\bar{\alpha}_0}\right)^{2/(2-n)} . \tag{4.B.8}$$

We obtain

$$A_{IR} = \frac{\#}{R^{2n/(2-n)}} + \frac{R}{\left(1+\frac{n}{2}\right) z_*^{1+n/2}} + \frac{1}{R}\frac{\alpha_1 + \frac{(2-n)^2}{2}\alpha_1^2}{\left(\frac{3n}{2}-1\right) z_*^{3n/2-1}} + \dots , \tag{4.B.9}$$

where the expansion is a double expansion as in (4.2.19). For $n = 2/3$ the answer is:

$$A_{IR} = \frac{\#}{R} + \frac{R}{\frac{4}{3} z_*^{1+n/2}} - \frac{27}{64}\frac{\log R}{R} + \dots \tag{4.B.10}$$

We know the coefficient of the first term from the analysis performed in the main text. In this approach it is given by a more complicated expression: the integral in the first line (with the lower limit sent to zero) and the $u = 1$ boundary terms in the second line in (4.B.6). It is related to $e_n$ by some simple factors. The second term is an uninteresting area law term. The third term is the $1/R$ term we are after. Combining this term with the boundary term in (4.B.3) we get for the $1/R$ term:

$$\begin{aligned} A = \#\, R + \frac{\#}{R^{2n/(2-n)}} \\ - \frac{1}{R}\left[\frac{1}{2}\int_0^{z_*} dz\, \frac{z^2}{\sqrt{f(z)}}\left[\int_z^\infty dv\, \frac{1}{v^2\sqrt{f(v)}}\right]^2 + \frac{2}{(3n/2-1)(2+n)^2}\frac{1}{z_*^{3n/2-1}}\right] + \dots , \end{aligned} \tag{4.B.11}$$

where we plugged in the value of $\alpha_1$ (4.2.16) and the UV expansion of $\rho_1$ (4.2.20). For $n > 2/3$ the two terms beautifully combine to give:

$$A = \#\, R + \frac{\#}{R^{2n/(2-n)}} - \frac{a_1}{2R} + \dots \tag{4.B.12}$$

$$a_1 = \int_0^\infty dz\, \frac{z^2}{\sqrt{f(z)}}\left[\int_z^\infty dv\, \frac{1}{v^2\sqrt{f(v)}}\right]^2 . \tag{4.B.13}$$

For $n = 2/3$ there are no terms coming from (4.B.3) that could contribute to the $\log R/R$ term of (4.B.10). Hence we obtain:

$$A = \#\, R - \frac{27}{64}\frac{\log R}{R} + \frac{\#}{R} + \dots \ . \tag{4.B.14}$$

For $n < 2/3$ we have to apply subtractions, then $a_1$ is given by

$$a_1 = \int_0^\infty dz \left( \frac{z^2}{\sqrt{f(z)}} \left[ \int_z^\infty dv \, \frac{1}{v^2\sqrt{f(v)}} \right]^2 - \frac{4}{(2+n)^2}\frac{1}{z^{3n/2}} \right) . \tag{4.B.15}$$

Note that in the main text we use a dimensionless version of $a_1$ denoted by $s_1$. Because we set $a = 1$ in this appendix, plugging in $\tilde{\mu} = 1$ in the expression of $s_1$ gives the result for $a_1$ obtained here.

## 4.C Details of the UV expansion of $\rho_1$ for the domain wall case

We are interested in the behavior of $\rho_1$ at large $z$ beyond the crossover scale $z_{CO}$: $z_{CO} \ll z \ll R$. We assume that $f(z)$ takes the form:

$$f(z) = f_\infty \left( 1 - \frac{\lambda}{z^{2\tilde{\alpha}}} \right) + \dots \qquad (z \gg z_{CO}) \ . \tag{4.C.1}$$

where we introduced $\lambda \equiv \tilde{\mu}^{-2\tilde{\alpha}}$. From (4.1.35)

$$\rho_1 = b_1 \rho_{hom}(z) + \xi(z) \tag{4.C.2}$$

with

$$\xi(z) \equiv (d-2) \int_0^z du \, \frac{u^{d-1}}{\sqrt{f(u)}} \int_u^\infty dv \, \frac{1}{v^{d-1}\sqrt{f(v)}} \ . \tag{4.C.3}$$

For large $z$, $\rho_{hom}(z)$ has the expansion

$$\rho_{hom}(z) = \frac{z^d}{d\sqrt{f_\infty}} \left( 1 + \frac{d\lambda}{2(d-2\tilde{\alpha})} z^{-2\tilde{\alpha}} + \dots \right) + O(z_{CO}^d) \ . \tag{4.C.4}$$

The large $z$ behavior of $\xi(z)$ is a bit more complicated. For $\tilde{\alpha} > 1$ we have

$$\begin{aligned}\xi(z) =& \int_0^z du \left[\frac{u^{d-1}}{\sqrt{f(u)}}(d-2)\int_u^\infty dv \frac{1}{v^{d-1}\sqrt{f(v)}} - \frac{u}{f_\infty}\right] + \frac{z^2}{2f_\infty} \\ =& \frac{z^2}{2f_\infty} + \gamma - \int_u^\infty du \left[\frac{u^{d-1}}{\sqrt{f(u)}}(d-2)\int_u^\infty dv \frac{1}{v^{d-1}\sqrt{f(v)}} - \frac{u}{f_\infty}\right] \\ =& \frac{z^2}{2f_\infty} + \gamma - \frac{\lambda}{2f_\infty}\frac{(d-2+\tilde{\alpha})}{(\tilde{\alpha}-1)(d-2+2\tilde{\alpha})} z^{2-2\tilde{\alpha}} + O(z^{2-4\tilde{\alpha}})\end{aligned} \tag{4.C.5}$$

with

$$\gamma = \int_0^\infty du \left[\frac{u^{d-1}}{\sqrt{f(u)}}(d-2)\int_u^\infty dv \frac{1}{v^{d-1}\sqrt{f(v)}} - \frac{u}{f_\infty}\right], \qquad \tilde{\alpha} > 1\,. \tag{4.C.6}$$

For $1 \geq \tilde{\alpha} > 1/2$ we have to do more subtractions:

$$\begin{aligned}\xi(z) =& \int_0^z du \left[\frac{u^{d-1}}{\sqrt{f(u)}}(d-2)\int_u^\infty dv \frac{1}{v^{d-1}\sqrt{f(v)}} - \frac{u}{f_\infty} - \frac{\lambda(d-2+\tilde{\alpha})}{(d-2+2\tilde{\alpha})f_\infty} u^{1-2\tilde{\alpha}}\right] \\ &+ \frac{z^2}{2f_\infty}\left(1 + \frac{\lambda(d-2+\tilde{\alpha})}{(1-\tilde{\alpha})(d-2+2\tilde{\alpha})} z^{-2\tilde{\alpha}}\right) \\ =& \frac{z^2}{2f_\infty}\left(1 + \frac{\lambda(d-2+\tilde{\alpha})}{(1-\tilde{\alpha})(d-2+2\tilde{\alpha})} z^{-2\tilde{\alpha}}\right) + \gamma + O\left(z^{2-4\tilde{\alpha}}\right)\,,\end{aligned} \tag{4.C.7}$$

where now $\gamma$ is given by

$$\gamma = \int_0^\infty du \left[\frac{u^{d-1}}{\sqrt{f(u)}}(d-2)\int_u^\infty dv \frac{1}{v^{d-1}\sqrt{f(v)}} - \frac{u}{f_\infty} - \frac{\lambda(d-2+\tilde{\alpha})}{(d-2+2\tilde{\alpha})f_\infty} u^{1-2\tilde{\alpha}}\right]. \tag{4.C.8}$$

For $\tilde{\alpha}$ outside the above ranges one has to do more subtractions, but the leading expressions remain the same as (4.C.7) with the explicit value of $\gamma$ being different.

## 4.D $1/R$ term in the $d = 3$ domain wall geometry

In the domain wall case we follow the same logic as in Appendix 4.B, i.e. we divide the area functional into UV and IR parts as in (4.B.1). The UV expansion for scaling

and domain wall geometries takes the same form, and correspondingly $A_{UV}$ has an identical form to (4.B.3). $z_*$ is an arbitrary point in the region (4.4.20).

$A_{IR}$ can be obtained by regarding $f(z)$ as a perturbation of $f_\infty$ and working to first order. We set up the IR problem a bit differently, than in section 4.4:

$$\rho(z) = r_0(z) + \lambda r_1(z) = \sqrt{R^2 - \frac{z^2}{f_\infty}} + \lambda r_1(z) \tag{4.D.1}$$

$$\lambda r_1(z) - \frac{z^2}{2 f_\infty R} = -\frac{\rho_1(z)}{R} + \dots \,, \tag{4.D.2}$$

where $\lambda = \tilde{\mu}^{-2\tilde{\alpha}}$ as in (4.C.1), and the above equation follows from

$$R - \frac{\rho_1(R)}{R} + \dots = \sqrt{R^2 - \frac{z^2}{f_\infty}} + \lambda r_1(z) + \dots \,. \tag{4.D.3}$$

Let us consider how the on-shell action $A_{IR}$ changes, if we change $f(z)$. If we regard $z$ as time, this is as a Hamilton–Jacobi problem in classical mechanics, when we are interested in how the on-shell action changes. In this analogy, we are holding the initial time and the endpoint of the trajectory fixed. There will be a term coming from the explicit change of $f(z)$ in the Lagrangian. Because the original trajectory was an extremum of the action there is only a boundary term coming from the change of trajectory. Finally, there is a term coming from the change of time, when the particle reaches the endpoint. Hence we get, in the order we listed the terms above:

$$\delta A_{IR} = \int_{z_*}^{z_t} dz \frac{\delta \mathcal{L}}{\delta f} \delta f - \Pi \, \delta\rho \Big|_{z_*} - \mathcal{H}(z_t) \delta z_t \,, \tag{4.D.4}$$

where $\delta z_m$ and $\delta\rho$ denote the induced variations due to $\delta f$, and the canonical variables have the expressions

$$\Pi = \frac{\partial \mathcal{L}}{\partial \rho'} = \frac{\rho^{d-2}}{z^{d-1}} \frac{\rho'}{\sqrt{\rho'^2 + \frac{1}{f}}}, \qquad \mathcal{H} = \Pi \rho' - \mathcal{L} = -\frac{\rho^{d-2}}{z^{d-1}} \frac{1}{f\sqrt{\rho'^2 + \frac{1}{f}}} \,. \tag{4.D.5}$$

Applying the above results to the current problem, we find that

$$\delta A_{IR} = \int_{z^*}^{z_m} dz \left.\frac{\delta \mathcal{L}}{\delta f}\right|_{r_0} \left(-\frac{f_\infty \lambda}{z^{2\tilde{\alpha}}}\right) - \left.\Pi(z_*)\right|_{r_0} \lambda r_1(z_*) \tag{4.D.6}$$

where we used $\mathcal{H}(z_t) = 0$. Evaluating these with $z_m = \sqrt{f_\infty}\, R$ we get:

$$\delta A_{IR} = \#\, R - f_\infty^{-(1+\tilde{\alpha})} \lambda \frac{R^{-2\tilde{\alpha}}}{1-4\tilde{\alpha}^2} + \frac{\lambda}{2(1-2\tilde{\alpha}) f_\infty^{3/2} R} z_*^{1-2\tilde{\alpha}} + \frac{1}{\sqrt{f_\infty}\, z_*} \lambda r_1(z_*) + \dots \,. \tag{4.D.7}$$

The zeroth order contribution gives:

$$A_{IR}^{(0)} = \frac{R}{\sqrt{f_\infty} z_*} - \frac{1}{f_\infty} = \#\, R - \frac{1}{f_\infty} \,. \tag{4.D.8}$$

Adding all this up and using (4.D.2) we get:

$$\begin{aligned} A =& \#\, R - \frac{1}{f_\infty} - f_\infty^{-1-\tilde{\alpha}} \lambda \frac{R^{-2\tilde{\alpha}}}{1-4\tilde{\alpha}^2} - \frac{1}{2R} \int_0^{z_*} dz\, \frac{z^2}{\sqrt{f(z)}} \left[\int_z^\infty dv\, \frac{1}{v^2 \sqrt{f(v)}}\right]^2 \\ &+ \frac{\sqrt{f(z_*)}}{z_*^2 R} \rho_1'(z_*) \rho_1(z_*) + \frac{\lambda}{2(1-2\tilde{\alpha}) \sqrt{f_\infty}\, R} z_*^{1-2\tilde{\alpha}} - \frac{1}{\sqrt{f_\infty}\, z_*\, R} \rho_1(z_*) + \frac{z_*}{2 f_\infty^{3/2} R} \,. \end{aligned} \tag{4.D.9}$$

Note that this result is in the double expansion (4.4.20), just like all expressions in the matching region appearing in the main text. Now the common theme of this chapter has to be applied: subtractions. Subtracting the divergence(s) from the integral allows us to go with the upper limit to infinity and gives the result:

$$A = \#\, R - \frac{1}{f_\infty} - f_\infty^{-1-\tilde{\alpha}} \lambda \frac{R^{-2\tilde{\alpha}}}{1-4\tilde{\alpha}^2} - \frac{a_1}{2R} \tag{4.D.10}$$

$$a_1 = \begin{cases} \int_0^\infty dz \left[\frac{z^2}{\sqrt{f(z)}} \left[\int_z^\infty dv\, \frac{1}{v^2\sqrt{f(v)}}\right]^2 - \frac{1}{f_\infty^{3/2}}\right] & \left(\frac{1}{2} < \tilde{\alpha}\right) \\ \int_0^\infty dz \left[\frac{z^2}{\sqrt{f(z)}} \left[\int_z^\infty dv\, \frac{1}{v^2\sqrt{f(v)}}\right]^2 - \frac{1}{f_\infty^{3/2}} \left(1 + \frac{3+2\tilde{\alpha}}{2(1+2\tilde{\alpha})} \frac{\lambda}{z^{2\tilde{\alpha}}}\right)\right] & \left(\frac{1}{4} < \tilde{\alpha} < \frac{1}{2}\right) \end{cases} \tag{4.D.11}$$

The rest of the terms in (4.D.9) (after adding back the subtracted part to the integral) can be shown to cancel to the order in $z_*/R$ and $1/(\tilde{\mu} z_*)$ that we wrote them down.

The final answer is:

$$\mathcal{S}_3 = \mathcal{S}_3^{(IR)} + K_{IR} \frac{f_\infty^{-\tilde{\alpha}} \lambda}{(1-2\tilde{\alpha}) R^{2\tilde{\alpha}}} + \frac{K s_1}{\tilde{\mu} R} + \dots \,, \tag{4.D.12}$$

where $s_1 = \tilde{\mu} a_1$, as explained around (4.2.28).

# 4.E Some results for closely separated fixed points

We review and extend some results from [6] for closely separated fixed points:

$$f(z) = 1 + \epsilon g(z) \qquad g(z) \to 1 - \frac{\lambda}{z^{2\tilde{\alpha}}} \quad (z \to \infty) \tag{4.E.1}$$

$$\mathcal{S}_d = \mathcal{S}_d^{UV} - \epsilon \frac{(d-1)!! K}{2(d-2)!!} \begin{cases} \int_0^1 dx \; g(xR) & d \text{ odd} \\ \int_0^1 dx \; \frac{x g(xR)}{\sqrt{1-x^2}} & d \text{ even.} \end{cases} \tag{4.E.2}$$

Let us start with the odd $d$ case and expand for large $R$ with the technique of subtraction:

$$\begin{aligned} \int_0^1 dx \; g(xR) &= 1 + \int_0^1 dx \; [g(xR) - 1] = 1 + [x g(xR)]_{x=0}^1 + \int_0^1 dx \; [-x g'(xR) R - 1] \\ &= 1 - \int_0^1 dx \; (xR) g'(xR) + \dots \\ &= 1 - \left[ \int_0^\infty dz \; z g'(z) \right] \frac{1}{R} + \dots \,, \end{aligned} \tag{4.E.3}$$

where we used partial integration and assumed fast enough ($\tilde{\alpha} > \frac{1}{2}$) decay at infinity. If the decay is slower, we need additional subtractions. For the even dimensional case we encounter an integral similar to (4.4.7), so we can use the approximation technique from there. After subtraction the integral is expected to be dominated by the $x \ll 1$

region and we have:

$$\begin{aligned}\int_0^1 dx\ \frac{xg(xR)}{\sqrt{1-x^2}} &= 1+\int_0^1 dx\ \frac{xg(xR)-x}{\sqrt{1-x^2}} = 1+\int_0^1 dx\ \left[xg(xR)-x\right]+\dots \\ &= 1-\frac{1}{2}\int_0^1 dx\ x^2 g'(xR)R+\dots \\ &= 1-\frac{1}{2}\left[\int_0^\infty dz\ z^2 g'(z)\right]\frac{1}{R^2}+\dots\ .\end{aligned} \tag{4.E.4}$$

The final result in odd $d$ is:

$$\mathcal{S}_d = \mathcal{S}_d^{UV} - \epsilon\frac{(d-1)!!K}{2(d-2)!!} + \epsilon K\frac{1}{2}\frac{(d-1)!!}{(d-2)!!}b(\tilde{\alpha})\frac{\lambda}{R^{2\tilde{\alpha}}} + \epsilon\frac{Ks_1}{\tilde{\mu}R}+\dots \tag{4.E.5}$$

$$s_1 = \frac{(d-1)!!\,\tilde{\mu}}{2(d-2)!!}\begin{cases}\int_0^\infty dz\ zg'(z) & (\tilde{\alpha}>\frac{1}{2})\\ \int_0^\infty dz\ \left[zg'(z)-\frac{2\tilde{\alpha}\lambda}{z^{2\tilde{\alpha}}}\right] & (\tilde{\alpha}<\frac{1}{2})\ ,\end{cases} \tag{4.E.6}$$

where $\lambda=\tilde{\mu}^{-2\tilde{\alpha}}$. Of course we might need to apply more subtractions, if $\tilde{\alpha}$ is small enough.

The final result for even $d$ takes the form:

$$\mathcal{S}_d = \mathcal{S}_d^{UV} - \epsilon\frac{(d-1)!!K}{2(d-2)!!} + \epsilon K\frac{1}{2}\frac{(d-1)!!}{(d-2)!!}b(\tilde{\alpha})\frac{\lambda}{R^{2\tilde{\alpha}}} + \epsilon\frac{Ks_2}{(\tilde{\mu}R)^2}+\dots \tag{4.E.7}$$

$$s_2 = \frac{(d-1)!!\,\tilde{\mu}^2}{4(d-2)!!}\begin{cases}\int_0^\infty dz\ z^2g'(z) & (\tilde{\alpha}>1)\\ \int_0^\infty dz\ \left[z^2g'(z)-\frac{2\tilde{\alpha}\lambda}{z^{2\tilde{\alpha}-1}}\right] & (\tilde{\alpha}<1)\ .\end{cases} \tag{4.E.8}$$

Let us compare (4.E.6) to (4.4.39). We are interested in $s_1$ to first order in $\epsilon$, which we repeat here for convenience for $\frac{1}{2}<\tilde{\alpha}$:

$$s_1 = \int_0^\infty dz\ \left[\frac{z^2}{\sqrt{f(z/\tilde{\mu})}}\left[\int_z^\infty dv\ \frac{1}{v^2\sqrt{f(v/\tilde{\mu})}}\right]^2 - \frac{1}{f_\infty^{3/2}}\right]\ . \tag{4.E.9}$$

Let us first take the integral over $v$. Using (4.E.1) we obtain:

$$\int_z^\infty dv\ \frac{1}{v^2\sqrt{f(v/\tilde{\mu})}} = \frac{1}{z}-\frac{\epsilon}{2}\int_z^\infty dv\ \frac{g(v/\tilde{\mu})}{v^2}\ . \tag{4.E.10}$$

The next step is to examine the full integrand:

$$\begin{aligned}
\frac{z^2}{\sqrt{f(z/\tilde{\mu})}}\left[\int_z^\infty dv\,\frac{1}{v^2\sqrt{f(v/\tilde{\mu})}}\right]^2 &= z^2\left(1-\frac{\epsilon}{2}\,g(z/\tilde{\mu})\right)\left(\frac{1}{z^2}-\frac{\epsilon}{z}\int_z^\infty dv\,\frac{g(v/\tilde{\mu})}{v^2}\right) \\
&= 1+\epsilon\left(-\frac{1}{2}\,g(z/\tilde{\mu})+z\int_z^\infty dv\,\frac{g(v/\tilde{\mu})}{v^2}\right) \qquad (4.E.11) \\
\frac{1}{f_\infty^{3/2}} &= 1-\frac{3\epsilon}{2}\,. \qquad (4.E.12)
\end{aligned}$$

Combining the above terms we get that $s_1$ has the expression to first order in $\epsilon$:

$$s_1=\epsilon\int_0^\infty dz\,\left[-\frac{1}{2}\,g(z/\tilde{\mu})+z\int_z^\infty dv\,\frac{g(v/\tilde{\mu})}{v^2}+\frac{3}{2}\right]\,. \qquad (4.E.13)$$

We can define a new function $\tilde{g}(z)\equiv g(z)-1$ that vanishes sufficiently fast as $z\to\infty$. In terms of this new function

$$\begin{aligned}
s_1 &= \epsilon\int_0^\infty dz\,\left[-\frac{1}{2}\,\tilde{g}(z/\tilde{\mu})+z\int_z^\infty dv\,\frac{\tilde{g}(v/\tilde{\mu})}{v^2}\right] \\
&= -\epsilon\int_0^\infty dz\,\tilde{g}(z/\tilde{\mu}) \qquad (4.E.14) \\
&= \epsilon\,\tilde{\mu}\int_0^\infty dz\,z g'(z)\,,
\end{aligned}$$

where in the second line we integrated the second term partially in $z$. In the third line we did a second partial integration in $z$, and used that $\tilde{g}'(z)\equiv g'(z)$.

For $\tilde{\alpha}<\frac{1}{2}$ the same steps lead to the subtracted version of (4.E.13):

$$s_1=\epsilon\int_0^\infty dz\,\left[-\frac{1}{2}\,g(z/\tilde{\mu})+z\int_z^\infty dv\,\frac{g(v/\tilde{\mu})}{v^2}+\frac{3}{2}-\frac{3+2\tilde{\alpha}}{2(1+2\tilde{\alpha})}\,\frac{1}{z^{2\tilde{\alpha}}}\right]\,. \qquad (4.E.15)$$

Defining $\tilde{g}(z)\equiv g(z)-1+\frac{\lambda}{z^{2\tilde{\alpha}}}$ allows us to absorb all the subtracted terms, and get the simple formula:

$$s_1=-\epsilon\int_0^\infty dz\,\tilde{g}(z/\tilde{\mu})\,. \qquad (4.E.16)$$

Partially integrating in $z$ and using $\tilde{g}'(z)\equiv g'(z)-\frac{2\tilde{\alpha}\lambda}{z^{2\tilde{\alpha}+1}}$ we obtain (4.E.6).

# Chapter 5

# Entanglement entropy for superconformal gauge theories with classical gauge groups

## 5.1 Introduction

In the absence of a perturbative understanding of the fundamental degrees of freedom, one can learn about M-theory only through various dualities. A promising avenue is to use the AdS/CFT correspondence [102–104] to extract information about M-theory that takes us beyond its leading (two-derivative) eleven-dimensional supergravity limit. Such progress is enabled by the discovery of 3-d superconformal field theories (SCFTs) dual to backgrounds of M-theory of the form $AdS_4 \times X$ [105–112], as well as the development of the technique of supersymmetric localization in these SCFTs [37, 113, 114] (see also [115]). For instance, computations in these SCFTs may impose constraints on the otherwise unknown higher-derivative corrections to the leading supergravity action.

In this chapter we study several 3-d SCFTs, with the goal of extracting some information about M-theory on $AdS_4 \times X$ that is not accessible from the two-derivative eleven-dimensional supergravity approximation. These theories can be engineered by

placing a stack of $N$ M2-branes at the tip of a cone over the space $X$. A good measure of the number of degrees of freedom in these theories, and the quantity we will focus on, is the $S^3$ free energy $F$ defined as minus the logarithm of the $S^3$ partition function, $F = -\log|Z_{S^3}|$ [21, 23, 24, 28]. At large $N$, the $F$-coefficient of an SCFT dual to $AdS_4 \times X$ admits an expansion of the form [38, 116]

$$F = f_{3/2}N^{3/2} + f_{1/2}N^{1/2} + \dots . \tag{5.1.1}$$

The coefficient $f_{3/2}$ can be easily computed from two-derivative 11-d supergravity [38, 116]

$$f_{3/2} = \sqrt{\frac{2\pi^6}{27\,\mathrm{Vol}(X)}}, \tag{5.1.2}$$

whereas the coefficient $f_{1/2}$ together with the higher-order corrections in (5.1.1) cannot [117, 118]. In this chapter we will calculate $f_{1/2}$ for various SCFTs with M-theory duals.

The universal terms in $Z_{S^3}$ and in the entanglement entropy of the vacuum state across $S^1$ are equal [19]. Thus, by calculating $F$ we are evaluating entanglement entropy. In this chapter we will use the language of free energies.

We focus on SCFTs with $\mathcal{N} \geq 4$ supersymmetry. In such theories, supersymmetric localization reduces the computation of $Z_{S^3}$ to certain matrix models [119]. For instance, for the $\mathcal{N} = 6$ ABJM theory [105], which is a $U(N)_k \times U(N)_{-k}$ Chern-Simons matter gauge theory, one has [37, 116]

$$\begin{aligned} Z_{S^3} = \frac{1}{(N!)^2}\int \prod_{i=1}^{N} d\lambda_i d\tilde{\lambda}_i \frac{\prod_{i<j}\sinh^2(\pi(\lambda_i-\lambda_j))\sinh^2(\pi(\tilde{\lambda}_i-\tilde{\lambda}_j))}{\prod_{i,j}\cosh^2(\pi(\lambda_i-\tilde{\lambda}_j))} \\ \times \exp\left[i\pi k\sum_i\left(\lambda_i^2-\tilde{\lambda}_i^2\right)\right], \end{aligned} \tag{5.1.3}$$

where the integration variables are the eigenvalues of the auxiliary scalar fields in the two $\mathcal{N} = 2$ vectormultiplets. This theory corresponds to the case where the internal

space $X$ is a freely-acting orbifold of $S^7$, $X = S^7/\mathbb{Z}_k$. The integral (5.1.3) can be computed approximately at large $N$ by three methods:

I. By mapping it to the matrix model describing Chern-Simons theory on the Lens space $S^3/\mathbb{Z}_2$, and using standard matrix model techniques to find the eigenvalue distribution [116]. This method applies at large $N$ and fixed $N/k$. To extract $f_{3/2}$ and $f_{1/2}$ in (5.1.1) one needs to expand the result at large 't Hooft coupling $N/k$.

II. By expanding $Z_{S^3}$ directly at large $N$ and fixed $k$ [38]. In this limit, the eigenvalues $\lambda_i$ and $\tilde{\lambda}_i$ are uniformly distributed along straight lines in the complex plane.

III. By rewriting (5.1.3) as the partition function of $N$ non-interacting fermions on the real line with a non-standard kinetic term [1]. The partition function can then be evaluated at large $N$ and small $k$ using statistical mechanics techniques.

Using the Fermi gas approach (III), for instance, one obtains [1]

$$Z = \mathcal{A}(k)\,\mathrm{Ai}\left[\left(\frac{\pi^2 k}{2}\right)^{1/3}\left(N - \frac{k}{24} - \frac{1}{3k}\right)\right] + \mathcal{O}\left(e^{-\sqrt{N}}\right)\,, \tag{5.1.4}$$

where $\mathcal{A}(k)$ is an $N$-independent constant. From this expression one can extract

$$f_{3/2} = k^{1/2}\frac{\sqrt{2}\,\pi}{3}\,, \qquad f_{1/2} = -\frac{\pi}{\sqrt{2}}\left(\frac{k^{3/2}}{24} + \frac{1}{3k^{1/2}}\right)\,. \tag{5.1.5}$$

These expressions can be reproduced from the first method mentioned above [116], and $f_{3/2}$ can also be computed using the second method [38].

While ABJM theory teaches us about M-theory on $\mathrm{AdS}_4 \times (S^7/\mathbb{Z}_k)$, it would be desirable to calculate $F$ for other SCFTs with M-theory duals, so one may wonder how general the above methods are and/or whether they can be generalized further. So far, the first method has been generalized to a class of $\mathcal{N} = 3$ theories obtained by adding fundamental matter to ABJM theory [120].[1] The second method can be

[1] Grassi and Mariño informed us that they have also applied the first method to the $\mathcal{N} = 4$ $U(N)$

applied to many $\mathcal{N} \geq 2$ theories with M-theory duals [23, 121–125], but so far it can only be used to calculate $f_{3/2}$. The third method has been generalized to certain $\mathcal{N} \geq 2$ supersymmetric theories with unitary gauge groups [126]; in all these models, $Z_{S^3}$ is expressible in terms of an Airy function.

We provide two extensions of the above methods. We first extend method (II) to calculate the $k^{3/2}$ contribution to $f_{1/2}$ in (5.1.5), and provide a generalization to other SCFTs. We then extend the Fermi gas approach (III) to SCFTs with orthogonal and symplectic gauge groups. This method allows us to extract $f_{1/2}$ exactly for these theories, and we find agreement with results obtained using method (II). The extension of the Fermi gas approach to theories with symplectic and orthogonal gauge groups requires a fairly non-trivial generalization of the Cauchy determinant formula that we prove in the Appendix. This formula allows us to write $Z_{S^3}$ as the partition function of non-interacting fermions that can move on half of the real line and obey either Dirichlet or Neumann boundary conditions at $x = 0$. We find that the result for $Z_{S^3}$ is again an Airy function.

The rest of this chapter is organized as follows. In Section 5.2 we describe the field theories that we will consider in this chapter. These theories are not new. They can be constructed in type IIA string theory using D2 and D6 branes, as well as O2 and O6 orientifold planes. In Section 5.3 we extend the large $N$ expansion (II) to the next order. In Section 5.4 we extend the Fermi gas approach (III) to our theories of interest. We end with a discussion of our results in Section 5.5. We include several appendices. In Appendix A we determine the moduli space of vacua using field theory techniques. Appendix 5.A provides a brief summary of the Fermi gas approach [1]. Appendix 5.B contain some details of our computations. Lastly, in Appendix 5.C we prove the generalization of the Cauchy determinant formula used in the Fermi gas approach.

gauge theory with an adjoint and $N_f$ fundamental hypermultiplets. They obtained the free energy in the large $N$ limit at fixed $N/N_f$.

## 5.2 Review of $\mathcal{N} = 4$ superconformal field theories and their string/M-theory description

### 5.2.1 Brane construction and M-theory lift

We restrict ourselves to the simplest $\mathcal{N} = 4$ superconformal field theories in $d = 3$ with weakly-curved eleven-dimensional supergravity duals. The field content of our theories of interest have an $\mathcal{N} = 4$ vectormultiplet with gauge group $U(N)$, $O(2N)$, $O(2N+1)$, or $USp(2N)$, a hypermultiplet transforming in a two-index tensor representation of the gauge group, and $N_f$ hypermultiplets transforming in the fundamental (vector) representation. The two-index tensor representation can be the adjoint in the case of $U(N)$, or it can be a rank-two symmetric or anti-symmetric tensor representation in the other cases.

These SCFTs can be realized as low-energy effective theories on the intersection of various D-branes and orientifold planes in type IIA string theory as follows. In all of our constructions, we consider D2-branes stretched in the 012 directions, D6-branes stretched in the 0123456 directions, as well as O2-planes parallel to the D2-branes and O6-planes parallel to the D6-branes—See Table 5.1. Our constructions will have either an O2-plane or an O6-plane, but not both. The gauge theory lives in the 012 directions, and the choice of gauge group and two-index tensor representation is dictated by the kind of O2 or O6-plane that is present. The role of the D6-branes is to provide the fundamental hypermultiplet flavors. See Figure 5-1 for a picture of the brane configurations, and Table 5.2 for which gauge theories correspond to which brane/orientifold constructions.

| Object | 0 | 1 | 2 | 3 | 4 | 5 | 6 | 7 | 8 | 9 |
|---|---|---|---|---|---|---|---|---|---|---|
| D2/O2 | • | • | • | | | | | | | |
| D6/O6 | • | • | • | • | • | • | • | | | |

Table 5.1: The directions in which the ingredients extend are marked by •.

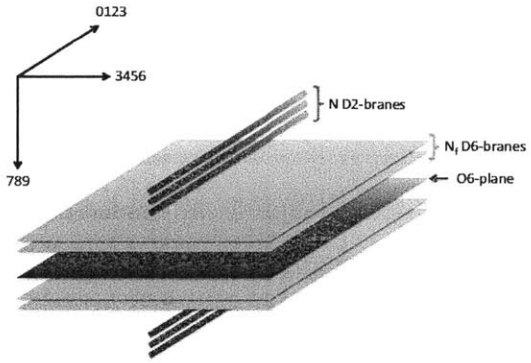


(a) Brane construction with an O6-plane.

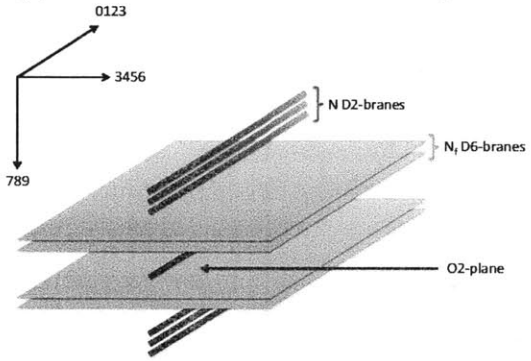


(b) Brane construction with an O2-plane.

Figure 5-1: Type IIA brane construction of the theories considered. Exactly which figure applies, and what type of orientifold plane is needed can be read from Table 5.2.

More precisely:

- $N$ D2-branes spanning the 012 directions and $N_f$ D6-branes extending in the 0123456 directions yields the $\mathcal{N} = 4$ $U(N)$ gauge theory with an adjoint hypermultiplet and $N_f$ fundamental hypermultiplets.

- To get the $O(2N)$ (or $O(2N+1)$) theory with an adjoint (antisymmetric tensor) hypermultiplet we add an O2$^-$-plane (or $\widetilde{\text{O2}}^-$-plane) coincident with the $2N$ D2-branes.[2] The $2N_f$ D6-branes[3] give $N_f$ fundamental flavors in the field theory living on the D2-branes.

[2]What we mean by this is that we have $N$ half D2-branes and their $N$ images. The $\widetilde{\text{O2}}^-$ can be thought of as having a half D2-brane stuck to an O2$^-$ plane, and hence naturally gives an $O(2N+1)$ gauge group.

[3]In the case of orientifold planes, the D6-branes should be more correctly referred to as $N_f$ half D6-branes and their $N_f$ images under the orientifold action.

- If, on the other hand, we want to construct the $O(2N)$ (or $O(2N+1)$) theory with a symmetric tensor hypermultiplet we add an O6$^+$-plane coincident with the $2N_f$ D6-branes. To get the $O(2N)$ theory we need $2N$ D2-branes, while to get $O(2N+1)$ we need a half D2-brane to be stuck at the O6$^+$-plane.

- Similarly, to get the $USp(2N)$ theory with an adjoint (symmetric tensor) hypermultiplet we add an O2$^+$-plane coincident with $2N$ D2-branes. The same theory can be obtained by using an $\widetilde{\text{O2}}^+$-plane.[4]

- To get the $USp(2N)$ gauge theory with an antisymmetric hypermultiplet, we should instead use an O6$^-$-plane.

- There are further ingredients in type IIA string theory, such as $\widetilde{\text{O6}}^\pm$-planes, but we do not use them in our constructions, because they do not yield 3-d SCFTs with known weakly-curved M-theory duals.[5][6]

The type IIA brane construction presented above can be straightforwardly lifted to M-theory, where one obtains $N$ M2-branes probing an 8-(real)-dimensional hyperkähler cone.[7] Indeed, if one ignores the D2-branes and orientifold planes for a moment, the configuration of $N_f$ separated D6-branes lifts to a configuration of $N_f$ unit mass Kaluza-Klein (KK) monopoles, and near every monopole core the spacetime is regular [130]. $N_f$ coincident D6-branes correspond to coincident KK monopoles, whose core now has an $A_{N_f-1}$ singularity; in other words, the transverse space to the

[4] In a similar construction involving $2N$ D3-branes coincident with an O3$^+$ or with an $\widetilde{\text{O3}}^+$ plane one does obtain two distinct gauge theories with symplectic gauge groups denoted by $USp(2N)$ and $USp'(2N)$, respectively. These theories differ in their spectra of dyonic line operators.

[5] We do not consider $\widetilde{\text{O6}}^\pm$ planes in our brane constructions, as they require a non-zero cosmological constant [127,128] in ten dimensions. These orientifold planes therefore only exist in massive type IIA string theory and their M-theory lifts are unknown. From the effective $2+1$-dimensional field theory perspective, an $\widetilde{\text{O6}}^-$-plane would introduce an extra fundamental half hypermultiplet compared to the O6$^-$ case. The extra half hypermultiplet introduces a parity anomaly, which can be canceled by adding a bare Chern-Simons term. This Chern-Simons term reduces the supersymmetry to $\mathcal{N}=3$ [128] and is related to the cosmological constant in ten dimensions.

[6] We remind the reader that it is impossible to have a half D2-brane stuck to an O6$^-$-plane, because the way the orientifold projection is implemented on the Chan-Paton factors requires an even number of such branes [129].

[7] The M-theory description is valid at large $N$ and fixed $N_f$. When $N_f$ is also large, a more useful description is in terms of type IIA string theory.

| $G+$ matter | D2 | D6 | O2$^-$ | $\widetilde{\text{O2}}^-$ | O2$^+$ | O6$^-$ | O6$^+$ | $\text{AdS}_4 \times X$ |
|---|---|---|---|---|---|---|---|---|
| $U(N)$ + adj | $N$ | $N_f$ | | | | | | $S^7/\mathbb{Z}_{N_f}$ |
| $O(2N)+A$ | $2N$ | $2N_f$ | ✓ | | | | | $(S^7/\hat{D}_{N_f})_{\text{free}}$ |
| $O(2N)+S$ | $2N$ | $2N_f$ | | | | | ✓ | $S^7/\hat{D}_{N_f+2}$ |
| $O(2N+1)+A$ | $2N$ | $2N_f$ | | ✓ | | | | $(S^7/\hat{D}_{N_f})_{\text{free}}$ |
| $O(2N+1)+S$ | $2N+1$ | $2N_f$ | | | | | ✓ | $S^7/\hat{D}_{N_f+2}$ |
| $USp(2N)+A$ | $2N$ | $2N_f$ | | | | ✓ | | $S^7/\hat{D}_{N_f-2}$ |
| $USp(2N)+S$ | $2N$ | $2N_f$ | | | ✓ | | | $(S^7/\hat{D}_{N_f})_{\text{free}}$ |

Table 5.2: The ingredients needed to construct a theory with gauge group $G$, $N_f$ fundamental flavors, and a two-index antisymmetric ($A$) or symmetric ($S$) hypermultiplet in Type IIA string theory. The dual M-theory background is also included.

monopole is $\mathbb{C}^2/\mathbb{Z}_{N_f}$ in this case. The infrared limit of the field theories living on the D2-branes is captured by M2-branes probing the region close to the core of the 11d KK monopole. Let us write the transverse directions to the M2-branes in complex coordinates. Let $z_1, z_2$ be the directions along which the KK monopole is extended, and $z_3, z_4$ be the directions transverse to it. Then the M2-branes probe the space $\mathbb{C}^2 \times \left(\mathbb{C}^2/\mathbb{Z}_{N_f}\right)$ [105], where the $\mathbb{Z}_{N_f}$ action on the coordinates is given by

$$(z_3, z_4) \to e^{\frac{2\pi i}{N_f}}(z_3, z_4) \ . \tag{5.2.1}$$

The orbifold acts precisely in the direction of the M-theory circle, which therefore rotates $(z_3, z_4)$ by the same angle and is non-trivially fibered over the 7 directions transverse to the D2-branes.[8]

Back-reacting the $N$ M2-branes and taking the near horizon limit yields $\text{AdS}_4 \times (S^7/\mathbb{Z}_{N_f})$, where the $\mathbb{Z}_{N_f}$ action on $S^7$ is that induced from $\mathbb{C}^4$, namely (5.2.1). This orbifold action is not free, hence $S^7/\mathbb{Z}_{N_f}$ is a singular space. Since we have not included orientifold planes yet, this $\text{AdS}_4 \times (S^7/\mathbb{Z}_{N_f})$ background of M-theory is dual

[8]Explicitly, the coordinates $x_3, \ldots, x_9$ transverse to the D2-branes can be identified with $(\text{Re}\, z_1, \text{Im}\, z_1, \text{Re}\, z_2, \text{Im}\, z_2, \text{Re}\,(z_3 z_4^*), \text{Im}\,(z_3 z_4^*), |z_3|^2 - |z_4|^2)$. The M-theory circle is parameterized by $\psi = \frac{1}{2}(\arg z_3 + \arg z_4) \in [0, 2\pi)$, and (5.2.1) identifies $\psi \sim \psi + 2\pi/N_f$.

to the $U(N)$ theory with an adjoint and $N_f$ fundamental hypermultiplets. Note that for $N_f = 1$ the monopole core is regular, the transverse space to the monopoles is $\mathbb{C}^2$, and the gravitational dual is M-theory on $AdS_4 \times S^7$. At low energies, M-theory on this background is dual to ABJM theory at Chern-Simons level $k = 1$ [105]; therefore, the $U(N)$ gauge theory with an adjoint and a flavor hypermultiplet described above is dual to ABJM theory at CS level $k = 1$ [119].

Introducing orientifolds in the type IIA construction corresponds to further orbifolding the 11d geometry.[9] The case of O2-planes is simpler: the orbifold in 11d is generated by the action:

$$\text{O2 lift:} \qquad (z_1, z_2, z_3, z_4) \to (-z_1, -z_2, iz_4^*, -iz_3^*) \ . \tag{5.2.2}$$

(See [131] for a similar orbifold action.) This action can be derived from the fact that in type IIA an O2-plane acts both by flipping the sign of all the transverse coordinates as well as of the R-R one-form $A_1$. This R-R one-form lifts to the off-diagonal components of the 11-d metric involving the M-theory circle and the type IIA coordinates (see for example [132]), so in 11d the orientifold acts by a sign flip on the M-theory circle. Eq. (5.2.2) then follows from the relations given in footnote 8. We should combine the orbifold action (5.2.2) with (5.2.1) (with $N_f \to 2N_f$). Together, the two generate the dicyclic (binary dihedral) orbifold group, $\hat{D}_{N_f}$ of order $4N_f$.[10] For $N_f = 0$ there are no D6-branes, hence the orbifold group is just $\mathbb{Z}_2$. For $N_f = 1$ the orbifold group is $\hat{D}_1 = \mathbb{Z}_4$.

In M-theory, we therefore have $N$ M2-branes probing a $\mathbb{C}^4/\hat{D}_{N_f}$ singularity, where $\hat{D}_{N_f}$ is generated by (5.2.1) (with $N_f \to 2N_f$) and (5.2.2). In the near-horizon limit, the eleven dimensional geometry is $AdS_4 \times (S^7/\hat{D}_{N_f})_{\text{free}}$. The subscript "free" emphasizes that the orbifold action induced from (5.2.1)–(5.2.2) on the $S^7$ base of $\mathbb{C}^4$ is free, and hence the corresponding eleven-dimensional background is smooth. Note

[9] We thank Oren Bergman and especially Ofer Aharony for helpful discussions on the lift of orientifolds to M-theory.

[10] Let us denote the O2 action in (5.2.2) by $a$ and the orbifold action (5.2.1) (with $N_f \to 2N_f$) by $b$. We then get the presentation of the dicyclic group $\hat{D}_{N_f} = \langle a, b | \, b^{2N_f} = 1, \, a^2 = b^{N_f}, \, ab = b^{2N_f - 1}a \rangle$.

that the $\hat{D}_{N_f}$ orbifolds here are not the same as those in [131] obtained from similar brane constructions.[11]

The O6 case is more involved. The O6$^-$-plane lifts to Atiyah-Hitchin space in M-theory [133, 134]. The O6$^-$-plane together with $2N_f$ coincident D6-branes away from the center of the Atiyah-Hitchin space can be thought of as a KK monopole with mass $(-4)$ (as the D6-brane charge of O6$^-$ is $(-4)$ [135]) and a KK monopole of mass $2N_f$, which we discussed above. When the D6-branes coincide with the O6$^-$-plane, we get a KK monopole of mass $2N_f - 4$ (away from the center). We should therefore consider the orbifold (5.2.1) with $N_f \to 2N_f - 4$. In addition, the O6 plane yields an extra orbifold in 11d generated by

$$\text{O6 lift:} \qquad (z_3, z_4) \to (iz_4^*, -iz_3^*) \ . \tag{5.2.3}$$

As in the O2 case, this action can be derived from the fact that in type IIA an O6-plane acts by flipping the sign of all the transverse coordinates and of the R-R one-form $A_1$. Together, (5.2.3) and (5.2.1) (with $N_f \to 2N_f - 4$) give a $D_{N_f}$ singularity. The corresponding orbifold group is again the dicyclic group, $\hat{D}_{N_f-2}$, so we have $N$ M2-branes probing a $\mathbb{C}^2 \times (\mathbb{C}^2/\hat{D}_{N_f-2})$ transverse space.[12]

The M-theory lift of the O6$^+$ plane is a peculiar kind of $D_4$ singularity, perhaps with extra fluxes that prevent the possibility of blowing it up [136, 137]. Further adding adding $2N_f$ D6-branes results in a $D_{N_f+4}$ singularity. The corresponding orbifold group is $\hat{D}_{N_f+2}$, so in this case we have $N$ M2-branes probing a $\mathbb{C}^2 \times (\mathbb{C}^2/\hat{D}_{N_f+2})$ transverse space. Note that if we shift $N_f \to N_f + 4$ in the O6$^-$ case, we get the same orbifold singularity as in the O6$^+$ case, perhaps with different torsion fluxes. As we

[11]The $N_f = 0$ case is special, because there are no D6-branes in this case. In M-theory one obtains a pair of $\mathbb{Z}_2$ singularities corresponding to a pair of OM2 planes sitting at opposite points on the M-theory circle. The gauge theory is simply $\mathcal{N} = 8$ SYM with $O(2N)$, $O(2N+1)$, or $USp(2N)$ gauge group, and just like $\mathcal{N} = 8$ SYM with gauge group $U(N)$, its infrared limit is non-standard. We expect $\mathcal{N} = 8$ SYM with orthogonal or symplectic gauge group to flow to an ABJ(M) theory with Chern-Simons level $k = 2$.

[12]The cases $N_f = 0, 1, 2$ are special. When $N_f = 0, 1$, the 11-d geometry is smooth, and we therefore expect that the low-energy dynamics is the same as that of ABJM theory at level $k = 1$. When $N_f = 2$, the 11-d geometry has a pair of $\mathbb{Z}_2$ singularities. Near each singularity the hyperkähler space looks like $\mathbb{C}^2 \times (\mathbb{C}^2/\mathbb{Z}_2)$.

will see, the corresponding field theories do not have the same $S^3$ partition functions, so they are not dual to each other.

For theories that are constructed with O6 planes, the near horizon limit of the M2-brane geometry is $\mathrm{AdS}_4 \times (S^7/\hat{D}_{N_f\pm 2})$, where the $\hat{D}_{N_f\pm 2}$ action on $S^7$ is that induced from (5.2.1) (with $N_f \to 2N_f \pm 4$) and (5.2.3). Within $\mathbb{C}^4$, the orbifold leaves the $\mathbb{C}^2$ at $z_3 = z_4 = 0$ fixed, hence $S^7/\hat{D}_{N_f\pm 2}$ is singular along the corresponding $S^3$.

In Appendix A we provide some evidence that the field theories mentioned above are indeed dual to M-theory on the backgrounds summarized in Table 5.2 by computing the Coulomb branch of the moduli space. In these moduli space computations an important role is played by certain BPS monopole operators that satisfy non-trivial chiral ring relations. The Coulomb branch of the $U(N)$ theory with an adjoint and $N_f$ fundamental hypermultiplets is $(\mathbb{C}^2 \times (\mathbb{C}^2/\mathbb{Z}_{N_f}))^N/S_N$, where the symmetric group $S_N$ permutes the factors in the product; this branch of moduli space is precisely what is expected for $N$ M2-branes probing the hyperkähler space $\mathbb{C}^2 \times (\mathbb{C}^2/\mathbb{Z}_{N_f})$. The Coulomb branch of the theories constructed from O2-planes is $(\mathbb{C}^4/\hat{D}_{N_f})^N/S_N$, again as expected for $N$ M2-branes probing $\mathbb{C}^4/\hat{D}_{N_f}$. The Coulomb branch of the theories constructed from O6-planes is $(\mathbb{C}^2 \times (\mathbb{C}^2/\hat{D}_{N_f\pm 2}))^N/S_N$ if the gauge group is $O(2N)$ or $USp(2N)$, matching the moduli space of $N$ M2-branes probing $\mathbb{C}^2 \times (\mathbb{C}^2/\hat{D}_{N_f\pm 2})$. If the gauge group is $O(2N+1)$ the moduli space has an extra factor of $\mathbb{C}^2$ corresponding to the half D2-brane stuck to the $\mathrm{O6}^+$ plane that cannot move in the directions transverse to the orientifold plane.

It is worth pointing out that the moduli space computations in Appendix A provide agreement with the 11-d geometry only if certain details of the field theory are chosen appropriately. For instance, the trace part of the symmetric tensor representations of $O(2N)$ and $O(2N+1)$ should be included, and so should the symplectic trace part of the anti-symmetric representation of $USp(2N)$. In the $O(2N)$ cases, one finds agreement only if the gauge group is $O(2N)$, and not for $SO(2N)$—the two differ in a $\mathbb{Z}_2$ gauging of the global charge conjugation symmetry present in the $SO(2N)$ case. In the $O(2N+1)$ case, the moduli space computation would yield the same answer

as if the gauge group were $SO(2N+1)$.[13]

In all the cases, the eleven-dimensional geometry takes the form:

$$\begin{aligned} ds^2 &= \frac{R^2}{4} ds^2_{\mathrm{AdS}_4} + R^2 ds^2_X \ , \qquad R = \left( \frac{2^5 \pi^6 N}{3 \, \mathrm{Vol}(X)} \right)^{1/6} \ell_p \ , \\ G_4 &= \frac{3}{8} R^3 \ \mathrm{vol}_{\mathrm{AdS}_4} \ , \end{aligned} \tag{5.2.4}$$

where $R$ is the AdS radius, $\mathrm{vol}_{\mathrm{AdS}_4}$ is the volume form on an $\mathrm{AdS}_4$ of unit radius, $X$ is the internal seven-dimensional manifold (tri-Sasakian in this case), and $\ell_p$ is the Planck length. This background should be accompanied by discrete torsion flux through a torsion three-cycle of $X$, but we do not attempt to determine this discrete torsion flux precisely. Since the volume of $X$ is given by the volume of the unit $S^7$ divided by the order of the orbifold group, we predict using (5.1.2) that

$$f_{3/2} = \frac{\sqrt{2}\pi}{3} \begin{cases} N_f^{1/2} & \text{no orbifold}, \\ [4N_f]^{1/2} & \mathrm{O2}, \\ [4(N_f \pm 2)]^{1/2} & \mathrm{O6}^{\pm}. \end{cases} \tag{5.2.5}$$

These results will be reproduced by the field theory calculations presented in the remainder of this chapter. See Table 5.5.

### 5.2.2 Matrix model for the $S^3$ free energy

The $S^3$ partition function of $U(N)$ gauge theory with one adjoint and $N_f$ fundamental hypermultiplets can be written down using the rules summarized in [125]:

$$Z = \frac{1}{2^N N!} \int d^N x \, \frac{\prod_{i<j} \left[ 4 \sinh^2 \left( \pi(\lambda_i - \lambda_j) \right) \right]}{\prod_{i<j} \left[ 4 \cosh^2 \left( \pi(\lambda_i - \lambda_j) \right) \right]} \times \prod_i \frac{1}{\left( 2 \cosh \left( \pi \lambda_i \right) \right)^{N_f}} \, . \tag{5.2.6}$$

[13]The gauging of the charge conjugation symmetry in the $SO(2N+1)$ gauge theory does not seem to affect the dynamics provided that $2N+1 > N_f$. When $2N+1 \leq N_f$, the $SO(2N+1)$ theory has baryonic operators of the form $q^{2N+1}$, where the color indices are contracted with the anti-symmetric tensor of $SO(2N+1)$. These operators are odd under charge conjugation, and are therefore absent from the $O(2N+1)$ theory. When $2N+1 > N_f$, however, the operator content of the $SO(2N+1)$ and $O(2N+1)$ gauge theories is the same. See also [138].

The normalization includes a division by the order of the Weyl group $|\mathcal{W}| = N!$ and the contributions from the $N$ zero weights in the adjoint representations.

The $S^3$ partition function for the theories with orthogonal and symplectic gauge groups is given by:

$$\begin{aligned}\widetilde{Z} = \mathcal{C} \int d^N\lambda \frac{\prod_{i<j}\left[16\sinh^2(\pi(\lambda_i-\lambda_j))\sinh^2(\pi(\lambda_i+\lambda_j))\right]}{\prod_{i<j}\left[16\cosh^2(\pi(\lambda_i-\lambda_j))\cosh^2(\pi(\lambda_i+\lambda_j))\right]} \\ \times \prod_i \frac{\left(4\sinh^2(\pi\lambda_i)\right)^a \left(4\sinh^2(2\pi\lambda_i)\right)^b}{\left(4\cosh^2(\pi\lambda_i)\right)^{N_f+c}\left(4\cosh^2(2\pi\lambda_i)\right)^d}.\end{aligned} \tag{5.2.7}$$

The constants $a$, $b$, $c$, $d$, and $\mathcal{C}$ are given in Table 5.3 for the various theories we study. The normalization $\mathcal{C}$ includes a division by the order of the Weyl group $\mathcal{W}$ (see Table 5.4) and the contributions from in the zero weights the matter representations:

$$\mathcal{C} = \frac{1}{2^z\,|\mathcal{W}|}, \tag{5.2.8}$$

where $z$ is the total number of zero weights in the hypermultiplet representations. In the $O(2N)$ and $O(2N+1)$ cases, (5.2.8) should be multiplied by an extra factor of $1/2$ coming from the gauging of the $\mathbb{Z}_2$ charge conjugation symmetry that distinguishes the $O(2N)$ and $O(2N+1)$ gauge groups from $SO(2N)$ and $SO(2N+1)$, respectively. In the rest of this chapter, we find it convenient to rescale $\widetilde{Z}$ by a factor of $2^N$ and calculate instead

$$Z = 2^N \widetilde{Z}. \tag{5.2.9}$$

The numerator in the integrand of (5.2.7) comes solely from the $\mathcal{N} = 4$ vector-multiplet; note that an $\mathcal{N} = 4$ vector can be written as an $\mathcal{N} = 2$ vector and an $\mathcal{N} = 2$ chiral multiplet with R-charge $\Delta_{\text{vec}} = 1$, and only the $\mathcal{N} = 2$ vector gives a non-trivial contribution to the integrand. The first factor in the denominator comes from the two-index hypermultiplet, while the additional factors come from both the two-index tensor and the $N_f$ fundamental hypermultiplets.

Note that there is a redundancy in the parameters $a, b$, and $c$. Using $\sinh 2\lambda =$

| $G$ + matter | $a$ | $b$ | $c$ | $d$ | $\mathcal{C}$ |
|---|---|---|---|---|---|
| $O(2N) + A$ | 0 | 0 | 0 | 0 | $1/(2^{2N}N!)$ |
| $O(2N) + S$ | 0 | 0 | 0 | 1 | $1/(2^{2N}N!)$ |
| $O(2N+1) + A$ | 1 | 0 | 1 | 0 | $1/(2^{2N+N_f+1}N!)$ |
| $O(2N+1) + S$ | 1 | 0 | 1 | 1 | $1/(2^{2N+N_f+2}N!)$ |
| $USp(2N) + A$ | 0 | 1 | 0 | 0 | $1/(2^{2N}N!)$ |
| $USp(2N) + S$ | 0 | 1 | 0 | 1 | $1/(2^{2N}N!)$ |

Table 5.3: The values of the constansts $a, b, c$, and $d$ appearing in (5.2.7) for gauge group $G$, $N_f$ fundamental flavors, and a two-index antisymmetric ($A$) or symmetric ($S$) hypermultiplet.

| $G$ | $\lvert\mathcal{W}\rvert$ |
|---|---|
| $U(N)$ | $N!$ |
| $SO(2N)$ | $2^{N-1}N!$ |
| $SO(2N+1)$ | $2^N N!$ |
| $USp(2N)$ | $2^N N!$ |

Table 5.4: The order of the Weyl group, $|\mathcal{W}|$, for various groups $G$. In the case where the gauge group is $O(2N)$ or $O(2N+1)$, one should use the Weyl groups of $SO(2N)$ and $SO(2N+1)$ in (5.2.8) and multiply the answer by an extra factor of $1/2$ coming from the gauging of the $\mathbb{Z}_2$ charge conjugation symmetry, as mentioned in the main text.

$2\sinh\lambda\cosh\lambda$, one can check that (5.2.7) is invariant under

$$b \to b - \Delta\,, \qquad a \to a + \Delta\,, \qquad c \to c - \Delta\,, \tag{5.2.10}$$

hence any expression involving $a$, $b$, and $c$ should only contain the combinations $c - a - 2b$ or $a + b$. This requirement provides a nice check of our results.

## 5.3 Large $N$ approximation

In this section we calculate the $S^3$ partition functions of the field theories presented above using the large $N$ approach of [38], which we extend to include one more order in the large $N$ expansion. Explicitly, we do three computations. In Section 5.3.1 we present the computation for ABJM theory, whose $S^3$ partition function was given in (5.1.3). In Section 5.3.2, we calculate the $F$-coefficient of the $\mathcal{N} = 4$ $U(N)$ gauge theory with one adjoint and $N_f$ fundamental hypermultiplets for which we wrote down the $S^3$ partition function in (5.2.6). Lastly, in Section 5.3.3 we generalize this computation to theories with a symplectic or orthogonal gauge group, for which the $S^3$ partition function takes the form (5.2.7) with various values of the parameters $a$, $b$, $c$, and $d$—see Table 5.3.

### 5.3.1 ABJM theory

At large $N$ one can calculate the $S^3$ partition function for ABJM theory (5.1.3) in a fairly elementary fashion using the saddle point approximation. Let us write

$$Z = \frac{1}{(N!)^2} \int \prod_{i=1}^{N} \left( d\lambda_i d\tilde{\lambda}_i \right) e^{-F(\lambda_i, \tilde{\lambda}_j)} , \tag{5.3.1}$$

for some function $F(\lambda_i, \tilde{\lambda}_j)$ that can be easily read off from (5.1.3). The factor of $(N!)^2$ that appears in (5.3.1) is nothing but the order of the Weyl group $\mathcal{W}$, which in this case is $S_N \times S_N$, $S_N$ being the symmetric group on $N$ elements. The saddle point equations are

$$\frac{\partial}{\partial \lambda_i} F(\lambda_i, \tilde{\lambda}_j) = \frac{\partial}{\partial \tilde{\lambda}_j} F(\lambda_i, \tilde{\lambda}_j) = 0 . \tag{5.3.2}$$

Since $F(\lambda_i, \tilde{\lambda}_j)$ is invariant under permuting the $\lambda_i$ or the $\tilde{\lambda}_j$ separately, the saddle point equations have a $S_N \times S_N$ symmetry. For any solution of (5.3.2) that is not invariant under this symmetry, as will be those we find below, there are $(N!)^2 - 1$ other solutions that can be obtained by permuting the $\lambda_i$ and the $\tilde{\lambda}_j$. That our saddle

point comes with multiplicity $(N!)^2$ means that we can approximate

$$Z \approx e^{-F_*}\,, \tag{5.3.3}$$

where $F_*$ equals the function $F(\lambda_i, \tilde{\lambda}_j)$ evaluated on any of the solutions of the saddle point equations. In other words, the multiplicity of the saddle precisely cancels the $1/(N!)^2$ prefactor in (5.3.1).

The saddle point equations (5.3.2) are invariant under interchanging $\tilde{\lambda}_i \leftrightarrow \lambda_i^*$, and therefore one expects to find saddles where $\tilde{\lambda}_i = \lambda_i^*$. If one parameterizes the eigenvalues by their real part $x_i$, the density of the real part $\rho(x) = \frac{1}{N}\sum_{i=1}^{N}\delta(x - x_i)$ and $\lambda_i$ become continuous functions of $x$ in the limit $N \to \infty$. The density $\rho(x)$ is constrained to be non-negative and to integrate to 1. Expanding $F(\lambda_i, \tilde{\lambda}_j)$ to leading order in $N$ (at fixed $N/k$), one obtains a continuum approximation:

$$\begin{aligned}\frac{F}{N^2} = &\int dx\ \rho(x) \int dx'\ \rho(x') \log\left|\frac{\cosh^2\left[\pi\left(\lambda(x) - \widetilde{\lambda}(x')\right)\right]}{\sinh\left[\pi\left(\lambda(x) - \lambda(x')\right)\right]\sinh\left[\pi\left(\widetilde{\lambda}(x) - \widetilde{\lambda}(x')\right)\right]}\right| \\ &- i\frac{k}{N}\int dx\ \rho(x)\left(\lambda(x)^2 - \widetilde{\lambda}(x)^2\right) + \mathcal{O}(1/N)\,.\end{aligned} \tag{5.3.4}$$

The corrections to this expression are suppressed by inverse powers of $N$. In the $N \to \infty$ limit the saddle point approximation becomes exact, and to leading order in $N$ one can simply evaluate $F$ on the solution to the equations of motion following from (5.3.4).

At large $N/k$, one should further expand [38]:

$$\lambda(x) = \sqrt{\frac{N}{k}}\,x + iy(x) + \cdots\,, \qquad \widetilde{\lambda}(x) = \sqrt{\frac{N}{k}}\,x - iy(x) + \cdots\,, \tag{5.3.5}$$

with corrections suppressed by positive powers of $\sqrt{k/N}$. Plugging (5.3.4) into (5.3.4)

and expanding at large $N/k$, we obtain

$$\begin{aligned}\frac{F[\rho,y]}{N^2} &= \left(\frac{k}{N}\right)^{1/2}\frac{\pi}{2}\int dx\ \left[\rho^2\left(1-16y^2\right)+8x\rho y\right] \\ &+\left(\frac{k}{N}\right)^{3/2}\pi\int dx\ \frac{1}{96}\rho\left(1-16y^2\right)\left[64\rho' yy'+16\rho\left(3y'^2+2yy''\right)-\left(1-16y^2\right)\rho''\right] \\ &+\ldots\ .\end{aligned} \tag{5.3.6}$$

Note that the double integral in (5.3.4) becomes a single integral in (5.3.6) after using the fact that, in the continuum limit (5.3.4), the scaling behavior (5.3.5) implies that the interaction forces between the eigenvalues are short-ranged. The expression in (5.3.6) should then be extremized order by order in $k/N$. To leading order, the extremum was found in [38]:

$$\begin{aligned}\rho(x) &= \begin{cases}\sqrt{\frac{1}{2}} & \text{for } |x|\le\frac{1}{\sqrt{2}}\,,\\ 0 & \text{otherwise}\,,\end{cases}\\ y(x) &= \begin{cases}\sqrt{\frac{1}{8}}\,x & \text{for } |x|\le\frac{1}{\sqrt{2}}\,,\\ 0 & \text{otherwise}\,.\end{cases}\end{aligned} \tag{5.3.7}$$

This eigenvalue distribution only receives corrections from the next-to-leading term in the expansion (5.3.6), so it is correct to plug (5.3.7) into (5.3.6) and obtain

$$F_* = N^2\left[\left(\frac{k}{N}\right)^{1/2}\frac{\sqrt{2}\,\pi}{3}-\left(\frac{k}{N}\right)^{3/2}\frac{\pi}{24\sqrt{2}}+\ldots\right]+\ldots\ . \tag{5.3.8}$$

If one wants to go to higher orders in the $k/N$ expansion, one would have to consider corrections to the eigenvalue distribution (5.3.7).

The result (5.3.8) is in agreement with the Fermi gas approach [1], when the latter is expanded at large $N/k$ and large $N$ as in (5.3.8). The coefficients $f_{3/2}$ and $f_{1/2}$ of the $N^{3/2}$ and $N^{1/2}$ terms in the large $N$ expansion of the free energy obtained through the Fermi gas approach were given in (5.1.5). Note that $F_*$ does not capture all the

terms at $\mathcal{O}(N^{1/2})$, but only the contribution that scales as $k^{3/2}$. This result is still meaningful, as the other terms of $\mathcal{O}(N^{1/2})$ in (5.1.5), coming from the fluctuations and finite $N$ corrections, have a different dependence on $k$.

### 5.3.2 $\mathcal{N} = 4$ $U(N)$ gauge theory with adjoint and fundamental matter

We now move on to a more complicated example, namely the $\mathcal{N} = 4$ $U(N)$ gauge theory introduced in Section 5.2 whose $S^3$ partition function was given in (5.2.6). Let us denote

$$Z = \frac{1}{|\mathcal{W}|} \int d^N\lambda \, e^{-F(\lambda_i)} \,. \tag{5.3.9}$$

Explicitly, we have

$$F(\lambda_i) = -\sum_{i<j} \log \tanh^2(\pi(\lambda_i - \lambda_j)) - \sum_i \log \frac{1}{(2\cosh(\pi\lambda_i))^{N_f}} \,. \tag{5.3.10}$$

As in the ABJM case, every saddle comes with a degeneracy equal to the order of the Weyl group ($S_N$ in this case), so we can approximate $Z \approx e^{-F_*}$, where $F_*$ equals $F(\lambda_i)$ evaluated on any given solution of the saddle point equations $\partial F/\partial\lambda_i = 0$.

In the $U(N)$ gauge theory the eigenvalues are real, and in the $N \to \infty$ limit we again introduce a density of eigenvalues $\rho(x)$. We will be interested in taking $N$ to infinity while working in the Veneziano limit where $t \equiv N/N_f$ is held fixed and then taking the limit of large $t$. At large $N$, the free energy is a functional of $\rho(x)$:

$$\begin{aligned} \frac{F[\rho]}{N^2} = &\int dx\, \rho(x) \int dx'\, \rho(x') \log\left|\coth\left(\pi(\lambda(x) - \lambda(x'))\right)\right| \\ &+ \frac{1}{t} \int dx\, \rho(x)\, \log\left(2\cosh(\pi\lambda(x))\right) \,. \end{aligned} \tag{5.3.11}$$

As in the ABJM case, the appropriate scaling at large $t$ is $\lambda \propto \sqrt{t}$, so we can

define

$$\lambda(x) = \sqrt{t}\, x\,. \tag{5.3.12}$$

It is convenient to further introduce another parameter $T$ and write (5.3.11) as

$$\begin{aligned}\frac{F[\rho]}{N^2} = &\int dx\, \rho(x) \int dx'\, \rho(x') \log \left|\coth\left(\pi\sqrt{t}(x-x')\right)\right| \\ &+ \frac{1}{\sqrt{t}} \int dx\, \frac{\rho(x)}{\sqrt{T}} \log\left(2\cosh(\pi\sqrt{T}x)\right)\,.\end{aligned} \tag{5.3.13}$$

Of course, we are eventually interested in setting $T = t$, but it will turn out to be convenient to have two different parameters and expand both at large $t$ and large $T$. Expanding in $t$ we get

$$\begin{aligned}\frac{F[\rho]}{N^2} = &\frac{\pi}{4}\frac{1}{\sqrt{t}} \int dx\, \rho(x)^2 - \frac{\pi}{192}\frac{1}{t^{3/2}} \int dx\, \rho'(x)^2 + o(t^{-3/2}) \\ &+ \frac{1}{\sqrt{t}} \int dx\, \frac{\rho(x)}{\sqrt{T}} \log\left(2\cosh(\pi\sqrt{T}x)\right)\,.\end{aligned} \tag{5.3.14}$$

If we assume that $\rho$ is supported on $[-x_*, x_*]$ for some $x_* > 0$, we should extremize (5.3.14) order by order in $N$ under the condition that $\rho(x) \geq 0$ and that

$$\int_{-x_*}^{x_*} dx\, \rho(x) = 1\,. \tag{5.3.15}$$

We can impose the latter condition with a Lagrange multiplier and extremize

$$\frac{\widetilde{F}[\rho]}{N^2} = \frac{F[\rho]}{N^2} - \pi\frac{\mu}{\sqrt{t}}\left(\int dx\, \rho(x) - 1\right) \tag{5.3.16}$$

instead of (5.3.14).

### Leading order result

To obtain the leading order free energy we can simply take the limit $T \to \infty$ in (5.3.14) and ignore the $1/t^{3/2}$ term in the first line of (5.3.14). The free energy takes

the form

$$\frac{F[\rho]}{N^2} = \frac{1}{\sqrt{t}} \int dx \, \left[ \frac{\pi}{4} \rho(x)^2 + \pi x \, \rho(x) \right] . \tag{5.3.17}$$

The normalized $\rho(x)$ that minimizes (5.3.17) is

$$\rho(x) = \begin{cases} (x_* - |x|)/x_*^2 & |x| \leq x_* \,, \\ 0 & \text{otherwise,} \end{cases} \qquad x_* \equiv \frac{1}{\sqrt{2}} . \tag{5.3.18}$$

The value of $F$ we obtain from (5.3.18) is

$$\frac{F_*}{N^2} = \frac{\pi\sqrt{2}}{3} \frac{1}{\sqrt{t}} + o(t^{-1/2}) . \tag{5.3.19}$$

After writing $t = N/N_f$, one can check that this term reproduces the expected $N^{3/2}$ behavior of a SCFT dual to $\mathrm{AdS}_4 \times S^7/\mathbb{Z}_{N_f}$.

### Subleading corrections

To obtain the $t^{-3/2}$ term in (5.3.19) we should find the $1/T$ corrections to the extremum of the $t^{-1/2}$ terms in (5.3.14), and we should evaluate the $t^{-3/2}$ term in (5.3.14) by plugging in the leading result (5.3.18).

Focusing on the $t^{-1/2}$ terms first, the equation of motion for $\rho$ gives

$$\rho(x) = 2\mu - \frac{2}{\pi\sqrt{T}} \log \left( 2\cosh(\pi\sqrt{T}x) \right) . \tag{5.3.20}$$

Up to exponentially small corrections (at large $T$), the normalization condition (5.3.15) fixes $\mu$ to

$$\mu = \frac{x_*}{2} + \frac{1}{x_*} \left( \frac{1}{4} + \frac{1}{24T} \right) . \tag{5.3.21}$$

Plugging this expression back into $F[\rho]$ and minimizing with respect to $x_*$, one obtains

$$x_* = \sqrt{\frac{1}{2} + \frac{1}{12T}}\,, \tag{5.3.22}$$

again only up to exponentially suppressed corrections.

Then (5.3.14) evaluates to

$$\frac{F_*}{N^2} = \frac{\pi\sqrt{2}}{3}\frac{1}{\sqrt{t}} + \frac{\pi}{6\sqrt{2}}\frac{1}{T\sqrt{t}} - \frac{\pi}{24\sqrt{2}}\frac{1}{t^{3/2}} + \dots\,, \tag{5.3.23}$$

where we included the $t^{-3/2}$ term. We see now that if we had taken $T \to \infty$ directly in (5.3.14) we would have missed the second term in (5.3.23). Setting $T = t = N/N_f$, we obtain

$$F_* = \frac{\pi\sqrt{2N_f}}{3}N^{3/2} + \frac{\pi N_f^{3/2}}{8\sqrt{2}}N^{1/2} + \dots\,. \tag{5.3.24}$$

In analogy with the ABJM case we expect that fluctuations and finite $N$ corrections will contribute to the free energy starting at $N^{1/2}$ order. However, they will have different $N_f$ dependence then the term (5.3.24), and the saddle point computation can be thought of as the first term in the large $N_f$ expansion.[14] These expectations will be verified in the Fermi gas approach in Section 5.4.

### 5.3.3 $\mathcal{N} = 4$ gauge theories with orthogonal and symplectic gauge groups

As a final example, let us discuss the $\mathcal{N} = 4$ theories with symplectic and orthogonal gauge groups for which the $S^3$ partition function was written down in (5.2.7). (See Table 5.3 for the values of the constants $a$, $b$, $c$, $d$, and $C$.) In this case one can define $F(\lambda_i)$ just as in (5.3.9). The saddle point equations $\partial F/\partial\lambda_i$ are now invariant both under permutations of the $\lambda_i$ and under flipping the sign of any number of $\lambda_i$. In particular, from any solution of the saddle point equations one can construct other

[14] One could think of $t = N/N_f$ as the analog of the 't Hooft coupling in this case.

solutions by flipping the sign of any number of $\lambda_i$. We can therefore restrict ourselves to saddles for which $\lambda_i \geq 0$ for all $i$. If $F_*$ is the free energy of any such saddle, we have $Z \approx e^{-F_*}$, up to a $\mathcal{O}(N^0)$ normalization factor coming from the constant $\mathcal{C}$ in (5.2.7) that we will henceforth ignore.

Instead of extremizing $F(\lambda_i)$ with respect to the $N$ variables $\lambda_i$, $i = 1, \ldots, N$, it is convenient to introduce $2N$ variables $\mu_i$, $i = 1, \ldots, 2N$, and extremize instead

$$F(\mu_i) = -\frac{1}{2}\sum_{i<j} \log \tanh^2(\pi(\mu_i - \mu_j)) - \sum_i \log \left| \frac{(2\sinh(\pi\mu_i))^a \, (2\sinh(2\pi\mu_i))^{b-1}}{(2\cosh(\pi\mu_i))^{N_f+c} \, (2\cosh(2\pi\mu_i))^{d-1}} \right| \tag{5.3.25}$$

under the constraint $\mu_{i+N} = -\mu_i$. In the case at hand, one can actually drop this constraint, because the extrema of the unconstrained minimization of $F(\mu_i)$ satisfy $\mu_{i+N} = -\mu_i$ (after a potential relabeling of the $\mu_i$).

If the $\mu_i$ are large, then extremizing (5.3.25) is equivalent up to exponentially small corrections to extremizing

$$F(\mu_i) = \frac{1}{2}\left[ -\sum_{i<j} \log \tanh^2(\pi(\mu_i - \mu_j)) - \sum_i \log \frac{1}{(2\cosh(\pi\mu_i))^{2\widetilde{N_f}}} \right], \tag{5.3.26}$$

where

$$\widetilde{N_f} \equiv N_f + c + 2d - a - 2b\,. \tag{5.3.27}$$

We performed a similar extremization problem in the previous section. From comparing (5.3.26) with (5.3.10), we see that the extremum of (5.3.26) can be obtained after replacing $N_f \to 2\widetilde{N_f}$, $N \to 2N$ in (5.3.24) and multiplying the answer by $1/2$:

$$F_* = \frac{2\pi\sqrt{2\widetilde{N_f}}}{3} N^{3/2} + \frac{\pi \widetilde{N_f}^{3/2}}{4\sqrt{2}} N^{1/2} + \ldots\,. \tag{5.3.28}$$

The first term reproduces the expected $N^{3/2}$ behavior of an SCFT dual to $AdS_4 \times X$ where $X$ is an orbifold of $S^7$ of order $4\widetilde{N_f}$, in agreement with (5.2.5). We will

reproduce (5.3.28) from the Fermi gas approach in the following section, where we will also be able to calculate the other terms of order $N^{1/2}$ that have a different $\widetilde{N_f}$ dependence from the one in (5.3.28).

## 5.4 Fermi gas approach

### 5.4.1 $\mathcal{N} = 4$ $U(N)$ gauge theory with adjoint and fundamental matter

For SCFTs with unitary gauge groups and $\mathcal{N} \geq 3$ supersymmetry, the Fermi gas approach of [1, 126] relies on the determinant formula

$$\frac{\prod_{i<j}\left[4\sinh\left(\pi(x_i-x_j)\right)\sinh\left(\pi(y_i-y_j)\right)\right]}{\prod_{i,j}\left[2\cosh\left(\pi(x_i-y_j)\right)\right]} = \det\frac{1}{2\cosh\left(\pi(x_i-y_j)\right)}, \tag{5.4.1}$$

which is nothing but a slight rewriting of the Cauchy determinant formula

$$\frac{\prod_{i<j}(u_i-u_j)(v_i-v_j)}{\prod_{i,j}(u_i+v_j)} = \det\frac{1}{u_i+v_j}. \tag{5.4.2}$$

that holds for any $u_i$ and $v_i$, with $i = 1, \ldots, N$. Eq. (5.4.1) can be obtained from (5.4.2) by writing $u_i = e^{2\pi x_i}$ and $v_i = e^{2\pi y_i}$.

Using (5.4.1) in the particular case $y_i = x_i$, we can write (5.2.6) in the form

$$Z = \frac{1}{N!}\int d^N x \prod_i \frac{1}{\left(4\cosh^2(\pi x_i)\right)^{N_f}} \det\frac{1}{2\cosh\left(\pi(x_i-x_j)\right)}. \tag{5.4.3}$$

$Z$ can then be rewritten as the partition function of an ideal Fermi gas of $N$ noninteracting particles, namely

$$Z = \frac{1}{N!}\sum_{\sigma\in S_N}(-1)^\sigma \int d^N x \prod_i \rho\left(x_i, x_{\sigma(i)}\right), \tag{5.4.4}$$

where $\rho(x_1, x_2) \equiv \langle x_1|\hat{\rho}|x_2\rangle$ is the one particle density matrix, and the sum is over the elements of the permutation group $S_N$. We can read off the density matrix by

comparing (5.4.4) with (5.4.3). In the position representation, $\rho$ is given by

$$\rho(x_1, x_2) = \frac{1}{(2\cosh(\pi x_1))^{N_f/2}} \frac{1}{(2\cosh(\pi x_2))^{N_f/2}} \times \frac{1}{2\cosh\left(\pi(x_1 - x_2)\right)} . \tag{5.4.5}$$

We can put this expression into a more useful form by writing it more abstractly in terms of the position and momentum operators, $\hat{x}$ and $\hat{p}$, as

$$\hat{\rho} = e^{-U(\hat{x})/2} e^{-T(\hat{p})} e^{-U(\hat{x})/2} , \tag{5.4.6}$$

In units where $h = 1$, which imply $[\hat{x}, \hat{p}] = i/(2\pi)$, one can show as in (5.B.3) that

$$U(x) = \log\left(2\cosh(\pi x)\right)^{N_f} , \qquad T(p) = \log\left(2\cosh(\pi p)\right) . \tag{5.4.7}$$

We then rescale $x \equiv y/(2\pi N_f)$ and $p \equiv k/(2\pi)$ to get

$$\hat{\rho} = \frac{1}{2\pi N_f} e^{-U(\hat{y})/2} e^{-T(\hat{k})} e^{-U(\hat{y})/2} , \tag{5.4.8}$$

where

$$U(y) = \log\left(2\cosh\left(\frac{y}{2N_f}\right)\right)^{N_f} , \qquad T(k) = \log\left(2\cosh\left(\frac{k}{2}\right)\right) . \tag{5.4.9}$$

The rescaling was motivated by the following nice properties:

$$\begin{aligned} &\left[\hat{y}, \hat{k}\right] = 2\pi i N_f , \\ &U(y) \to \frac{y}{2} \qquad (y \to \infty) , \\ &T(k) \to \frac{k}{2} \qquad (k \to \infty) . \end{aligned} \tag{5.4.10}$$

We identify $\hbar = 2\pi N_f$, and perform a semiclassical computation of the canonical free energy of the Fermi gas. In Appendix 5.A we give a brief review of the relevant results from [1]. These results enable us to calculate the free energy from the above ingredients. In summary, we calculate the Fermi surface area as a function of the

energy for the Wigner Hamiltonian (5.A.11). In the semiclassical approximation, to zeroth order the phase space volume enclosed by the Fermi surface is:

$$V_0 = 8E^2 \ , \tag{5.4.11}$$

while the corrections are:

$$\begin{aligned} \Delta V = 4 \Bigg[ & \int_0^\infty dy \ (y - 2U(y)) + \int_0^\infty dp \ (k - 2T(k)) + \frac{\hbar^2}{24} \int_0^\infty dy \, U''(y) \\ & - \frac{\hbar^2}{48} \int_0^\infty dk \, T''(k) \Bigg] \ . \end{aligned} \tag{5.4.12}$$

We can perform the calculation and conclude that $n(E)$ defined in (5.A.1) takes the form:

$$n(E) = \frac{V}{2\pi\hbar} = \frac{V_0 + \Delta V}{2\pi\hbar} = \frac{2E^2}{\pi^2 N_f} - \frac{N_f}{8} - \frac{1}{6N_f} \ . \tag{5.4.13}$$

In (5.A.5) we parametrized the $E$ dependence of $n(E)$ as

$$\begin{aligned} n(E) &= C\,E^2 + n_0 + \mathcal{O}\left(E\,e^{-E}\right) \ , \\ B &\equiv n_0 + \frac{\pi^2 C}{3} \ , \end{aligned} \tag{5.4.14}$$

so from (5.4.13) we can read off

$$C = \frac{2}{\pi^2 N_f} \ , \qquad B = -\frac{N_f}{8} + \frac{1}{2N_f} \ , \tag{5.4.15}$$

and the partition function takes the form [1]

$$Z(N) = \mathcal{A}(N_f)\,\mathrm{Ai}\left[C^{-1/3}(N - B)\right] + \mathcal{O}\left(e^{-\sqrt{N}}\right) \ . \tag{5.4.16}$$

$\mathcal{A}(N_f)$ is an $N$-independent constant that our approach only determines perturbatively for small $N_f$, and we are not interested in its value. Expanding the $F = -\log Z$

we obtain:

$$F = f_{3/2}N^{3/2} + f_{1/2}N^{1/2} + \dots \,, \qquad f_{3/2} = \frac{2}{3\sqrt{C}} \,, \qquad f_{1/2} = -\frac{B}{\sqrt{C}} \,. \tag{5.4.17}$$

We conclude that the free energy goes as:

$$F = \frac{\pi\sqrt{2N_f}}{3}N^{3/2} + \frac{\pi}{\sqrt{2}}\left(\frac{N_f^{3/2}}{8} - \frac{1}{2\sqrt{N_f}}\right)N^{1/2} + \dots \,. \tag{5.4.18}$$

The Fermi gas computation is in principle only valid in the semiclassical, small $\hbar$, i.e. small $N_f$ regime. However, because the small $N_f$ series expansions terminate, we obtain the exact answer. Then we can compare to the matrix model result (5.3.24) valid at large $N_f$, and find perfect agreement to leading order in $N_f$.[15]

As discussed in Section 5.2, at $N_f = 1$ the $U(N)$ theory is dual to ABJM theory at $k = 1$, and the free energy computation in both representations should give the same result [119]. Plugging $k = 1$ into (5.1.1) and (5.1.5) indeed gives (5.4.18) with $N_f = 1$.

### 5.4.2 $\mathcal{N} = 4$ gauge theories with orthogonal and symplectic gauge groups

To generalize the Fermi gas approach to SCFTs with orthogonal and symplectic gauge groups, one needs the following generalization of the Cauchy determinant formula (5.4.2):

$$\frac{\prod_{i<j}(u_i - u_j)(v_i - v_j)(u_i u_j - 1)(v_i v_j - 1)}{\prod_{i,j}(u_i + v_j)(u_i v_j + 1)} = \det \frac{1}{(u_i + v_j)(u_i v_j + 1)} \,, \tag{5.4.19}$$

[15] Grassi and Mariño informed us that they calculated the free energy of this theory in the large $N$, fixed $N/N_f$ limit using method (I) discussed in Section 5.1. Their result is

$$F = \frac{\pi\sqrt{2N_f}}{3}N^{3/2}\left(1 + \frac{N_f}{8N}\right)^{3/2}$$

up to exponentially small corrections in $N/N_f$ and subleading terms in $1/N$. This expression agrees with the large $N$, fixed $N/N_f$ limit of the Fermi gas result (5.4.15)–(5.4.16) of this section. We thank Marcos Mariño for sharing these results with us.

which holds for any $u_i$ and $v_i$, with $i = 1, \ldots, N$.[16] Upon writing $u_i = e^{2\pi x_i}$ and $v_i = e^{2\pi y_i}$, this expression becomes

$$\frac{\prod_{i<j} \left[16 \sinh\left(\pi(x_i - x_j)\right) \sinh\left(\pi(y_i - y_j)\right) \sinh\left(\pi(x_i + x_j)\right) \sinh\left(\pi(y_i + y_j)\right)\right]}{\prod_{i,j} \left[4 \cosh\left(\pi(x_i - y_j) \cosh\left(\pi(x_i + y_j)\right)\right]} = \det \frac{1}{4 \cosh\left(\pi(x_i - y_j)\right) \cosh\left(\pi(x_i + y_j)\right)} . \tag{5.4.20}$$

In addition to this generalization of the Cauchy determinant formula, our analysis involves an extra ingredient. The one-particle density matrix of the resulting Fermi gas will be expressible not only just in terms of the usual position and momentum operators $\hat{x}$ and $\hat{p}$ as before, but also in terms of a reflection operator $R$ that we will need in order to project onto symmetric or anti-symmetric wave-functions on the real line.

Using (5.4.20) in the particular case $y_i = x_i$, one can rewrite (5.2.7) as

$$Z = 2^N \mathcal{C} \int d^N x \prod_i \frac{\left(4 \sinh^2(\pi x_i)\right)^a \left(4 \sinh^2(2\pi x_i)\right)^b}{\left(4 \cosh^2(\pi x_i)\right)^{N_f + c} \left(4 \cosh^2(2\pi x_i)\right)^{d-1/2}} \times \det \frac{1}{4 \cosh\left(\pi(x_i - x_j)\right) \cosh\left(\pi(x_i + x_j)\right)} . \tag{5.4.21}$$

As in (5.4.4) we recognize the appearence of the partition function of an ideal Fermi gas of $N$ noninteracting particles, and can read off the one-particle density matrix $\hat{\rho}$ from comparing (5.4.4) with (5.4.21). From Table 5.4 we see that $2^N \mathcal{C} \approx 1/(2^N N!)$, up to a $\mathcal{O}(N^0)$ pre-factor that we will henceforth ignore. In the position representa-

[16] After completing this chapter, it was pointed out to us by Miguel Tierz that this determinant formula can be found in the literature. See, for example, [139].

tion, $\rho(x_1, x_2) \equiv \langle x_1|\hat{\rho}|x_2\rangle$ is given by

$$\begin{aligned}\rho(x_1,x_2) = \frac{1}{2}&\sqrt{\frac{\left(4\sinh^2(\pi x_1)\right)^a \left(4\sinh^2(2\pi x_1)\right)^b}{\left(4\cosh^2(\pi x_1)\right)^{N_f+c} \left(4\cosh^2(2\pi x_1)\right)^{d-1/2}}} \\ &\times \sqrt{\frac{\left(4\sinh^2(\pi x_2)\right)^a \left(4\sinh^2(2\pi x_2)\right)^b}{\left(4\cosh^2(\pi x_2)\right)^{N_f+c} \left(4\cosh^2(2\pi x_2)\right)^{d-1/2}}} \\ &\times \frac{1}{4\cosh\left(\pi(x_1-x_2)\right)\cosh\left(\pi(x_1+x_2)\right)}\,.\end{aligned} \tag{5.4.22}$$

To put this expression in a more useful form, we note that if we set $h = 1$, we can write

$$\frac{4\cosh(\pi x_1)\cosh(\pi x_2)}{4\cosh\left(\pi(x_1-x_2)\right)\cosh\left(\pi(x_1+x_2)\right)} = \left\langle x_1 \left| \frac{1+R}{2\cosh(\pi\hat{p})} \right| x_2 \right\rangle\,, \tag{5.4.23}$$

where $R$ is the reflection operator that sends $x \to -x$. For the derivation of this identity see Appendix 5.B. Then we can write

$$\hat{\rho} = e^{-U_+(\hat{x})/2} e^{-T(\hat{p})} \left(\frac{1+R}{2}\right) e^{-U_+(\hat{x})/2}\,, \tag{5.4.24}$$

where

$$U_+(x) = \log \frac{\left(4\cosh^2(\pi x)\right)^{N_f+c+1} \left(4\cosh^2(2\pi x)\right)^{d-1/2}}{\left(4\sinh^2(\pi x)\right)^a \left(4\sinh^2(2\pi x)\right)^b}\,, \qquad T(p) = \log\left(2\cosh(\pi p)\right)\,. \tag{5.4.25}$$

Similarly, we could use the identity

$$\frac{4\sinh(\pi x_1)\sinh(\pi x_2)}{4\cosh\left(\pi(x_1-x_2)\right)\cosh\left(\pi(x_1+x_2)\right)} = \left\langle x_1 \left| \frac{1-R}{2\cosh(\pi\hat{p})} \right| x_2 \right\rangle\,, \tag{5.4.26}$$

and write

$$\hat{\rho} = e^{-U_-(\hat{x})/2} e^{-T(\hat{p})} \left(\frac{1-R}{2}\right) e^{-U_-(\hat{x})/2}\,, \tag{5.4.27}$$

with

$$U_-(x) = \log \frac{\left(4\cosh^2(\pi x)\right)^{N_f+c} \left(4\cosh^2(2\pi x)\right)^{d-1/2}}{\left(4\sinh^2(\pi x)\right)^{a-1} \left(4\sinh^2(2\pi x)\right)^{b}}, \tag{5.4.28}$$

and the same expression for $T(p)$ as before.

To be able to use $\widetilde{N_f}$ as a parameter analogous to $k$ in ABJM theory, we rescale $x \equiv y/(4\pi\widetilde{N_f})$ and $p \equiv k/(2\pi)$. Under this rescaling, we have

$$\begin{aligned} \hat{\rho} &= e^{-U_\pm(\hat{x})/2} e^{-T(\hat{p})} e^{-U_\pm(\hat{x})/2} \left(\frac{1 \pm R}{2}\right) \\ \rightarrow \quad \hat{\rho} &= \frac{1}{4\pi\widetilde{N_f}} e^{-U_\pm(\hat{y})/2} e^{-T(\hat{k})} e^{-U_\pm(\hat{y})/2} \left(\frac{1 \pm R}{2}\right), \end{aligned} \tag{5.4.29}$$

where we used that $U(\hat{x})$ commutes with $R$, and for the $(+)$ sign

$$\begin{aligned} U_+(y) &= \log \frac{\left(4\cosh^2\left(\frac{y}{4\widetilde{N_f}}\right)\right)^{N_f+c+1} \left(4\cosh^2\left(\frac{y}{2\widetilde{N_f}}\right)\right)^{d-1/2}}{\left(4\sinh^2\left(\frac{y}{4\widetilde{N_f}}\right)\right)^{a} \left(4\sinh^2\left(\frac{y}{2\widetilde{N_f}}\right)\right)^{b}}, \\ T(k) &= \log\left(2\cosh\left(\frac{k}{2}\right)\right), \end{aligned} \tag{5.4.30}$$

while for the $(-)$ sign

$$U_-(y) = \log \frac{\left(4\cosh^2\left(\frac{y}{4\widetilde{N_f}}\right)\right)^{N_f+c} \left(4\cosh^2\left(\frac{y}{2\widetilde{N_f}}\right)\right)^{d-1/2}}{\left(4\sinh^2\left(\frac{y}{4\widetilde{N_f}}\right)\right)^{a-1} \left(4\sinh^2\left(\frac{y}{2\widetilde{N_f}}\right)\right)^{b}}, \tag{5.4.31}$$

and $T(k)$ is as above.

After rescaling, we get the following nice properties:

$$\begin{aligned} \left[\hat{y}, \hat{k}\right] &= 4\pi\widetilde{N_f}\, i\,, \\ U_\pm(y) &\rightarrow \frac{y}{2} \qquad (y \rightarrow \infty)\,, \\ T(k) &\rightarrow \frac{k}{2} \qquad (k \rightarrow \infty)\,. \end{aligned} \tag{5.4.32}$$

We then identify $\hbar = 4\pi\widetilde{N_f}$, and calculate the area of the Fermi surface as a function

of energy using the Wigner Hamiltonian (5.A.11). It is important to bear in mind that the projector halves the density of states, as consecutive energy eigenvalues correspond to eigenfunctions of opposite parity.[17] To zeroth order, the phase space volume enclosed by the Fermi surface is again given by (5.4.11), and the correction is given by (5.4.12).

The $\int_0^\infty dy\, U''(y)$ part of the latter formula seems to be problematic at first sight. For generic $a, b$ parameter values

$$U(y) \sim \log|y| \qquad (y \to 0)\ , \tag{5.4.33}$$

and the integral is divergent. Physically, this divergence would be the consequence of the careless semi-classical treatment of a Fermi gas in a singular potential (5.4.33). We will not have to deal with such subtleties, however, for the following reason. In the cases of interest we either have $a+b=0$ or $a+b=1$—see Table 5.3. If $a+b=0$, we choose $U(y)$ of (5.4.30) corresponding to the projection by $(1+R)/2$, which is regular at the origin. If $a+b=1$ we choose $U(y)$ of (5.4.31) corresponding to the projection by $(1-R)/2$, and the potential is again regular. With these choices, we can go ahead and calculate (5.4.12).

For the number of eigenvalues below energy $E$ we get:

$$n(E) = \frac{V}{4\pi\hbar} = \frac{V_0+\Delta V}{4\pi\hbar} = \frac{E^2}{2\pi^2\widetilde{N_f}} - \frac{\widetilde{N_f}+1-2d}{8} - \frac{1}{24\widetilde{N_f}}\ , \tag{5.4.34}$$

where we have $4\pi\hbar$ instead of the conventional $2\pi\hbar$ due to the projection. The constants $C$ and $B$ from (5.4.16) take the values

$$C = \frac{1}{2\pi^2\widetilde{N_f}}\ , \qquad B = n_0 + \frac{\pi^2 C}{3} = -\frac{\widetilde{N_f}+1-2d}{8} + \frac{1}{8\widetilde{N_f}}\ . \tag{5.4.35}$$

[17] We can also think of the projection as Neumann or Dirichlet boundary conditions at the origin.

Analogously to (5.4.36), the free energy $F$ has the following large $N$ expansion:

$$F = \frac{2\sqrt{2}\,\pi}{3}\,\widetilde{N}_f^{\,1/2}\,N^{3/2} + \pi\left(\frac{\widetilde{N}_f^{\,3/2}}{4\sqrt{2}} + \frac{(1-2d)\,\widetilde{N}_f^{\,1/2}}{4\sqrt{2}} - \frac{1}{4\sqrt{2}\,\widetilde{N}_f^{\,1/2}}\right) N^{1/2} + \ldots \,. \tag{5.4.36}$$

This result matches with the saddle point computation of Section 5.3.3—see (5.3.28). As another check, note that the answer (5.4.36) is invariant under the redefinition of parameters in (5.2.10), as should be the case.

## 5.5 Discussion and outlook

We summarize the results obtained in this chapter for the partition function of $\mathcal{N}=4$ gauge theories with classical gauge groups with matter consisting of one two-index tensor (anti)symmetric and $N_f$ fundamental hypermultiplets. The partition function takes the form

$$Z(N) = \mathcal{A}(N_f)\,\mathrm{Ai}\left[C^{-1/3}(N-B)\right] + \mathcal{O}\left(e^{-\sqrt{N}}\right)\,, \tag{5.5.1}$$

where $C$ and $B$ are given in Table 5.5. Using the relation $f_{3/2} = 2/(3\sqrt{C})$ from (5.4.17), we get agreement with the supergravity calculation (5.2.5).

From Table 5.5 one can see that there can be different field theories with the same $\mathrm{AdS}_4\times X$ dual. For instance, the theories $O(2N)+A$, $O(2N+1)+A$, and $USp(2N)+S$ are all dual to $\mathrm{AdS}_4\times(S^7/\hat{D}_{N_f})_{\text{free}}$, whereas $O(2N)+S$ and $O(2N+1)+S$, as well as $USp(2N)+A$ with the shift $N_f \to N_f+4$, are all dual to $\mathrm{AdS}_4\times(S^7/\hat{D}_{N_f+2})$, where the orbifold action on $S^7$ is not free. As mentioned in Section 5.2, the supergravity backgrounds must be distinguished by discrete torsion flux of the three-form gauge potential. Remarkably, the $S^3$ free energies of $O(2N)$ and $O(2N+1)$ theories agree both with symmetric and antisymmetric matter to all orders in $1/N$. However, there are non-perturbative differences, as the two matrix models are not the same.[18] For

[18]The equivalence (5.2.10) does not take the two integrands into each other. See Table 5.3.

other pairs of theories with a same dual M-theory geometry, the subleading $N^{1/2}$ contributions to the free energy are different.

More generally, the results collected in Table 5.5, together with the results of [1, 126] for $U(N)$ quiver theories, represent predictions for M-theory computations that go beyond the leading two-derivative 11-d supergravity. In the case of ABJM theory, the $k^{3/2}$ contribution to $f_{1/2}$ appearing (5.1.1) is accounted for by the shift in the membrane charge from higher derivative corrections on the supergravity side [117]. It would be very interesting to derive the shifts in membrane charge and to take into account higher derivative corrections on the supergravity side for the other examples. Note that from the large $N$ expansion of the Airy function (5.5.1), one obtains a universal logarithmic term in the free energy equal to $-\frac{1}{4}\log N$; this term matches a one-loop supergravity computation on $AdS_4 \times X$ [118].[19] Perhaps one could derive the full Airy function behavior from supergravity calculations.

| $G$ + matter | IIA orientifold | M-theory on $AdS_4 \times X$ | $C$ | $B$ |
|---|---|---|---|---|
| $U(N)$ + adj | no orientifold | $S^7/\mathbb{Z}_{N_f}$ | $\frac{2}{\pi^2 N_f}$ | $-\frac{N_f}{8}+\frac{1}{2N_f}$ |
| $O(2N)+A$ | $O2^-$ | $(S^7/\hat{D}_{N_f})_{\text{free}}$ | $\frac{1}{2\pi^2 N_f}$ | $-\frac{N_f+1}{8}+\frac{1}{8N_f}$ |
| $O(2N)+S$ | $O6^+$ | $S^7/\hat{D}_{N_f+2}$ | $\frac{1}{2\pi^2(N_f+2)}$ | $-\frac{N_f-1}{8}+\frac{1}{8(N_f+2)}$ |
| $O(2N+1)+A$ | $\widetilde{O2}^-$ | $(S^7/\hat{D}_{N_f})_{\text{free}}$ | $\frac{1}{2\pi^2 N_f}$ | $-\frac{N_f+1}{8}+\frac{1}{8N_f}$ |
| $O(2N+1)+S$ | $O6^+$ | $S^7/\hat{D}_{N_f+2}$ | $\frac{1}{2\pi^2(N_f+2)}$ | $-\frac{N_f-1}{8}+\frac{1}{8(N_f+2)}$ |
| $USp(2N)+A$ | $O6^-$ | $S^7/\hat{D}_{N_f-2}$ | $\frac{1}{2\pi^2(N_f-2)}$ | $-\frac{N_f-1}{8}+\frac{1}{8(N_f-2)}$ |
| $USp(2N)+S$ | $O2^+$ | $(S^7/\hat{D}_{N_f})_{\text{free}}$ | $\frac{1}{2\pi^2 N_f}$ | $-\frac{N_f-1}{8}+\frac{1}{8N_f}$ |

Table 5.5: The values of the constants $C$ and $B$ appearing in (5.5.1) for a gauge theory with gauge group $G$, $N_f$ fundamental flavors, and a two-index antisymmetric ($A$) or symmetric ($S$) hypermultiplet. We also listed the type IIA construction, and dual M-theory geometry. To compare with the gravity calculation (5.2.5), one needs the relation $f_{3/2} = 2/(3\sqrt{C})$.

It would be desirable to generalize the methods in this chapter to more complicated quiver theories with classical gauge groups and Chern-Simons interactions. Although

[19] We thank Nikolay Bobev for discussions on this issue.

at first sight it may seem straightforward to generalize the large $N$ approximation of Section 5.3 to the more general setup, there are additional complications related to the non-smoothness of the eigenvalue distributions at leading order in large $N$ and the non-exact cancellation of long-range forces between eigenvalues at subleading order. We leave such a general treatment for future work. The Fermi gas approach explored in Section 5.4 is very powerful, but it relies crucially on non-trivial determinant formulae. It would be interesting to understand better the set of SCFTs with orthogonal and symplectic gauge groups that lend themselves to this approach. One may hope that the $S^3$ partition functions of all theories with $\mathcal{N} \geq 3$ supersymmetry can be written as non-interacting Fermi gases.

## 5.A Lightning review of the Fermi gas method of [1]

In this Appendix we review briefly the approach of [1] for computing the partition function of a non-interacting Fermi gas. For such a system, the number of energy eigenvalues below some energy $E$ is given by:

$$n(E) = \mathrm{Tr}\,\theta(E - \hat{H}) = \sum_n \theta(E - E_n) \ , \tag{5.A.1}$$

where $E_n$ is the $n$th energy eigenvalue of the full system. The density of states is defined by

$$\rho(E) = \frac{dn(E)}{dE} = \sum_n \delta(E - E_n) \ . \tag{5.A.2}$$

In the thermodynamic limit, $\rho(E)$ becomes a continuous function. The grand canonical potential of the non-interacting gas is given by:

$$J(\mu) = \int_0^\infty dE\ \rho(E) \log\left(1 + e^{-E+\mu}\right) \ , \tag{5.A.3}$$

where $\mu$ is the chemical potential. The canonical partition function and the free energy can be obtained from evaluating

$$\begin{aligned} Z(N) &= \frac{1}{2\pi i} \int d\mu \; e^{J(\mu)-\mu N} , \\ F(N) &= -\log Z(N) . \end{aligned} \tag{5.A.4}$$

In the thermodynamic limit where $N \to \infty$, we only need the asymptotic form of $n(E)$ in order to determine the free energy to all orders in $1/N$. In the models of interest, we find that

$$n(E) = C\, E^2 + n_0 + \mathcal{O}\left(E\, e^{-E}\right) . \tag{5.A.5}$$

Then a short calculation gives

$$\begin{aligned} J(\mu) &= \frac{C}{3}\,\mu^3 + B\,\mu + A + \mathcal{O}\left(\mu\, e^{-\mu}\right) , \qquad B = n_0 + \frac{\pi^2\, C}{3} , \\ Z(N) &= \mathcal{A}\,\mathrm{Ai}\left[C^{-1/3}(N-B)\right] + \mathcal{O}\left(e^{-\sqrt{N}}\right) , \end{aligned} \tag{5.A.6}$$

where $A$ and $\mathcal{A} = C^{-1/3} e^{A}$ are $N$-independent constants.

The constants $C$ and $n_0$ can be determined by semiclassical methods, as they describe the large energy behavior of the density of states of the non-interacting Fermi gas. The semiclassical computation can be performed in the Wigner–Kirkwood formalism. Firstly, we introduce the Wigner transform of an operator $\hat{A}$:

$$A_W(x,p) = \int dy \; \langle x - \frac{y}{2} | \hat{A} | x + \frac{y}{2} \rangle \, e^{ipy/\hbar} . \tag{5.A.7}$$

The Wigner transform obeys the product rule

$$\begin{aligned} \left(\hat{A}\hat{B}\right)_W &= A_W \star B_W , \\ \star &\equiv \exp\left[\frac{i\hbar}{2}\left(\overleftarrow{\partial_x}\,\overrightarrow{\partial_p} - \overleftarrow{\partial_p}\,\overrightarrow{\partial_x}\right)\right] . \end{aligned} \tag{5.A.8}$$

The trace of an operator is given by the phase space integral of the Wigner transform:

$$\mathrm{Tr}\,\hat{A} = \int \frac{dx\,dp}{2\pi\,\hbar}\, A_W(x,p)\ . \tag{5.A.9}$$

In the Fermi gases of interest in this chapter, we will encounter one particle density matrices of the form[20]

$$\hat{\rho} = e^{-U(\hat{x})/2} e^{-T(\hat{p})} e^{-U(\hat{x})/2}\ , \tag{5.A.10}$$

where $U(x)$ and $T(p)$ approach linear functions exponentially fast for large $x$ or $p$. One can then calculate the Wigner Hamiltonian

$$\begin{aligned} \rho_W &\equiv e_\star^{-H_W}\ , \\ H_W(x,p) &= T(p) + U(x) + \frac{\hbar^2}{24}\left[U'(x)^2\,T''(p) - 2T'(p)^2\,U''(x)\right] + \mathcal{O}(\hbar^4)\ . \end{aligned} \tag{5.A.11}$$

Combining (5.A.1) and (5.A.9) we get

$$n(E) = \int \frac{dx\,dp}{2\pi\,\hbar}\, \theta(E - \hat{H})_W(x,p)\ . \tag{5.A.12}$$

Along the lines of the argument in [1], one can show that up to exponentially small corrections $n(E)$ is given by the phase space area

$$n(E) = \int_{H_W^{(2)}(x,p)\le E} \frac{dx\,dp}{2\pi\,\hbar} + \mathcal{O}\left(E\,e^{-E}\right)\ , \tag{5.A.13}$$

where $H_W^{(2)}$ is the Wigner Hamiltonian through $\mathcal{O}(\hbar^4)$ displayed in (5.A.11). $n(E)$ is just the Fermi surface area the non-interacting Fermi gas fills up. (5.A.13) can be evaluated using the explicit form of $U(x)$ and $T(p)$.

[20] We have additional an projection operator multiplying this density matrix. We discuss the consequences of the projector in the main text.

## 5.B Derivation of (5.4.23)

Let us note that using simple trigonometric identities

$$\frac{4\cosh(\pi x_1)\cosh(\pi x_2)}{4\cosh\left(\pi(x_1-x_2)\right)\cosh\left(\pi(x_1+x_2)\right)} = \frac{1}{2\cosh\left(\pi(x_1-x_2)\right)} + \frac{1}{2\cosh\left(\pi(x_1+x_2)\right)} . \tag{5.B.1}$$

Using the Fourier transform

$$\int dx\; e^{2\pi i p x}\,\frac{1}{\cosh \pi p} = \frac{1}{\cosh \pi x} , \tag{5.B.2}$$

it is easy to see that

$$\frac{1}{2\cosh\left(\pi(x_1-x_2)\right)} = \left\langle x_1 \left| \frac{1}{2\cosh(\pi\hat{p})} \right| x_2 \right\rangle , \tag{5.B.3}$$

where in $h=1$ units $\hat{p} = -\frac{1}{2\pi i}\,\partial_x$ in position space. Finally, we make use of $R|x_2\rangle = |-x_2\rangle$ to combine (5.B.1) and (5.B.3):

$$\frac{4\cosh(\pi x_1)\cosh(\pi x_2)}{4\cosh\left(\pi(x_1-x_2)\right)\cosh\left(\pi(x_1+x_2)\right)} = \left\langle x_1 \left| \frac{1+R}{2\cosh(\pi\hat{p})} \right| x_2 \right\rangle . \tag{5.B.4}$$

This expression is the same as (5.4.23), which is what we set out to show.

## 5.C Derivation of the determinant formula

The Cauchy determinant formula states that for any numbers $u_i$ and $v_i$, with $1 \leq i,j \leq N$, the following identity holds

$$\frac{\prod_{i<j}(u_i-u_j)(v_i-v_j)}{\prod_{i,j}(u_i+v_j)} = \det \frac{1}{u_i+v_j} . \tag{5.C.1}$$

In this Appendix we derive a similar determinant formula[21]:

$$\frac{\prod_{i<j}(u_i-u_j)(v_i-v_j)(u_iu_j-1)(v_iv_j-1)}{\prod_{i,j}(u_i+v_j)(u_iv_j+1)}=\det\frac{1}{(u_i+v_j)(u_iv_j+1)}\,. \tag{5.C.2}$$

The proof of (5.C.2) is very similar to the proof of the Cauchy formula (5.C.1). Let us compute the determinant of the matrix $M^{(N)}$ where

$$M^{(N)}_{ij}=\frac{1}{(u_i+v_j)(u_i+v_j^{-1})}\,. \tag{5.C.3}$$

Subtracting the last column from each column $j<N$, one obtains the following entries

$$\begin{aligned}&\frac{1}{(u_i+v_j)(u_i+v_j^{-1})}-\frac{1}{(u_i+v_N)(u_i+v_N^{-1})}\\&=\frac{u_i(v_N-v_j)(v_N-v_j^{-1})}{v_N(u_i+v_N)(u_i+v_N^{-1})}\times\frac{1}{(u_i+v_j)(u_i+v_j^{-1})}\,.\end{aligned} \tag{5.C.4}$$

Extracting a factor of $1/(u_i+v_N)(u_i+v_N^{-1})$ from each row $i$ and a factor of $(v_N-v_j)(v_N-v_j^{-1})/v_N$ from each column $j<N$, one obtains

$$\det M^{(N)}=\frac{\prod_{j=1}^{N-1}(v_N-v_j)(v_N-v_j^{-1})}{v_N^{N-1}\prod_{i=1}^{N}(u_i+v_N)(u_i+v_N^{-1})}\begin{vmatrix}\frac{u_1}{(u_1+v_1)(u_1+v_1^{-1})}&\cdots&\frac{u_1}{(u_1+v_N)(u_1+v_N^{-1})}&1\\ \frac{u_2}{(u_2+v_1)(u_2+v_1^{-1})}&\cdots&\frac{u_2}{(u_2+v_N)(u_2+v_N^{-1})}&1\\ \vdots&\vdots&\ddots&\vdots\\ \frac{u_N}{(u_N+v_1)(u_N+v_1^{-1})}&\cdots&\frac{u_N}{(u_N+v_N)(u_N+v_N^{-1})}&1\end{vmatrix}\,. \tag{5.C.5}$$

In the determinant in (5.C.5) we now subtract the last row from each row $i<N$.

[21] This formula has previously appeared in the literature. See for example [139]. We thank Miguel Tierz for pointing this fact out to us.

The entries for $i, j < N$ become

$$\frac{u_i}{(u_i+v_j)(u_i+v_j^{-1})} - \frac{u_N}{(u_N+v_j)(u_N+v_j^{-1})} = \frac{(u_N-u_i)(u_Nu_i-1)}{(u_N+v_j)(u_N+v_j^{-1})}\frac{1}{(u_i+v_j)(u_i+v_j^{-1})}. \tag{5.C.6}$$

Extracting a factor of $(u_N - u_i)(u_Nu_i - 1)$ from each row $i < N$ and a factor of $1/(u_N + v_j)(u_N + v_j^{-1})$ from each column $j < N$ one obtains

$$\det M^{(N)} = \frac{\prod_{i=1}^{N-1}(u_N-u_i)(u_Nu_i-1)\prod_{j=1}^{N-1}(v_N-v_j)(v_N-v_j^{-1})}{v_N^{N-1}\prod_{i=1}^{N}(u_i+v_N)(u_i+v_N^{-1})\prod_{j=1}^{N-1}(u_N+v_j)(u_N+v_j^{-1})}\det M^{(N-1)}. \tag{5.C.7}$$

By induction, we can then show

$$\det M^{(N)} = \frac{\prod_{j>i}(u_j-u_i)(u_iu_j-1)(v_j-v_i)(v_j-v_i^{-1})}{\prod_{i=1}^{N}v_i^{i-1}\prod_{i,j}(u_i+v_j)(u_i+v_j^{-1})}. \tag{5.C.8}$$

Since

$$\det\frac{1}{(u_i+v_j)(u_iv_j+1)} = \frac{1}{\prod_{i=1}^{N}v_i}\det M^{(N)}, \tag{5.C.9}$$

after rearranging the factors of $v_i$ in (5.C.8) we have

$$\det\frac{1}{(u_i+v_j)(u_iv_j+1)} = \frac{\prod_{j>i}(u_j-u_i)(u_iu_j-1)(v_j-v_i)(v_iv_j-1)}{\prod_{i,j}(u_i+v_j)(u_iv_j+1)}, \tag{5.C.10}$$

which is the same expression as (5.C.2).

# Appendix A

# Quantum-corrected moduli space

As a check that the field theories presented in Table 5.2 are dual to M-theory on $AdS_4 \times X$, where $X$ is the quotient of $S^7$ in Table 5.2, one can make sure that the moduli space of these field theories does indeed match the moduli space of $N$ M2-branes probing the 11d geometry. We will do so at the level of algebraic geometry, without explicitly constructing the full hyperkähler metric on the moduli space. In this computation, monopole operators play a crucial role, because they parameterize certain directions in the moduli space [106, 107]. It is very important to include quantum corrections to their scaling dimensions, which essentially determine their OPE as in [106, 107, 110, 111].

To define monopole operators, one should first consider monopole backgrounds. We use the convention where for a gauge theory with gauge group $G$, the gauge field $\mathcal{A}$ corresponding to a GNO monopole background centered at the origin takes the form

$$\mathcal{A} = H(\pm 1 - \cos\theta)d\phi\,, \tag{A.0.1}$$

where $H$ is an element of the Lie algebra $\mathfrak{g}$. Using the gauge symmetry, one can rotate $H$ into the Cartan $\{h_i\}$ subalgebra, namely

$$H = \sum_{i=1}^{r} q_i h_i\,, \tag{A.0.2}$$

where $r$ is the rank of $G$. The Dirac quantization condition requires

$$q \cdot w \in \mathbb{Z}/2 \tag{A.0.3}$$

for any allowed weight $w$ of an irreducible representation of $G$. These monopole backgrounds should be considered only modulo the action of the Weyl group.

The background (A.0.1) above breaks all supersymmetry by itself. To define a supersymmetric background, one should supplement (A.0.1) with a non-trivial profile for one of the three real scalars in the $\mathcal{N} = 4$ vectormultiplet. Let this scalar be $\sigma$; we must take $\sigma = H/|x|$. The choice of such a scalar breaks the $SO(4)_R$ symmetry of the $\mathcal{N} = 4$ supersymmetry algebra to an $SO(2)_R$ subgroup corresponding to an $\mathcal{N} = 2$ subalgebra. In this $\mathcal{N} = 2$ language, one can define chiral monopole operators $\mathcal{M}_q$ corresponding to the GNO background described above. Being chiral, one can identify their scaling dimension $\Delta_q$ with the $SO(2)_R$ charge. As shown in [107, 140], the BPS monopole operator $\mathcal{M}_q$ acquires at one-loop the R-charge

$$\Delta_q = \sum_{\text{hypers}} |q \cdot w| - \sum_{\text{vectors}} |q \cdot w| \,, \tag{A.0.4}$$

where the sums run over all the weights $w$ of the fermions in the hyper and vectormultiplets. As far as the $\mathcal{N} = 4$ supersymmetry is concerned, these chiral monopole operators $\mathcal{M}_q$ are the highest weight states of $SO(4)_R$ representations of dimension $2\Delta_q + 1$. However, only the chiral operators with scaling dimension (A.0.4) will be relevant for us.

## A.1 $\mathcal{N} = 4$ $U(N)$ gauge theory with adjoint and $N_f$ fundamental hypermultiplets

Let us start by reviewing the construction of the geometric branch of the moduli space for the $\mathcal{N} = 4$ $U(N)$ gauge theory with an adjoint hyper and $N_f$ fundamental hypermultiplets. In $\mathcal{N} = 2$ notation, the matter content of the theory consists of

adjoint chiral multiplets with bottom components $X$, $Y$ (coming from the adjoint $\mathcal{N}=4$ hypermultiplet), and $Z$ (coming from the $\mathcal{N}=4$ vectormultiplet), as well as chiral multiplets with bottom components $q_i$, $i=1,\ldots,N_f$ transforming in the fundamental of $U(N)$ and $\widetilde{q}_i$ transforming in the conjugate representation. The $\mathcal{N}=2$ superpotential,

$$W = \mathrm{tr}\,(Z[X,Y] + \widetilde{q}_i Z q_i)\ , \tag{A.1.1}$$

is consistent with the R-charges of $X$, $Y$, $q_i$, and $\widetilde{q}_i$ being equal $1/2$, and that of $Z$ being equal 1, as can be derived for instance using the $F$-maximization procedure [23, 113, 141].

In the $N=1$ case, the moduli space of this theory should match precisely the eight-dimensional transverse space probed by the M2-branes. Indeed, in this case the chiral multiplets corresponding to $X$ and $Y$ completely decouple, and the expectation values of these complex fields parameterize a $\mathbb{C}^2$ factor in the moduli space of vacua. The rest of the moduli space is parameterized by expectation values for $Z$ and for the monopole operators $T=\mathcal{M}_{1/2}$ and $\widetilde{T}=\mathcal{M}_{-1/2}$. These operators are not independent; in the chiral ring, they satisfy a relation that can be determined as follows. According to (A.0.4), we can calculate their R-charge to be

$$\Delta = \frac{N_f}{2} + 0 - 0 = \frac{N_f}{2}\,, \tag{A.1.2}$$

where in the middle equality we exhibited explicitly the contributions from the $N_f$ fundamentals, the adjoints, and the $\mathcal{N}=4$ vector, respectively. One then expects the OPE [106, 107, 110, 111]

$$T\widetilde{T} \sim Z^{N_f}\,, \tag{A.1.3}$$

which should be imposed as a relation in the chiral ring. Giving $T$, $\widetilde{T}$, and $Z$ expectation values obeying (A.1.3) describes the orbifold $\mathbb{C}^2/\mathbb{Z}_{N_f}$, as can be seen from

"solving" (A.1.3) by writing $T = a^{N_f}$, $\widetilde{T} = b^{N_f}$, and $Z = ab$. The coordinates $a$ and $b$ parameterize $\mathbb{C}^2/\mathbb{Z}_{N_f}$ because both $(a, b)$ and $(ae^{2\pi i/N_f}, be^{-2\pi i/N_f})$ yield the same point in (A.1.3). The moduli space of the $U(1)$ theory is therefore $\mathbb{C}^2 \times (\mathbb{C}^2/\mathbb{Z}_{N_f})$, where the $\mathbb{C}^2$ factor is parameterized by the free fields $X$ and $Y$, and the $\mathbb{C}^2/\mathbb{Z}_{N_f}$ factor is really just the complex surface (A.1.3). Defining

$$z_1 = X\,, \qquad z_2 = Y\,, \qquad z_3 = a\,, \qquad z_4 = b^*\,, \tag{A.1.4}$$

we obtain the description of $\mathbb{C}^2 \times (\mathbb{C}^2/\mathbb{Z}_{N_f})$ used around eq. (5.2.1).

When $N > 1$, the theory has a Coulomb branch where the fundamentals vanish and the adjoint fields $X$, $Y$, and $Z$ have diagonal expectation values

$$X = \mathrm{diag}\{x_1, x_2, \ldots, x_N\}\,, \qquad Y = \mathrm{diag}\{y_1, y_2, \ldots, y_N\}\,, \qquad Z = \mathrm{diag}\{z_1, z_2, \ldots, z_N\} \tag{A.1.5}$$

(to ensure vanishing of the F-term potential), thus breaking the gauge group generically to $U(1)^N$. In addition, there are BPS monopole operators corresponding to

$$H = \mathrm{diag}\{q_1, q_2, \ldots, q_N\}\,; \tag{A.1.6}$$

we can denote the BPS monopole operators with $q_i = \pm 1/2$ and $q_j = 0$ with $i \neq j$ by $T_i$ (for the plus sign) and $\widetilde{T}_i$ (for the minus sign). An argument like the one in the Abelian case above shows that for every $i$, we have

$$T_i \widetilde{T}_i \sim z_i^{N_f}\,. \tag{A.1.7}$$

For each $i$ we therefore have a $\mathbb{C}^2 \times (\mathbb{C}^2/\mathbb{Z}_{N_f})$ factor in the moduli space parameterized by $(x_i, y_i, z_i, T_i, \widetilde{T}_i)$. The Weyl group of $U(N)$ acts by permuting these factors, so the Coulomb branch of the $U(N)$ theory is the symmetric product of $N$ $\mathbb{C}^2 \times (\mathbb{C}^2/\mathbb{Z}_{N_f})$ factors. This space is precisely the expected Coulomb branch of $N$ M2-branes probing $\mathbb{C}^2 \times (\mathbb{C}^2/\mathbb{Z}_{N_f})$. In addition to the Coulomb branch, the moduli space also has a Higgs

branch where the fundamental fields $q$ and $\widetilde{q}$ acquire expectation values. This branch is not realized geometrically, however, and is therefore of no interest to us.

## A.2 The $USp(2N)$ theories

Let us now consider the $\mathcal{N} = 4$ $USp(2N)$ theories with $N_f$ fundamental and either a symmetric or an anti-symmetric hypermultiplet. As in the $U(N)$ case, let us denote the bottom components of the $\mathcal{N} = 2$ matter multiplets by $X$, $Y$ (transforming either in the symmetric or anti-symmetric representations of $USp(2N)$), $Z$ (transforming in the adjoint (symmetric) representation of $USp(2N)$), $q_i$, and $\widetilde{q}_i$ (transforming in the fundamental representation). A superpotential like (A.1.1) determines the R-charges of these operators just like in the $U(N)$ case.

In the $N = 1$ case, we expect that the Coulomb branch of the $USp(2) \cong SU(2)$ theory should match the geometry probed by the M2-branes. In this case, $Z$ is an adjoint field, while $X$ and $Y$ are either adjoint-valued or singlets under $SU(2)$ (corresponding to symmetric or anti-symmetric $USp(2N)$ tensors, respectively). On the Coulomb branch, the gauge group is broken to $U(1)$ by expectation values for the adjoint fields. Without loss of generality, we can consider these expectation values to be in the $J_3 = \frac{1}{2}\sigma_3$ direction and take $Z = zJ_3$. If $X$ and $Y$ are adjoint-valued, we should also take $X = xJ_3$, $Y = yJ_3$ (such that the bosonic potential following from the first term in (A.1.1) vanishes); if $X$ and $Y$ are $SU(2)$ singlets, we can take $X = x$ and $Y = y$. The expectation values of the fundamental fields $q_i$ and $\widetilde{q}_i$ must vanish for any of the vacua on the Coulomb branch.

As in the $U(1)$ case, a full description of the moduli space also involves monopole operators. For an $SU(2)$ gauge theory, the monopole operators can be taken to correspond to a GNO background (A.0.1) with

$$H = qJ_3\,. \tag{A.2.1}$$

Since the possible weights $w$ are half-integral, the Dirac quantization condition (A.0.3)

implies $q \in \mathbb{Z}$. Note that all these operators are topologically trivial, because the group $SU(2)$ has trivial topology. The operators with smallest charge are $T = \mathcal{M}_1$ and $\widetilde{T} = \mathcal{M}_{-1}$. In fact, in the $SU(2)$ gauge theory, $T$ and $\widetilde{T}$ are identified under the action of the Weyl group, but on the Coulomb branch they will be distinct. According to (A.0.4), the R-charge of $T$ and $\widetilde{T}$ is

$$\Delta = \begin{cases} N_f + 2 - 2 = N_f & \text{if } X, Y \text{ are adjoints}, \\ N_f + 0 - 2 = N_f - 2 & \text{if } X, Y \text{ are singlets}, \end{cases} \tag{A.2.2}$$

where, as in (A.1.2), in the middle equality we exhibited explicitly the contributions from the $N_f$ fundamental, from the adjoints / singlets, and from the $\mathcal{N} = 4$ vector, respectively. From (A.2.2), one expects the OPE

$$T\widetilde{T} \sim \operatorname{tr} Z^{2\Delta} = (\operatorname{tr} Z^2)^{\Delta}, \tag{A.2.3}$$

where the trace is taken in the fundamental representation of $SU(2)$. The relation (A.2.3) should be imposed as a relation in the chiral ring. Note that $\Delta$ in (A.2.2) is always an integer, so $\operatorname{tr} Z^{2\Delta}$ does not vanish. Also note that if $N_f = 0$ in the adjoint case and $N_f \leq 2$ in the singlet case we obtain monopole operators with R-charge $\Delta \leq 0$, which signifies that one of the assumptions in our UV description of the theory must break down as we flow to the IR critical point. Such theories were called "bad" in [140], and we will not examine them. See also footnotes 11 and 12.

We are now ready to give the full description of the Coulomb branch. It is parameterized by the complex fields $x$, $y$, $z$, $T$, and $\widetilde{T}$. The latter three satisfy

$$T\widetilde{T} \sim z^{2\Delta}, \tag{A.2.4}$$

as can be easily seen from (A.2.3). In addition, $SU(2)$ has a $\mathbb{Z}_2$ Weyl group, which sends $J_3 \to -J_3$ and consequently also acts non-trivially on the Coulomb branch by

flipping the sign of the adjoint fields and interchanging $T$ with $\widetilde{T}$:

$$\begin{aligned} X,\, Y \text{ adjoints (symmetric):} \quad & (x,y,z,T,\widetilde{T}) \sim (-x,-y,-z,\widetilde{T},T)\,, \\ X,\, Y \text{ singlets (anti-symmetric):} \quad & (x,y,z,T,\widetilde{T}) \sim (x,y,-z,\widetilde{T},T)\,. \end{aligned} \tag{A.2.5}$$

We can relate this description of the Coulomb branch to the one used in Section 5.2.1. First, we solve (A.2.4) by writing $T = a^{2\Delta}$, $\widetilde{T} = (c^*)^{2\Delta}$, and $z = ac^*$, for some complex coordinates $a$ and $c$. There is a redundancy in this description that forces us to make the identification

$$(a,c) \sim e^{\pi i/\Delta}(a,c)\,. \tag{A.2.6}$$

In terms of $a$ and $c$, the Weyl group identifications (A.2.5) yield

$$\begin{aligned} X,\, Y \text{ adjoints (symmetric):} \quad & (x,y,a,c) \sim (-x,-y,ic^*,-ia^*)\,, \\ X,\, Y \text{ singlets (anti-symmetric):} \quad & (x,y,a,c) \sim (x,y,ic^*,-ia^*)\,. \end{aligned} \tag{A.2.7}$$

Redefining $x = z_1$, $y = z_2$, $a = z_3$, $c = z_4$, we obtain precisely the orbifold description used in Section 5.2.1. In the case where $X$ and $Y$ are adjoint fields, the Coulomb branch is a freely acting $\hat{D}_{N_f}$ orbifold of $\mathbb{C}^4$, while in the case where $X$ and $Y$ are singlets the Coulomb branch is a $\hat{D}_{N_f-2}$ orbifold of $\mathbb{C}^4$ (more precisely $\mathbb{C}^2 \times (\mathbb{C}^2/\hat{D}_{N_f-2})$) that now has fixed points because the coordinates $z_1 = x$ and $z_2 = y$ are invariant under the action (A.2.6)–(A.2.7).

When $N > 1$, the moduli space of vacua has a Coulomb branch where the fundamentals vanish and $X$, $Y$, and $Z$ acquire expectation values and break $USp(2N)$ generically to $U(1)^N$. A straightforward analysis shows that if $X$ and $Y$ are symmetric tensors, the Coulomb branch is the $N$th symmetric power of the space $\mathbb{C}^4/\hat{D}_{N_f}$ found above in the $N = 1$ case; if $X$ and $Y$ are anti-symmetric tensors, the Coulomb branch is the $N$th symmetric power of $\mathbb{C}^2 \times (\mathbb{C}^2/\hat{D}_{N_f-2})$. These spaces are precisely the expected moduli spaces of $N$ M2-branes probing $\mathbb{C}^4/\hat{D}_{N_f}$ or $\mathbb{C}^2 \times (\mathbb{C}^2/\hat{D}_{N_f-2})$. In addition to the Coulomb branch, the theory also has a Higgs branch where the fun-

damentals $q_i$ and $\widetilde{q}_i$ acquire VEVs, but the Higgs branch is not realized geometrically in M-theory.

It is worth noting that if $X$ and $Y$ are anti-symmetric tensors of $USp(2N)$, one could consider imposing a symplectic tracelessness condition on these fields. When $N = 1$, the fields $X$ and $Y$ would be completely absent, because what survived in the analysis above was precisely their symplectic trace. The moduli space would therefore be only $\mathbb{C}^2/\hat{D}_{N_f}$ if the symplectic trace were removed from $X$ and $Y$, and it would not match the eleven-dimensional geometry. The correct field theory that arises from the brane construction of Section 5.2.1 is that where $X$ and $Y$ are not required to be symplectic traceless.

## A.3 The $O(2N)$ theories

The discussion of the Coulomb branch for $\mathcal{N} = 4$ $O(2N)$ gauge theory with either a symmetric or anti-symmetric hypermultiplet and $N_f$ hypermultiplets in the the fundamental representation of $O(2N)$ parallels the discussion of the $USp(2N)$ case above. Let $X$, $Y$, $Z$, $q_i$, and $\widetilde{q}_i$ be the bottom components of the chiral multiplets arising from the $\mathcal{N} = 4$ hyper and vectormultiplets as before. Now $Z$ transforms in the adjoint (anti-symmetric) representation of $O(2N)$, while $X$ and $Y$ transform either in the symmetric or antisymmetric tensor representations of $O(2N)$. While the representations of $O(2N)$ are real, and therefore there exists the possibility of considering real scalar fields, our scalar fields $X$, $Y$, $Z$, $q_i$, and $\widetilde{q}_i$ are all complex.

In the case $N = 1$, one can again study the Coulomb branch where the fundamentals all vanish and $X$, $Y$, and $Z$ have expectation values. Let

$$J = \begin{pmatrix} 0 & -i \\ i & 0 \end{pmatrix} \tag{A.3.1}$$

be the Hermitian generator of $O(2)$. On the Coulomb branch, we should take $Z = zJ$. If $X$ and $Y$ are symmetric matrices, the scalar potential vanishes if these matrices

commute with $Z$, so we should take $X = xI_2$ and $Y = yI_2$, where $I_2$ is the $2 \times 2$ identity matrix. If $X$ and $Y$ are anti-symmetric matrices, the only option is $X = xJ$ and $Y = yJ$ for some complex numbers $x$ and $y$.

The monopole operators for an $O(2)$ gauge theory correspond to backgrounds (A.0.1) with

$$H = qJ\,. \tag{A.3.2}$$

Since the possible weights of $O(2)$ representations are all integral, Dirac quantization implies $q \in \mathbb{Z}/2$. The monopole operators of smallest charge are $T = \mathcal{M}_{1/2}$ and $\widetilde{T} = \mathcal{M}_{-1/2}$. These operators are independent at generic points on the Coulomb branch. If the gauge group were $SO(2)$ they would also be distinct at the CFT fixed point at the origin of the Coulomb branch, but for an $O(2)$ gauge group they get identified: Indeed, one can consider the charge conjugation

$$C = \begin{pmatrix} 1 & 0 \\ 0 & -1 \end{pmatrix} \in O(2)\,, \tag{A.3.3}$$

(which in the $O(2)$ theory is gauged) under which $J \to CJC^{-1} = -J$. Charge conjugation identifies $T$ with $\widetilde{T}$ at the origin of moduli space because it identifies the defining backgrounds (A.3.1). The R-charge of $T$ and $\widetilde{T}$ is

$$\Delta = \begin{cases} N_f + 2 - 0 = N_f + 2 & \text{if } X,\, Y \text{ are symmetric}\,, \\ N_f + 0 - 0 = N_f & \text{if } X,\, Y \text{ are anti-symmetric}\,. \end{cases} \tag{A.3.4}$$

These R-charges imply that $T$ and $\widetilde{T}$ satisfy the OPE (A.2.3), as in the $SU(2)$ case.

The Coulomb branch is parameterized by the complex parameters $x$, $y$, $z$, $T$, and $\widetilde{T}$ satisfying the constraint (A.2.4). Charge conjugation (A.3.3) imposes the further

identifications

$$\begin{aligned} X,\, Y \text{ symmetric:} \qquad & (x,y,z,T,\widetilde{T}) \sim (x,y,-z,\widetilde{T},T)\,, \\ X,\, Y \text{ anti-symmetric:} \qquad & (x,y,z,T,\widetilde{T}) \sim (-x,-y,-z,\widetilde{T},T)\,. \end{aligned} \tag{A.3.5}$$

Writing $T = a^{2\Delta}$, $\widetilde{T} = (c^*)^{2\Delta}$, and $z = ac^*$ as in the $SU(2)$ case, we obtain a description of the Coulomb branch in terms of the complex parameters $(x,y,a,c)$ subject to the identifications $(a,c) \sim e^{\pi i/\Delta}(a,c)$ and

$$\begin{aligned} X,\, Y \text{ symmetric:} \qquad & (x,y,a,c) \sim (x,y,-z,ic^*,-ia^*)\,, \\ X,\, Y \text{ anti-symmetric:} \qquad & (x,y,a,c) \sim (-x,-y,ic^*,-ia^*)\,. \end{aligned} \tag{A.3.6}$$

Denoting $x = z_1$, $y = z_2$, $a = z_3$, and $c = z_4$ as in the $SU(2)$ case we obtain the same description of the eight-dimensional hyperkähler space that appears in the eleven-dimensional geometry, as described in Section 5.2.1.

In the $N > 1$ case, one can check that the Coulomb branch is the $N$th symmetric power of $\mathbb{C}^2 \times (\mathbb{C}^2/\hat{D}_{N_f})$ or $\mathbb{C}^4/\hat{D}_{N_f}$, depending on whether $X$ and $Y$ are symmetric or anti-symmetric tensors, respectively. This geometry matches precisely the moduli space of $N$ M2-branes probing, respectively, $\mathbb{C}^2 \times (\mathbb{C}^2/\hat{D}_{N_f})$ or $\mathbb{C}^4/\hat{D}_{N_f}$. As in the $U(N)$ and $USp(2N)$ theories discussed above, there is also a Higgs branch where the fundamentals have expectation values, but this branch is not realized geometrically in M-theory.

Note that having an $O(2N)$ gauge group as opposed to $SO(2N)$ was very important for matching the eleven-dimensional geometry. In an $SO(2)$ gauge theory, the identifications (A.3.5) and (A.3.6) would not be present. Note also that in the case where $X$ and $Y$ are symmetric tensors of $O(2N)$, one has in principle the possibility of imposing a tracelessness condition on $X$ and $Y$. When $N = 1$, the moduli space would then be $\mathbb{C}^2/\hat{D}_{N_f}$, and would therefore have complex dimension two. For the field theory that arises from the orientifold construction in string theory one should therefore not require $X$ and $Y$ to be traceless.

## A.4 The $O(2N+1)$ theories

Lastly, let us consider the $\mathcal{N}=4$ $O(2N+1)$ gauge theories with either a symmetric or anti-symmetric tensor hypermultiplet and $N_f$ fundamental hypermultiplets. We use the same notation for the bottom components of the various $\mathcal{N}=2$ chiral multiplets as in the previous section.

In the $N=1$ case, we can take the theory to the Coulomb branch by giving an expectation value to $Z=zJ_{12}$ to the complex scalar $Z$ belonging to the $\mathcal{N}=4$ vectormultiplet. Here,

$$J_{12}=\begin{pmatrix} 0 & -i & 0 \\ i & 0 & 0 \\ 0 & 0 & 0 \end{pmatrix} \tag{A.4.1}$$

is the generator of rotations in the 12-plane in color space. To ensure that the scalar potential vanishes, one should also take $X=xJ_{12}$ and $Y=yJ_{12}$ in the case where $X$ and $Y$ are anti-symmetric tensors, and $X=\mathrm{diag}\{x,x,\widetilde{x}\}$, $Y=\mathrm{diag}\{y,y,\widetilde{y}\}$ in the case where $X$ and $Y$ are symmetric tensors. In both cases, the vanishing of the F-term potential requires $q_i=\widetilde{q}_i=0$.

The relevant BPS monopole operators in this case correspond to

$$H=qJ_{12}\,. \tag{A.4.2}$$

Dirac quantization implies $q\in\mathbb{Z}/2$, and as before we denote $T=\mathcal{M}_{1/2}$ and $\widetilde{T}=\mathcal{M}_{-1/2}$. The operators $T$ and $\widetilde{T}$ are distinct on the Coulomb branch, but at the CFT

fixed point they get identified. Indeed, the gauge transformations corresponding to

$$O = \begin{pmatrix} 1 & 0 & 0 \\ 0 & -1 & 0 \\ 0 & 0 & \pm 1 \end{pmatrix} \in O(3) \tag{A.4.3}$$

send $J_{12} \to O J_{12} O^{-1} = -J_{12}$, so they identify $T$ with $\widetilde{T}$. Note that the minus sign in (A.4.3) yields a group element of $SO(3)$ as well, while the plus sign does not; the transformation corresponding to the plus sign is the charge conjugation symmetry of the $SO(3)$ theory, which is gauged when the gauge group is $O(3)$. Unlike the $O(2)$ case discussed above, the operators $T$ and $\widetilde{T}$ are not identified only in the $O(3)$ gauge theory. They would be identified in the $SO(3)$ gauge theory as well. The R-charge of $T$ and $\widetilde{T}$ is

$$\Delta = \begin{cases} N_f + 3 - 1 = N_f + 2 & \text{if } X, Y \text{ are symmetric}, \\ N_f + 1 - 1 = N_f & \text{if } X, Y \text{ are anti-symmetric}. \end{cases} \tag{A.4.4}$$

Based on these R-charges, one can infer that $T$ and $\widetilde{T}$ satisfy the OPE (A.2.3).

The Coulomb branch in this case is parameterized by $x$, $y$, $z$, $T$, $\widetilde{T}$, as well as $\widetilde{x}$ and $\widetilde{y}$ in the symmetric tensor case. The fields $z$, $T$, and $\widetilde{T}$ satisfy the chiral ring relation (A.2.4). The transformation (A.4.3) imposes the same relations as in (A.3.5)–(A.3.6) and does not act on $\widetilde{x}$ and $\widetilde{y}$. The Coulomb branch is therefore $\mathbb{C}^4/\hat{D}_{N_f+2}$ if $X$ and $Y$ are anti-symmetric tensors, just like in the $O(2)$ case discussed above. If $X$ and $Y$ are symmetric tensors, the Coulomb branch is $\mathbb{C}^2 \times \mathbb{C}^2 \times \mathbb{C}^2/\hat{D}_{N_f+2}$, where the extra $\mathbb{C}^2$ factor relative to the $O(2)$ case is parameterized by $\widetilde{x}$ and $\widetilde{y}$.

This discussion generalizes to $N > 1$. If $X$ and $Y$ are anti-symmetric tensors, the Coulomb branch is the $N$th symmetric power of $\mathbb{C}^4/\hat{D}_{N_f+2}$, as expected from $N$ M2-branes probing $\mathbb{C}^4/\hat{D}_{N_f}$. If $X$ and $Y$ are symmetric tensors, the Coulomb branch is $\mathbb{C}^2$ times the $N$th symmetric power of $\mathbb{C}^2 \times \mathbb{C}^2/\hat{D}_{N_f+2}$. This moduli spaces is also

as expected from $N$ M2-branes probing $\mathbb{C}^2 \times (\mathbb{C}^2/\hat{D}_{N_f})$, together with a fractional M2-brane that is stuck at the $\mathbb{C}^2/\hat{D}_{N_f}$ singularity and can only explore the $\mathbb{C}^2$ part of the geometry. This fractional M2-brane corresponds to the half-D2-brane that is stuck to the $O6^+$-plane. As in the previous cases, the moduli space also has a Higgs branch where the fundamental fields $q_i$ and $\widetilde{q}_i$ have expectation values, but this branch is not realized geometrically.

# Bibliography


[1] M. Marino and P. Putrov, "ABJM theory as a Fermi gas," *J.Stat.Mech.* **1203** (2012) P03001, 1110.4066.

[2] L. Amico, R. Fazio, A. Osterloh, and V. Vedral, "Entanglement in many-body systems," *Rev.Mod.Phys.* **80** (2008) 517–576, quant-ph/0703044.

[3] J. Eisert, M. Cramer, and M. Plenio, "Area laws for the entanglement entropy - a review," *Rev.Mod.Phys.* **82** (2010) 277–306, 0808.3773.

[4] L. Bombelli, R. K. Koul, J. Lee, and R. D. Sorkin, "A Quantum Source of Entropy for Black Holes," *Phys.Rev.* **D34** (1986) 373–383.

[5] M. Srednicki, "Entropy and area," *Phys.Rev.Lett.* **71** (1993) 666–669, hep-th/9303048.

[6] H. Liu and M. Mezei, "A Refinement of entanglement entropy and the number of degrees of freedom," *JHEP* **1304** (2013) 162, 1202.2070.

[7] M. P. Hertzberg and F. Wilczek, "Some Calculable Contributions to Entanglement Entropy," *Phys.Rev.Lett.* **106** (2011) 050404, 1007.0993.

[8] A. Zamolodchikov, "Irreversibility of the Flux of the Renormalization Group in a 2D Field Theory," *JETP Lett.* **43** (1986) 730–732.

[9] J. L. Cardy, "Operator Content of Two-Dimensional Conformally Invariant Theories," *Nucl.Phys.* **B270** (1986) 186–204.

[10] T. Appelquist, A. G. Cohen, and M. Schmaltz, "A New constraint on strongly coupled gauge theories," *Phys.Rev.* **D60** (1999) 045003, hep-th/9901109.

[11] S. Sachdev, "Polylogarithm identities in a conformal field theory in three-dimensions," *Phys.Lett.* **B309** (1993) 285–288, hep-th/9305131.

[12] A. V. Chubukov, S. Sachdev, and J. Ye, "Theory of two-dimensional quantum Heisenberg antiferromagnets with a nearly critical ground state," *Phys.Rev.* **B49** (1994) 11919–11961.

[13] T. Nishioka and K. Yonekura, "On RG Flow of $tau_{RR}$ for Supersymmetric Field Theories in Three-Dimensions," *JHEP* **1305** (2013) 165, 1303.1522.

[14] A. Cappelli, D. Friedan, and J. I. Latorre, "C theorem and spectral representation," *Nucl.Phys.* **B352** (1991) 616–670.

[15] D. Anselmi, D. Freedman, M. T. Grisaru, and A. Johansen, "Nonperturbative formulas for central functions of supersymmetric gauge theories," *Nucl.Phys.* **B526** (1998) 543–571, hep-th/9708042.

[16] J. L. Cardy, "Is There a c Theorem in Four-Dimensions?," *Phys.Lett.* **B215** (1988) 749–752.

[17] Z. Komargodski and A. Schwimmer, "On Renormalization Group Flows in Four Dimensions," *JHEP* **1112** (2011) 099, 1107.3987.

[18] Z. Komargodski, "The Constraints of Conformal Symmetry on RG Flows," *JHEP* **1207** (2012) 069, 1112.4538.

[19] H. Casini, M. Huerta, and R. C. Myers, "Towards a derivation of holographic entanglement entropy," *JHEP* **1105** (2011) 036, 1102.0440.

[20] R. C. Myers and A. Sinha, "Seeing a c-theorem with holography," *Phys.Rev.* **D82** (2010) 046006, 1006.1263.

[21] R. C. Myers and A. Sinha, "Holographic $c$-theorems in arbitrary dimensions," *JHEP* **1101** (2011) 125, 1011.5819.

[22] S. Ryu and T. Takayanagi, "Aspects of Holographic Entanglement Entropy," *JHEP* **0608** (2006) 045, hep-th/0605073.

[23] D. L. Jafferis, I. R. Klebanov, S. S. Pufu, and B. R. Safdi, "Towards the F-Theorem: N=2 Field Theories on the Three-Sphere," *JHEP* **1106** (2011) 102, 1103.1181.

[24] I. R. Klebanov, S. S. Pufu, and B. R. Safdi, "$F$-Theorem without supersymmetry," *JHEP* **1110** (2011) 038, 1105.4598.

[25] I. R. Klebanov, S. S. Pufu, S. Sachdev, and B. R. Safdi, "Entanglement Entropy of 3-d Conformal Gauge Theories with Many Flavors," *JHEP* **1205** (2012) 036, 1112.5342.

[26] B. R. Safdi, "Exact and Numerical Results on Entanglement Entropy in (5+1)-Dimensional CFT," *JHEP* **1212** (2012) 005, 1206.5025.

[27] C. A. Agon, M. Headrick, D. L. Jafferis, and S. Kasko, "Disk entanglement entropy for a Maxwell field," *Phys.Rev.* **D89** (2014) 025018, 1310.4886.

[28] H. Casini and M. Huerta, "On the RG running of the entanglement entropy of a circle," *Phys.Rev.* **D85** (2012) 125016, 1202.5650.

[29] H. Liu and M. Mezei, "Probing renormalization group flows using entanglement entropy," *JHEP* **1401** (2014) 098, 1309.6935.

[30] H. Casini, C. Fosco, and M. Huerta, "Entanglement and alpha entropies for a massive Dirac field in two dimensions," *J.Stat.Mech.* **0507** (2005) P07007, cond-mat/0505563.

[31] H. Casini and M. Huerta, "Entanglement and alpha entropies for a massive scalar field in two dimensions," *J.Stat.Mech.* **0512** (2005) P12012, cond-mat/0511014.

[32] H. Casini and M. Huerta, "Entanglement entropy in free quantum field theory," *J.Phys.* **A42** (2009) 504007, 0905.2562.

[33] I. R. Klebanov, T. Nishioka, S. S. Pufu, and B. R. Safdi, "On Shape Dependence and RG Flow of Entanglement Entropy," *JHEP* **1207** (2012) 001, 1204.4160.

[34] T. Grover, "Chiral Symmetry Breaking, Deconfinement and Entanglement Monotonicity," 1211.1392.

[35] E. Dyer, M. Mezei, and S. S. Pufu, "Monopole Taxonomy in Three-Dimensional Conformal Field Theories," 1309.1160.

[36] M. Mezei and S. S. Pufu, "Three-sphere free energy for classical gauge groups," *JHEP* **1402** (2014) 037, 1312.0920.

[37] A. Kapustin, B. Willett, and I. Yaakov, "Exact Results for Wilson Loops in Superconformal Chern-Simons Theories with Matter," *JHEP* **1003** (2010) 089, 0909.4559.

[38] C. P. Herzog, I. R. Klebanov, S. S. Pufu, and T. Tesileanu, "Multi-Matrix Models and Tri-Sasaki Einstein Spaces," *Phys.Rev.* **D83** (2011) 046001, 1011.5487.

[39] T. Grover, A. M. Turner, and A. Vishwanath, "Entanglement Entropy of Gapped Phases and Topological Order in Three dimensions," *Phys.Rev.* **B84** (2011) 195120, 1108.4038.

[40] A. Kitaev and J. Preskill, "Topological entanglement entropy," *Phys.Rev.Lett.* **96** (2006) 110404, hep-th/0510092.

[41] M. Levin and X.-G. Wen, "Detecting Topological Order in a Ground State Wave Function," *Phys.Rev.Lett.* **96** (2006) 110405.

[42] B. Swingle and T. Senthil, "Universal crossovers between entanglement entropy and thermal entropy," *Phys.Rev.* **B87** (2013) 045123, 1112.1069.

[43] N. Ogawa, T. Takayanagi, and T. Ugajin, "Holographic Fermi Surfaces and Entanglement Entropy," *JHEP* **1201** (2012) 125, 1111.1023.

[44] L. Huijse, S. Sachdev, and B. Swingle, "Hidden Fermi surfaces in compressible states of gauge-gravity duality," *Phys.Rev.* **B85** (2012) 035121, 1112.0573.

[45] E. Shaghoulian, "Holographic Entanglement Entropy and Fermi Surfaces," *JHEP* **1205** (2012) 065, 1112.2702.

[46] N. Iizuka, S. Kachru, N. Kundu, P. Narayan, N. Sircar, *et. al.*, "Bianchi Attractors: A Classification of Extremal Black Brane Geometries," *JHEP* **1207** (2012) 193, 1201.4861.

[47] S.-S. Lee, "Low-energy effective theory of Fermi surface coupled with U(1) gauge field in 2+1 dimensions," *Phys.Rev.* **B80** (Oct., 2009) 165102, 0905.4532.

[48] M. M. Wolf, "Violation of the entropic area law for Fermions," *Phys.Rev.Lett.* **96** (2006) 010404, quant-ph/0503219.

[49] D. Gioev and I. Klich, "Entanglement Entropy of Fermions in Any Dimension and the Widom Conjecture," *Phys.Rev.Lett.* **96** (2006) 100503.

[50] B. Swingle, "Entanglement Entropy and the Fermi Surface," *Phys.Rev.Lett.* **105** (2010) 050502, 0908.1724.

[51] Y. Zhang, T. Grover, and A. Vishwanath, "Entanglement entropy of critical spin liquids," *Phys.Rev.Lett.* **107** (2011) 067202, 1102.0350.

[52] P. Calabrese, M. Mintchev, and E. Vicari, "Entanglement entropies in free-fermion gases for arbitrary dimension," *EPL (Europhysics Letters)* **97** (Jan., 2012) 20009, 1110.6276.

[53] J. Callan, Curtis G. and F. Wilczek, "On geometric entropy," *Phys.Lett.* **B333** (1994) 55–61, hep-th/9401072.

[54] C. Holzhey, F. Larsen, and F. Wilczek, "Geometric and renormalized entropy in conformal field theory," *Nucl.Phys.* **B424** (1994) 443–467, hep-th/9403108.

[55] P. Calabrese and J. L. Cardy, "Entanglement entropy and quantum field theory," *J.Stat.Mech.* **0406** (2004) P06002, hep-th/0405152.

[56] H. Casini and M. Huerta, "A Finite entanglement entropy and the c-theorem," *Phys.Lett.* **B600** (2004) 142–150, hep-th/0405111.

[57] H. Casini and M. Huerta, "A c-theorem for the entanglement entropy," *J.Phys.* **A40** (2007) 7031–7036, cond-mat/0610375.

[58] S. N. Solodukhin, "Entanglement entropy, conformal invariance and extrinsic geometry," *Phys.Lett.* **B665** (2008) 305–309, 0802.3117.

[59] L.-Y. Hung, R. C. Myers, and M. Smolkin, "On Holographic Entanglement Entropy and Higher Curvature Gravity," *JHEP* **1104** (2011) 025, 1101.5813.

[60] M. Huerta, "Numerical Determination of the Entanglement Entropy for Free Fields in the Cylinder," *Phys.Lett.* **B710** (2012) 691–696, 1112.1277.

[61] S. Ryu and T. Takayanagi, "Holographic derivation of entanglement entropy from AdS/CFT," *Phys.Rev.Lett.* **96** (2006) 181602, hep-th/0603001.

[62] T. Nishioka, S. Ryu, and T. Takayanagi, "Holographic Entanglement Entropy: An Overview," *J.Phys.* **A42** (2009) 504008, 0905.0932.

[63] J. de Boer, M. Kulaxizi, and A. Parnachev, "Holographic Entanglement Entropy in Lovelock Gravities," *JHEP* **1107** (2011) 109, 1101.5781.

[64] J. T. Liu, W. Sabra, and Z. Zhao, "Holographic c-theorems and higher derivative gravity," *Phys.Rev.* **D85** (2012) 126004, 1012.3382.

[65] A. Sinha, "On higher derivative gravity, $c$-theorems and cosmology," *Class.Quant.Grav.* **28** (2011) 085002, 1008.4315.

[66] M. F. Paulos, "Holographic phase space: $c$-functions and black holes as renormalization group flows," *JHEP* **1105** (2011) 043, 1101.5993.

[67] T. Albash and C. V. Johnson, "Holographic Entanglement Entropy and Renormalization Group Flow," *JHEP* **1202** (2012) 095, 1110.1074.

[68] D. Freedman, S. Gubser, K. Pilch, and N. Warner, "Renormalization group flows from holography supersymmetry and a c theorem," *Adv.Theor.Math.Phys.* **3** (1999) 363–417, hep-th/9904017.

[69] L. Girardello, M. Petrini, M. Porrati, and A. Zaffaroni, "The Supergravity dual of N=1 superYang-Mills theory," *Nucl.Phys.* **B569** (2000) 451–469, hep-th/9909047.

[70] D. Freedman, S. Gubser, K. Pilch, and N. Warner, "Continuous distributions of D3-branes and gauged supergravity," *JHEP* **0007** (2000) 038, hep-th/9906194.

[71] A. Brandhuber and K. Sfetsos, "Nonstandard compactifications with mass gaps and Newton's law," *JHEP* **9910** (1999) 013, hep-th/9908116.

[72] M. Bianchi, D. Z. Freedman, and K. Skenderis, "How to go with an RG flow," *JHEP* **0108** (2001) 041, hep-th/0105276.

[73] B. Gouteraux and E. Kiritsis, "Generalized Holographic Quantum Criticality at Finite Density," *JHEP* **1112** (2011) 036, 1107.2116.

[74] X. Dong, S. Harrison, S. Kachru, G. Torroba, and H. Wang, "Aspects of holography for theories with hyperscaling violation," *JHEP* **1206** (2012) 041, 1201.1905.

[75] A. Lewkowycz and J. Maldacena, "Generalized gravitational entropy," *JHEP* **1308** (2013) 090, 1304.4926.

[76] R. C. Myers and A. Singh, "Comments on Holographic Entanglement Entropy and RG Flows," *JHEP* **1204** (2012) 122, 1202.2068.

[77] L.-Y. Hung, R. C. Myers, and M. Smolkin, "Some Calculable Contributions to Holographic Entanglement Entropy," *JHEP* **1108** (2011) 039, 1105.6055.

[78] C. R. Graham and E. Witten, "Conformal anomaly of submanifold observables in AdS / CFT correspondence," *Nucl.Phys.* **B546** (1999) 52–64, hep-th/9901021.

[79] A. Schwimmer and S. Theisen, "Entanglement Entropy, Trace Anomalies and Holography," *Nucl.Phys.* **B801** (2008) 1–24, 0802.1017.

[80] R. Corrado, K. Pilch, and N. P. Warner, "An N=2 supersymmetric membrane flow," *Nucl.Phys.* **B629** (2002) 74–96, hep-th/0107220.

[81] E. Witten, "Anti-de Sitter space, thermal phase transition, and confinement in gauge theories," *Adv.Theor.Math.Phys.* **2** (1998) 505–532, hep-th/9803131.

[82] A. Pakman and A. Parnachev, "Topological Entanglement Entropy and Holography," *JHEP* **0807** (2008) 097, 0805.1891.

[83] A. Khavaev, K. Pilch, and N. P. Warner, "New vacua of gauged N=8 supergravity in five-dimensions," *Phys.Lett.* **B487** (2000) 14–21, hep-th/9812035.

[84] T. Hirata and T. Takayanagi, "AdS/CFT and strong subadditivity of entanglement entropy," *JHEP* **0702** (2007) 042, hep-th/0608213.

[85] T. Nishioka and T. Takayanagi, "AdS Bubbles, Entropy and Closed String Tachyons," *JHEP* **0701** (2007) 090, hep-th/0611035.

[86] I. R. Klebanov, D. Kutasov, and A. Murugan, "Entanglement as a probe of confinement," *Nucl.Phys.* **B796** (2008) 274–293, 0709.2140.

[87] I. Bah, A. Faraggi, L. A. Pando Zayas, and C. A. Terrero-Escalante, "Holographic entanglement entropy and phase transitions at finite temperature," *Int.J.Mod.Phys.* **A24** (2009) 2703–2728, 0710.5483.

[88] M. Headrick, "Entanglement Renyi entropies in holographic theories," *Phys.Rev.* **D82** (2010) 126010, 1006.0047.

[89] H. Casini and M. Huerta, "Remarks on the entanglement entropy for disconnected regions," *JHEP* **0903** (2009) 048, 0812.1773.

[90] B. Swingle, "Mutual information and the structure of entanglement in quantum field theory," 1010.4038.

[91] M. Fujita, "Holographic Entanglement Entropy for d=4 N=2 SCFTs in F-theory," *Prog.Theor.Phys.* **128** (2012) 285–300, 1112.5535.

[92] N. Ogawa and T. Takayanagi, "Higher Derivative Corrections to Holographic Entanglement Entropy for AdS Solitons," *JHEP* **1110** (2011) 147, 1107.4363.

[93] J. Dowker, "Entanglement entropy for odd spheres," 1012.1548.

[94] R. Lohmayer, H. Neuberger, A. Schwimmer, and S. Theisen, "Numerical determination of entanglement entropy for a sphere," *Phys.Lett.* **B685** (2010) 222–227, 0911.4283.

[95] J. Latorre, C. Lutken, E. Rico, and G. Vidal, "Fine grained entanglement loss along renormalization group flows," *Phys.Rev.* **A71** (2005) 034301, quant-ph/0404120.

[96] A. Riera and J. Latorre, "Area law and vacuum reordering in harmonic networks," *Phys.Rev.* **A74** (2006) 052326, quant-ph/0605112.

[97] J. Cardy and P. Calabrese, "Unusual Corrections to Scaling in Entanglement Entropy," *J.Stat.Mech.* **1004** (2010) P04023, 1002.4353.

[98] I. R. Klebanov, T. Nishioka, S. S. Pufu, and B. R. Safdi, "Is Renormalized Entanglement Entropy Stationary at RG Fixed Points?," *JHEP* **1210** (2012) 058, 1207.3360.

[99] E. Shaghoulian, "FRW cosmologies and hyperscaling-violating geometries: higher curvature corrections, ultrametricity, Q-space/QFT duality, and a little string theory," *JHEP* **1403** (2014) 011, 1308.1095.

[100] D. T. Son and A. O. Starinets, "Minkowski space correlators in AdS / CFT correspondence: Recipe and applications," *JHEP* **0209** (2002) 042, hep-th/0205051.

[101] N. Itzhaki, J. M. Maldacena, J. Sonnenschein, and S. Yankielowicz, "Supergravity and the large N limit of theories with sixteen supercharges," *Phys.Rev.* **D58** (1998) 046004, hep-th/9802042.

[102] J. M. Maldacena, "The Large N limit of superconformal field theories and supergravity," *Adv.Theor.Math.Phys.* **2** (1998) 231–252, hep-th/9711200.

[103] S. Gubser, I. R. Klebanov, and A. M. Polyakov, "Gauge theory correlators from noncritical string theory," *Phys.Lett.* **B428** (1998) 105–114, hep-th/9802109.

[104] E. Witten, "Anti-de Sitter space and holography," *Adv.Theor.Math.Phys.* **2** (1998) 253–291, hep-th/9802150.

[105] O. Aharony, O. Bergman, D. L. Jafferis, and J. Maldacena, "$\mathcal{N} = 6$ superconformal Chern-Simons-matter theories, M2-branes and their gravity duals," *JHEP* **0810** (2008) 091, 0806.1218.

[106] D. L. Jafferis, "Quantum corrections to $\mathcal{N} = 2$ Chern-Simons theories with flavor and their $AdS_4$ duals," 0911.4324.

[107] D. Gaiotto and D. L. Jafferis, "Notes on adding D6 branes wrapping $\mathbb{RP}^3$ in $AdS_4 \times \mathcal{P}^3$," *JHEP* **1211** (2012) 015, 0903.2175.

[108] D. L. Jafferis and A. Tomasiello, "A Simple class of $\mathcal{N} = 3$ gauge/gravity duals," *JHEP* **0810** (2008) 101, 0808.0864.

[109] S. Franco, I. R. Klebanov, and D. Rodriguez-Gomez, "M2-branes on Orbifolds of the Cone over $Q^{1,1,1}$," *JHEP* **0908** (2009) 033, 0903.3231.

[110] F. Benini, C. Closset, and S. Cremonesi, "Quantum moduli space of Chern-Simons quivers, wrapped D6-branes and AdS4/CFT3," *JHEP* **1109** (2011) 005, 1105.2299.

[111] F. Benini, C. Closset, and S. Cremonesi, "Chiral flavors and M2-branes at toric CY4 singularities," *JHEP* **1002** (2010) 036, 0911.4127.

[112] D. Martelli and J. Sparks, "$AdS_4/CFT_3$ duals from M2-branes at hypersurface singularities and their deformations," *JHEP* **0912** (2009) 017, 0909.2036.

[113] D. L. Jafferis, "The Exact superconformal R-symmetry extremizes $Z$," *JHEP* **1205** (2012) 159, 1012.3210.

[114] N. Hama, K. Hosomichi, and S. Lee, "Notes on SUSY Gauge Theories on Three-Sphere," *JHEP* **1103** (2011) 127, 1012.3512.

[115] V. Pestun, "Localization of gauge theory on a four-sphere and supersymmetric Wilson loops," *Commun.Math.Phys.* **313** (2012) 71–129, 0712.2824.

[116] N. Drukker, M. Marino, and P. Putrov, "From weak to strong coupling in ABJM theory," *Commun.Math.Phys.* **306** (2011) 511–563, 1007.3837.

[117] O. Bergman and S. Hirano, "Anomalous radius shift in AdS(4)/CFT(3)," *JHEP* **0907** (2009) 016, 0902.1743.

[118] S. Bhattacharyya, A. Grassi, M. Marino, and A. Sen, "A One-Loop Test of Quantum Supergravity," *Class.Quant.Grav.* **31** (2013) 015012, 1210.6057.

[119] A. Kapustin, B. Willett, and I. Yaakov, "Nonperturbative Tests of Three-Dimensional Dualities," *JHEP* **1010** (2010) 013, 1003.5694.

[120] R. C. Santamaria, M. Marino, and P. Putrov, "Unquenched flavor and tropical geometry in strongly coupled Chern-Simons-matter theories," *JHEP* **1110** (2011) 139, 1011.6281.

[121] D. Martelli and J. Sparks, "The large N limit of quiver matrix models and Sasaki-Einstein manifolds," *Phys.Rev.* **D84** (2011) 046008, 1102.5289.

[122] S. Cheon, H. Kim, and N. Kim, "Calculating the partition function of N=2 Gauge theories on $S^3$ and AdS/CFT correspondence," *JHEP* **1105** (2011) 134, 1102.5565.

[123] D. R. Gulotta, C. P. Herzog, and S. S. Pufu, "From Necklace Quivers to the $F$-theorem, Operator Counting, and $T(U(N))$," *JHEP* **1112** (2011) 077, 1105.2817.

[124] D. R. Gulotta, C. P. Herzog, and S. S. Pufu, "Operator Counting and Eigenvalue Distributions for 3D Supersymmetric Gauge Theories," *JHEP* **1111** (2011) 149, 1106.5484.

[125] D. R. Gulotta, C. P. Herzog, and T. Nishioka, "The ABCDEF's of Matrix Models for Supersymmetric Chern-Simons Theories," *JHEP* **1204** (2012) 138, 1201.6360.

[126] M. Marino and P. Putrov, "Interacting fermions and N=2 Chern-Simons-matter theories," 1206.6346.

[127] Y. Hyakutake, Y. Imamura, and S. Sugimoto, "Orientifold planes, type I Wilson lines and nonBPS D-branes," *JHEP* **0008** (2000) 043, hep-th/0007012.

[128] J. de Boer, R. Dijkgraaf, K. Hori, A. Keurentjes, J. Morgan, *et. al.*, "Triples, fluxes, and strings," *Adv.Theor.Math.Phys.* **4** (2002) 995–1186, hep-th/0103170.

[129] E. G. Gimon and J. Polchinski, "Consistency conditions for orientifolds and d manifolds," *Phys.Rev.* **D54** (1996) 1667–1676, hep-th/9601038.

[130] A. Sen, "Kaluza-Klein dyons in string theory," *Phys.Rev.Lett.* **79** (1997) 1619–1621, hep-th/9705212.

[131] O. Aharony, O. Bergman, and D. L. Jafferis, "Fractional M2-branes," *JHEP* **0811** (2008) 043, 0807.4924.

[132] O. Bergman, E. G. Gimon, and S. Sugimoto, "Orientifolds, RR torsion, and K theory," *JHEP* **0105** (2001) 047, hep-th/0103183.

[133] N. Seiberg, "IR dynamics on branes and space-time geometry," *Phys.Lett.* **B384** (1996) 81–85, hep-th/9606017.

[134] N. Seiberg and E. Witten, "Gauge dynamics and compactification to three-dimensions," hep-th/9607163.

[135] A. Sen, "A Note on enhanced gauge symmetries in M and string theory," *JHEP* **9709** (1997) 001, hep-th/9707123.

[136] K. Landsteiner and E. Lopez, "New curves from branes," *Nucl.Phys.* **B516** (1998) 273–296, hep-th/9708118.

[137] E. Witten, "Toroidal compactification without vector structure," *JHEP* **9802** (1998) 006, hep-th/9712028.

[138] O. Aharony, S. S. Razamat, N. Seiberg, and B. Willett, "3$d$ dualities from 4$d$ dualities for orthogonal groups," *JHEP* **1308** (2013) 099, 1307.0511.

[139] G. Kuperberg, "Symmetry classes of alternating-sign matrices under one roof," *ArXiv Mathematics e-prints* (Aug., 2000) math/0008184.

[140] D. Gaiotto and E. Witten, "S-Duality of Boundary Conditions In $\mathcal{N} = 4$ Super Yang-Mills Theory," *Adv.Theor.Math.Phys.* **13** (2009) 721, 0807.3720.

[141] C. Closset, T. T. Dumitrescu, G. Festuccia, Z. Komargodski, and N. Seiberg, "Contact Terms, Unitarity, and $F$-Maximization in Three-Dimensional Superconformal Theories," *JHEP* **1210** (2012) 053, 1205.4142.